2017

Heme Oxygenase 1 expression after traumatic brain injury and effect of pharmacological manipulation on functional recovery.

Nicholas H. Russell
Virginia Commonwealth University

0 Preamble

0.1 Cover Page

Heme Oxygenase 1 expression after traumatic brain injury and effect of pharmacological manipulation on functional recovery.

A dissertation submitted in partial fulfillment of the requirements for the degree of Doctor of Philosophy at Virginia Commonwealth University.

By

Nicholas Hyatt Russell
M. ChE., Carnegie Mellon University, 2011
B.S. Mechanical Engineering and Biomedical Engineering, Carnegie Mellon University, 2010

Director: Linda L. Phillips, Ph.D.

Professor, Department of Anatomy and Neurobiology.

Virginia Commonwealth University

Richmond, Virginia

May 2017

0.2 Acknowledgements

To Anna, Carolina, and Eleanor.

I would like to thank my advisor, Dr. Linda L. Phillips for her continued support, mentoring, and guiding through the course of my research and writing. She has been truly invested in my success as a student and researcher and has provided me with a foundation in lifelong research skills. I would also like to thank my Ph.D. advisory committee: Dr. Clive Baumgarten, Dr. Andrew Ottens, Dr. John T. Povlishock, and Dr. Dong Sun who have each provided me with invaluable resources and guidance through the course of my studies. I am also forever grateful to Dr. Gordon L. Archer, and Sandra Sorrell for their support and guidance through the many stages of the MD-PhD Program.

I am further ever in the debt of the members of the Phillips' lab where I have made my home these past years. Raiford T. Black and Lesley K. Harris provided invaluable technical knowledge for my studies in Western Blot and Zymogram. Nancy N. Lee both trained me in the craniectomy surgery and provided significant expertise in immunohistochemistry. Terry L. Smith provided continued support for a variety of experiments repeated short notice. Dr. Thomas M. Reeves provided a sounding board for statistical rigor and hypotheticals that assisted the interpretation of multi-component assays.

I would also like to thank the students of Dr. Phillips; Dr. Julie L. Chan, Dr. Adele E. Doperalski, and Dr. Melissa A. Powell. They each independently provided training, humor, and camaraderie throughout and were always eager to share advice and knowledge. The style and format of this document was influenced by the work of Dr. Phillips' previous students: Dr. Julie Chan, Dr. Melissa Powell, & Dr. Kelly Warren. I would also like to thank my cohort of MD-PhD classmates and select Neuroscience classmates who also provided significant camaraderie and technical support; Adam Blakeney, Marc Cantwell, Sheela Damles, Mackenzie Lind, Spencer Harris, Mike Waters, and Pavel Lizhnyak.

Finally I would like to thank my family who have supported me throughout the process from my earliest application through to the present day. This includes my Mom and Dad, my brother Ben, and my sister Amanda. Most importantly I would like to thank and dedicate this body of work to my wife Anna, and my two daughters Carolina and Eleanor; without their sustained support this work would not have been possible.

This work was supported by NIH grants: NIH-NS56247, NS44372, NS57758, 5P30NS047463

0.3 Table of Contents

0 Preamble 1

0.1 Cover Page 1

0.2 Acknowledgements 2

0.3 Table of Contents 3

0.4 List of Figures 13

0.5 List of Tables 16

0.6 List of Abbreviations 17

0.7 Abstract 23

1 Chapter 1: Introduction 26

1.1 Impact, Epidemiology, and Classification 26

1.1.1 Table 1-1: TBI ED Visits, Hospitalizations, and Deaths by Age 27

1.2 Traumatic Brain Injury Pathophysiology 29

1.2.1 Table 1-2: Categories of Neuropathological Damage 30

1.2.2 Figure 1-1: Neurovascular Unit 33

1.3 Molecular Mechanisms of Injury 36

1.4 NVU and Inflammatory Response 42

1.5 Neuroplasticity and the Extracellular Environment after TBI 47

1.5.1 Figure 1-2: Reactive Synaptogenesis 49

1.5.2 Table 1-3: MMPs and Their Classifications 55

1.5.3 Figure 1-3: Domain Structure of the MMP Family 58

1.6 Gelatinases, NVU and TBI..... 60

1.7 Heme Oxygenase..... 62

1.7.1 Discovery, Structure, Biological Role 62

1.7.2 NVU Breach, HO-1 and Cytotoxicity..... 65

1.7.3 HO Genetics, Gene Regulation, and Signal Transduction..... 66

1.7.4 Figure 1-4: HO-1 Gene Regulation..... 67

1.7.5 HO Subcellular Localization..... 69

1.7.6 HO-1 Sources of Activation..... 69

1.7.7 Figure 1-5: HO-1 Activation Pathways 71

1.8 Non Traumatic Role for HO-1 73

1.9 HO-1 and Traumatic Brain Injury..... 74

1.9.1 Figure 1-6: HO-1 Expression 1-7d Post-Injury 75

1.10 Novel Role in Traumatic Brain Injury Recovery 78

1.10.1 Pharmacological Inducers of HO-1 81

1.10.2 A Proposed Mechanism for HO-1 Induced Cytoprotection after TBI..... 82

1.11 Choice of FPI as Experimental Model 84

1.11.1 The Hippocampus as a TBI Model 87

1.11.2 Figure 1-7: Mid-Dorsal Coronal Section of Rodent Brain 90

1.11.3 The Neocortex as a TBI Model 93
1.11.4 Figure 1-8: Simplified Cortical Excitatory Circuits 94
1.11.5 Hypotheses Tested and Dissertation Organization by Chapter 98
2 Chapter 2 100
2.1 Abstract Chapter 2 101
2.2 Introduction Chapter 2 103
2.2.1 Figure 2-1: Pathway of Heme Metabolism 105
2.3 Methods Chapter 2 109
2.3.1 Experimental Animals 109
2.3.2 Surgical Preparation for Rat Central Fluid Percussion Injury 109
2.3.3 Central Fluid Percussion Injury 110
2.3.4 Protein Extraction 111
2.3.5 Western Blotting 115
2.3.6 Tissue Fixation 116
2.3.7 Immunohistochemistry 116
2.3.8 Statistics 117
2.3.9 Table 2-1 Antibodies used in Western Blot Experiments 118
2.3.10 Table 2-2: Antibodies used in Immunohistochemistry Experiments 118
2.4 Chapter 2 Data 119
2.4.1 Figure 2-3: Widefield Hemorrhage after cFPI 1-7d Post-Injury 121

2.4.2 Figure 2-4: Enlarged view of 3d Post-Injury Hemorrhage 123

2.4.3 Figure 2-5: HO-1 Response to Injury Over Time 126

2.5 HO-1 Change Neocortex vs Hippocampus 128

2.5.1 Figure 2-6: Acute Changes in HO-1 vs GFAP or IBA1 in Hippocampus and Neocortex 129

2.5.2 Figure 2-7: HO-1 Western Blot Time Course 1-15d 133

2.5.3 Figure 2-8: HO-1 and Glial Reactivity in Reactive Neocortex 1-7d Post-Injury . 136

2.5.4 Figure 2-9: HO-1 and Glial Reactivity in Necrotic Neocortex 3-7d 138

2.5.5 Figure 2-10: HO-1 and Reactive Glia in Hippocampus 1-7d Post-Injury 141

2.5.6 Summary of Observations in HO-1 143

2.6 FTL Change Neocortex vs Hippocampus 144

2.6.1 Figure 2-11:FTL vs LCN2 in Neocortex 1-15d Post-Injury 145

2.6.2 Figure 2-12:FTL vs LCN2 in Hippocampus 1-15d Post-Injury 147

2.6.3 Figure 2-13: FTL vs LCN2 Hippocampal Fissure 1-7d Post-Injury..... 149

2.6.4 Figure 2-14: FTL Western Blot 1-15d Post-Injury 152

2.6.5 Summary of Observations in FTL 154

2.7 LCN2 Change Neocortex vs Hippocampus 155

2.7.1 Figure 2-15: Acute HO-1 vs LCN2 Hippocampus Widefield 156

2.7.2 Figure 2-16: Acute HO-1 vs LCN2 Hippocampus and Neocortex Confocal 158

2.7.3 Figure 2-17: HO-1 vs LCN2 Hippocampus 1-7d Post-Injury Widefield 161

2.7.4 Figure 2-18: LCN2 Western Blot 1-7d Post-Injury 164
2.7.5 Summary of Observations in LCN2 166
2.8 Gelatinase Response Neocortex vs Hippocampus 167
2.8.1 Figure 2-19: Zymography of MMP2 and MMP9 1-7d Post-Injury in Neocortex 169
2.8.2 Figure 2-20: Zymography of MMP2 and MMP9 1-7d Post-Injury in Hippocampus 172
2.8.3 Summary of Observations in Zymograms 174
2.9 Chapter 2 Discussion 175
2.9.1 Summary of Results in Chapter 2 175
2.9.2 Hemorrhage and HO-1 Response to mild-moderate FPI 176
2.9.3 Correlated Post-injury changes in heme processing pathway molecules 179
2.9.4 Neocortical HO-1 Response Relative to Hemorrhagic Damage at NVU 184
2.9.5 Hippocampal HO-1 Response Relative to Absence of Hemorrhagic Damage 187
2.9.6 Impact of these results on post-injury management of hemorrhage 190
3 Chapter 3 193
3.1 Abstract Chapter 3 194
3.2 Introduction Chapter 3 196
3.3 Methods Chapter 3 199
3.3.1 Experimental Animals 199
3.3.2 Surgical Preparation for Rat Central Fluid Percussion Injury 199

3.3.3 Central Fluid Percussion Injury 200

3.3.4 Protein Extraction 201

3.3.5 Figure 3-1: cFPI Device 203

3.3.6 Western Blotting 205

3.3.7 Tissue Fixation 206

3.3.8 Immunohistochemistry 206

3.3.9 Drug Injection Protocol 207

3.3.10 Figure 3-2: Rotarod Device 209

3.3.11 Rotarod 211

3.3.12 Morris Water Maze 211

3.3.13 Figure 3-3: Morris Water Maze Apparatus 213

3.3.14 Statistics 215

3.3.15 Table 3-1: Antibodies Used in Western Blot Experiments 216

3.3.16 Table 3-2 Antibodies Used in Immunohistochemistry Experiments 216

3.4 Chapter 3 Data 217

3.5 Heme Pigment Disappearance in Drug Treated Animals 218

3.5.1 Figure 3-4: Heme Procesing Cartoon: 220

3.5.2 Figure 3-5: Loss of Heme Pigment After Drug Treatment 1d Post-Injury 223

3.6 Drug Treated HO-1 Shift responding to pigment changes, LCN2 unaffected 225

3.6.1 HO-1 Results 225

3.6.2 Figure 3-6: HO-1 Western Blot Results Drug Treated 1-15d Post-Injury 227

3.6.3 Table 3-3: HO-1 Western Blot Result Table 1-15d Post-Injury 229

3.6.4 Figure 3-7: HO-1 vs LCN2 Neocortex Drug Treated 1d Post-Injury 232

3.6.5 Figure 3-8: HO-1 vs LCN2 Hippocampus Drug Treated 1d Post-Injury 234

3.6.6 Figure 3-9: HO-1 vs IBA1 Neocortex Drug Treated 3d Post-Injury 237

3.6.7 Figure 3-10: HO-1 vs IBA1 Hippocampus Drug Treated 3d Post-Injury 239

3.6.8 Figure 3-11: HO-1 vs GFAP Neocortex Drug Treated 7d Post-Injury 241

3.6.9 Figure 3-12: HO-1 vs FTL Neocortex Drug Treated 15d Post-Injury 243

3.7 Summary of Observations HO-1 245

3.8 LCN2 Results 246

3.8.1 Figure 3-13: LCN2 Western Blot Results Drug Treated 1-7d Post-Injury 248

3.8.2 Table 3-4: LCN2 Western Blot Result Table 1-7d 250

3.9 Rotarod Behavioral Results 251

3.9.1 Figure 3-14: Rotarod Contact Time 1-7d Post-Injury 253

3.9.2 Table 3-5: Rotarod ANOVA Model 255

3.9.3 Figure 3-15: Rotarod Max RPM 1-7d Post-Injury 256

3.9.4 Table 3-6: Rotarod Max RPM ANOVA Model 258

3.9.5 Figure 3-16: Rotarod Contact Time Box Plots 1,3,5,7d Post-Injury 260

3.9.6 Figure 3-17: Cumulative Rotarod Metrics 262

3.9.7 Summary of Observations Rotarod 264

3.10 Zymogram changes and long term sequelae of tissue damage (FTL) 265
3.10.1 Zymogram Results 265
3.10.2 Figure 3-18: Zymography for MMP2, MMP9 in Drug Treated Neocortex 268
3.10.3 Figure 3-19: Zymography for MMP2, MMP9 in Drug Treated Hippocampus 270
3.10.4 Summary of Observations Zymography 272
3.10.5 FTL Results 273
3.10.6 Figure 3-20: FTL Western Blot Results Drug Treated 1-15d Post-Injury 275
3.10.7 Table 3-7: FTL Western Blot ANOVA Model 277
3.11 Long Term Behavioral Shifts 278
3.11.1 Morris Water Maze 278
3.12 General Metrics: Path Length, Platform Latency, Swim Speed 280
3.12.1 Figure 3-21: Morris Water Maze Path Length during Training 11-14d Post-Injury 280
3.12.2 Figure 3-22: Morris Water Maze Latency to Platform Post-Injury 11-14d 282
3.12.3 Figure 3-23: Morris Water Maze Swim Speed 11-14d Post-Injury 284
3.12.4 Water Maze Heat Maps for Individual Groups 286
3.12.5 Figure 3-24: Morris Water Maze Probe Trials for Individual Sham Animals 288
3.12.6 Figure 3-25Morris Water Maze Probe Trials for Individual TBI Animals 289
3.12.7 Figure 3-26Morris Water Maze Probe Trials for Individual TBI+HMN Animals 290
3.12.8 Figure 3-27Morris Water Maze Probe Trials for Individual TBI+SFN Animals . 291

3.12.9 MWM Summaries and Analysis 292
3.12.10 Figure 3-28: Morris Water Maze Probe Trial Heat Maps by Condition 294
3.12.11 Figure 3-29: Morris Water Maze Probe Trial Quadrant Score by Group 296
3.12.12 Figure 3-30: Morris Water Maze Proximity Score by Group 298
3.12.13 Figure 3-31: Morris Water Maze Relative Proximity Score by Group 300
3.12.14 Table 3-8: Morris Water Maze Training Quadrant Score ANOVA Model 302
3.12.15 Table 3-9: Morris Water Maze Probe Trial Proximity Score 303
3.12.16 Table 3-10: Morris Water Maze All Days Relative Proximity Score 304
3.13 Discussion Chapter 3 306
3.13.1 Summary Chapter 3 306
3.13.2 Discussion Chapter 3 307
4 Chapter 4: Discussion 325
4.1 Summary of Results 325
4.2 Post-Injury Heme Processing 326
4.3 Hemorrhagic Processing in the Neocortex vs Hippocampus 328
4.4 HO-1 Expression/Evidence of Bleeds 329
4.5 Lipocalin 2 and Gelatinase Role in Heme Processing and Recovery 331
4.5.1 Lipocalin 2 is a known effector of Angiogenesis and Dendritic Spine Remodeling 331
4.5.2 Gelatinases as effective targets for both synaptic and vascular remodeling 334

4.5.3 Mechanisms of Select Agents 337
4.6 Behavioral outcomes after Treatment 338
4.7 HO-1 as a Therapeutic Target 339
4.8 Differential Drug Treatment Effects 343
4.9 Future Directions 346
4.9.1 Pathway Mechanism Experiments 346
4.9.2 Pathway Manipulation Experiments 348
4.9.3 Behavioral Outcomes 348
4.10 Final Remarks 350
5 List of References 351
6 Appendices 394
6.1 Description of Injury Model 394
6.2 Commentary on Randomization, Blinding, Animal Sex Selection 394
6.3 Drug Blood Brain Barrier Transport 395
6.4 Sham Drug Treated Animal Behavior 396
6.4.1 Morris Water Maze 396
6.5 Appendix Data for Chapter 3 398
6.6 Affymetric Rat Genome Microarray Screening 407
7 Vita 408

0.4 List of Figures

1.2.2 Figure 1-1: Neurovascular Unit 33

1.5.1 Figure 1-2: Reactive Synaptogenesis 49

1.5.3 Figure 1-3: Domain Structure of the MMP Family 58

1.7.4 Figure 1-4: HO-1 Gene Regulation 67

1.7.7 Figure 1-5: HO-1 Activation Pathways 71

1.9.1 Figure 1-6: HO-1 Expression 1-7d Post-Injury 75

1.11.2 Figure 1-7: Mid-Dorsal Coronal Section of Rodent Brain 90

1.11.4 Figure 1-8: Simplified Cortical Excitatory Circuits 94

2.2.1 Figure 2-1: Pathway of Heme Metabolism 105

2.3.4.1 Figure 2-2: cFPI Device 113

2.4.1 Figure 2-3: Widefield Hemorrhage after cFPI 1-7d Post-Injury 121

2.4.2 Figure 2-4: Enlarged view of 3d Post-Injury Hemorrhage 123

2.4.3 Figure 2-5: HO-1 Response to Injury Over Time 126

2.5.1 Figure 2-6: Acute Changes in HO-1 vs GFAP or IBA1 in Hippocampus and Neocortex 129

2.5.2 Figure 2-7: HO-1 Western Blot Time Course 1-15d 133

2.5.3 Figure 2-8: HO-1 and Glial Reactivity in Reactive Neocortex 1-7d Post-Injury 136

2.5.4 Figure 2-9: HO-1 and Glial Reactivity in Necrotic Neocortex 3-7d 138

2.5.5 Figure 2-10: HO-1 and Reactive Glia in Hippocampus 1-7d Post-Injury 141

2.6.1 Figure 2-11:FTL vs LCN2 in Neocortex 1-15d Post-Injury 145

2.6.2 Figure 2-12:FTL vs LCN2 in Hippocampus 1-15d Post-Injury 147

2.6.3 Figure 2-13: FTL vs LCN2 Hippocampal Fissure 1-7d Post-Injury 149

2.6.4 Figure 2-14: FTL Western Blot 1-15d Post-Injury 152

2.7.1 Figure 2-15: Acute HO-1 vs LCN2 Hippocampus Widefield..... 156

2.7.2 Figure 2-16: Acute HO-1 vs LCN2 Hippocampus and Neocortex Confocal 158

2.7.3 Figure 2-17: HO-1 vs LCN2 Hippocampus 1-7d Post-Injury Widefield..... 161

2.7.4 Figure 2-18: LCN2 Western Blot 1-7d Post-Injury 164

2.8.1 Figure 2-19: Zymography of MMP2 and MMP9 1-7d Post-Injury in Neocortex 169

2.8.2 Figure 2-20: Zymography of MMP2 and MMP9 1-7d Post-Injury in Hippocampus.. 172

3.3.5 Figure 3-1: cFPI Device 203

3.3.10 Figure 3-2: Rotarod Device..... 209

3.3.13 Figure 3-3: Morris Water Maze Apparatus 213

3.5.1 Figure 3-4: Heme Procesing Cartoon:..... 220

3.5.2 Figure 3-5: Loss of Heme Pigment After Drug Treatment 1d Post-Injury 223

3.6.2 Figure 3-6: HO-1 Western Blot Results Drug Treated 1-15d Post-Injury 227

3.6.4 Figure 3-7: HO-1 vs LCN2 Neocortex Drug Treated 1d Post-Injury 232

3.6.5 Figure 3-8: HO-1 vs LCN2 Hippocampus Drug Treated 1d Post-Injury..... 234

3.6.6 Figure 3-9: HO-1 vs IBA1 Neocortex Drug Treated 3d Post-Injury 237

3.6.7 Figure 3-10: HO-1 vs IBA1 Hippocampus Drug Treated 3d Post-Injury..... 239

3.6.8 Figure 3-11: HO-1 vs GFAP Neocortex Drug Treated 7d Post-Injury..... 241

3.6.9 Figure 3-12: HO-1 vs FTL Neocortex Drug Treated 15d Post-Injury 243

3.8.1 Figure 3-13: LCN2 Western Blot Results Drug Treated 1-7d Post-Injury 248

3.9.1 Figure 3-14: Rotarod Contact Time 1-7d Post-Injury..... 253

3.9.3 Figure 3-15: Rotarod Max RPM 1-7d Post-Injury..... 256

3.9.5 Figure 3-16: Rotarod Contact Time Box Plots 1,3,5,7d Post-Injury..... 260

3.9.6 Figure 3-17: Cumulative Rotarod Metrics 262

3.10.2 Figure 3-18: Zymography for MMP2, MMP9 in Drug Treated Neocortex 268

3.10.3 Figure 3-19: Zymography for MMP2, MMP9 in Drug Treated Hippocampus 270

3.10.6 Figure 3-20: FTL Western Blot Results Drug Treated 1-15d Post-Injury 275

3.12.1 Figure 3-21: Morris Water Maze Path Length during Training 11-14d Post-Injury ... 280

3.12.2 Figure 3-22: Morris Water Maze Latency to Platform Post-Injury 11-14d 282

3.12.3 Figure 3-23: Morris Water Maze Swim Speed 11-14d Post-Injury 284

3.12.5 Figure 3-24: Morris Water Maze Probe Trials for Individual Sham Animals 288

3.12.6 Figure 3-25Morris Water Maze Probe Trials for Individual TBI Animals 289

3.12.7 Figure 3-26Morris Water Maze Probe Trials for Individual TBI+HMN Animals 290

3.12.8 Figure 3-27Morris Water Maze Probe Trials for Individual TBI+SFN Animals 291

3.12.10 Figure 3-28: Morris Water Maze Probe Trial Heat Maps by Condition 294

3.12.11 Figure 3-29: Morris Water Maze Probe Trial Quadrant Score by Group 296

3.12.12 Figure 3-30: Morris Water Maze Proximity Score by Group 298

3.12.13 Figure 3-31: Morris Water Maze Relative Proximity Score by Group 300

0.5 List of Tables

1.1.1 Table 1-1: TBI ED Visits, Hospitalizations, and Deaths by Age 27

1.2.1 Table 1-2: Categories of Neuropathological Damage 30

1.5.2 Table 1-3: MMPs and Their Classifications 55

2.3.9 Table 2-1 Antibodies used in Western Blot Experiments 118

2.3.10 Table 2-2: Antibodies used in Immunohistochemistry Experiments 118

3.3.15 Table 3-1: Antibodies Used in Western Blot Experiments 216

3.3.16 Table 3-2 Antibodies Used in Immunohistochemistry Experiments 216

3.6.3 Table 3-3: HO-1 Western Blot Result Table 1-15d Post-Injury 229

3.8.2 Table 3-4: LCN2 Western Blot Result Table 1-7d 250

3.9.2 Table 3-5: Rotarod ANOVA Model 255

3.9.4 Table 3-6: Rotarod Max RPM ANOVA Model 258

3.10.7 Table 3-7: FTL Western Blot ANOVA Model 277

3.12.14 Table 3-8: Morris Water Maze Training Quadrant Score ANOVA Model 302

3.12.15 Table 3-9: Morris Water Maze Probe Trial Proximity Score 303

3.12.16 Table 3-10: Morris Water Maze All Days Relative Proximity Score 304

0.6 List of Abbreviations

ACH……...……...Acetylcholine

ADAM-10…… A Disintegrin and metalloproteinase domain-containing protein-10

AD……..... Alzheimer's Disease

AMPA……..….. α-amino-3-hydroxy-5-methyl-4-isoxazolepropionic acid

ANOVA……...Analysis of Variance

APP…….Amyloid Precursor Protein

ARE……..Antioxidant Response Element

BBB……...……..... Blood Brain Barrier

BDNF…….Brain Derived Neurotrophic Factor

CA…… Cornu ammonis

CAM……..Cell Adhesion Molecules

CCI…….. Controlled cortical impact

CNS……... Central Nervous System

CO…….Carbon Monoxide

CT……Computed Tomography

CTE…… Chronic traumatic encephalopathy

DAI……. Diffuse axonal injury

DG……. Dentate Gyrus

DMSO……..... Dimethyl sulfoxide

DTI……Diffusion Tensor Imaging

EAA…….Excitatory Amino Acid

ECM……. Extracellular matrix

ED……....Emergency Department

ER……....Endoplasmic Reticulum

Fe…….Iron

fMRI……Functional magnetic resonance imaging

FTL…….Ferritin Light Chain

FPI…….Fluid Percussion Injury

GCL……. Granule cell layer

GCS…….. Glasgow coma scale

GFAP…….. Glial fibrillary acidic protein

HI……..….. Hypoxic-ischemic injury

HIV……...….Human Immunodeficiency Virus

HMN……...Hemin

HO……..Heme Oxygenase

HO-1……...……Heme Oxygenase 1

HO-2……..…….Heme Oxygenase 2

HOAc……..…..Glacial acetic acid

HPF…….Hippocampal Formation

IACUC……..Institutional Animal Care and Use Committee

IBA1…….….. Ionized calcium binding adaptor molecule 1

IHC……... Immunohistochemistry

ICP……... Intracranial pressure

IL……..Interleukin

IFN-γ……...Interferon-γ

IP…… Intraperitoneal

IQR……..Interquartile Range

KDa……..… Kilodalton

KO…….……..…..Knock out

LCN2……..……..Lipocalin 2

LOC……..……. Loss of consciousness

LTP……..…..Long-term potentiation

LTD…….Long Term Depression

MANOVA……...…. Multivariate analysis of variance

MCAO…….…. Middle cerebral artery occlusion

MeOH……...……. Methanol

MI…….….. Myocardial infarction

ML……..……. Molecular layer

MMP……..… Matrix metalloproteinase

MS…….Multiple Sclerosis

mTBI……. Mild traumatic brain injury

mTBST……..….Tris Buffered Saline + Tween + milk

MWM……..… Morris water maze

MRI…….Magnetic Resonance Imaging

MT-MMP……...Membrane Type-Matrix Metalloproteinase

NAC……N-acetylcysteine

NCC……Neural Crest Cell

NGAL…….…… Neutrophil gelatinase-associated lipocalin (aka Lipocalin 2)

NO……..…Nitric Oxide

NMDA……..…..N-methyl-D-aspartate

NSC…….....Neural Stem Cell

OB……..Olfactory Bulb

PBS…….. Phosphate buffered saline

PD…….. Parkinson's Disease

PET……..Positron Emission Tomography

PNS……. Peripheral nervous system

PTA…….Post Traumatic Amnesia

PTSD……..….Post Traumatic Stress Disorder

RES…….Reticuloendothelial System

ROS……..… Reactive oxygen species

ROD……..... Relative optical density

SAH……..... Subarachnoid hemorrhage

SCI……..…….. Spinal cord injury

SEM……...……..….. Standard error of the mean

SFN……...Sulforaphane

SWI……... Susceptibility Weighted Imaging

SWIM……...Susceptibility Weighted Imaging and Mapping

TAI…….…….. Traumatic axonal injury

TBI……...….. Traumatic brain injury

TBI+HMN……...…Traumatic Brain Injury treated with Hemin

TBI+SFN…….....Traumatic Brain Injury treated with Sulforaphane

TBS……....Tris Buffered Saline

TBST…….. Tris Buffered Saline + Tween

TGF-β……..Transforming growth factor β

TIMP……...Tissue Inhibitor of Metalloproteinase

TJ…….....Tight Junction

UEC……...Unilateral Entorhinal Cortex Lesion

VCU……..…Virginia Commonwealth University

VEGF……Vascular Endothelial Growth Factor

WB…… Western blot

WT…….Wild type

0.7 Abstract

Heme Oxygenase 1 expression after traumatic brain injury and effect of pharmacological manipulation on functional recovery.

By Nicholas Hyatt Russell, M.ChE., B.S.

A dissertation submitted in partial fulfillment of the requirements for the degree of Doctor of Philosophy at Virginia Commonwealth University.

Virginia Commonwealth University, 2017

Major Director: Linda L. Phillips, Ph.D.
Professor, Department of Anatomy and Neurobiology.

Traumatic brain injury (TBI) is a multimodal constellation of injuries derived from acute mechanical trauma to the brain. TBI has an impact across all parts of society and has resulted in a large number of victims living with resulting neurocognitive and physical impairments due to the limited availability of generalizable treatment options. As a result, it is necessary in TBI to understand all aspects of underlying tissue pathology and attempt to treat these underlying injuries, individually if necessary. Here we have focused on examining heme processing and hemorrhagic injury in a diffuse model of TBI. There are two parts to this study, the first is to examine whether there is a heme processing response in non-hemorrhagic tissue and thus if treatment of heme processing pathways may be a viable treatment paradigm. The second part is to try and influence heme processing by upregulating expression of heme catabolic proteins. In particular we focus on **heme oxygenase 1 (HO-1)**, the inducible form of the rate limiting enzyme in heme catabolism, and compare it both in tissues that experience distinct but limited hemorrhage (the neocortex), and tissue that rarely experiences significant hemorrhages (the hippocampus). The model used was a central fluid percussion injury model that has been extensively characterized to produce diffuse injury throughout the tissue. Using an overpressure

of 2.0±0.1 ATM we produce a mild-moderate injury which characteristically shows limited hemorrhage in white matter tracks laying above the lateral ventricles and which extend into the layer VI and V neocortex overlaying. We tracked the temporal and spatial profile of HO-1 expression via **western blot (WB)** and **immunohistochemistry (IHC)**, identifying that HO-1 peaks at 3d post-injury in both tissues examined and generally localizes within the reactive glia with distinct profiles depending on distance from the necrotic bleed. In the hippocampus expression was limited almost entirely within **glial fibrillary acidic protein + (GFAP+)** astroglia while in the neocortex the immediate penumbra to the bleed results in extensive **ionized calcium binding adaptor molecule 1+ (IBA1+)** microglial co-staining, with an outer penumbra consisting of GFAP+ astroglia. We further characterized the temporal and spatial expression of a small number of other heme processing related proteins. We examined **Lipocalin 2 (LCN2)**, a small iron sequestering siderocalin, which can be upregulated by the same promoter as HO-1 and which is involved both in the acute iron sequestering response and in the extracellular matrix response since it is known to persistently activate matrix metalloproteinases. We examined **Ferritin (FTL)** as a marker of iron deposition (evidence of heme degradation) and long term tissue damage. Further, we observed the timeline of heme pigment processing and the rise of iron dense aggregates observed via Perls' stain. Characterizing the expression of these additional metrics demonstrated that the hippocampus exhibits a robust iron processing response which at times shows protein elevation relative to Sham that is higher than in the neocortex. At the same time there is a notable absence of heme pigment or iron aggregate formation. After characterizing this response we next moved to influence heme processing via the post-injury injection of either **Hemin (HMN)** or **Sulforaphane (SFN)**, two known activators of the HO-1 transcriptional activator Nrf2. We observed that both drugs caused similar shifts in the heme

processing response. By 1d post-injury the majority of heme pigment typically observed after injury was absent and the peak expression of HO-1 was shifted to 1d rather than 3d post-injury. Behavioral testing via the rotarod 1-7d post-injury showed a robust improvement in the Sulforaphane treated animals which approached Sham performance ability by 2d. In the later term behavioral testing via the **Morris water maze (MWM)** 11-15d post-injury robust improvement was demonstrated by the Hemin treated animals which showed focused search patterns during their probe trial which were similar to the Sham performance. The Sulforaphane treated animals did not appear to show improvement in the Morris water maze testing paradigm however closer examination revealed that there is a marked shift in search pattern utilization that occurs in the Sulforaphane group which demonstrates that even a single injection given in a critical post-injury window can have profound effects on behavioral performance even 15d later.

Collectively the studies presented in these two chapters provide evidence that there is an underlying hemorrhagic or hemorrhagic-like injury response which is generalizable to multiple tissues even in circumstances of diffuse brain injury. Further, post-injury treatment targeted the hemorrhagic response can produce robust behavioral effects if provided in a critical window suggesting that heme pathology is a contributory factor to continued impairment following TBI.

1 Chapter 1: Introduction

1.1 Impact, Epidemiology, and Classification

Traumatic Brain Injury (TBI) is a constellation of largely mechanically induced injuries that result in temporary or permanent neurological impairment including long term cognitive and motor deficits. Though some injuries are relatively minor and resolve spontaneously many require patients to undergo extensive psychological and physical therapy (Hyder et al., 2007; Asikainen et al., 1998; Faul et al., 2010; Weightman et al., 2010). While TBI is a serious global health issue with 2.2 million new incidents in the US (Faul et al., 2010) and 10 million worldwide (Hyder et al., 2007), it is the potential long term sequelae that lead to nearly 5.3 million Americans living with the effects of TBI and contribute to TBI being associated with 52,000 deaths yearly (**Table 1**; Rutland-Brown et al., 2006). The cost of rehabilitation and loss of productivity has resulted in a financial burden that currently exceeds $60 billion annually (Langlois et al., 2006; Finkelstein et al., 2006; Rutland-Brown et al., 2006) with some estimates as high as $221 billion annually when factoring in loss of quality of life (Coronado et al., 2011; Coronado et al., 2014). It is important to note that these numbers are derived from clinical contacts and do not include the large number of injuries that are more mild and do not result in **emergency department (ED)** treatment (Goldstein, 1990; Coburn, 1992).

Due to its multimodal nature TBI affects a wide swath of American society impacting every age group though the most likely source of injury changes with age and societal behavior. The Centers for Disease Control and Prevention categorizes the most common causes of TBI as; Motor Vehicle Traffic, Falls, Assault, Struck by/Against, Self-Inflicted, and Other. Young children 0-4 most commonly experience TBI due to assault while older children through young adults (5-14 and 15-24) primarily experience injury from motor vehicle traffic accidents. Older

adults (25-44 and 45-64) in contrast experience more self inflicted injuries while in patients over 65 years old the primary cause of injury is due to falls. When added together, TBI incidents outnumber the combined cases of multiple sclerosis, breast cancer, and **spinal cord injury (SCI)** and demonstrate wider distribution throughout society (Weber and Maas, 2007).

1.1.1 Table 1-1: TBI ED Visits, Hospitalizations, and Deaths by Age

	Emergency department visits*		Hospitalizations†		Deaths		Total‡	
Age, y	No.§	Rate‖	No.§	Rate‖	No.	Rate‖	No.§	Rate‖
0–4	216,000	1091.2	18,000	92.1	1,035	5.2	235,000	1188.5
5–14	188,000	458.2	24,000	59.3	1,250	3.1	213,000	520.5
15–24	313,000	760.1	56,000	135.4	9,053	22.0	378,000	917.5
25–44	254,000	301.0	58,000	69.1	13,904	16.5	326,000	386.7
45–64	163,000ƒ	237.9ƒ	50,000	72.4	11,698	17.0	225,000ƒ	327.3ƒ
65+	90,000ƒ	251.8ƒ	84,000	234.1	13,796	38.4	188,000ƒ	524.3ƒ
Total‡	1,224,000	420.9	290,000	99.9	50,757	17.5	1,565,000	538.2

*Persons who were hospitalized, died, were transferred to another facility, or had an unknown disposition were excluded.
†Persons who died while being hospitalized were excluded.
‡Numbers, rates, and percentages may not sum to totals due to rounding.
§Numbers have been rounded to the nearest 1000.
‖Rate per 100,000 population.
ƒSample size, or sample size of one of the components, is 30–59; the value of the estimate was reported but may not be stable.

Table 1: Numbers and rates of traumatic brain injury-related emergency department visits, hospitalization, and deaths, by age group, in United States, Reproduced with permission from Rutland-Brown 2006.

TBI has historically been classified as mild, moderate, or severe based on various clinical guides that tend to blur boundaries between categories making comparisons across studies somewhat difficult due to variable clinical assessments (Malec et al., 2007). Additionally, the widespread use of semi-appropriate scales, including the **Glasgow Coma Scale (GCS),** has resulted in

somewhat lumped categorization of larger symptom constellations [editor note: the GCS was initially designed as a pre and post-operative scale of neurological function to determine if a neurological surgical intervention was helpful, it was not originally intended as a clinical assessment of injury or recovery]. Alternative or additional measurements, including **post-traumatic amnesia (PTA)** and **loss of consciousness (LOC),** can be assessed to determine relative severity of TBI. More data driven metrics also exist including the usage of **computer tomography (CT)**, **magnetic resonance imaging (MRI)**, **functional MRI (fMRI)**, **positron emission tomography (PET)**, **diffusion tensor imaging (DTI)**, and **susceptibility weighted imaging (SWI)** all of which can be used to more discretely classify injury.

In addition to the 2.2 million ED visits that are recorded each year there is also a significantly larger population that is affected by mild TBI, including the majority of what would be considered 'concussions' in a sports setting where the individual may seek out a degree of medical help (e.g. from a sports trainer) but does not visit an ED and thus is not recorded. This leads to a potentially unknown number of patients who may be experiencing progressive TBI consequences (Goldstein, 1990; Coburn, 1992) which may include sensory deficits, movement disorders, cognition changes, and memory loss. Severe TBI is obvious and frequently fatal and even moderate TBI demonstrates clear neurological deficits that are fairly obvious in both the immediate and long term to the average person. Mild TBI, in contrast, is more insidious with its relatively minor initial presentation that may progress to or at least is associated with an array of chronic delayed functional deficits and early onset typically age related neurological disorders including forms of Parkinsonianism and Alzheimers disease. More recent epidemiological studies have examined the effects of mild TBI due to sports or military related injuries (Pellman et al., 2006; Phillips and Woessner, 2015) and have implicated TBI in the development of **post-**

traumatic stress disorder (Benedictus et al., 2010; Greenwald et al., 2012), **chronic traumatic encephalopathy (CTE)** (Goldstein and McKee, 2012; Saulle and Greenwald, 2012; McKee et al., 2009), epilepsy (Annegers et al., 1998; Ferguson et al., 2009; Frey, 2003), Parkinson's (Bower et al., 2003; Goldman et al., 2006), and Alzheimer's (Mortimer et al., 1985; Fleminger, 2003; Sivanandam and Thakur, 2012). In a real and significant sense it seems that TBI induces new neurological dysfunction, contributes to early age related dysfunction, or causes an overlaying condition resulting in early diagnoses of other neurological diseases. This is particularly concerning given a number of studies that have shown that repeated sub-concussive injuries can result in similar outcomes to discrete injuries.

1.2 Traumatic Brain Injury Pathophysiology

TBI consists of largely mechanically induced injuries that include a wide range of events varying from skull fractures and penetrating ballistic injury to whiplash and mid frequency vibration. The amplitude, timing, direction, and energy of the applied force relates directly to how and where mechanical stress is applied to the brain and where structural tissue damage results. As a result of the diverse sources of TBI, a number of broad categories have been developed to help divide the pathophysiology into more interpretable segments. Broad categories include whether the injury is focal or diffuse and whether the molecular processes are primary or secondary (Lovell et al., 1994; Granacher, 2008; Povlishock and Katz, 2005). Focal injury tends to be local to the propagating pressure wave that resulted after the injury and tends to be associated with gross tissue disruption and damage. Diffuse injury in contrast is characterized by a generalized stretch injury that causes wide disruption of tissue cytoskeletal elements and causes broad tissue level dysfunction by triggering necrotic and apoptotic cascades (Povlishock and Katz, 2005). An example is **diffuse axonal injury (DAI**) where shear induced damage to the

axolemma leads to inappropriate ion dysregulation and protease activity which impairs axonal transport and function (Povlishock and Katz, 2005). Primary injury is typified by the mechanical damage occurring at the moment of impact while the secondary insults are the downstream processes that result as the tissue attempts to recover (Werner and Engelhard, 2007).

1.2.1 Table 1-2: Categories of Neuropathological Damage

	Focal	Diffuse
Primary injury	Focal cortical contusion	Diffuse axonal injury
	Deep cerebral hemorrhage	Petechial white matter hemorrhage
	Extracerebral hemorrhage	
Secondary injury	Delayed neuronal injury	Delayed neuronal injury
	Microvascular injury	Microvascular injury
	Focal hypoxic-ischemic injury (HII)	Diffuse hypoxic-ischemic injury (HII)
	Herniation	Diffuse hypometabolism
	Regional and diffuse hypometabolism	

Table 2: *Categories of neuropathological damage.* Examples of different injury pathologies that can be experienced after Traumatic Brain Injury. Reproduced with permission from Povlishock & Katz, 2005.

An example of a classic generalizable focal injury is the whiplash related coup-contrecoup injury that typically occurs in a motor vehicle or sports setting. In this injury a rapid acceleration/deceleration event occurs (with or without striking an object), which generates focal brain injuries on opposite sides of the brain in the plane of motion as the brain bounces and rebounds off the interior of the cranium (Silver et al., 2011; Andriessen et al., 2010). Classically this occurs in a forward motion injury and results in injury to the frontal lobe and the occipital lobe on opposite sides of the brain. The focal injuries mentioned can include laceration, contusion, or hemorrhage of the tissue; the hemorrhage that develops demonstrates significant crossover with ischmia/reperfusion and hemorrhagic injury in stroke (Lin et al., 1993; del Zoppo and Hallenbeck, 2000; Chodobski et al., 2011; Mark and Davis, 2002).

In contrast, a classic diffuse injury occurs due to rapid shaking or rotation that induces large shear/stretch tensors in the tissue (*www.biausa.org*). Stretch injury results in **diffuse axonal injury (DAI)** (Strich, 1961; Gennarelli et al., 1982; Adams et al., 1991; Adams et al., 1989; Adams et al., 1982; Povlishock and Katz, 2005), which is a neuronal pathology characterized by axonal bulb swellings due to disrupted microtubules and impaired intracellular transport (Povlishock et al., 1983; Povlishock and Kontos, 1985). This process contemporaneously has been linked to focal alterations of the axolemma (Pettus et al., 1994; Maxwell et al., 1997). DAI is frequently associated with impaired neurological function in instances which lack focal injury; impaired axonal transport results can result in neuronal death, axonal degeneration, or simply deafferentation of the specific circuit leading to neurologic dysfunction. The process is mediated by the uncontrolled influx of extracellular ions (e.g. Ca^{2+}) which activate cysteine proteases, calpains, and caspases that in turn disrupt the cytoskeleton inhibiting axonal transport and thus axonal function (Buki et al., 2000; Buki et al., 1999).

Current therapies are largely focused on molecular pathobiology underlying the prolonged impairments seen in TBI with anti-inflammatory agents and a heavy dose of nootropics used to mask underlying deficits (Povlishock and Katz, 2005; Silver, 2012; Silver and Miller, 2004). A significant issue with attempting to treat TBI is the reality of pharmacopeia, which can efficiently mask underlying deficits; e.g., treating neurologic dysfunction with stimulants such as amphetamine improves patient outcome which doesn't necessarily correlate with recovery. There is a well-documented cascade of events that occurs after TBI including initial cell membrane permeability and the release of excitatory amino acids (e.g. glutamate, aspartate). This can cause neuroexcitation injury where extreme levels of neuronal firing lead to inappropriate and dysfunctional output. An important consequence of this cell damage and

excessive neuroexcitation is the widespread disruption of the **blood brain barrier (BBB)** and **neurovascular unit (NVU)**, which impairs trophic support and dynamic response to energy demand as well as the ability to expel cytotoxic materials efficiently. The result is an increased local vulnerability to neurotoxicity and disruptions in the typical distribution of injury-induced cytokines/chemokines (Farkas, 2006; Schmidt and Grady, 1993; Habgood et al., 2007).

1.2.2 Figure 1-1: Neurovascular Unit

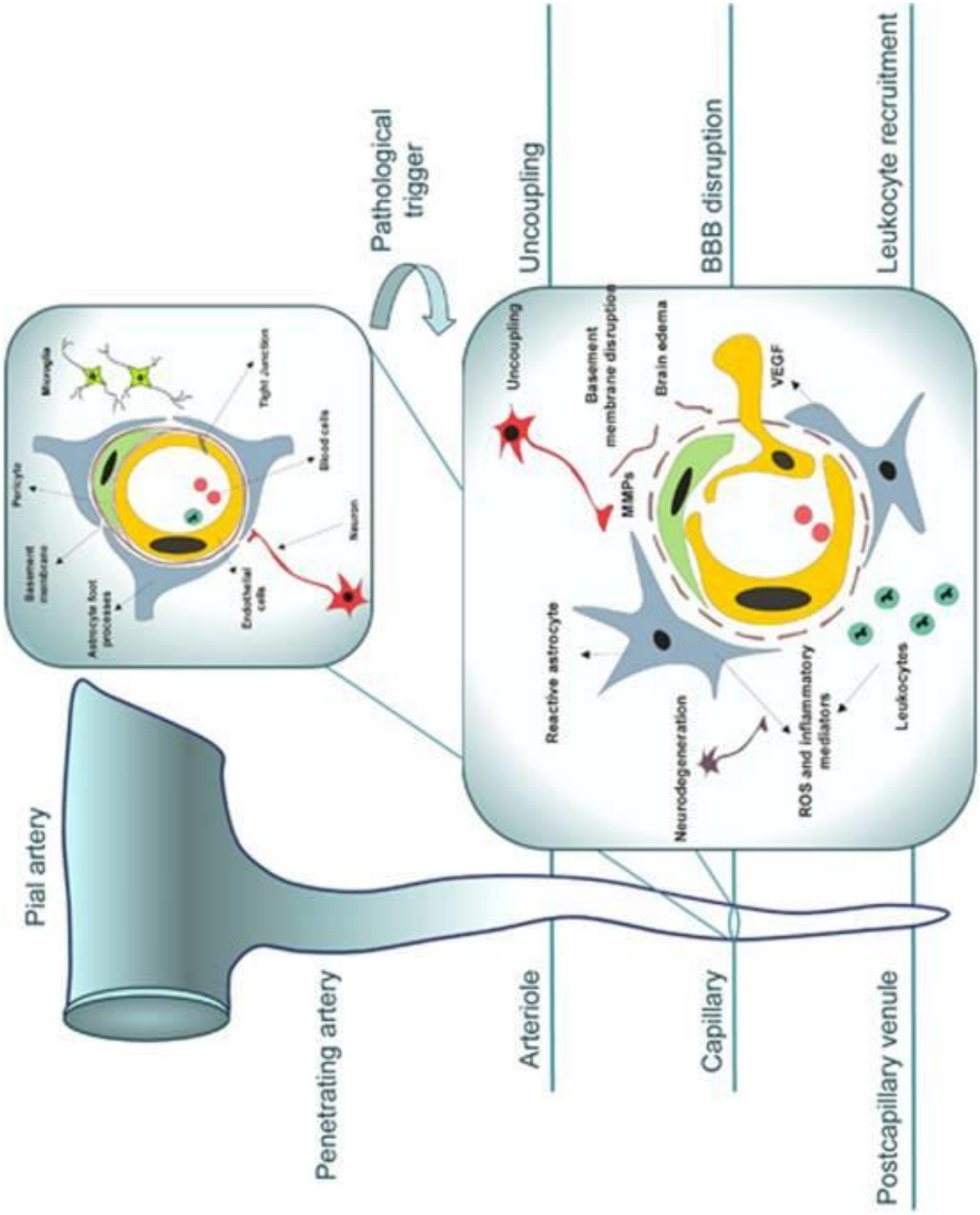

Figure 1-1: *Neurovascular unit (NVU) reorganization in response to pathogenic stimulus. Highly structured multicellular anatomy of the NVU (shown in the upper right inset) undergoes profound changes in response to pathogenic stimulus, such as tissue hypoxia, schematically shown in the lower inset. The subsequent 'sequence of events' leading to neuronal injury includes the expression and release of pro-angiogenic factors, such as vascular endothelial growth factor (VEGF), by astrocytes and surrounding cells and upregulation of their receptors in brain endothelial cells, stimulating endothelial proliferation and migration with consequent disruption of tight junctions and increased blood–brain barrier (BBB) permeability. Release of metaloproteases by migrating endothelial cells and pericytes leads to proteolytic disruption of the basement membrane and additional release of pro-angiogenic breakdown products of the extracellular matrix. Accompanying influx of serum proteins and water through disrupted BBB results in vasogenic edema, which further disconnects cellular interactions within the NVU; toxic serum components cause astrocyte activation. Upregulation and secretion of inflammatory mediators from both activated astrocytes and endothelial cells stimulates the expression of adhesion molecules in endothelial cells and the recruitment of inflammatory cells into the brain. Reactive oxygen species and proteases released from leukocytes and activated perivascular cells cause oxidative injury to neurons. Secondary injury to neurons, if prolonged or repeated, could cause dissociation of neuronal projections from the NVU, uncoupling and subsequent retrograde degeneration. Some of the described events and their manifestation occur at specific sites of the brain microcirculatory tree: uncoupling at the level of arterioles, BBB disruption at the level of capillaries, and leukocyte recruitment at the level of postcapillary venules.* Reproduced with permission from Stanimirovic & Friedman, 2012.

In a functional sense, the NVU can be considered to be the critical component of the vascular/brain interface that supports the BBB and its selective trophic support to the brain parenchyma. The NVU (Figure 1-1) typically consists of endothelial cells linked by numerous tight junction proteins which are non-fenestrated, wrapped with cytoplasm of associated pericytes and covered by an **extracellular matrix (ECM)** basal lamina (comprised primarily of type IV collagen). These in turn are wrapped by astrocytic end feet which are in direct contact with adjacent neurons with the whole system monitored by immune cells on both sides of the barrier. This setup provides a consistent steady state environment for efficient neuronal function and is resistant to rapid transient variance in peripheral conditions. The corollary, however, is that disruption of any one component can lead to neuronal dysfunction. This can range from gross mechanical tissue disruption, where the NVU is physically torn apart, to instances of basal lamina breakdown due to excess gelatinase activity or to the effects of inflammatory cytokines. It is known that TBI can induce each of these responses. Of course, TBI vascular injury is associated with the disruption of the NVU, but the analysis of post-injury vascular damage is more typically made with reference to large global effects on brain circulation rather than individual effects on the cells positioned at the brain/parenchyma interface. Chief among the negative components of such global vascular injury (ignoring gross tissue disruption) is the loss of vascular autoregulation which leads to inappropriate vasospasm and inefficient trophic support. Numerous authors have demonstrated this impaired microcirculation in a variety of traumatic **central nervous system (CNS)** models (Lin et al., 2001; Kenney et al., 2016; Bartnik-Olson et al., 2014; Baranova et al., 2008; Park et al., 2009b; Gao et al., 2010; Wei et al., 2009; Cherian et al., 2011). **Central Fluid Percussion Injury (cFPI**) models in particular have shown microvascular losses through 2 weeks after injury (Schwarzmaier et al., 2010).

1.3 Molecular Mechanisms of Injury

Focal brain injury sets in motion a series of events following the initial insult, a pattern that has been reasonably well studied both in vivo and in vitro. There is tissue wide damage which affects not only neurons but all of the glial and vascular components supporting those neurons, as well as the ground substance which enmeshes the tissue. Frank membrane disruption occurs in a small number of cells, lysing and releasing cytosolic contents into the surrounding tissue, which exposes cell organelles to the extracellular environment. Many of the molecules released induce modulators of cell signaling including chemokines and cytokines which are also intimately involved in the stabilization of the NVU. Their release leads to extensive disruption of cerebral blood flow and oncotic dysregulation, leading to both impaired O_2/CO_2 exchange and increased **intracranial pressure (ICP)**.

Following TBI, primary mechanical disruption of the neuronal membrane results in uncontrolled pre-synaptic depolarization causing excessive release of **excitatory amino acids** (**EAA**, e.g. glutamate, aspartate) leading to neuroexcitatory impairments (Hayes et al., 1992; Yoshino et al., 1992; Palmer et al., 1993). The excitation hypothesis was first proposed by Rothman and Olney based on the observed neurotoxic potential of glutamate acting on **N-methyl-D-aspartate (NMDA)** receptors (Rothman and Olney, 1987; Bullock et al., 1998). This process occurs in conjunction with membrane ionic dysregulation, another pathophysiologic condition which can occur for a variety of reasons, but directly leads to impaired cellular function and neuronal signaling. It may follow neuronal cell membrane disruption, but can also result from glial cell insult where supporting astrocytes ineffectively recycle neurotransmitters or inappropriately release calcium into the extracellular space. Effects of this pathology are manifest as damaged neuronal membranes and altered extracellular ionic gradients, often

characterized by rapid increases in extracellular EAA's (Faden et al., 1989; Hayes et al., 1992). The classic hypothesis of increased EAA receptor activation centers around a two phase process driven by ionic gradient dysregulation. In the first phase Na^+ and Cl^- gradients aberrantly fall leading to osmotic swelling and occasional cell death. The second phase is more cell directed and involves Ca^{2+} dependent cell degeneration driven by induced downstream neurotoxic cascades triggering cell death responses (Arundine and Tymianski 2004). Excess transmitter release leads to excessive activation of excitatory receptors (e.g. NMDA) causing dramatic post-synaptic intracellular shifts in Na^+, K^+, Ca^{2+} ions (McIntosh, 1994; Katayama et al., 1990; Hayes et al., 1992; Wolf et al., 2001). This excessive neuroexcitation has been identified as a significant contributor to post-injury functional impairments. Interestingly, it has been reported that mechanical cell deformation in isolation is sufficient to induce altered glutamate receptor function (Zhang et al., 1996). Early studies with experimental animal models of TBI have demonstrated excessive EAA release in the hippocampus, with later reports showing that selective receptor blockade can mitigate long term cognitive deficits (Gorman et al., 1989; Katayama et al., 1989; Hayes et al., 1986; Lyeth et al., 1988). Notably, the excessive release of transmitters has been identified as being exacerbated by the breakdown in the BBB that occurs after injury.

Towards identifying this as a root cause of continued impairment, both dopamine and NMDA antagonists have been used in animal studies to help elucidate the mechanism of impairment (Zhu et al., 2000; Massucci et al., 2004; Wagner et al., 2005; Faden et al., 1989; Hayes et al., 1992; Hamm et al., 1993; Phillips et al., 1998; Bales et al., 2009). NMDA antagonist therapies in animal models have demonstrated therapeutic efficacy but, as is unfortunately typical in TBI translational therapies to date, clinical trials have had disappointing

results (Muir, 2006); to some extent this may be due to greater complexity of human injury or simply the less controlled nature of injury relative to animal models. Dopamine agonists have also been tested therapeutically, with promising experimental results in animal models (Dixon et al., 1999; Kline et al., 2004; Wagner et al., 2005; Wagner et al., 2007), as have serotoninergic receptor agonists (Cheng et al., 2008; Olsen et al., 2012) and stimulation of GABA receptors (O'Dell et al., 2000), but each continue to show disappointing clinical results (Levin and Diaz-Arrastia, 2015; Warden et al., 2006). Thus, pharmacologic targeting of specific mechanisms has the potential to improve outcome following human TBI, but it seems abundantly obvious from the current history of clinical failures that treating TBI as a mono-factorial condition, with a single primary driving pathology, is unlikely to prove fruitful.

As discussed above, one hallmark of diffuse TBI models is the generation of DAI, where a significant portion of the axon pathology is restricted to the long axons of white matter tracts. It has been demonstrated that, even in the absence of l**oss of consciousness (LOC)**, **mild TBI (mTBI)** can induce diffuse axonal injury (Browne et al., 2011), result in long term cognitive impairment (Molgaard et al., 1990; Susan L. Hillier, 1997; Asikainen et al., 1998), and increase risk of developing neurodegenerative conditions (Graves et al., 1990; Fleminger, 2003). Due to the long term ramifications of tract disruption, DAI has been a much targeted research focus to identify imaging or circulating biomarkers to aid in TBI diagnosis and ultimately treatment (Smith et al., 2013). DAI has been described as being a result of acceleration-deceleration causing shearing of tissue layers with long anisotropic axons being particularly vulnerable compared to the more isotropic dendritic structures (Gennarelli et al., 1982; Meaney et al., 1995; Smith et al., 1997; Smith and Meaney, 2000). Beyond primary mechanical disruption of the cell membrane there are numerous secondary neurodegenerative effects directly tied to initial

disruption of axons, including deafferentation, neuronal death, and ECM breakdown. Some neurons will experience mechanoporation of their axonal membrane mediated by a breakdown in axonal transport proximal to cytoskeletal disruption. As noted above, rapid acceleration/deceleration events mechanically deform long axons which, due to their cytoskeletal structure, are selectively vulnerable to out of axis shear stress. This DAI is characterized by local axonal swellings described as 'beads on a string', which occur most frequently in (but not limited to) white matter tracts including the corpus callosum, parasagittal white matter, internal capsule, and thalamus (Adams et al., 1989; Adams et al., 1991; Graham et al., 1995; Gultekin and Smith, 1994; Vascak et al., 2017). Much of the observed histological change can be attributed to a breakdown in axonal transport dynamics. **Amyloid precursor protein (APP)**, which pools as a result of local disruption of anterograde axonal transport, is considered the gold standard in identifying DAI or more specifically, **traumatic axonal injury** (Povlishock et al., 1992; Povlishock and Christman, 1995). After TBI, APP has been primarily associated with two forms of TAI pathology: retraction balls in disconnected axons, and varicosities in intact axons (Adams et al., 1989; Smith and Meaney, 2000; Povlishock et al., 1983; Povlishock and Kontos, 1985; Povlishock and Becker, 1985; Povlishock and Katz, 2005). These axon varicosities can develop into reactive axonal swellings within a few hours after injury, enlarging through at least 2d post injury. This process leads to severe ionic imbalance, Ca^{2+} influx and mechanical failure of the axon cytoskeleton. The result is a sealed off distal end of the axonal swelling and development of the characteristic axon retraction balls (Povlishock et al., 1983; Povlishock and Becker, 1985; Povlishock and Kontos, 1985; Povlishock et al., 1992; Povlishock and Katz, 2005). The axon segment distal to the retraction ball undergoes Wallerian degeneration, a semi-controlled 'apoptosis', leading to complete axotomy (Povlishock et al., 1992; Povlishock, 1992;

Povlishock and Pettus, 1996; Kelley et al., 2006; Büki and Povlishock, 2006). A consequence of this axotomy is the eventual atrophy of the presynaptic terminal, dissociation of the synaptic junction and deafferentation (Grady et al., 1989; Steward, 1989; Erb and Povlishock, 1991). Together, these secondary pathologies affecting membrane and axon integrity have been observed in a wide variety of brain regions both post experimentally and post mortem (Povlishock, 1992; Povlishock and Katz, 2005).

TBI has also been shown to induce cell death among susceptible populations, although with a wide range of intensity, depending on specific injury or model used. Certain brain regions have been identified as being particularly vulnerable to cell death – largely white matter or cortical structures including the hippocampus, neocortex, as well as the cerebellum, and thalamus (Ross et al., 1993; Kotapka et al., 1992; Adams et al., 1985). Animal models have demonstrated neurodegeneration as early as minutes to hours after insult and it is easy to recognize that grossly damaged cells with disrupted membrane integrity rapidly necrose (Sutton et al., 1993; Dietrich et al., 1994; Hicks et al., 1996). Ultrastructural analysis of dying neurons due to secondary insult has also been examined by Dietrich and colleagues, demonstrating neuronal profiles with pyknotic nuclei, swollen mitochondria, vacuolated cytoplasm, and disrupted membranes (Dietrich et al., 1994). This cell loss due to secondary insult is particularly robust in the peri-injury region surrounding a focal lesion, as well as with diffuse TBI. It has been demonstrated in the same injury-susceptible regions seen histologically, including the neocortex, hippocampus, **dentate gyrus (DG)**, thalamus, and caudate/putamen (Farkas and Povlishock, 2007). In each case, high vulnerability is likely due to the structural nature of the fiber tracts involved, proximity to the applied injury, or unique anatomical location that results in particularly damaging strain responses. Regardless of brain region, both apoptotic and necrotic

mechanisms of cell death are represented after TBI (Raghupathi et al., 2002; Portera-Cailliau et al., 1997; Nicotera et al., 1999b; Nicotera et al., 1999a). That being said, injury severity is probabilistic in these vulnerable brain regions, with apoptosis predominating for both mTBI and ischemic injury (Raghupathi et al., 2002; Du et al., 1996), while moderate and severe TBI demonstrating increased levels of necrotic cell death (Conti et al., 1998; Newcomb et al., 1999a; Newcomb et al., 1999b). While TBI-induced cell death is often an acute process it has also been observed as a chronic, delayed neurodegenerative event (Hicks et al., 1996; Conti et al., 1998). Finally, it is important to note that while post-injury damage and death of neuronal populations are well established, the majority of affected neurons in the injured brain do not die, and remain capable of recovery after some period of time. This regenerative potential is an active area of TBI research with some investigators identifying the onset of the regenerative process at the time of initial axon disconnection from the synapse due to axonal swelling (Pettus et al., 1994; Maxwell et al., 1997; Stone et al., 2004).

From a cellular perspective, much of the aforementioned TBI pathology might be linked with trauma-induced change in the NVU. For example, the same gross mechanical insult that damages axons also damages other anisotropic structures such as small intra-parenchymal vessels and capillaries. Under normal circumstances the brain vasculature is a tightly controlled structure that effectively permits the highly selective movement of certain metabolic and trophic support molecules into the brain, while screening out many unwanted blood constituents. Historically, this led to the concept of the brain as an ‘immune-privileged’ organ, and while this view may no longer be fully accurate (Ransohoff and Brown, 2012), it is true that the brain vasculature, NVU and BBB comprise an efficient structure, highly susceptible to insult within any single component. After TBI, mechanical uncoupling of the NVU leads directly to the

movement of blood into the surrounding brain tissue, resulting in the release of red blood cell heme and the activation of pathways responsible for recycling free iron. This process disrupts critical metabolic support to affected neurons. Importantly, NVU damage also increases the molecular signals stimulating local reactive neuroglia to increase their production and release of pro inflammatory cytokines, leading to the breakdown of adjacent extracellular matrix supporting injured neurons. In tandem, NVU disruption and BBB opening disrupts ionic gradients in the local neuronal environment, further contributing to axon membrane damage, deafferentation, cell death and major circuit dysfunction.

1.4 NVU and Inflammatory Response

Mechanisms that underpin NVU disruption are not well understood, but it is clear that a combination of mechanical disruption, flow abnormalities, nitric oxide mediated vasodilation, and inflammatory cytokines all play a role in loosening the tight junctions that normally compartmentalize the vascular constituents from the brain parenchyma (Janigro et al., 1994; Kobari et al., 1994; Cobbs et al., 1997; Lu et al., 2001; Kenney et al., 2016). The resulting disruption impairs the stability of the neurochemical environment leading to highly variable functional changes in specific cellular populations (Saunders et al., 1999; Habgood et al., 2007). When functioning properly the NVU has numerous intercellular tight junctions between endothelial cells and the small capillaries are wrapped by pericytes and astrocytic end feet preventing the transmission of large molecules and the relatively selective uptake of contents into the astroglia rather than into the brains extracellular space (Ek et al., 2003; Ek et al., 2006; Kenney et al., 2016). Following injury this carefully ordered structure is disrupted and large (potentially toxic) molecules are able to enter the CNS impairing normal functions (Habgood et al., 2007). This is easily characterized in animal models and post mortem tissue by staining for

albumin – a large protein involved in the conjugation and trafficking of waste products which is normally partitioned into the intravascular space. This can drastically affect the post-injury change in oncotic pressure of the capillary beds resulting in local tissue swelling and an increase in ICP.

The resident immune cells of the CNS (astroglia and microglia) are capable of producing a robust immune response and releasing of associated cytokines (Ransohoff and Brown, 2012). These cells typically reside at or near the NVU structure. Each glial type also exemplifies a common immune and neural development function. As an example, microglia are involved in embryonic development and normal synaptic striping serving a phagocyte-like role (Bilimoria and Stevens, 2015; Fiske and Brunjes, 2000; Blinzinger and Kreutzberg, 1968; Kettenmann et al., 2013). Astroglia similarly are involved in synapse formation and secrete soluble signals that direct synaptogenesis and stabilize the resulting connections (Hughes et al., 2010; Ransohoff and Brown, 2012). These resident immune cells are notable for having distinct morphologies when immunologically active. While there are currently a large number of descriptors for microglia engaged in more specific activities, the cells can generally be described as resting or active. Resting microglia (synonymous with surveillant or ramified) possess small cell bodies with an abundant surrounding web of long fine process that actively sample and survey the environment. Activated microglia (or reactive) retract these processes, develop larger, rounded cell bodies and become more mobile. Activated microglia are further divided into two main categories; M1 (classically active) and M2 (alternatively active). The different subtypes predominate at different times post injury.

Classically active microglia (M1) are highly responsive to pro-inflammatory molecules including TNF-α and LPS and in turn produce further pro-inflammatory cytokines (Ponomarev

et al., 2007). Alternatively active microglia (M2) in contrast are responsive to anti-inflammatory molecules including IL-4 and IL-13 (Colton and Wilcock, 2010). Further, M2 microglia express proteins (including Arginase-1) involved in ECM repair and remodeling (Colton, 2009). Both types are activated after injury and are required to develop an appropriate immune response but they can become harmful if expressed excessively and chronically (Holmin and Mathiesen, 1999; Bartfai et al., 2007; Ramlackhansingh et al., 2011). Excessive microglial activation has been shown to decrease neurogenesis, be pro-apoptotic, and damage healthy neurons (Lazarini et al., 2012; Block and Hong, 2007; Block and Hong, 2005; Ponomarev et al., 2007). Further, reactive microglia have been linked to the induction and development of neurodegenerative disease states including MS (Correale, 2014) and inducing aberrant synaptic striping (Ziebell et al., 2015).

Similarly, astrocytes become reactive after injury and are characterized by cellular hypertrophy and increased expression of vimentin and glial fibrillary acidic protein (GFAP; (Herrmann et al., 2008). Astrocytes produce a different profile of secreted molecules after injury compared to microglia and they tend towards greater secretion of ECM molecules and growth factors (Zhao et al., 2004; Ransohoff and Brown, 2012). Astrocyte secreted Thrombospondins are key signals for synapse formation. They are more heavily involved local maintenance of nearby neurons and serve to buffer $[K^+]_e$, recycle glutamate, modulate blood flow, and secrete anti-inflammatory cytokines (e.g. IL-1; (Ransohoff and Brown, 2012). Astrocytes reduce the neurotoxic effect of excess glutamate (Schousboe et al., 2014; Schousboe and Waagepetersen, 2005; Kumar and Loane, 2012) and neuron dysfunction is exacerbated when astrocyte function is impaired (Myer et al., 2006). Excessive astrocyte reactivity has also been shown to be damaging,

and **knockout (KO)** mice lacking vimentin and GFAP have shown impaired recovery after CNS injury (Menet et al., 2003; Wilhelmsson et al., 2004).

As noted above, the disruption of the NVU allows blood constituents and brain specific proteins to bilaterally cross the barrier triggering an immediate, local inflammatory response (Morganti-Kossmann et al., 2001). Release of inflammatory cytokines from hemorrhagic sites within the injured area and through fenestration of the NVU barrier permits inflammatory cells, including neutrophils and other leukocytes, to infiltrate the brain parenchyma (Chodobski et al., 2011). These cells selectively migrate to damaged brain tissue, and in turn release further chemoattractants to recruit additional vascular cells (Bellander et al., 2001; Fluiter et al., 2014; Lozano et al., 2015). This feeds a recurrent cycle of cytokine and chemokine production to promote a sustained inflammatory response, further inducing barrier permeability (Chodobski et al., 2011). Local release of both cytokines and chemokines also induces endogenous glial activation which stimulates additional leukocyte recruitment, exacerbating NVU 'leakiness' (Ziebell and Morganti-Kossmann, 2010; Morganti-Kossmann et al., 2001; Kenney et al., 2016)(Ziebell and Morganti Kossman, 2010, Morganti Kossman 2001, Kenney 2016, Shlosberg 2010). Experimental models and clinical data have specifically identified tissue, CSF and blood elevations of both pro- and anti-inflammatory cytokines during the acute post-injury period (Hofman, 1989; Shohami et al., 1994; Breder et al., 1988; Spangelo et al., 1990; Frugier et al., 2010; Rothwell, 2000). Even diffuse injury models have shown cytokine/chemokine elevation within 6 hours post-injury, the 'acute phase' of response, which has been characterized by microglial activation near injured neurons (Kelley et al., 2007). Local glia have been shown to be heavily involved in both monitoring the injured environment and secreting cytokines/chemokines (Singhal et al., 2002; Cederberg and SiesjÃ¶, 2009).

Pro-inflammatory cytokines induced by TBI include not only TNF-α (an acute phase regulator of inflammation; (Hofman, 1989; Shohami et al., 1994), but also IL-1β (a human pyrogen; (Rothwell and Luheshi, 2000), IL-6 (pyrogen secreted by macrophages after trauma or burn injury; (Breder et al., 1988; Frugier et al., 2010), IL-12 (a T-cell stimulating factor; (Stahel et al., 1998), and IFN-γ (activator of macrophages and MHC II inducer; (Frugier et al., 2010; Lozano et al., 2015; Hernandez-Ontiveros et al., 2013). Interestingly, each of these cytokines can be linked to beneficial effects after peripheral trauma or infection but their sustained elevation may be harmful and maladaptive, particularly within the brain. For example, it has been shown that TNF-α inhibition does not improve long term neurocognitive outcomes after TBI, while IL-6 suppression impairs recovery (Penkowa et al., 2000; Scherbel et al., 1999; Sullivan et al., 1999). This well-established immune response from systemic cytokines is also supported by the fact that other brain expressed molecules can function as local cytokines, e.g. osteopontin (Shin et al., 2012). The overall effect of these cytokines is to further increase the targeting of both peripheral and resident immune cells to areas of injury.

As is typical for many other organ systems, there is mixed evidence for the role of inflammation after TBI, particularly in regards to extent and timing (Correale and Villa, 2004; Lucas et al., 2006; Shohami, 1999; Morganti-Kossmann et al., 2002). Cytokines in particular have been identified as having both neurotoxic and neuroprotective effects (Morganti-Kossmann et al., 2007). To a significant extent, this dual role is commonly observed in multiple peripheral traumatic responses although the potential for deleterious outcomes is amplified in CNS injury. Early inflammation is linked to the release of potentially toxic cytosolic contents into the extracellular space. This triggers a number of responses some of which involve the generation of reactive oxygen species (ROS) and **nitric oxide (NO)** by the surrounding tissue and is supported

by resident microglia and astroglia that monitor and maintain the extracellular space (Juliet et al., 2008; Singhal et al., 2002; Cederberg and SiesjÃ¶, 2009). A number of studies have examined the effects of attenuating specific portions of this acute phase inflammatory response, reporting improvements in post-TBI outcomes. Several pro-inflammatory molecules have been targeted including IL-1, IL-1 receptor, TNF-alpha and S-nitrosoglutathione. For example, IL-1 exacerbates neuronal injury (Rothwell, 1999) and treatment with an IL-1R antagonist improves post TBI outcome (Relton and Rothwell, 1992; Loddick and Rothwell, 1996; Tehranian et al., 2002; Lucas et al., 2006). Further, inhibiting elevated TNF-alpha levels improves post TBI outcome (Shohami et al., 1997), and exposure to S-glutathione shows increased repair and protection after TBI (Khan et al., 2011). By contrast, a number of pharmacologic studies that have targeted post-injury elevation of IL-6 (Penkowa et al., 2000) and IL-10 (Knoblach and Faden, 1998; Kremlev and Palmer, 2005) report improved outcome following TBI. Since management of inflammation has long been considered a possible means to foster the post-injury neuroplasticity underlying this improved outcome, several TBI studies have focused on the interaction between inflammation, extracellular environment and successful neuroplasticity.

1.5 Neuroplasticity and the Extracellular Environment after TBI

While historically the CNS was considered a hard-wired and permanent structure in adulthood, neural plasticity and modest regeneration in mature systems has become an accepted theory (Hebb, 1950; Keyvani and Schallert, 2002). Plasticity has been observed in nearly every form of traumatic neural injury studied, demonstrating the CNS is a plastic structure after injury including in the spinal cord (Liu, 1958), hindbrain/midbrain (Goodman and Horel, 1966), septal nuclei (Raisman, 1969), superior colliculus (Lund and Lund, 1971), the hippocampus (Steward, 1976; Lynch et al., 1976; Scheff et al., 1977; Christman et al., 1997; Hulsebosch et al., 1998;

Harris et al., 2010), and the neocortex (Bashir et al., 2012; D'Amato and Hicks, 1978; Levin et al., 1994).

In addition to the previously described immunological cascades that occur after injury there are also well defined phases of local ECM degradation and recovery which are directly associated with restored neuronal function. Generally, recovery appears to be mediated through the interactions of cytoskeletal proteins and the ECM mediated by **cell adhesion molecules (CAMs)**, **Matrix Metalloproteinases (MMPs**), and growth factors, each of which correlates with separation of neuronal connections and their reintegration for cell/tissue stability after injury. Of particular note is the stability requirements of dendritic and somatic synaptic contacts which begin to dysregulate and separate when tissue stability is lost (Levy et al., 2014). Animal models and human patients each demonstrate specific cellular and synaptic dysfunction following injury (Cotman et al., 1977; Nadler and Cotman, 1978; Grady et al., 1989; Steward, 1989; Phillips and Reeves, 2001). Because neocortex, cerebellum, thalamus, and hippocampus regions are susceptible to brain injury, and are easily injured and dissected for study in rodent models, these animal models of synaptic deafferentation have been able to effectively document time dependent stages of synaptic recovery (Adams et al., 1985; Kotapka et al., 1992; Ross et al., 1993; Loesche and Steward, 1977).

1.5.1 Figure 1-2: Reactive Synaptogenesis

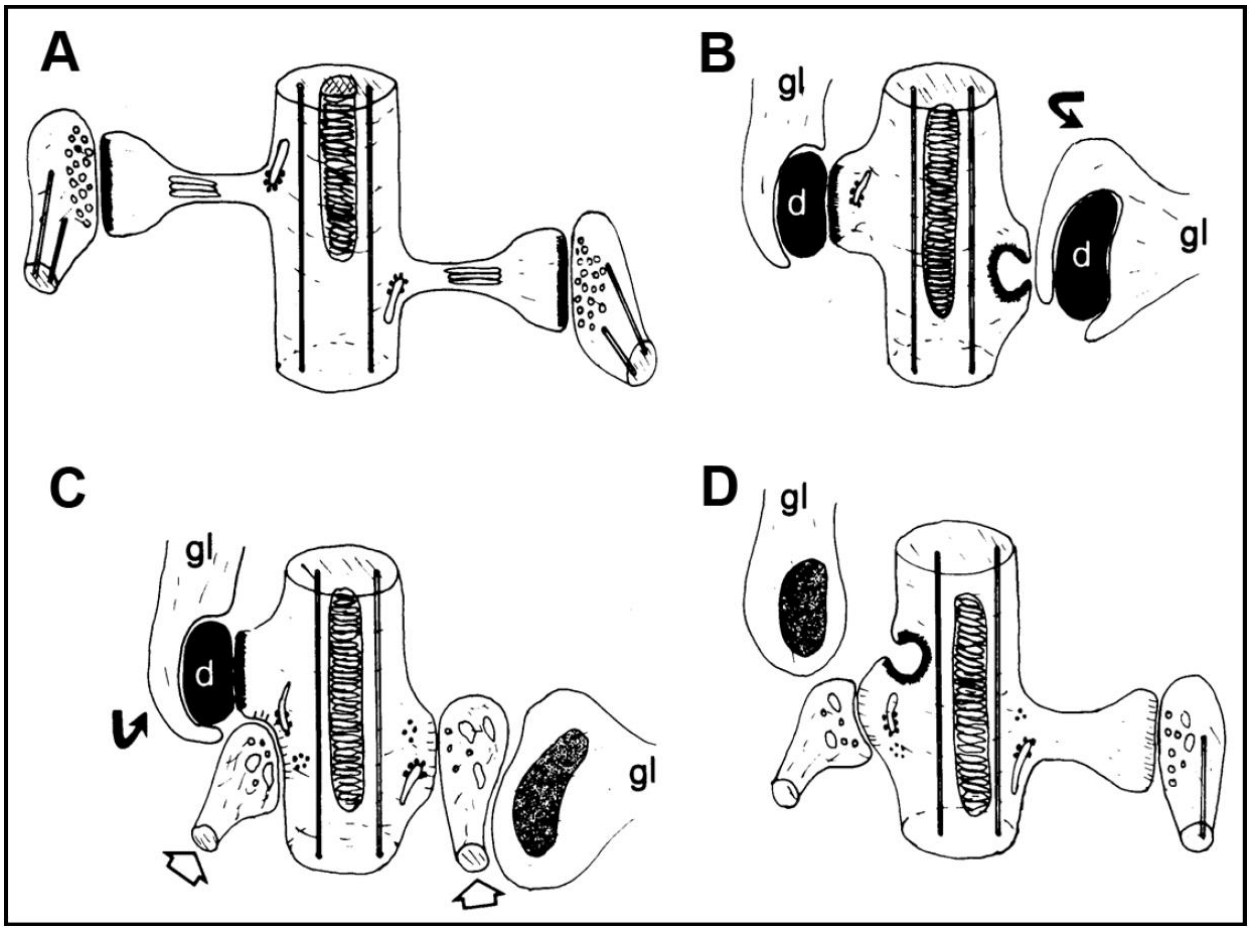

Figure 1-2**:** *Stages of Reactive Synaptogenesis. Following deafferentation normal synapses (A) first undergo a degenerative phase (1-5d postinjury; B) characterized by reactive glia (gl) which remove degenerating terminals (d). Next, synapses enter the regenerative phase (6-15d postinjury; C) where sprouting of new axons occurs (arrows) before maturing during stabilization (15d+ postinjury; D)* Reproduced with permission from Steward et al., 1988.

TBI induces axotomy and loss of presynaptic input, followed by the plasticity of reinnervation. Synaptogenesis is the formation of new synapses among neurons and is a normal process occurring during embryonic development. It has been shown that local synaptic plasticity and synaptogenesis occurs in response to trauma, much as it does during loss and re-emergence of **long term potentiation (LTP)** and **long term depression (LTD)** metrics (Miyazaki et al., 1992; Reeves et al., 1995)**.** DAI has been shown similarly to drive plasticity (Grady et al., 1989; Levin, 1995; Povlishock et al., 1992) in a process guided by glia, matrix proteins, and secreted growth factors. The term 'reactive' synaptogenesis describes the process where a previously established synapse has been damaged or lost and the reorganization /regeneration occurs over time, divided into distinct degenerative, regenerative, and stability phases (1-5days, 6-15 days and 15+ days respectively; see **Figure 1-2**). A number of animal models have been developed to focus on reactive synaptogenesis and have made frequent use of the hippocampus as a model brain structure with well-characterized synaptic reorganization. An example is the **unilateral entorhinal cortex lesion (UEC)** model developed by Steward 1979 which involves lesioning the entorhinal cortex on one side. Since the majority of EC input targets ispilateral dentate gyrus via the perforant path, such lesions predominantly deafferent the hippocampus of one hemisphere to induce unilateral reactive synaptogenesis. Between1-5 days after injury degeneration and clearance of debris predominates: axon terminals die and retract; cellular debris is removed by phagocytic cells. At 6-15 days after injury new axon terminals appear as collateral sprouts of intact non EC projections and reinnervation of the deafferented tissue begins (Lynch et al., 1976; Steward, 1976; Deller et al., 2007; Frotscher et al., 1997). By 15+ days after injury, the deafferented zone shows continued stabilization of newly formed synapses as they mature and functionally strengthen (Steward and Vinsant, 1983). This process

has been identified in many other brain tissues and while the cellular events proceed in a similar order the time course may shift, as in the **olfactory bulb (OB)** (Graziadei et al., 1978; Graziadei et al., 1979) and neocortex (Stroemer et al., 1995).

It is known that reactive synaptogenesis occurs in response to a variety of brain insults and including those resulting from effects of DAI and diffuse injury in general. Since these is much evidence to suggest that hemorrhage is sufficient to cause injury and reactive synaptogenesis (e.g. it is the basis for **subarachnoid hemorrhage (SAH)** animal models) and TBI models generate varied degrees of brain hemorrhage, it is clear that perturbations of the NVU play a role in the process of post-injury neuroplasticity. The most direct connection between NVU and this plasticity lies in the role of reactive glia. It has been observed that the supporting glia drive the process of post-injury synaptogenesis. Microglia become reactive and migrate to the deinnervated zone within 24 hours after injury and peak in number around day 3 before returning to baseline conditions at day 8 (Cotman, 1999). Astrocytes similarly follow, peaking at day 4 and remaining active through day 14. Both are involved in clearing degenerated terminal and debris. Rate of synapse reformation correlates with rate of degenerated terminal clearance and persistent degeneration delays glial reactivity and sprouting (Steward, 1992). At sites of NVU disruption, highly reactive and mobile glia secrete a variety of injury-induced molecules into the brain matrix, including both thrombospondins, which regulate endothelial cell proliferation (Chamak et al., 1995; Moller et al., 1996; Christopherson et al., 2005) and matrix metalloproteinases (MMPs), that modify the cytoarchitecture of the brain parenchyma around the insult (Rosenberg, 1995; Phillips et al., 2014) .

Extracellular Matrix, Metalloproteinases and Neuroplasticity

The **extracellular matrix (ECM)** is the ground substance into which tissue is embedded and provides the external structure and organization to brain tissue with its numerous adhesion substrates that support growth, development, and maturation of synapses (Ruoslahti, 1996; Venstrom and Reichardt, 1993; Dityatev and Schachner, 2003). In a field dominated by studies of neural circuits and neuronal subpopulations, the CNS ECM has been described as being less organized than other organ systems, possibly as a result of the continuous remodeling necessary for a lifetime of ongoing neural plasticity (Pittman and Buettner, 1989; Romanic and Madri, 1994). The brain ECM does however contribute significantly to the structural stability of the brain and in doing so supports neuronal homeostasis and mediates the interactions of cellular components (Jones, 1996; Wee Yong et al., 1998). For example, integrin glycoproteins regulate the adhesion and cell signaling of neurons, glia, meningeal epithelium and endothelial cells in both cell-cell and cell-ECM interactions (Hynes, 1992; Milner and Campbell, 2002).

Just as ECM proteins play a major role in guiding and stabilizing synaptogenesis during development, effective ECM maintenance is also required for successful synaptic recovery following traumatic injury. A number of specific cell populations have been identified which interact with ECM to direct different phases of synaptic reorganization including microglia, astroglia, and olfactory ensheathing cells (Giulian et al., 1989; Chao et al., 1992; Bessis et al., 2007; Ekdahl et al., 2009; Christopherson et al., 2005; Barnett, 2004; Steward, 1989; Ullian, 2001). Microglial injury response not only involves the production and release of cytokines, but also generation of MMPs and proteoglycans in an effort to recruit additional macrophages, debride damaged tissue and stabilize remaining viable tissue (Hanisch, 2002; Gottschall and Yu, 1995; Gottschall et al., 1995; Yokoyama et al., 2006). This microglial action facilitates in

reshaping the ECM during the acute degenerative phase (John et al., 2003; Ethell and Ethell, 2007). Astrocytes are also responsive after injury and take on a reactive form which secretes growth factors and MMPs (Goss et al., 1998; Madathil et al., 2013; Wells et al., 1996; Muir et al., 2002), molecules which stimulate neurite growth and modify local environment to permit sprouting of terminals during the synapse regenerative phase (Falo et al., 2008; Warren et al., 2012).

These participant MMPs are a family of secreted divalent cation (Zn^{2+}/Ca^{2+}) activated proteolytic enzymes, best characterized by their ability to modify and degrade ECM during both normal physiologic and pathogenic conditions (Romanic and Madri, 1994; Asahi et al., 2001). This ability has broad ramifications at the tissue level and causes the modification in function of membrane receptors, adhesion molecules, and growth factors during developmental processes including embryonic development, wound healing, and angiogenesis (Van Hove et al., 2012; Verslegers et al., 2013). Most relevant to traumatic brain injury, glial and neuronal sourced MMPs may facilitate synaptic recovery after TBI through modification of the ECM (Wee Yong, 2010).

1.5.2 Table 1-3: MMPs and Their Classifications

Table 2
Matrix metalloproteinases and their domain composition

Enzyme	MMP	Chromosomal location (human)	Domain composition												
			SS	Pro	CS	RX[R/K]R	Cat	FN2	Lk 1	Hpx	Lk 2	TM	GPI	Cyt	CysR-Ig
Collagenases															
Insterstitial collagenase; Collagenase 1	MMP-1	11q22-q23	+	+	+	–	+	–	+	+					
Neutrophil collagenase; Collagenase 2	MMP-8	11q21-q22	+	+	+	–	+	–	+	+					
Collagenase 3	MMP-13	11q22.3	+	+	+	–	+	–	+	+					
Collagenase 4 (*Xenopus)*	MMP-18	Not found in humans	+	+	+	–	+	–	+	+					
Gelatinases															
Gelatinase A	MMP-2	16q13	+	+	+	–	+	+	+	+					
Gelatinase B	MMP-9	20q11.2-q13.1	+	+	+	–	+	+	+	+					
Stromelysins															
Stromelysin 1	MMP-3	11q23	+	+	+	–	+	–	+	+					
Stromelysin 2	MMP-10	11q22.3-q23	+	+	+	–	+	–	+	+					
Matrilysins															
Matrilysin 1	MMP-7	11q21-q22	+	+	+	–	+	–	–	–					
Matrilysin 2	MMP-26	11p15	+	+	+	–	+	–	–	–					
Stromelysin 3	MMP-11	22q11.2	(+)	(+)	+	+	+	–	+	+					
Membrane-type MMPs															
(A)Transmembrane type															
MT1-MMP	MMP-14	14q11-q12	+	+	+	+	+	–	+	+	+	+	–	+	
MT2-MMP	MMP-15	15q13-q21	+	+	+	+	+	–	+	+	+	+	–	+	
MT3-MMP	MMP-16	8q21	+	+	+	+	+	–	+	+	+	+	–	+	
MT5-MMP	MMP-24	20q11.2	+	+	+	+	+	–	+	+	+	+	–	+	
(B) GPI-anchored															
MT4-MMP	MMP-17	12q24.3	+	+	+	+	+	–	+	+	+	–	+	–	
MT6-MMP	MMP-25	16p13.3	+	+	+	+	+	–	+	+	+	–	+	–	
Others															
Macrophage elastase	MMP-12	11q22.2-q22.3	+	+	+	–	+	–	+	+					
–	MMP-19	12q14	+	+	+	–	+	–	+	+					
Enamelysin	MMP-20	11q22.3	+	+	+	–	+	–	+	+					
–	MMP-21		+	+	+	+	+	–	+	+					
CA-MMP	MMP-23	1p36.3	+	+	–	+	+	–	–	–	–	–	–	–	+
–	MMP-27	11q24	+	+	+	–	+	–	+	+					
Epilysin	MMP-28	17q21.1	+	+	+	+	+	–	+	+					

Groups of MMPs are listed with their trivial names and chromosomal location. SS, signal peptide; Pro, pro-domain; CS, cysteine switch motif; RX[R/K]R, proprotein convertase recognition sequence; FN2, fibronectin type II motif; LK, linker; TM, transmembrane domain; GPI, glycosylphophatidylinositol anchoring sequence; Cyt, cytoplasmic domain; CyR-Ig, cysteine rich and Ig domain.

Table 3: *Matrix metalloproteinases and their domain composition.* Reproduced with permission from Nagase et al., 2006.

MMPs are classified based on their primary substrates and whether they are secreted or membrane bound (see **Table 1-3, Figure 1-3**). These classes include collagenases, gelatinases, stromelysins, matrilysins, and **membrane-types (MT-MMPs)** (NAGASE et al., 2006). They all contain similar structural homology including a signaling peptide and a catalytic domain, and they are produced as inactive zymogens (pro-MMPs) which must be cleaved to expose the Zn^{2+}-cysteine bond at the catalytic site which characterizes the functionally active form (Van Wart and Birkedal-Hansen, 1990; Becker et al., 1995). MMPs are thus regulated via proteolytic activation, although they can also be regulated by post-translational modification, **tissue inhibitors of matrix metalloproteinases (TIMPs)**, and more indirectly by cell compartmentalization (Chakraborti et al., 2003; Baker, 2002).

MMPs have been well studied as effectors of reorganization of synaptic plasticity (Yong et al., 2001; Yong, 2005; Wlodarczyk et al., 2011; Dityatev and Schachner, 2003; Lo et al., 2002). They have been identified as influencing axonal growth, synaptic modification, and recovery after injury (Szklarczyk et al., 2002a; Vaillant, 2003; Fredrich and Illing, 2010; Yong et al., 2001; Dityatev and Schachner, 2003). These effects have largely been identified as being a result of glial reactivity and secretion (Oh et al., 1999; Giraudon et al., 1997; Sternlicht and Werb, 2001). Studies in our laboratory have connected aberrant MMP activity to disrupted synaptic reorganization post hippocampal deafferentation. These studies have indicated that membrane type 5 matrix metalloproteinase (MT5-MMP) and a disintigrin and metalloproteinase-10 (ADAM-10) are both capable of cleaving N-cadherin which is partially responsible for synaptic stabilization (Warren et al., 2012). Warren et al., 2012 showed that when contrasting models of adaptive and maladaptive plasticity, persistent ADAM-10 expression during maladaptive plasticity is correlated with attenuated N-cadherin production and ultimately

reduced functional recovery. MMP inhibition was further found to reduce ADAM-10, shifting the N-cadherin expression profile to one that begins to match the synaptic recovery profile. Other gelatinases (MMP-2, MMP-9) and stromelysins (MMP-3, MMP-10, MMP-11) have also been identified as critical to the pathophysiology of CNS injury. It is abundantly evident that the time dependent nature of MMP expression underlies successful vs unsuccessful recovery after injury. As an example, MMP-3 was found to disrupt the BBB/NVU and to promote injury via that mechanism (Rosenberg et al., 1998; Van Hove et al., 2012), while other studies have found MMP-3 to be associated with successful neuronal outgrowth following sciatic nerve crush injury (Demestre et al., 2004; Shubayev and Myers, 2004). Elevated MMP-9 has similarly been associated with both increased injury after TBI, as well as positive mediation of dendritic remodeling during LTP in in vitro models of learning and memory (Dziembowska and Wlodarczyk, 2012; Bozdagi et al., 2007).

1.5.3 Figure 1-3: Domain Structure of the MMP Family

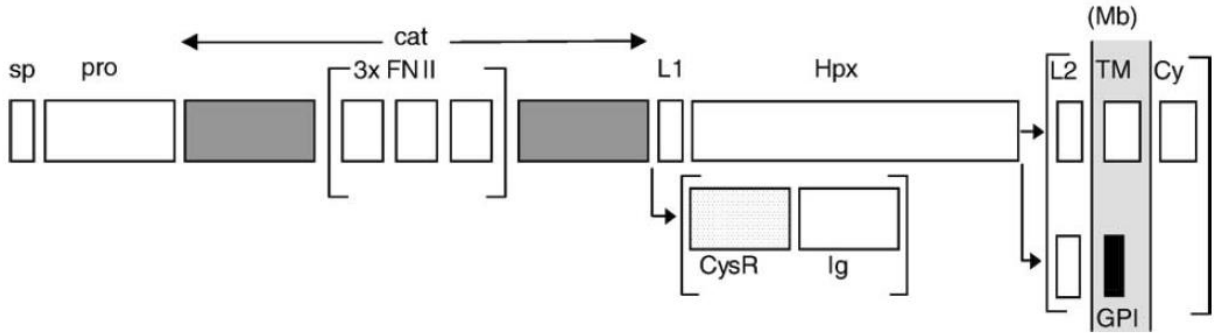

Figure 1-3: *Domain structures of the MMP family. See* Table 3 *for the domain arrangement for each MMP. Sp, signal sequence; pro, pro-domain; cat, catalytic domain, FNII, fibronectin type II motif; L1, linker 1; Hpx, hemopexin domain; L2, linker 2; Mb, plasma membrane; TM, transmembrane domain; Cy, cytoplasmic tail; CysR, cysteine rich; Ig, immunoglobulin domain; GPI, glycosylphosphatidilyinositol anchor.* Reproduced with permission from Nagase et al., 2006.

1.6 Gelatinases, NVU and TBI

Of the MMPs known to respond to brain injury, those that directly target the major components of basal lamina ECM are most relevant to NVU disruption after TBI. Collagen is one of the principal matrix proteins making up this basal lamina, which is degraded along with NVU breakdown. One MMP family consistently associated with this degradation is the gelatinases, MMP-2 (72 kDa, Gelatinase A), and MMP-9 (92 kDa, Gelatinase B). It should be noted that these enzymes target a form of collagen different from the animal derived collagen which, when irreversibly hydrolyzed, is used largely as a gelling thickening agent in food. Here we are referring largely to type IV collagen (a large precursor to culinary gelatin) which is the primary type of collagen within the extracellular matrix supporting the NUV, acting to stabilize vascular epithelium.

MMP-2 and MMP-9 have been extensively associated with a variety of physiologic and disease processes including blastocyst implantation, inflammatory disease, cancer, and cardiovascular disorders (Van den Steen et al., 2002; Stamenkovic, 2003; Klein and Bischoff, 2010). Their structure consists of a hemopexin domain and fibronectin repeats that are located upstream of the catalytic site (Handsley et al., 2005); **see again Figure 1-3**). Gelatinases have been identified as targets for modulation and treatment of TBI pathobiology because their elevated expression is linked to effective synaptic reorganization. Notably, neural development occurs in the presence of high levels of gelatinase mRNA, especially during the first postnatal week in vascular cell types including pericytes and endothelial cells (Ayoub et al., 2005; Planas

et al., 2001; Szklarczyk et al., 2002a) as well as in glial subpopulations: MMP-2 in astrocytes and MMP-9 in white matter tracts (Planas et al., 2001; Szklarczyk et al., 2002a).

Another important cell function supported by gelatinases in the developing CNS is the direction of tissue migration of **neural crest cells (NCCs)**, **neural stem cells (NSCs)**, neurons, and astrocytes (Perris and Perissinotto, 2000; Perris, 1997; Kazanis and ffrench-Constant, 2011; Barros et al., 2011). MMP9 inhibitors can impair migration of these NCC and NSC cells in avian and rodent embryonic models (Duong and Erickson, 2003; Ingraham et al., 2011). MMP-9 KO mice and in vitro assay models have shown altered granule cell migration (Vaillant, 2003; Ayoub et al., 2005) and MMP-2 positive pericytes are associated with vascular sprouting (Girolamo et al., 2004; Virgintino et al., 2007). Gelatinases are also highly expressed in dendrites; which is unsurprising given that a large number of their substrates are cytoskeletal components, growth factors, cell adhesion molecules, and axonal guidance receptors, and they have been linked to dendritic and axonal outgrowth (Tian et al., 2007; Gonthier et al., 2009; Saygili et al., 2010; Lin et al., 2008). Thus, gelatinases have the potential to direct CNS angiogenesis, including the establishment/maintenance of NVUs. These brain/vascular interfaces can, in turn, influence cell activation/migration after TBI, generating molecules which foster axonal outgrowth, myelination and synaptogenesis crucial for post-injury recovery. For example, MMP-9 influences emergence of LTP via regulating extracellular proteolysis and transmitter receptor tracking/activation at the recovering synapse (Bozdagi et al., 2007; Michaluk et al., 2009) . Further, MMP-9 mRNA has also been shown to be transported and activated during LTP (Sbai et al., 2008; Dziembowska and Wlodarczyk, 2012). Similarly, MMP-9 KO animals display altered hippocampal dependent function (Nagy, 2006; Meighan et al., 2006). Indeed, a number of studies have demonstrated increased MMP expression following CNS injury in both

experimental animal models and human trauma victims (Clark et al., 1997; Rosenberg et al., 1998; Heo et al., 1999). Overall, increased MMP expression correlates with increased damage, which is thought to occur as a result of widespread proteolysis and the disruption of the basal lamina (Rosenberg, 1995; Rosenberg et al., 1998; Wang, 2000; Gursoy-Ozdemir et al., 2004; Michaluk and Kaczmarek, 2007). Additional studies have linked gelatinases to modulation of growth factors and inflammatory cytokines (Rosell and Lo, 2008; Gottschall and Yu, 1995; Giraudon et al., 1997). MMP-9 is considered the gelatinase most responsible for this effect since studies with MMP-2 KO mice did not show reduce injury pathology (Asahi et al., 2001), while loss of MMP-9 was protective against ischemia and TBI (Asahi et al., 2000b; Wang, 2000). Such protection was posited to be through increased BBB/NVU integrity in the absence of MMP-9 (Conant and Gottschall, 2005; Gidday, 2005) (Conant and Gottschall 2005, Gidday 2005). Together, these data would argue that loss of NVU integrity is a primary TBI pathobiology and point to the critical role of tissue response pathways activated by local hemorrhage at the breeched NVU. One of the most important first responders to this breech is inducible Heme Oxygenase 1 (HO-1).

1.7 Heme Oxygenase

1.7.1 Discovery, Structure, Biological Role

Heme Oxygenase (HO) enzymes were initially discovered in 1968 and were largely characterized as endoplasmic reticulum proteins due to their presence in microsomal fractions of tissue homogenate (Ishikawa et al., 1991; Yoshida et al., 1988; Shibahara et al., 1989). Since that time HO-1 has been identified as containing a hydrophobic terminal domain segment more suggestive of membrane compartmentalization (Ishikawa et al., 1991; Shibahara et al., 1985; Yoshida et al., 1988). The overall structure of HO-1 is a flexible bi-helical protein structure that

surrounds a central heme pocket (Lad et al., 2003; Schuller et al., 1999). A widely conserved histidine imidazole functions as a heme iron ligand which is stabilized by two distal glycine residues. A 32 kDa inducible protein, HO-1 is homologically similar to **heme oxygenase 2 (HO-2)**, a 36 kDa constituently expressed protein.

HO-1 and HO-2 both catalyze identical biochemical reactions. They are the canonical enzymes that reduce molecular heme into biliverdin-IXa and though they have similar substrate specificity and cofactor requirements they have different kinetic properties with K_m values of 0.24 and 0.67 uM respectively among other physical differences (Maines, 1992; Maines et al., 1986; Trakshel et al., 1986). A low Km indicates the enzyme requires only a small amount of substrate to saturate and maximal velocity is reached at low substrate concentrations; a high Km requires high substrate concentration to achieve maximal reaction volume. The substrate of an enzyme with lowest Km is assumed to be the native substrate.

The primary biological role of HO is to reduce heme from senescent erythrocytes, hemorrhage, or cytochrome enzymes (Tenhunen et al., 1969; Tenhunen et al., 1970; Pimstone et al., 1971b; Pimstone et al., 1971a). It has been identified that HO-1 is highly upregulated during inflammatory wound processes and responds to a variety of inflammatory and pro-oxidant stimuli (Ryter et al., 2006; Chang et al., 2005). Despite the name, it is known that HO-1 is the primary driving force behind erythrocyte related heme degradation both normally and pathologically. While KO of HO-1 or HO-2 are viable, HO-1 KO animals experience impaired wound healing and some degree of hemochromatosis despite elevated HO-2 throughout the tissue, a phenotype observed in a human case report of an individual with HO-1 deficiency (Poss and Tonegawa, 1997a; Poss and Tonegawa, 1997b; Kawashima et al., 2002; Yachie et al., 1999). HO-2 KOs in contrast do not show any obvious phenotypic change beyond increased HO-1

expression. Normally, HO-1 is highly elevated in the **reticuloendothelial system** (**RES** or mononuclear phagocyte system), a system of phagocytic cells located in reticular connective tissue that processes damaged or senescent erythrocytes and is involved with the formation of bile pigments and storage of iron. Major sites of RES activity include the spleen, liver, and lymph nodes with additional small populations scattered throughout other tissues. During traumatic vascular injury HO-1 is highly induced n the local tissue, typically expressed by macrophages involved in erythrophagocytosis. In a typical hemorrhagic injury there is a delay of ~24-48 hours before HO-1 expression increases (Cao et al., 2016; Lu et al., 2014) and this appears to be primarily driven by the lag in erythrocyte lysis after injury. Ultimately, when the available heme substrate has been processed fully HO-1 returns to near baseline levels.

HO-1 is transcriptionally controlled by a variety of antioxidant/anti-ischemic transcription factors (Ryter et al., 2006; Alam, 1994; Alam et al., 1994; Alam et al., 1995). Chief among them is Nrf2, a constituently present transcription factor known to activate the consensus ARE sequence which controls antioxidant response proteins, including HO-1(**Figure 1-4**). Under normal conditions Nrf2 is continuously produced and resides in the cytoplasm bound by the repressor protein Keap1 and experiencing continual steady state degradation via cullin3 mediated ubiquitinization. Under oxidative stress (e.g. ROS, Fe, Electrophilic Attack) Keap1 conformationally changes due to cysteine mediated disulfide bond disruption (Hu et al., 2011). This change releases Nrf2 which is sufficiently small to spontaneously cross the nuclear pore. Once inside the nucleus Nrf2 binds to the consensus ARE sequence and promotes transcription of downstream targets. In regards to HO-1 this largely functions as a feed-forward mechanism which amplifies expression of HO-1 until HO-1 substrate is fully digested. This feed-forward mechanism occurs because the breakdown products of HO-1 mediated heme B catabolism (Fe

specifically) are known to induce Keap1 conformational change releasing Nrf2 which in turn increases HO-1, increases heme catabolic rate, and increases the local concentration of Fe which drives expression in a closed loop. This whole process is initiated due to small quantities of HO (e.g. HO-2) that are constituently present and provide the induction trigger. There are other known mechanisms which induce HO-1 expression but to date there is no evidence that they play a role in the selected model of TBI and the dominant focus of endogenous HO-1 induction has settled on the Nrf2/Keap1 axis as the dominant mechanism.

1.7.2 **NVU Breach, HO-1 and Cytotoxicity**

During the reduction of Heme via HO-1 catalytic cleavage there are several molecules that are released which have potential cytotoxic sequelae: **carbon monoxide (CO), Iron (Fe),** and **Biliverdin**. Carbon monoxide has a number of well-known cytotoxic effects where it tends to bind metalloproteins and heme moieties with high affinity preventing normotypic function. In mass quantities this is the typical outcome seen in CO poisoning where a sufficient fraction of erythrocyte hemoglobin becomes saturated with CO and fails to function normally in oxygen exchange with the tissue. At the scale we are discussing this is less likely and more typical dysfunction involves dysregulation of cytochrome enzymes and mimicry of NO on NO receptors causing inappropriate vascular response. Iron similarly has a number of cytotoxic effects, primary of which is the rapid cycling between oxidative states that encompasses the Fenton and Haber Weiss cycles. In these cycles Fe acts as a charge receptor/donator and by rapidly cycling between states generates hydroxyl radicals from metal catalyzed decomposition of hydrogen peroxide (Halliwell and Gutteridge, 1999).

1.7.3 HO Genetics, Gene Regulation, and Signal Transduction

HO-1 and HO-2 are the products of the genes hmox1 and hmox2 which are 14 kb and 12 kb respectively and are both organized into 5 exons and 4 introns (Alam et al., 1994; Cruse and Maines, 1988; Maines et al., 1986; McCoubrey and Maines, 1994; Shibahara et al., 1989). There are a number of potential promoter regions that have been identified for HO-1 (Shibahara et al., 1993), and the two major ones identified in the mouse are the E1 (268 bp) and E2 (161 bp) regions located at -4kb and - 10kb respectively and similar sequences exist in humans (Alam and Den, 1992; Alam, 1994; Alam et al., 1994; Alam et al., 1995; Alam and Cook, 2003). Both regions contain the Stress Response Element (T/C)GCTGAGTCA and respond to a variety of stimuli, being targets for Jun, Fos, CREB, ATF, Maf, and CNC-bZIP regulation (Alam and Cook, 2003; Alam et al., 2000; Balogun et al., 2003; Elbirt et al., 1998; Kiemer et al., 2003; Kietzmann et al., 2003; Kronke et al., 2003; Numazawa et al., 1997; Oguro et al., 1998; Shibahara, 2003). This can be seen in **Figure 1-4** adapted from Ryter et al., 2006. Signal transduction is mediated through a wide variety of kinases including MAPKs, Tyrosine Kinases, PI3K, and Protein Kinases A,G,C, generally operating through Keap1/Nrf2 or nuclear factors. This can be seen in **Figure 1-5** adapted from Ryter et al., 2006.

1.7.4 Figure 1-4: HO-1 Gene Regulation

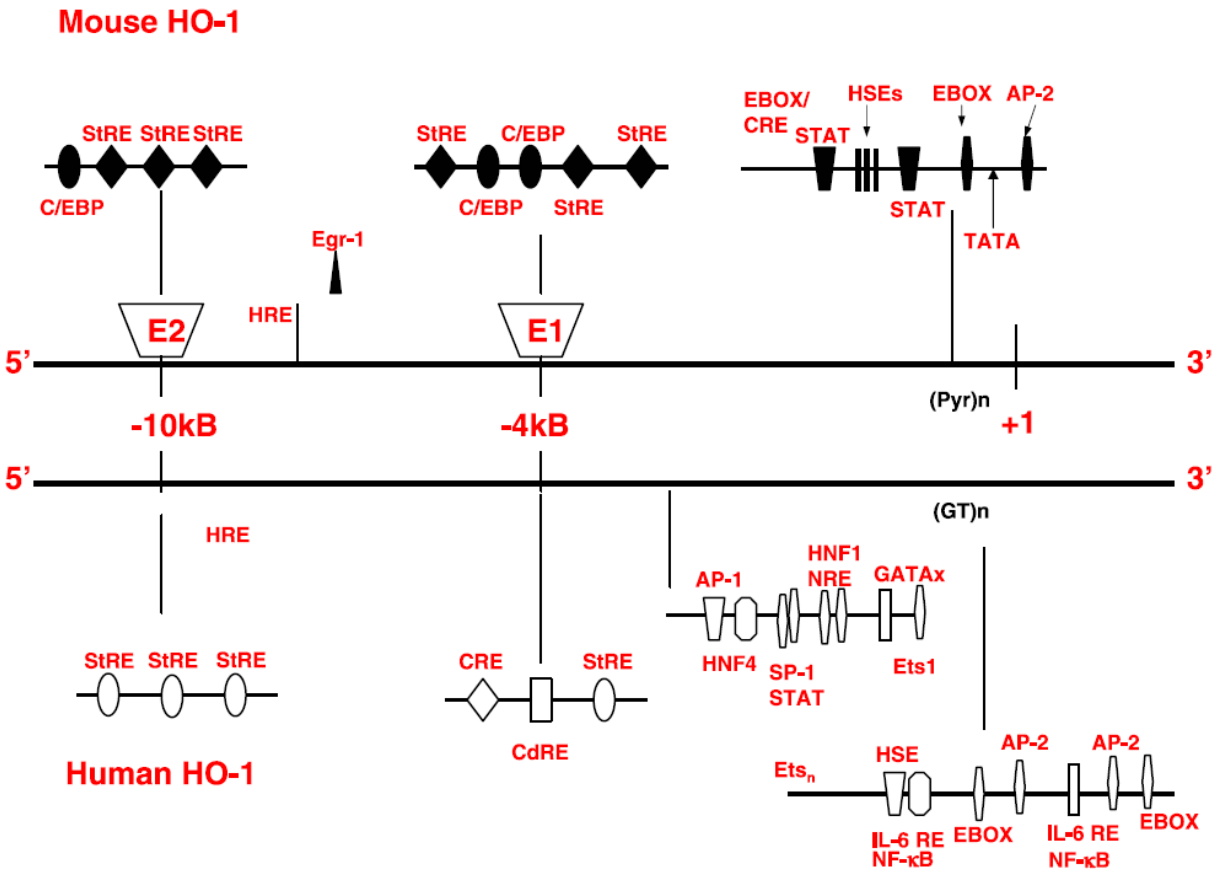

Figure 1-4: *Regulatory domains of the mouse and human ho-1 genes. The scheme depicts the known regulatory elements in the mouse and human ho-1 genes. The -4 and -10 kb regions (E1,E2) are marked for reference. Sequences identified primarily in the context of rat ho-1 are shown in the hatched boxes. (…).* Reproduced with permission from Ryter et al., 2006.

1.7.5 HO Subcellular Localization

Subcellular Localization HO-1 has typically been characterized as an **endoplasmic reticulum (ER)** associated protein and both HO-1 and HO-2 contain C terminal hydrophobic domains suggesting membrane compartmentalization (Ishikawa et al., 1991; Shibahara et al., 1985; Yoshida et al., 1988). Evidence also exists for wider distribution including at the plasma membrane caveolae, mitochondria (Kim et al., 2004), and nucleus (Li Volti et al., 2004; Maines et al., 2001) in an inducer dependent fashion.

1.7.6 HO-1 Sources of Activation

Increased synthesis of HO-1 occurs as a general response to stress in biological systems. Generally the increased synthesis is the result of transcriptional activation of the hmox1 gene resulting in de novo synthesis of mRNA (Alam et al., 1989; Keyse et al., 1990; Lin et al., 1990; Mitani et al., 1992; Mitani et al., 1993; Rizzardini et al., 1993; Sardana et al., 1982; Shibahara et al., 1987). Table 3, adapted from Ryter et al., 2006 provides an only partially complete listing of a wide variety of stressors. Ryter also note that there are three general hypotheses about HO-1 induction that will be discussed here.

The first general hypothesis is that an increase in intracellular heme content as a response to a stressor will mediate induction of HO-1. This is primarily based on the observation that heme is a potent inducer of HO-1 (and its enzymatic target) and that a number of chemicals known to induce HO-1 are associated with transient increases in the hepatic heme pool (Kikuchi and Yoshida, 1983). This hypothesis is, however, limited by the observation that inducers exist which do not cause elevations in intracellular heme (Kikuchi and Yoshida, 1983). An interesting point here is that an increase in the hepatic iron pool is suggestive of increased

erythrophagocytosis suggesting that either stressors are inducing erythrocyte senescence or that HO-1 induces erythrocyte degradation.

The second general hypothesis is that an increase in intracellular reactive oxygen species (ROS) causes induction of HO-1 in a redox regulated pathway. This hypothesis is founded on the observation that many of the inducing agents are oxidants associated with the intracellular production of **reactive oxygen species (ROS)** and further that induction of HO-1 by many inducers can be inhibited by the antioxidant **N-acetyl-L-cysteine (NAC)** in millimolar concentrations (Borger and Essig, 1998; Camhi et al., 1995; Durante et al., 1999; Favatier and Polla, 2001; Foresti et al., 1997; Foresti et al., 1999; Gong and Hart, 1997; Hartsfield et al., 1997; Hill-Kapturczak et al., 2003; Liu et al., 2004; Rizzardini et al., 1994; Terry et al., 1999). The weakness in this hypothesis is that the ROS production of some inducers (particularly some cytokines and hypoxia) is not settled and that antioxidants do not universally inhibit HO-1 induction. Even worse, some phenolic antioxidant compounds including quercetin and curcumin induce HO-1 (Lim et al., 2001; Motterlini et al., 2000; Scapagnini et al., 2002; Tanigawa et al., 2007). One of the HO-1 inducers utilized in this thesis (Sulforaphane) utilizes a similar mechanism and it is worth mentioning that there is some confusion in the literature and generally between molecules that are true antioxidants (aka are reductive a la N-Acetyl-L-Cysteine) or molecules that are weak oxidants and instead activate redox triggers effectively without being sufficiently oxidative to cause tissue damage.

1.7.7 Figure 1-5: HO-1 Activation Pathways

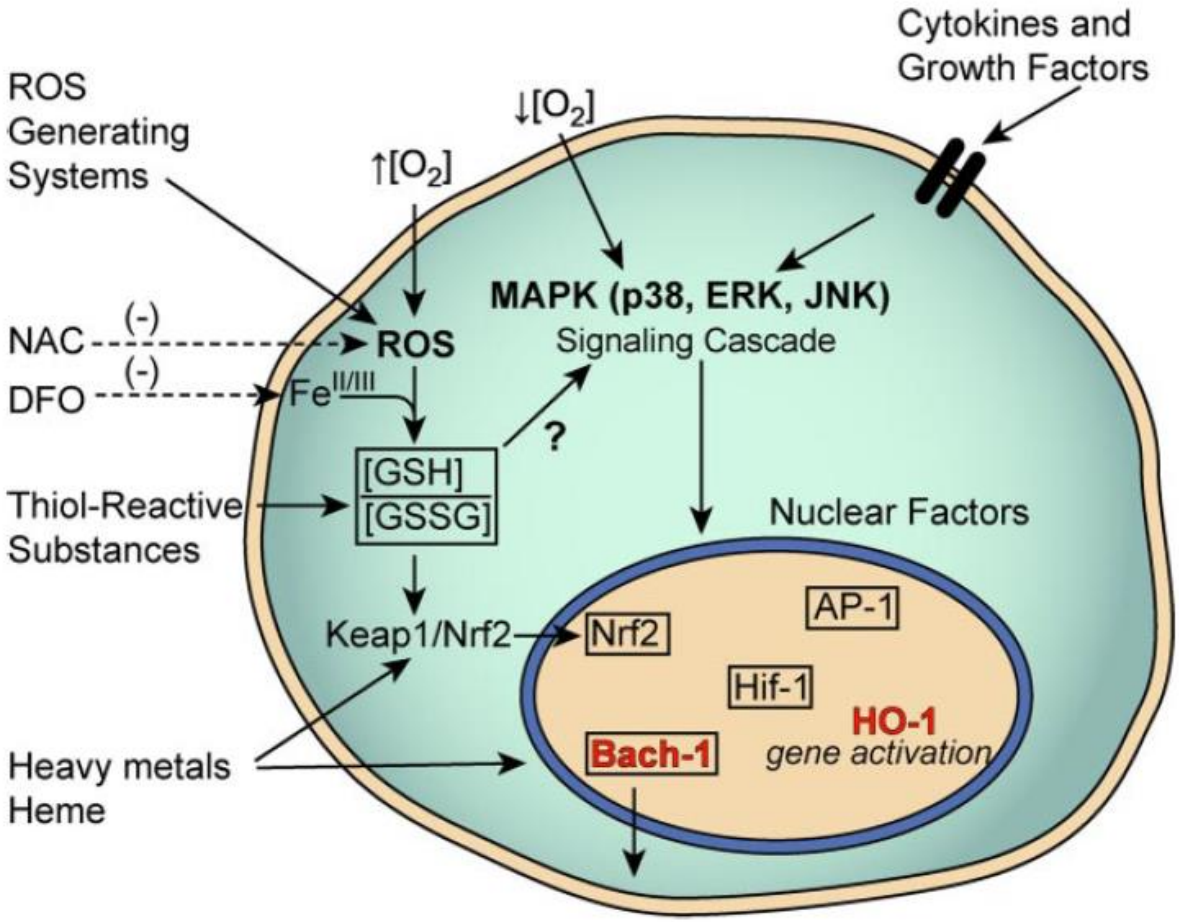

Figure 1-5. *Signaling pathways leading to ho-1 activation. The scheme shows the potential interrelationships between intracellular and nuclear signaling events that lead to transcriptional activation of the ho-1 gene by various inducing agents. Increased of intracellular reactive oxygen species lead to perturbation of intracellular thiol equilibrium, leading to reduction of GSH/GSSG ratio, and redox regulation of Keap1. Treatment with heavy metals and/or heme promotes Nrf2 nuclear translocation and nuclear export of the transcriptional repressor Bach1. Activation of MAPK by environmental stresses and cytokines has also been implicated in ho-1 activation. (…)* Reproduced with permission from Ryter et al., 2006.

The third general hypothesis is that alteration of intracellular thiol equilibrium via the ratio of intracellular reduced vs. oxidized glutathione acts as a primary sensor for oxidative stress (Ryter et al., 2006). This hypothesis originates in the observation that many inducers which produce reactive oxidative species or can react with free thiol groups can consume, complex, or reduce the availability of intracellular glutathione (Ewing and Maines, 1993; Lautier et al., 1992; Naughton et al., 2002; Oguro et al., 1998; Rizzardini et al., 1994; Trakshel et al., 1991; Yoshida et al., 1987). The main weakness in this hypothesis is requiring direct redox regulation of transcription factors and while well characterized in bacteria they have been poorly investigated in mammals. Ryter et al., suggest that the cytoplasmic factor Keap1 is a potential redox sensor leading to the release of the bound substrate Nrf2, a transcription factor (Dinkova-Kostova et al., 2002; Wakabayashi et al., 2004; Levonen et al., 2004) and may result in increased HO-1 expression.

1.8 Non Traumatic Role for HO-1

There is evidence that HO-1 plays a role in a variety of neurodegenerative conditions. In **Alzheimer disease (AD)** it has been observed that plasma HO-1 and lymphocyte HO-1 mRNA are reduced (Schipper et al., 2000), while at the same time senile plaques are known to display elevated HO-1 co-localized with β-amyloid (Schipper et al., 1995) and it appears that β-amyloid induces HO-1 expression (Pappolla et al., 1998). In **Parkinson's disease (PD)** HO-1 is highly expressed in Lewy bodies (Castellani et al., 1996) and oxidative stress has notably been shown to increase HO-1 in a dopaminergic cell line (Yoo et al., 2003). In an intriguing study, a specially modified form of HO-1 was shown to prevent MPTP induction of PD in a mouse model (Youn et al., 2014). Other conditions including amyotrophic lateral sclerosis, Friedreich's ataxia,

Huntington's disease, and many others have also been studied, but less stringently than in AD and PD and the current evidence in each case is unsettled.

1.9 HO-1 and Traumatic Brain Injury

As discussed above, TBI generates a heterogeneous collection of pathologies that can often be broken down into two major types: focal or diffuse. Focal injury results in cortical contusion, severe vascular damage, cell death and overt hemorrhage, frequently accompanied by ischemia. Diffuse injury, in contrast, is primarily characterized by dispersed axonal injury, minimal to moderate vascular disruption and reduced necrosis. This suggests that there are at least two different injury paradigms where NVU and HO response may be linked to TBI. Experimental models incorporating diffuse injury permit studies where the effects of the TBI on the NVU can be more cleanly examined, as in the midline fluid percussion injury (Albert-Weissenberger and Siren, 2010). Indeed NVU disruption and HO response are each demonstrable in both grey and white matter sites within 24 hours following in a moderate level midline fluid percussion injury as seen in **Figure 1-6**.

1.9.1 Figure 1-6: HO-1 Expression 1-7d Post-Injury

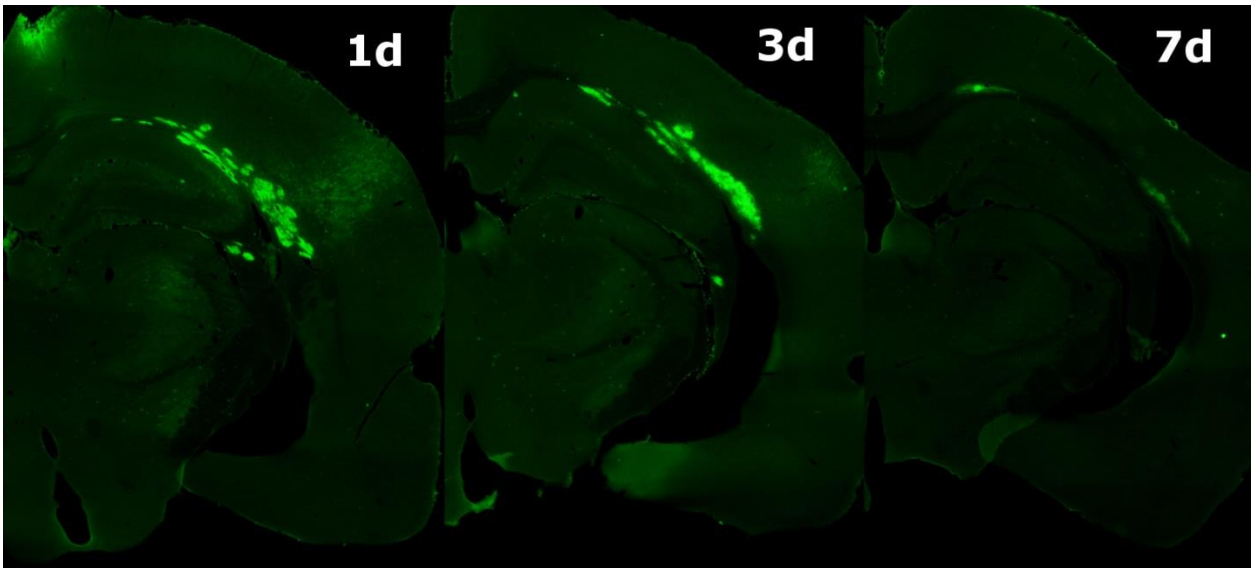

Figure 1-6. Showing HO-1 elevation 1-7d post midline fluid percussion TBI. Note hemorrhagic/necrotic regions under the medial longitudinal fissure and in the white matter tracts of corpus callosum. This is in contrast to non-hemorrhagic/necrotic regions in the auditory cortex, hippocampus, thalamus, striatum and internal capsule.

Following midline **fluid percussion injury (FPI)** focal vascular hemorrhage and necrosis causes an increase in HO-1, mostly likely through the gross efflux of red blood cells and release of heme into the surrounding tissue. In regards to the NVU, the primary responsive cells are leukocytes and microglia, which co-stain with both microglia/macrophage specific marker IBA1 and HO-1. These cells are found below the injury hub site and in white matter tracts (Phillips Lab, unpublished data), an expected result given that heme can induce HO-1. This is in direct contrast to the diffuse injury response seen in the hippocampus and auditory cortex of the same animals. There, a more diffuse injury is expected which was, surprisingly, accompanied by significant HO-1 up-regulation in cells co-staining with the astrocyte marker GFAP. Interestingly, midline FPI is known to generate minimal hippocampal hemorrhage, with no gross loss of either cell structure or evidence of cell death. This points to a parallel, non-hemorrhagic, non-heme driven induction of HO-1.

HO-1 has been reported to increase after TBI by a variety of techniques including gene chip, qRT-PCR, western blot, and immunofluorescence (Phillips Lab unpublished data, (Raghavendra Rao et al., 2003; Fukuda et al., 1995)). Fukuda et al, observed HO-1 upregulation within 24 hours following lateral FPI, leading to widespread signal at 72 hours before declining at 5 days post-injury. Co-expression was primarily with microglia and astrocytes identified with OX42 (microglia specific) and GFAP (Fukuda et al., 1996). The same group further observed that a spinal cord injury model also demonstrated HO-1 elevation in microglia and macrophages from 24 hours to at least 42 days post-injury (Mautes et al., 2000). They further established that HO-1 was induced by hyperosmolar mannitol (Richmon et al., 1998) or heme injected into the subarachnoid space (Turner et al., 1998). Further, HO-1 could be reduced by an Endothilin A

antagonist (Sato and Noble, 1998), stabilized the blood-spinal cord barrier (Lin et al., 2007a) and reduced barrier disruption after injury (Yamauchi et al., 2004).

1.10 Novel Role in Traumatic Brain Injury Recovery

At the NVU HO-1 is most likely produced by astrocytes and microglia following TBI. Indeed, the Noble group at UCSF has shown that after TBI HO-1 is elevated in both astrocytes and microglia. HO-1 is at least partially induced as a result of direct heme interactions, particularly at sites of microvascular bleeds and gross hemorrhage (Phillips Lab, unpublished data). Conspicuously absent is HO-1 production in the endothelium, which is likely also elevated but masked by the much greater response in the glia due to leakage of blood and its constituents through the BBB. What is particularly interesting is that with midline FPI there is evidence of HO-1 elevation in areas experiencing gross hemorrhage (such as the neocortex) as well as those lacking hemorrhage (such as the hippocampus). This finding implies multiple activation mechanisms are responsible for post-injury HO-1 increase or that there are hemorrhagic processes currently unidentified. Transient ischemia or mild hypoxia present one potential mechanism for NVU injury in the hippocampus but this is clouded by the alternatives of increased inflammatory cytokines, eicosanoids, or ionic dysregulation, all driven by changes in the BBB, perhaps resulting from local mechanical shear stress.

Trauma → ↑Heme → ↑HO-1→↑free iron→↑LCN2→↑MMP9 activation→↑ECM modulation

Diagram 1. A proposed novel pathway for HO-1 driven ECM modulation

It has become clear that HO-1 has a number of tissue effects that may play a role after injury. The first is in heme clearance that has been addressed previously. A simple proposed pathway for this role is outlined in **Diagram 1** where free heme causes an increase in HO-1

leading to increased free ferrous iron. This in turn leads to an increase in the iron scavenger Lipocalin 2 (LCN2) and resulting increased activation of MMP-9, a collagenase involved in tissue remodeling. At each step there are also branch points with multiple additional effects including local vasodilation as a result of CO release and antioxidant activity of biliverdin mediated through biliverdin reductase. This suggested pathway provides an HO-1 driven effector of tissue remodeling though this pathway is somewhat spatially restricted. It is expected that HO-1 operating near the vasculature or within the luminal side of the NVU basal membrane would allow for rapid egress of ferrous iron and other breakdown products from the brain while HO-1 operating further into the parenchyma may result in iron accumulation locally in the tissue. This may explain the reported benefit from endothelial cell up-regulation of HO-1 via sulphoraphane in an ischemic hypoxia/reperfusion model (Alfieri et al., 2013) while also addressing toxicity concerns associated with Parkinson's Disease (Castellani et al., 1996; Yoo et al., 2003).

A second role appears to be as a novel cytoprotective, anti-inflammatory protein with neuroprotective potential, though this role is both spatially and situationally complex. In a number of disease states that lack hemorrhage HO-1 pharmacologic up-regulation has been shown to be beneficial, including in hepatic encephalopathy (Jiang et al., 2009), Alzheimer's Disease (Barone et al., 2014), and Parkinson's Disease (Cuadrado and Rojo, 2008) . This may be due to HO-1's ability to degrade porphyrins and potentially prevent Cytochrome C heme C degradation products from activating pro-apoptotic Bcl2 family proteins. This role is made more difficult to understand, since baseline HO-1 increase in AD is associated with worse pathology. These divergent views can be unified when considering HO-1 as both a sensor and effector of pathology and recovery. In this view high HO-1 in AD indicates an underlying pathology that activates HO-1, possibly in a glutathione mediated way, and further HO-1 induction can be

beneficial. However, this is in contrast to PD where HO-1 also likely indicates an underlying pathology but further induction becomes negative due to the tendency of HO-1 to degrade heme (including intracellular heme) and the weak ability of dopaminergic neurons to remove the excess iron that results. The situation becomes even more complex when it is noted that even in the absence of apparent hemorrhage LCN2, an iron scavenger and transporter, is significantly up-regulated in areas also demonstrating increased HO-1 expression. Additionally, both CO and Biliverdin/Bilirubin produced by HO-1 are known to be neuroprotective in low concentrations and yet grossly neurotoxic at high concentrations.

From the previously observed expression of HO-1 after TBI and knowledge of the NVU structure I propose three scenarios where HO-1 expression in the NVU affects injury recovery, each characterized by a different primary cell response.

The first situation is an endothelial driven response where HO-1 pre-injury induction in the endothelium occurs as a result of circulating HO-1 activators that act on the endothelial cells without penetrating into the brain parenchyma. In this situation HO-1 acts to stabilize the endothelial **tight junctions (TJ)** as noted previously (Lin et al., 2007a; Yamauchi et al., 2004). This likely has two effects: reducing BBB disruption and also limiting heme efflux when disruption occurs. Further, via receptor mediated transport free heme may be taken up by the endothelium and processed with degradation products expelled back into the circulation limiting buildup of Biliverdin or iron within the brain parenchyma.

The second situation causes a microglial driven response to gross heme influx in situations of hemorrhage and necrosis, where microglia and other macrophages are selectively recruited and highly express HO-1 in an effort to degrade heme. This would primarily follow the

most classical pathway of heme induction of HO-1 but HO-1 may also drive the activation of MMP9 via LCN2 upregulation as described in **Diagram 1**. This case notably involves the gross disruption of the NVU by MMP activation to result in significant degradation of basal the lamina and cellular architecture.

The third situation would involve an astrocyte driven response where thiol/glutathione disruption caused by the breakdown of endothelial TJ and basal lamina permits efflux of undesired molecules. In this case HO-1 may be elevated in an effort to assist TJ integrity as well as an anti-apoptotic to prevent astrocyte cell death after being flooded with undesirable metabolic waste products not effectively removed from the brain parenchyma. This situation lends itself to the possibility of persistent activation of HO-1 if trapped waste products continually disrupt the glutathione redox balance. This would negatively impact the cell and surrounding parenchyma by continual slow accumulation of iron from the degradation of intracellular non-hemoglobin heme sources.

1.10.1 Pharmacological Inducers of HO-1

A number of chemical inducers of HO-1 expression have been identified by confirmation of increases in mRNA, promotor activity, protein expression, or enzymatic activity. An excellent summary chart of these compounds has been published by Ryter et al 2006, which is partially reproduced below. It is noteworthy that generalized cell stress is frequently sufficient to cause an induction somewhere along the HO-1 pathway though this level of induction is highly variable. Of particular interest to my study are two inducers: Hemin (Heme) and Sulforaphane. The first is the natural substrate of HO-1 and is commercially available as Heme Chloride or Heme Arginate. In various forms it is approved for human medical use as a treatment of acute intermittent porphyria. It has been shown to reliably increase HO-1 expression and is somewhat

selective in how it triggers the generalized antioxidant transcriptional response. In brief, Hemin is processed identically to endogenous heme, it is taken in by phagocytic cells and is reduced from Heme to Biliverdin and then Bilirubin releasing CO, and Fe along the way. Fe has been identified as one of the major players in the feed-forward mechanism of HO-1 amplification and as Hemin is degraded it induces increased expression of HO-1. The major proposed pathway for heme driven HO-1 amplification revolves around the Nrf2 repressor protein Keap1. Keap1 functions as an antioxidant sensor and when disrupted it releases bound Nrf2 allowing for increased transcription of the consensus ARE sequence genes which include HO-1. Along the way Fe is also active in increasing reactive oxidant species locally and triggering iron response element gene expression.

Sulforaphane, in contrast, has a different mechanism of action that ultimately increases HO-1. Sulforaphane is an organosulfur isothiocyanate molecule that is derived from Brassicaceae vegetables (e.g. mustards, brussels sprouts). The isothiocyanates generally function as weak electrophiles and due to their properties are effective in triggering cellular antioxidant sensors without providing a large pro-oxidant stimuli. Sulforaphane has been proposed to activate HO-1 via the Nrf2 repressor protein Keap1 via specific cysteine residue binding and appears to be effective at causing separation of Keap1 from Nrf2 leading to an increase in HO-1 expression (Hu et al., 2011). In this context the molecule does not trigger increased HO-1 expression through its action as a substrate and it does not produce potentially cytotoxic molecules along the way.

1.10.2 A Proposed Mechanism for HO-1 Induced Cytoprotection after TBI

In a typical TBI there is local extravasation of erythrocytes from damaged blood vessels into the surrounding brain parenchyma. The erythrocytes then proceed to spontaneously lyse

over the course of 24-72 hours with a significant initial delay after the injury which is coincident with a decrease in CD47 (Cao et al., 2016; Lu et al., 2014). When the red cells begin to lyse they do so in response to the local tissue environment (pH, stasis, temperature, cytokines, etc) and appear to lyse *en masse* with a large bolus of hemoglobin and heme released simultaneously. The result is quick saturation of the HO enzymes and rapid breakdown of heme which releases cytotoxic species. As HO-1 processes the substrate it experiences feed forward amplification and the ARE sequence is recruited to increase various buffering molecules that limit the potential cytotoxic effects of heme catabolism. Due to the nature of the feed forward process the production of buffering molecules necessarily lags behind the inducing stimulus which, in this case, is a collection of molecules that need to be buffered proximally.

This provides a few key pieces of information that are fundamental to the present thesis of HO-1 role in response to TBI. We know that: 1. a traumatic injury to the NVU has occurred and that a bleed/s is/are likely concurrent, 2. the damaging effects of the bleed have a temporal delay, 3. the enzyme responsible for heme degradation is controlled by a transcriptional promotor that also controls expression of buffering compounds. As a direct result, we have foreknowledge of future injury that the tissue is not yet responsive to. The underlying proposed hypothesis is straightforward: *early induction of HO-1 will be coincident with increased production of buffering compounds which then limit peak of HO-1 feed-forward signal, resulting in a net HO-1 reduction, attenuation of the 'peak bolus' of cytotoxic compounds and more stable substrate processing.* A corollary hypothesis is that *if such regulation of HO-1 expression is accomplished the reduction in cytotoxic insult will lead to improved histopathological and behavioral outcomes after TBI.*

The proposed experiments will first establish post-injury response of select HO-1 pathway molecules following diffuse midline FPI, then test if early HO-1 induction through IP injection of either Hemin or Sulforaphane (delivered 1 hour after FPI) will affect extent of pathobiology or behavioral deficits. This approach has potential for translational value in that it could identify safe, acute post-injury treatments to reduce the consequences of initial NVU damage and permit a greater functional recovery over time after injury.

1.11 Choice of FPI as Experimental Model

There are multiple experimental models of TBI and the midline FPI, using a mild-moderate injury, was chosen as being most applicable to this study. Examples of other commonly used injury models include Blast Injury, **Controlled Cortical Impact (CCI)**, and Weight Drop Models which will be addressed in turn.

Blast injury models seek to replicate the shockwave induced injury that originates from high speed propagating air waves as a way to model blast injuries that typically occur from explosives (e.g. in a wartime setting). The severity of injury is modified by adjusting the peak overpressure and impulse that is experienced by the animal with typical injuries occurring in the 10-20 psi range (~0.7-1.5 ATM overpressure). The model is a closed head model that avoids some of the concerns surrounding the surgical preparation involved in other TBI models but is somewhat limited due to the substantial differences between shockwave induced injuries and focal or diffuse impact injuries. The insult is effective at modeling blast damage to the brain but has historically shown several unexpected differences when compared to other injury models (VandeVord, P., 2017-03-01 VCU Traumatic Brain Injury Seminar Series).

Controlled Cortical Impact models provide a well characterized set of focal TBI injuries (Dixon et al., 1991). A craniectomy surgery is performed to expose the intact dura and then an impactor tip is forced against the surface of the brain with speed, depth, tip type, and dwell time all varying to induce different degrees of highly reproducible injury. The resulting injury is focal in nature and tends to be both grossly hemorrhagic and necrotic, typically applied laterally. When adjusted to produce a mild insult there have been competing reports as to whether mTBI in this model is able to produce behavioral deficits due to the required restrictions on speed, depth, and dwell time.

Weight drop models use a free falling weight which strikes either the intact skull or exposed dura to produce an injury. The height and mass of the object dropped can be adjusted to alter the severity of the injury. The most popular variant of the weight drop insult is the Marmarou model of Impact Acceleration (Petraglia et al., 2014; Marmarou et al., 1994; Foda and Marmarou, 1994) which uses a plate attached to the animal skull to prevent fracture and gives the animal a degree of freedom to allow the head to move resulting in a largely diffuse injury that avoids contusion or hippocampal cell death.

The mechanics of the midline Fluid Percussion model are interrelated with each of the other models, as they all share specific commonalities and differences (Petraglia et al., 2014). In the fluid percussion model a craniectomy is performed and a fluid overpressure pulse is applied to the intact dura (Sullivan et al., 1976). The result is a direct pressure wave injury contained within the skull that avoids hemorrhage at the impact site while producing extensive diffuse injury throughout the brain, including in the neocortex and hippocampus (Dixon et al., 1987). Depending upon severity, the model can produce hemorrhage in specific susceptible tissue regions while inducing widespread axonal and neuronal injury. The injury is characterized by the

overpressure that is used though some consider subject LOC time to be a better metric since the in line position of the pressure sensor could influence the measurement of pressure delivered to the animal. This model provides a diffuse tissue injury similar to some aspects of the blast and CCI models and allows for a midline injury like the weight drop and blast injuries, however, it avoids impact site hemorrhage, and generates a broad injury effect within many areas of the brain that is well characterized.

We selected midline FPI as a model of choice for this study because we sought to model human mild-moderate diffuse TBI. Although this rat model demonstrates reasonably sized white matter hemorrhages characteristic of moderate injury, the model also provides a dynamic range of tissue damage across other brain regions. For example, the hippocampus is largely non-hemorrhagic, yet known to be functionally damaged in the model, while the neocortex which frequently shows small frank petechial hemorrhages originating along the gray/white matter interface and along a subset of radially oriented blood vessels (notably not at the hub site where the overpressure is applied). Thus, FPI allows for the direct comparison between distinct injury sites with and without overt hemorrhage. In this dissertation study I will first examine whether such hemorrhagic differences affect the response of injury-induced HO-1 pathway proteins by contrasting cortical and hippocampal regions (it is important to note here that while the neocortex has overt hemorrhage it is not overwhelmingly hemorrhagic/necrotic). Next, I will determine if acute pharmacological modulation of HO-1 response will change the time course of structural and behavioral recovery. This approach has value in that it offers promise for discriminating the role of HO-1 pathways in brain regions vulnerable to milder, non-contusional forms of injury and probes whether HO-1 manipulation can alter TBI pathology or functional outcome. Since the absolute size of the bleeds in this rat model are consistent with those seen in

human mTBI, we proffer that information about the recovery of rat hemorrhagic tissue in FPI would also closely match that seen in milder forms of human TBI.

1.11.1 The Hippocampus as a TBI Model

1.11.1.1 Structure and Function

The hippocampus is a seahorse shaped structure in primates located in the medial temporal lobe. It is selected for study in TBI models due to prominent its role in learning and memory along with the associated cortical regions which make up the hippocampal formation. The hippocampal formation is divided into six anatomical areas: the subiculum, the hippocampus proper (further divided into four **cornu ammonis (CA)** sectors CA1-CA4), the dentate gyrus, the presubiculum, the parasubiculum, and the entorhinal cortex. The CA fields are comprised of pyramidal neurons whose cell bodies form the pyramidal later (stratum pyramidale). Basal dendrites of these neurons are located in the stratum oriens while apical dendrites extend to the stratum radiatum, lacunosum, and moleculare. CA dendrites receive a variety of inputs from both the Direct and Trisynaptic (indirect) perforant pathways. The dentate gyrus is divided into the hilus/polymorph layer, the **granule cell layer** (**GCL**; stratum granulare, containing the cell bodies of the granule neurons), and the stratum moleculare containing the dendrites of the granule cells. These granule cell dendrites receive stratified inputs from the perforant pathway originating in the entorhinal cortex as the initial part of the Trisynaptic pathway.

Circuitry in the hippocampus is both internal and external – externally information is shared reciprocally with the structures of the limbic system as well as the entorhinal cortex, other associated cortices, and the septum. Flow of information within the hippocampus is largely

unidirectional and the major pathway is known as the ‘Trisynaptic Circuit’. The main output pathway of the entorhinal cortex is the perforant pathway which perforates the subiculum to project mainly into the granule cell layer of the dentate gyrus (with some projections into CA1 and CA3). Dentate gyrus axons known as mossy fibers then pass information to CA3 pyramidal cell dendrites. CA3 axons, known as Schaffer Collaterals, next loop to CA1, whereupon CA1 axons project back to the entorhinal cortex. This whole process involves three synapses EC-DG, DG-CA3, and CA3-CA1 which provide the circuit with its name.

Damage to the hippocampus generally results in memory impairment and disorientation (Eichenbaum et al., 2007; Nadel et al., 1975) and early observations led to the discovery of long term potentiation or LTP (Bliss and Lomo, 1973). LTP was first identified by Bliss and Lomo in 1973 noting that repetitive stimulation of the performant path fibers to the dentate area of the hippocampus led to reduced firing latency and increased spike amplitude in dentate granule neurons (Bliss and Lomo, 1973). This has since been expanded into a more generalizable model of synaptic/circuit development where increased stimulation leads to a strengthened pathway and has been observed in all portions of the Trisynaptic pathway (Kandel et al., 2013). The corollary of long term depression (LTD) also exists where loss of stimuli leads to decreased synapse strength and functionality. There are three main historical theories of hippocampal function that have come in and out of vogue over the years; Behavioral Inhibition, Memory, and Spatial Theory. The behavioral inhibition theory was the first described by Jeffrey Gray (Gray and McNaughton, 2003) who noted that animals with hippocampal damage tended to by hyperactive leading to the conclusion that the hippocampus was useful in inhibiting overactive behavior. The memory theory was produced from the treatment observations of a certain Patient HM who in an attempt to alleviate his epileptic seizures had his hippocampi surgically destroyed. The result was

that Patient HM suffered from severe anterograde amnesia as well as partial retrograde amnesia where he could not produce new memories moving forward but was still able to remember events from his childhood leading up to several days/weeks before his surgery. The last theory is the spatial map theory which is based off the observations that electrode recording data show that specific hippocampal regions in a rat brain lit up when in specific spatial locations suggesting that the hippocampus is involved in developing a spatial map of the surrounding environment (O'Keefe and Conway, 1978). The specific cells have since been characterized as 'place cells' which in network form a 'place field' and they develop within minutes of entering a new environment and maintain stability for weeks-months afterwards (Kandel et al., 2013)**.** When assembled together all three theories share commonalities in memory consolidation/encoding and situational awareness.

1.11.2 Figure 1-7: Mid-Dorsal Coronal Section of Rodent Brain

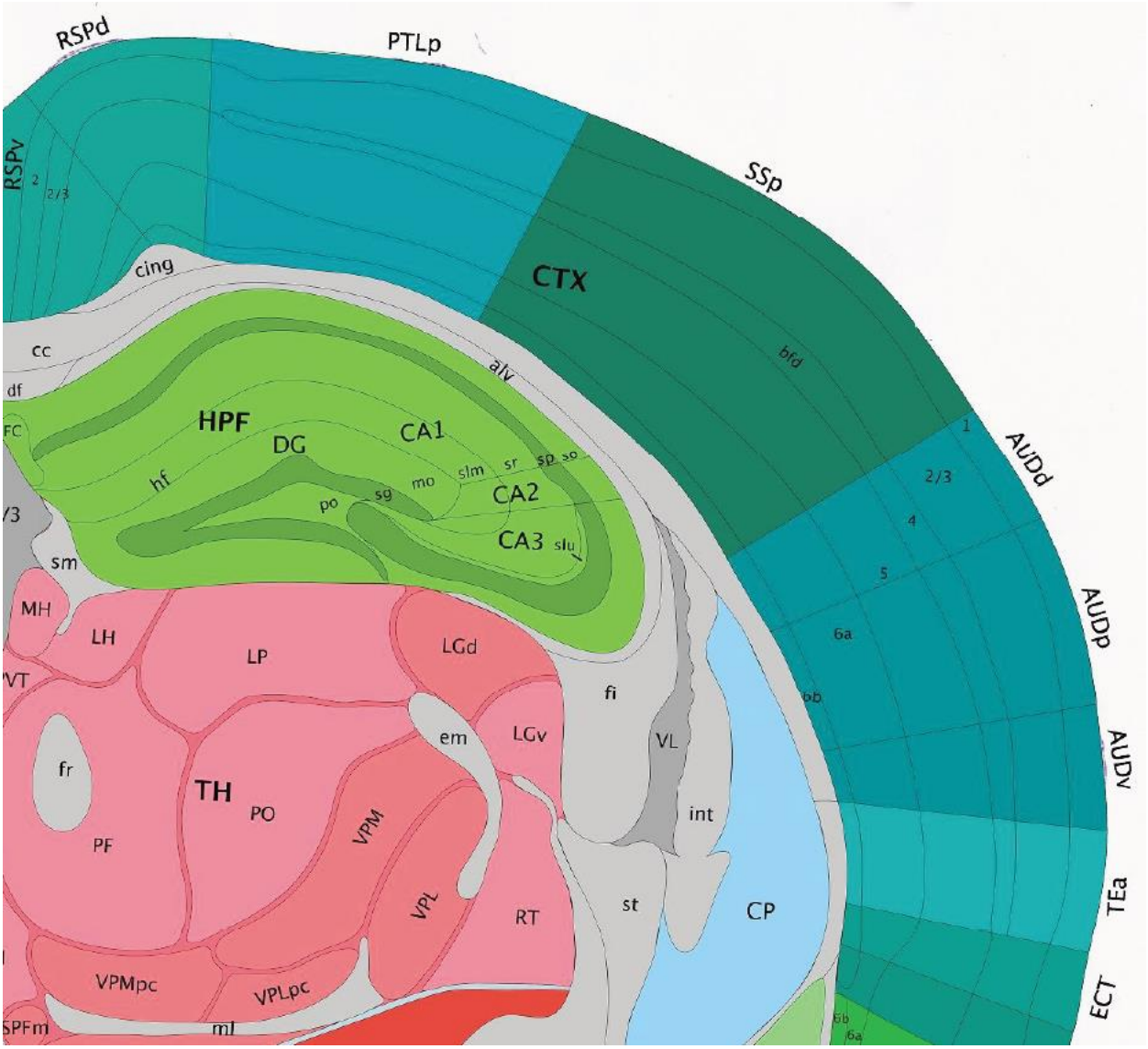

Figure 1-7. This image is from the Allen mouse brain atlas. A section through the mid-dorsal **hippocampal formation (HPF)** is illustrated, showing the major cell layers. In our FPI model we primarily induce tissue damage in the somatosensory cortex and auditory cortex overlying the hippocampus, as well as hemorrhagic bleeds in the white matter of the corpus callosum.

1.11.2.1 Hippocampal Plasticity

The two principle mechanisms of CNS plasticity, neurogenesis and synaptogenesis, are both activated after injury in the hippocampus. The hippocampus is well established as one of the limited adult brain regions with continued neurogenesis (Gould, 2007). In the DG the subgranular zone generates neuronal precursors and the process is stimulated by CNS injuries including both focal and diffuse TBI (Kernie et al., 2001; Dash et al., 2001; Bye et al., 2011). The subgranular zone precursors are capable of differentiating into neurons/glia and migrate to the injured tissue enhancing cognitive recovery (Magavi et al., 2000; Sun et al., 2005; Sun et al., 2007). Treatments with VEGF after TBI have demonstrated increased neuronal differentiation and improve neurological recovery in conjunction with decreased lesion volume (Thau-Zuchman et al., 2010). New neurons migrate to the granule cell layer integrating into the circuits of the dentate gyrus **molecular layer (ML)** and the cornus ammu of the hippocampus (Dash et al., 2001; Emery et al., 2005).

Previous studies have well established injury induced synaptogenesis in the hippocampus after TBI with associated synaptic sprouting and synapse replacement (Steward et al., 1988; Scheff et al., 2005). Our laboratory has shown this is in part mediated by the ECM and its interactions with MMPs and CAMs (Falo et al., 2006; Falo et al., 2008; Harris et al., 2011; Warren et al., 2012; Chan et al., 2014). Others have demonstrated the acute phase of this process is reliant on inflammatory processes to include cellular phagocytosis of damaged tissue (Morganti-Kossmann et al., 2002). Neurogenesis and synaptogenesis has been directly linked to robust microglial response following TBI (Sun et al., 2005; Bye et al., 2011). It has been suggested that examining molecules with specific time dependent expression during the process of post-injury repair may lead to identifying targets for possible therapeutic intervention.

1.11.3 The Neocortex as a TBI Model

1.11.3.1 Structure and Function

The neocortex is the outer layer of neural tissue in the brain and plays key roles in higher order brain function including cognition, sensory perception, language, and memory. The previously described hippocampus is part of the allocortex, characterized by having only 3-4 neuronal cell layers in contrast to the remaining neocortex, which has 6 layers of neuronal cell bodies.

1.11.4 Figure 1-8: Simplified Cortical Excitatory Circuits

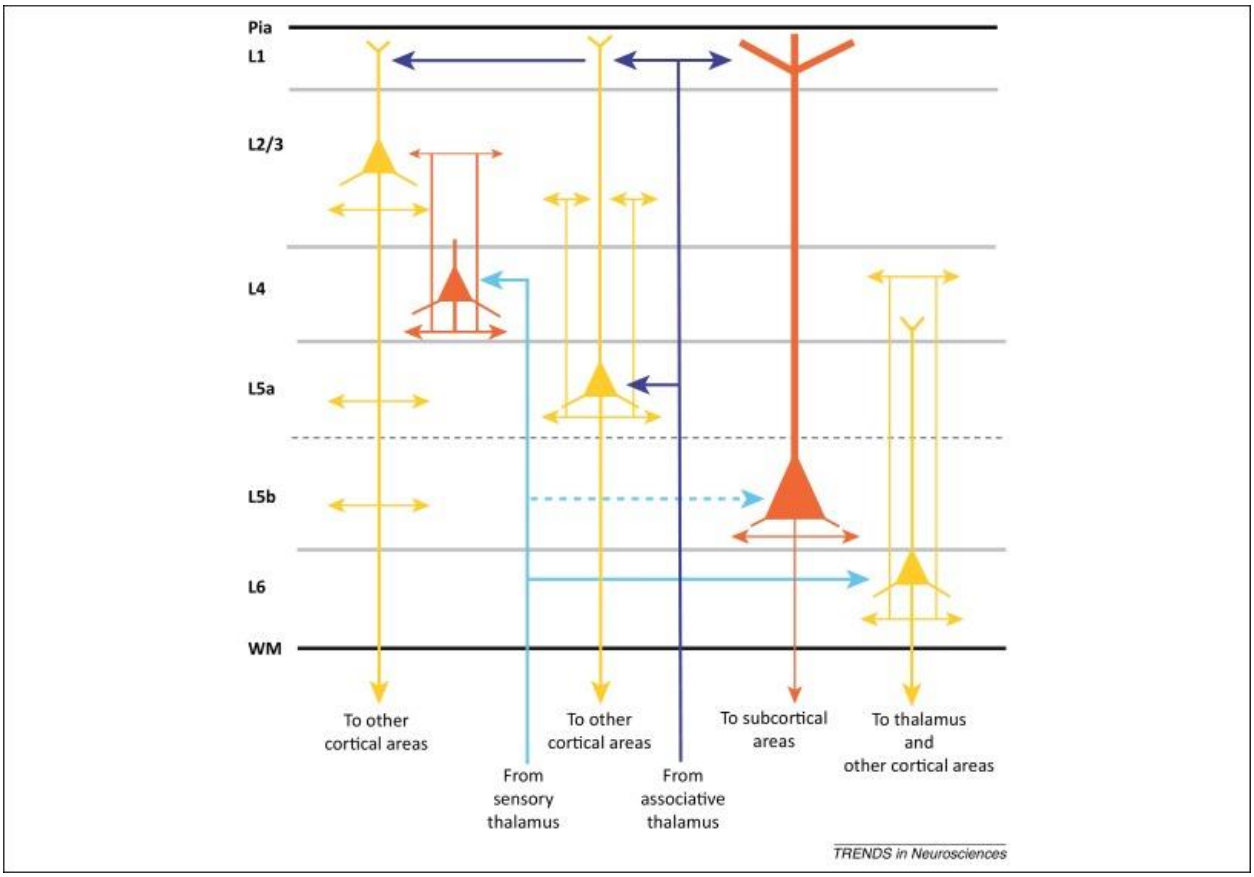

Figure 1-8. Simplified diagram of excitatory neurocortical circuits. Reproduced with permission from Allene et al., 2015.

The various layers of the neocortex have extensive connections between adjacent regions and layers and the size of each layer is highly dependent on specific region of the neocortex and form of processing that locally occurs. Layer I (outermost) is the molecular layer and consists mainly of apical dendritic tufts of pyramidal neurons and laterally oriented axons. Staining with Golgi Stain demonstrates an absence of cell bodies in this layer. Layer II/III is the external granule cell layer/external pyramidal layer consisting of small pyramidal neurons/stellate neurons and midsized pyramidal neurons respectively that receive extensive input from Layer I and layers IV/V. Layer IV is the internal granular layer and is the main recipient of thalamic sensory input. Layer IV projects laterally and to layers II/III. Layer V is the internal pyramidal cell layer which receives extensive input form layers II/III, and is the primary output pathway from the neocortex. Lastly layer VI (innermost) is the polymorph/multiform layer which receives input from sensory thalamus and projects to adjacent layer VI and IV. The cell bodies in Layer VI are variable and blend into the white matter forming the deep limit of the neocortex. As may be evident from the description, the structure of the neocortex is highly integrated with continued projections within and between layers and within and between regions.

During traumatic brain injury a variety of models produce differing degrees of cortical damage. For example, CCI injury if sufficiently severe can completely obliterate the neocortex on one side down to layer VI. In our rat mild-moderate midline FPI model we observe frank hemorrhage extending from the white matter into Layer VI, with small petechial disruption of vasculature occasionally seen in the overlaying cortical field and on the pial surface (**see Figure 1-6**). Relative to cell replacement after injury, there has been some debate over whether neurogenesis exists in the neocortex, with some limited evidence shown that neural precursors can exist in the neocortex (Li et al., 2015; Whitman and Greer, 2009). More recent studies in a rat model of

ischemia have found that during CNS injury neurogenesis does occur in the neocortex but the neurons failure to mature (Li et al., 2015). Extension to humans is even weaker and a rather neat experiment using adult subjects older than 18 in 1945 (and thus post radioisotopes released by atomic weaponry; “bomb pulse” dating (Pravalie, 2014; Speller et al., 2012) however demonstrated that while more C14 (radioactive Carbon Isotope) was found in some hippocampal sub populations of neurons this increase was absent in the neocortex suggesting that adult neurogenesis did not occur (Bhardwaj et al., 2006); admittedly, for our purposes, this was not in the context of CNS injury.

1.11.4.1 Brain Injury and Cortical Plasticity

Cortical plasticity is dependent on both local synaptogenesis and long range axonal sprouting. As previously mentioned neurogenesis is largely absent and the current dearth of strong evidence suggests that the contribution of neurogenesis to recovery plasticity may be trivial. It has been suggested that a large part of behavioral recovery after injury may be simply due to alternative circuit reactivity underlying overall behavioral compensation (Whishaw et al., 1991; Cirstea and Levin, 2000). There is also a suggestion that the peri-injury regions near damaged tissue, particularly the vulnerable NVU, may play a more significant role in neurological recovery (Cramer et al., 1997; Jaillard et al., 2005; Teasell et al., 2005). Neuroanatomical changes occur with significant neurite outgrowth 3-14 days post injury (Stroemer et al., 1995). To some extent the absence of a true neurogenic process can make cortical recovery difficult to study due to an absence of definitive markers of neuronal replacement. This particularly presents a problem when moving from small animal models into human patients. As an example, the recovery of physically small (but appropriately sized) infarcts in a rat model of stroke may be relatively easy to overcome due to the very limited

distance of axonal sprouting necessary to bridge the damaged or destroyed tissue. In a human with a comparable proportionally sized injury, the distance required for regenerating axons to achieve synaptic repair is significantly larger from a cellular perspective. To date, one of the few treatments to show potential for cortical neuroprotection after TBI in human patients has been the combination hypothermia and hematoma evacuation, in a study occurring at the University of Pittsburgh (**D. Okonkwo Neurotrauma 2016 presentation, https://clinicaltrials.gov/ct2/show/NCT02064959**)

1.11.5 Hypotheses Tested and Dissertation Organization by Chapter

Based upon established TBI pathobiology and the concurrent induction of HO-1, we hypothesize that the time course of HO-1 response can be manipulated pharmacologically to drive early post-injury rise in HO-1, attenuating the 'peak bolus' of cytotoxic compounds and resulting in more stable substrate processing. Under such manipulation, the injured tissues will have higher acute levels of iron buffering, which, in turn, would limit peak of HO-1 feed-forward signal for a net HO-1reduction and more stable enzyme activity over time post-injury. We posit that such regulation of HO-1 expression will reduce cytotoxic insult and lead to improved histopathological and behavioral outcomes after TBI.

In the following chapters we report results of two studies which test these hypotheses, examining post-injury consequences of HO-1 heme processing and the effects of acute treatments to manipulate HO-1 response in a rat midline FPI model of mild-moderate traumatic brain injury. Chapter 2 will discuss observed regional differences in heme processing proteins between non-hemorrhagic (hippocampal) and hemorrhagic (neocortical) tissue. We find that even tissue classically interpreted as non-hemorrhagic still demonstrates a robust HO-1/heme processing-like response. Chapter 3 will discuss the effect of two heme processing treatment

paradigms, Hemin and Sulforaphane, exploring how they each affect HO-1 pathway response and the extent of behavioral recovery after injury. We find that both treatment paradigms are effective at attenuating the heme processing response and improving acute (1-3d) outcome in motor behavior, but only one treatment is effective at inducing long term (11-15d) improvement in cognitive behavior. Chapter 4 will then complete the document, providing a discussion of how the present results extend our understanding of HO-1 role in TBI, suggest novel therapeutic options and give direction for possible future studies in the field of neurotrauma.

2 Chapter 2

Chapter 2

HO-1 and Heme Processing Response Following Traumatic Brain Injury

2.1 Abstract Chapter 2

Heme Oxygenase 1 (HO-1) is the inducible form of the rate limiting enzyme in heme catabolism. HO-1 is highly upregulated in circumstances of hemorrhage and undergoes forward feedback amplification via the transcription factor Nrf2 which itself can be induced by the products of heme catabolism. As such, an acute increase in HO-1 substrate (heme) causes an acute spike in HO-1 expression in the tissue. Since there has been some uncertainty about the extent of hemorrhage in diffuse injury after traumatic brain injury (TBI) we sought to examine the expression of HO-1 along with several other markers of hemorrhage in tissues that are known to experience limited frank hemorrhage (the neocortex) contrasted to tissues that are largely absent of hemorrhage (the hippocampus). This work was performed in a central fluid percussion model of TBI which generated a mild-moderate injury with characteristic diffuse axonal injury throughout the tissue and limited hemorrhage originating in the white matter tracks overlaying the lateral ventricles which typically extends into layers V and VI of the neocortex. We tracked our observations through 15d post-injury. Our results showed striking similarities in the hippocampal and cortical measures of HO-1 regardless of observed hemorrhage in the tissue. In both cases HO-1 expression peaked at 3d and expression was notably higher relative to Sham in the hippocampus compared to the neocortex. This finding was consistently supported by measurements of other injury and hemorrhagic markers. The iron scavenging protein Lipocalin 2 (LCN2) was markedly elevated at 1d post-injury and had expression ~10 fold higher in the hippocampus. Ferritin, an iron storage protein and marker of prior hemorrhagic injury, was similarly elevated in both tissues, peaking at 7d and while expression was higher at 7d in the neocortex the hippocampus showed persistent elevation through 15d that was higher than the

neocortical measure. These results appear to show that there is a consistent underlying hemorrhagic processing response which occurs in both the hippocampus and neocortex and is suggested that the underlying process may be generalizable in diffuse injury.

2.2 Introduction Chapter 2

Traumatic Brain Injury (TBI) is an enduring public health burden that to date has been resistant to therapeutic intervention. Fundamental to understanding how to treat TBI is deconstructing the multimodal injury that occurs into discrete parts that can be studied. Many different animal models have been developed as a result, each tending to produce a characteristic injury representative of one or another aspect of TBI. To further understand the diffuse injury that frequently develops after TBI we have documented the post-injury time course of heme processing using a central fluid percussion injury (FPI) model.

Classically diffuse injury has been characterized by extensive point disruptions of the axolemma in long axons and has been interpreted to be relatively independent of other injury process (e.g. gross tissue necrosis or hemorrhage related damage). It has been previously noted in more hemorrhagic models of TBI that heme processing proteins, including HO-1, are upregulated after injury. Our prior observations with gene chip assay showed that HO-1 was consistently elevated in all brain regions examined and in both rat and mouse tissue. We found this curious since the model used has been characterized as demonstrating limited hemorrhage largely restricted to the corpus callosum and white/grey matter (WM/GM) interface. Nonetheless our samples universally demonstrated upregulation even in tissue (the hippocampus) that has not been described as hemorrhagic in this model.

This is interesting for a variety of reasons. Free heme has been well characterized as inducing local tissue pathology (Chang et al., 2005). The blood brain barrier/neurovascular unit (BBB/NVU) and its relative impermeability to blood constituents provides a unique condition for

tissue heme processing/elimination, and metabolites of heme are known to have cytotoxic properties (Ryter et al., 2006; Chang et al., 2005). In our application of the FPI, we tend not to observe overt bleeds in the hippocampus but it remains possible that there might be a minor, undetected hemorrhagic process that underlies the injury. The role of this potentially undetected change in the NVU is the main focus of the first portion of this study. We hypothesized that the hippocampus may experience heme injury pathology that has not been previously identified and this may be a secondary component of diffuse injury that, to date, has not been recognized as significant. Towards this end we examined the change of heme driven response molecules within the injured hippocampus and compared these results to change in the same proteins within the neocortex overlaying the major WM/GM interface bleed, which includes small petechial hemorrhages.

The characteristic injury in the FPI model is diffuse axonal injury, a process that occurs through a mechanism whereby focal membrane disruption in the axolemma leads to ion dysregulation, cytoskeletal disruption, and axonal functional impairment, resulting in persistent neurocognitive dysfunction. It is possible that a similar effect may occur in the NVU since the relatively fine membrane shearing that results in axolemmal damage could similarly result in disruption of cell membrane-basal lamina connections, even in the absence of gross tissue displacement. To date no successful treatments for TBI induced axonal injury have been demonstrated and we are interested in exploring if an underlying heme processing response is complicating the known injury process to affect treatment efficacy.

2.2.1 Figure 2-1: Pathway of Heme Metabolism

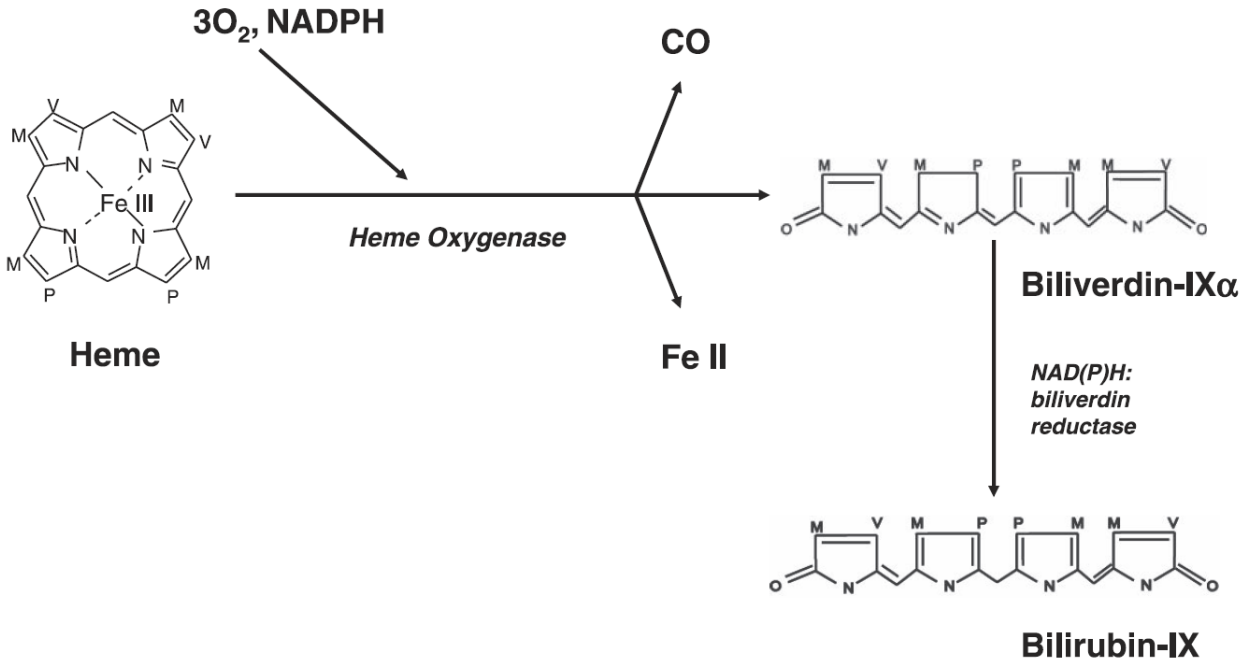

Figure 2-1: *The pathway of heme metabolism. Heme oxygenase enzymes (HO; E.C. 1.14.99.3; heme-hydrogen donor: oxygen oxidoreductase) catalyze the rate-limiting step in heme metabolism. Both HO enzymes (HO-1 and HO-2) oxidize heme (ferriprotoporphyrin IX) to the bile pigment biliverdin-IXα.The reaction requires 3 mol of molecular oxygen and NADPH:cytochrome P-450 reductase as a source of electrons. The cleavage of the heme ring releases the coordinated iron, as well as the α-methene bridge carbon as carbon monoxide (CO). The principal HO reaction product, biliverdin-Ixα, is further metabolized to bilirubin-Ixα by NAD(P)H:biliverdin reductase (BVR). M, methyl; V, vinyl; P, propionate.* Pathway of Heme Metabolism reproduced with permission from Ryter et al., 2006.

Heme Oxygenase 1 (HO-1) is the inducible form of the rate limiting enzyme in heme catabolism. HO-1 catabolizes heme into the potential neurotoxins carbon monoxide (CO), Iron (Fe), and Biliverdin by cleaving heme at the alpha-methene bridge which directly releases CO and removes the binding stability of Fe in the center of the Heme structure leaving behind the open metalloporphyrin Biliverdin (**Figure 2-1**). HO-1 is induced by a variety of stimuli, chief amongst them heme substrate itself, and HO-1 has a high degree of specificity for free heme (e.g. heme B unbound by hemoglobin or neuroglobin) over other forms of heme or metalloporphyrins (Kutty and Maines, 1982; Maines et al., 1986; Maines, 1988; Yoshinaga et al., 1982). Heme B only accumulates in tissue under pathologic conditions (Maines, 1988) and has known pathogenicity that results both from its own effects and those of its breakdown products (Huang et al., 2002; Maines and Trakshel, 1993; Regan and Panter, 1996; Ryter et al., 2000; Wu et al., 2003). Heme and the products of heme catabolism have been shown to be individually bioactive (Platt and Nath, 1998). Two major enzymes exist to degrade heme, HO-1 the inducible form and HO-2 the constituently expressed form. HO-1 has been shown to be the dominant form involved in erythrocyte senescence, but there have been conflicting reports after CNS injury as to which form predominates. In large part this is likely to be due to time dependent changes in expression as HO-1 requires an induction trigger. Additionally, a rather unique aspect of hemorrhage is that extravasated erythrocytes require several days before they are lysed/phagocytosed and release their cytosolic stores of heme in a process that appears to be mediated by CD47 loss.

Previous studies have shown elevations of HO-1 in grossly hemorrhagic models of brain injury and in this study we examine HO-1 expression using a model of diffuse mixed mild/moderate TBI with minimal hemorrhage, contrasting a region which experiences small

frank bleeds (neocortex) with a region that generally lacks hemorrhage (hippocampus). The study is performed within rat midline FPI, a model that is frequently chosen to study the cellular effects of diffuse brain injury. Here we examine time dependent differences of induced HO-1 expression and hemorrhage between two brain regions known to be selectively vulnerable to diffuse injury: the neocortex and the hippocampus (Farkas and Povlishock, 2007). Both brain regions are associated with the well characterized neurocognitive deficits that persist after injury, showing variable recovery 7-30d post injury depending on injury severity, metric, and test sensitivity. The well-defined time course of reactive synaptogenesis underlies the capacity for this post-injury recovery, having clear early degenerative and later regenerative phases. Key to our interest in the HO-1 pathway is the rapid rise in IBA1+ and GFAP+ reactivity that occurs ~3-4d post-injury associated with debris clearance and axonal degeneration. Moreover, this early degeneration exactly matches the rise in IBA1+, GFAP+ reactivity known to occur in response to hemorrhage and suggests that there may be a mixed or co-signaling interaction between reactive glia and HO-1pathways. That is, brain regions known to be particularly affected by aggressive immune cell scavenging may be responding not only to local axonal pathology but also to nearby heme driven activation.

In this first study, we propose to map time dependent changes in HO-1 after rat midline FPI, correlating these measures with markers of heme catabolism, tissue damage and extracellular matrix (ECM) proteins critical to tissue remodeling. To understand how these molecules relate to the parallel process of synaptic recovery, animals were grouped into select cohorts whose brains were harvested for fresh tissue homogenates (hippocampus and neocortex) or aldehyde tissue perfusion (whole brain) on days 1, 3, 7, 14/15 post-injury.

2.3 Methods Chapter 2

2.3.1 Experimental Animals

The procedures in this study met national guidelines for the care and use of laboratory animals with all experimental protocols approved by the VCU Institutional Animal Care and Use Committee (IACUC). Male Sprague-Dawley rats (290-360g, ENVIGO, Huntingdon, UK) were used in these experiments, housed in pairs when possible under a temperature (22^{o}C) and humidity (66%) controlled environment with food and water provided ad libitum and subjected to a 12 hour dark-light cycle. Rats were randomly assigned to either TBI (n=26), or Sham-injured (n=21) groups and evaluated at 1d, 3d, 7d, or 14d/15 post-injury by WB or **immunohistochemistry (IHC)**. For all analysis Sham-injured animals served as controls for the TBI animals.

2.3.2 Surgical Preparation for Rat Central Fluid Percussion Injury

Twenty-four hours prior to central fluid percussion injury animals underwent surgical preparation to mitigate acute inflammatory response confounding. Rats were anesthetized with 4% isoflurane in carrier gas (70% N_2O, 30% O_2) for 4 minutes, heads shaved, and maintained on 2% isoflurane in carrier gas delivered via nose cone for the duration of the surgery. Surgical site is cleaned with iodine solution followed by 70% ethanol and a surgical drape placed over the animal. Body temperature was maintained at 37^{o}C via heating pad (Stryker, Kalamazoo, MI), and animal vital signs (heart rate, arterial oxygen saturation, respiratory rate, pulse distention, and breath distention) monitored via pulse oximeter (MouseOX; Starr Life Sciences, Oakmont,

PA). While under anesthesia rats were secured in a stereotaxic device (Harvard Apparatus, Holliston, MA) via ear bars and a midline incision used to expose the cranium to permit a midline sagittal craniectomy midway between the lambda and bregma sutures of 4.8 mm diameter to allow visualization of intact dura mater. Two 3/16 in steel machine screws were implanted into the skull 1 cm from craniectomy center in the 1st and 3rd quadrants. The craniectomy was fitted with a modified (tapered) Luer Lock hub (2.6 mm i.d.) fixed with cyanoacrylate adhesive. Additional stability is provided using dental acrylic (Coltene/Whaledent, Inc., Cuyahoga Falls, OH) to secure screws and Luer Lock hub into a single complex. The hub was finally filled with saline to limit clotting and tissue damage prior to injury. The incision wound was sutured over the complex and treated with triple antibiotic ointment and lidocaine. Animals were monitored for post-surgical stress in a heated holding cage during the acute recovery phase prior to being returned to their home cage.

2.3.3 Central Fluid Percussion Injury

The fluid percussion injury device consists of a weighted pendulum and a 0.9% saline filled acrylic cylinder (Custom Design and Fabrication, Petersburg, VA) which is fitted with a metal pressure transducer (Entram Devices, Inc., model EPN-0300-100A). Injury is induced by releasing the weighted pendulum from a pre-determined empirically derived height which strikes a greased rubber piston on one end of the cylinder producing a pressure wave which injects a small volume of saline into the dura of the animal attached to the other end of the cylinder via the Luer Lock fitting (**Figure 2-2;**(Dixon et al., 1987). Height of the pendulum corresponds monotonically with injury peak pressure which in turn corresponds with injury severity. Twenty-four hours after preparative surgery, animals were anesthetized 4% isoflurane in carrier gas for 4

minutes and given a scalp incision to expose the hub complex. Animals were then attached to the fluid percussion device by filling the hub with sterile 0.9% saline to ensure a seal free of air bubbles and clots. Animals then received a mild-moderate fluid percussion injury (2.0 ± 0.1 ATM overpressure) via saline injection into the closed cranial cavity. The pressure pulse was measured by the transducer and displayed on an oscilloscope (Tektronix 1000 S, Beaverton, OR) and the peak of the pressure wave recorded. Prior to recovery of consciousness, the hub was removed and the incision sutured closed and treated with topical triple antibiotic and lidocaine. To determine and confirm injury severity, reflexes (tail, paw, ear, corneal blink) and righting times were recorded prior to acute recovery. Sham injured animals underwent the same surgical preparation and hub removal procedures but did not receive central fluid percussion injury. For Sham injured animals reflexes and righting time were not recorded as they do not differ from naïve anesthesia treated animals.

2.3.4 Protein Extraction

Rats were anesthetized with 4% isoflurane in carrier gas (70% O_2, 30% NO_2) for 4 min and sacrificed by decapitation at the appropriate experimental interval 1, 3, 7, 15d after FPI/Sham injury. Neocortex trimmed of white matter and obvious hemorrhages sampled from the central square of a 3x3 grid arranged on the surface was collected along with whole hippocampal bulbs trimmed of any extraneous tissue (n=4-7/group). Tissue samples were homogenized on ice in 250 uL of RIPA Lysis Buffer (EMD Millipore, Billerica, MA) with cOmplete protease inhibitor + EDTA (Roche Diagnostics, Mannheim, Germany) prior to separation via 14,000 g centrifugation for 20 min at 4^{o}C. Supernatant was aliquoted and stored with separated nuclear pellet at -80^{o}C. Protein concentration of extract was determined using

Pierce BCA Protein Assay Reagent kit (Thermo-Fisher, Waltham, MA) on a Fluostar Optima plate reader (BMG Labtech, Inc., Cary, NC).

2.3.4.1 Figure 2-2: cFPI Device

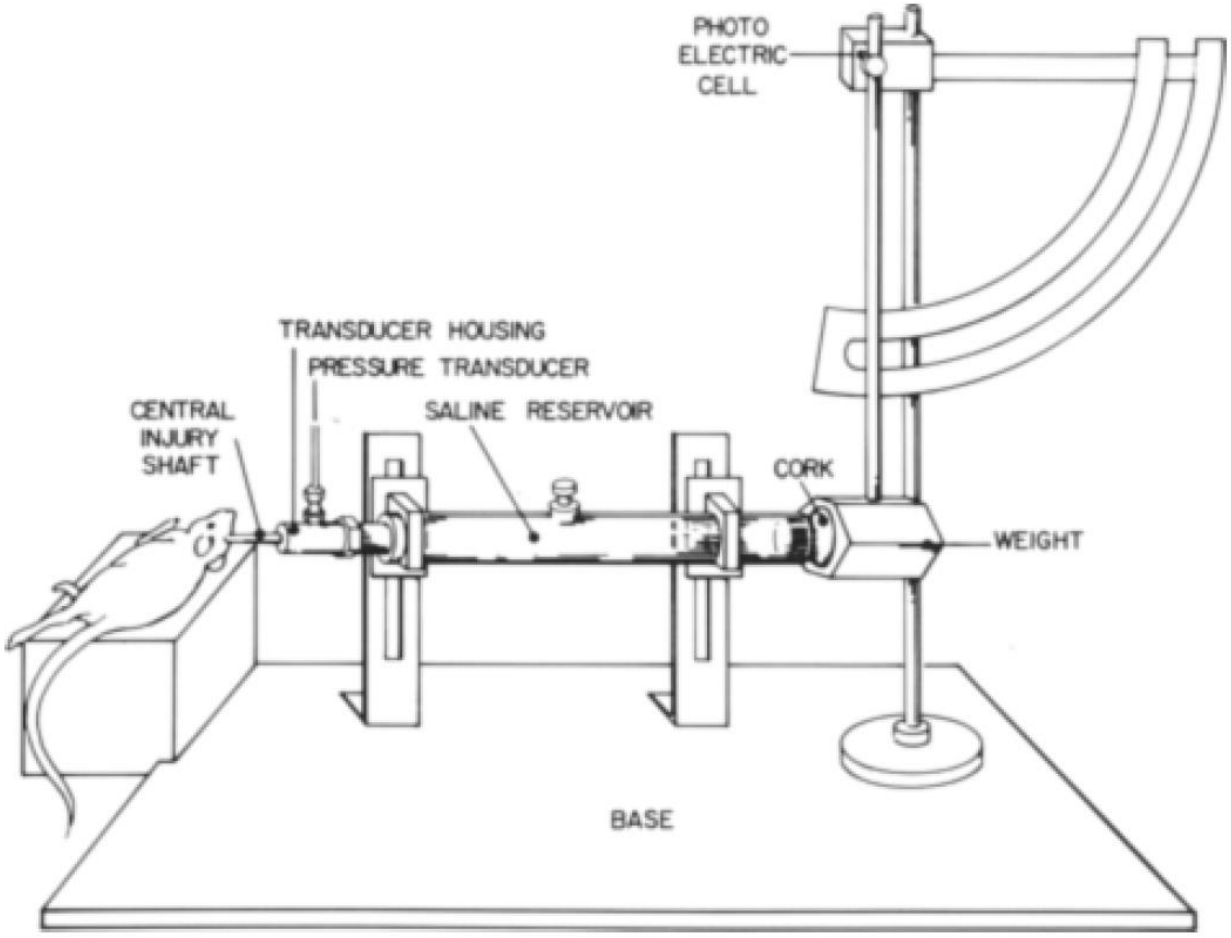

Figure 2-2: *Diagram of fluid percussion model of brain injury. A 4 mm central craniectomy central craniectomy is connected to one end of a Plexiglass cylinder filled with physiologic saline. At the other end in the cylinder is a Plexiglas cork mounted on O-rings. Injury is produced by striking the cork with a 4.8 kg pendulum dropped from a specific height. The pressure transient is recorded on a storage oscilloscope with an extra-cranial transducer.* Figure and text reproduced with permission from Dixon et al., 1987. In our paradigm we note several small changes including a central craniectomy 4.8 mm in diameter and the addition of a firm rubber tip on the end of the cylinder cork.

2.3.5 Western Blotting

Western Blot (WB) analysis was carried out using Bio-Rad products on their Criterion Gel system using 18 or 26 lane Criterion XT Bis-Tris Gels (Hercules, CA). 50 or 25 ug of protein were prepared in XT Sample Buffer with XT Reducing Agent and homogenized prior being denatured at 95^{o}C for 5 mins. Samples were electrophoresed on 4-12% or 12% gels in MOPS running buffer at 200v for 45 min (after 50v x 5 min stacking period) or until tracking dye approached the gel foot. Protein was transferred onto PVDF or Nitrocellulose membranes at 100v for 1 hour in a Tris-Glycine buffer with 10% **methanol (MeOH).** Post-transfer the remaining protein on the gels was stained with 0.1% Coomassie Brilliant blue in 40% MeOH+10% **glacial acetic acid (HOAc)** overnight prior to de-stain and visualization to confirm even protein load and transfer. Meanwhile, membranes were rinsed with nano-pure deionized water before buffering with **Tris-buffered saline (TBS)** and blocking for 1 hour with 5% non-fat milk in TBS with 0.5% Tween (mTBST). Membranes were incubated with appropriate antibody at 1:1K or 1:2k **(see Table 2-1)** dilution overnight at 4^{o}C. After incubation, membranes were washed with mTBST and then incubated with the appropriate HRP-linked secondary for 1 hour at room temperature. Membranes were then washed in TBST to remove excess non-specific signal and finally in TBS to remove tween surfactant effects. Membranes were visualized via chemiluminescence using Super Signal West Dura Extended Duration Substrate (Thermo-Fisher, Waltham, MA). Quantitative data was collected using a Syngene G:Box with protein bands subjected to densitometric analsysis using Gene Tools software (Syngene, Frederick, MD). Protein data was expressed as fold change relative to time matched Sham control animals processed on the same membrane. Confirmation of load control was determined using beta actin

(Sigma-Aldrich, St. Louis, MO) with a known caveat that signal may modestly change during TBI.

2.3.6 Tissue Fixation

Rats were anesthetized with 4% isoflurane in carrier gas (70% O_2, 30% NO_2) for 4 min with sodium pentobarbital (400 mg/kg IP) and sacrificed via transcardial perfusion; flushed with 0.9% saline with a clamped descending aorta and snipped right atrium. When perfusion runs clear tissue is perfused with 4% paraformaldehyde in phosphate buffer (0.1 M $NaHPO_4$, pH=7.4). Once tissue was fixed whole intact brains were removed from the cranium and placed in excess tissue fixative for 24 hours prior to transfer into 0.03% NaN_3 in 1.0 M **Phophate Buffered Saline (PBS)** and storage at 4^o C. Prior to utilization for immunohistochemistry tissue was blocked and sectioned into 40 um coronal slices using a Leica Vibratome (VT1000S; Leica Biosystems Inc., Buffalo Grove, IL). Sections were stored separated and organized in PBS + Azide at 4^oC.

2.3.7 Immunohistochemistry

Free floating sections were selected based on rostral-caudal position and permeabilized in 5% peroxidase for 30 mins. Tissue was washed in PBS and the blocked using fish gelatin in PBS + 0.05% triton X-100. Tissue was incubated overnight with primary antibody in blocking buffer (**see Table 2-2**) at 4^oC. The following day sections were washed with PBS prior to further blocking for 30 minutes and incubated with secondary fluorescently tagged antibody in blocking buffer for 2 hours at room temperature. Sections were then washed in PBS, rinsed in Phosphate

Buffer to remove salt artifact and mounted on Superfrost Plus slides (Fisher Scientific, Pittsburgh, PA), and allowed to air dry. When dry sections were coverslipped using Vectashield + DAPI (Vector Laboratories, Burlingame, CA). Fluorescent signal was visualized on a confocal Zeiss LSM 700 (Carl Zeiss, Thornwood, NY), on an apotome Zeiss AxioImager M2 (Carl Zeiss, Thornwood, NY), or on a widefield Olympus BX51 (Olympus, Tokyo, JP).

2.3.8 Statistics

The effects of injury condition and time post-injury were evaluated using the statistical software R using 2-way **Analysis of Variance (ANOVA)** analysis with post hoc TukeyHSD pairwise analysis of major effects. Pairwise analysis of timecourse interactions were computed using t-tests with Benjamini-Hochberg correction. In circumstances where the assumption of normality is violated, as observed via qualitative analysis Q-Q intervals and Cook's distance, data was normalized via log transform and timecourse interactions detected using Wilcoxon-Mann-Whitney tests. Western Blot and Zymography results are reported as mean ± **standard error of the mean (SEM)**. In all cases the analysis is done using two tailed tests where appropriate and with an alpha level of 0.05. Further, zymogram results involve multiple gelatinase metrics located on the same gel and are further analyzed via **Multivariate Analysis of Variance (MANOVA)** prior to subgroup ANOVA.

2.3.9 Table 2-1 Antibodies used in Western Blot Experiments

Antibody Target	Antibody Host and Type	Antibody Source and Serial Number	Typical Secondary Used 1:15k	Typical Membrane Used	Concentration Used
HO-1	Rabbit, Polyclonal	Stressgen, ADI-OSA-150	Harlan, 611-103-122, Goat anti-Rabbit	PVDF	1:1k 1:2k
FTL	Goat, Polyclonal	ABCAM AB Thermofisher	Santa Cruz, SC-2352, Bovine anti-Goat	PVDF	1:2k
LCN2	Goat, Polyclonal	R&D Systems AF3508	Santa Cruz, SC2352	Nitrocellulose	1:1k

2.3.10 Table 2-2: Antibodies used in Immunohistochemistry Experiments

Antibody Target	Antibody Host and Type	Antibody Source and Serial Number	Typical Secondary Used 1:1k	Concentration Used
HO-1	Rabbit, Polyclonal	Stressgen, ADI-OSA-150	Alexa-488	1:300
FTL	Goat, Polyclonal	ABCAM AB Thermofisher	Alexa-488/594	1:300
LCN2	Goat, Polyclonal	R&D Systems AF3508	Alexa-594	1:200
GFAP	Chicken, Polyclonal	Encor Biotechnologies	Alexa-594	1:200
IBA1	Goat, Polyclonal	AB5076	Alexa-594	1:300

2.4 Chapter 2 Data

We began our study of heme processing and manipulation by observing the endogenous progression of a hemorrhagic injury over time. Rats were surgically prepared with a day -1 craniectomy with a hub implant attached to their skull midline between lambda and bregma. Rats received a cFPI injury ~2.0 ATM overpressure with righting times ~7:00 minutes. After injury at periodic survival intervals select animals were anesthetized and perfused for later tissue histology.

We observed that heme pigment was easily identifiable in coronal tissue sections at 1d and 3d post injury with a significant reduction to near absence at 7d post injury (**Figure 2-3**). At 1d we see a loose organization of bleeds that seem to originate in the white matter of the callosum and along the grey/white interface into cortical layer VI. No observable bleeds are found in the hippocampus though occasional heme pigment is observed adjacent to the alveus. At 3d post injury the bleeds have both condensed cellularly and reached their point of maximum expansion concurrently with cortical thinning compressing the bleed boundary and a portion of the red heme pigment has shifted towards a yellowish color indicative of bilirubin, heme's degradative product (**Figure 2-4**). At 7d Heme pigment is largely absence though limited quantities of bilirubin pigment are still observable and cortical thinning has continued.

In general even though we are using a midline cFPI model we only occasionally see signs of injury or tissue disruption underneath the hub site. Instead the major locus of bleed in our model appears to be in the white matter tracks of the corpus callosum and along the white

matter/gray matter interface with bleeds frequently extending into layer VI neocortex and occasionally further to layers V & IV.

2.4.1 Figure 2-3: Widefield Hemorrhage after cFPI 1-7d Post-Injury

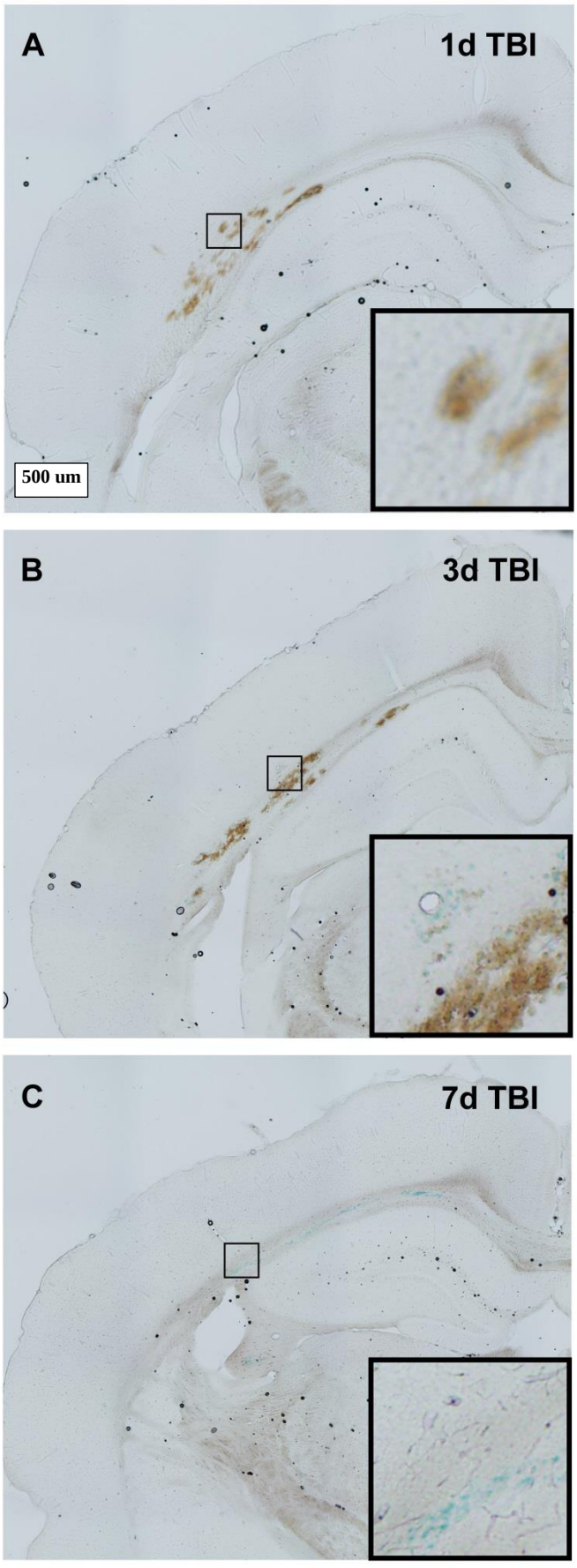

Figure 2-3: Widefield 4x single neocortex images (A-C) showing typical progression of bleed resolution 1d (A), 3d(B), and 7d(C) post injury. At 1d pigment is typically seen as a reddish-brown discoloration of the tissue. By 3d (B) some pigment has been reduced and deposits of iron begin to appear via Perls stain (blue pigment). By 7d (C) minimal heme is seen with some bilirubin (yellow pigment) observed and notable deposits of iron are observed.

2.4.2 Figure 2-4: Enlarged view of 3d Post-Injury Hemorrhage

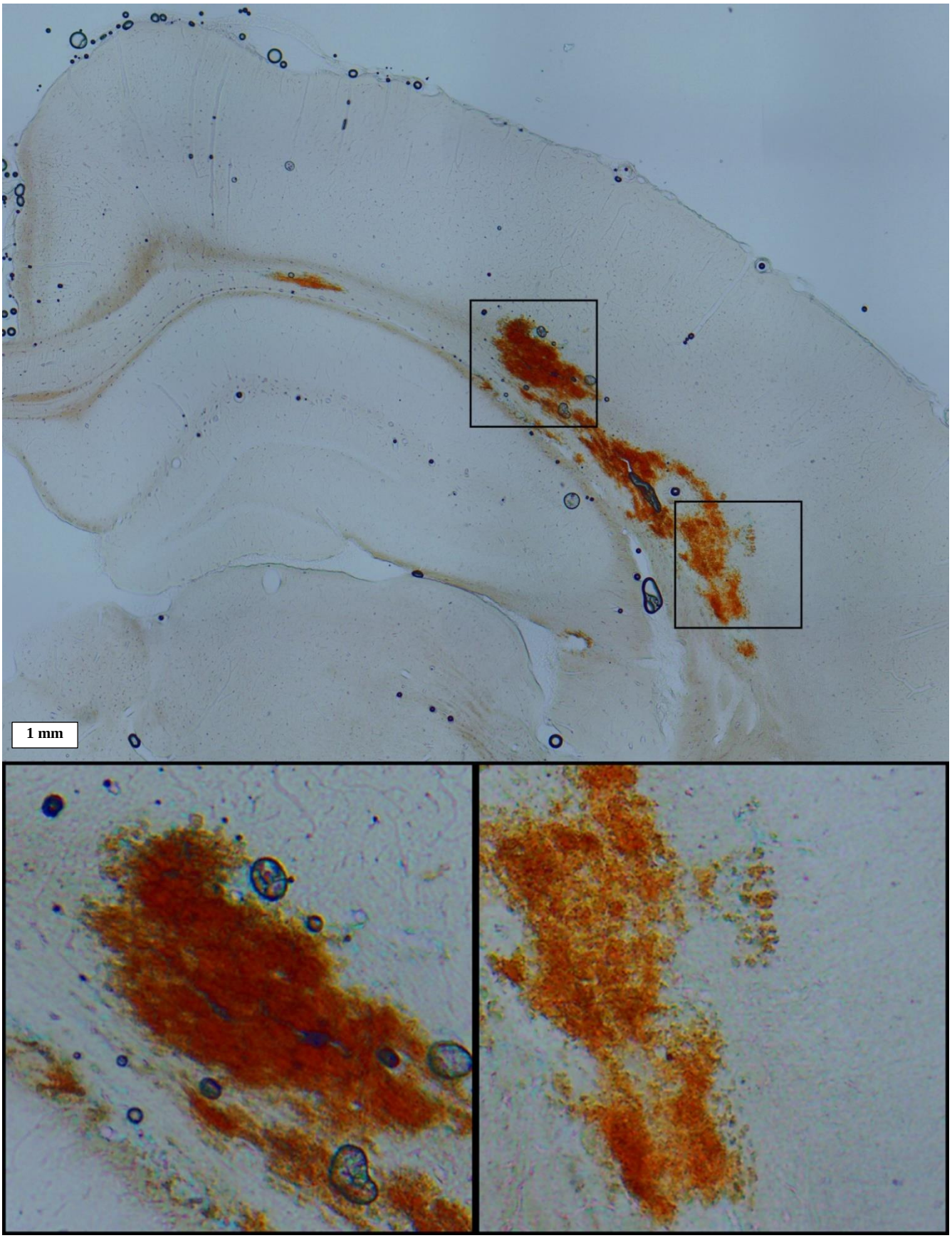

Figure 2-4: Widefield 4x single neocortex image showing a detailed perspective of a typical bleed at 3d post-injury showing both reddish heme pigment and yellowish bilirubin concurrent with Perls stain in higher detail. Particularly contrast the dense reddish pigment seen in the l inset compared to the thinner and more processed r inset which shows generalized shift towards yellow pigment with blue pigment (iron deposits) scattered around the periphery.

After examining the progression of heme pigment we next examined the expression of HO-1, the inducible form of the enzyme responsible for heme processing in the tissue.

We observe that HO-1 is greatly elevated after TBI (**Figure 2-5**). In 4x widefield images it is apparent that there is a high degree of immunoreactivity throughout the neocortex that overlays bleed injuries in the WM-WM/GM interface. Frequently we found this injury to variably lateralize and frequently one side demonstrated a more severe and expansive bleed. Higher magnification (10x) reveals extensive expression directly adjacent to the bleed sites (though with some autofluorescence artifact due to the bleed) and in the hippocampus. There is increased expression in the dentate gyrus and molecular layer or CA1. Over time we see consolidation of HO-1 expression; at 1d we see bright immunofluorescence that appears to remain stable through 3d before declining from 7d-15d. We also observe that over time the cells that most highly express HO-1 are found in different positions progressively. In the hippocampus HO-1 expression in the inferior dentate molecular layer disappears after day 3 while expression persists in the superior molecular layer and expands across the hippocampal fissure into the molecular layer of CA1.

2.4.3 Figure 2-5: HO-1 Response to Injury Over Time

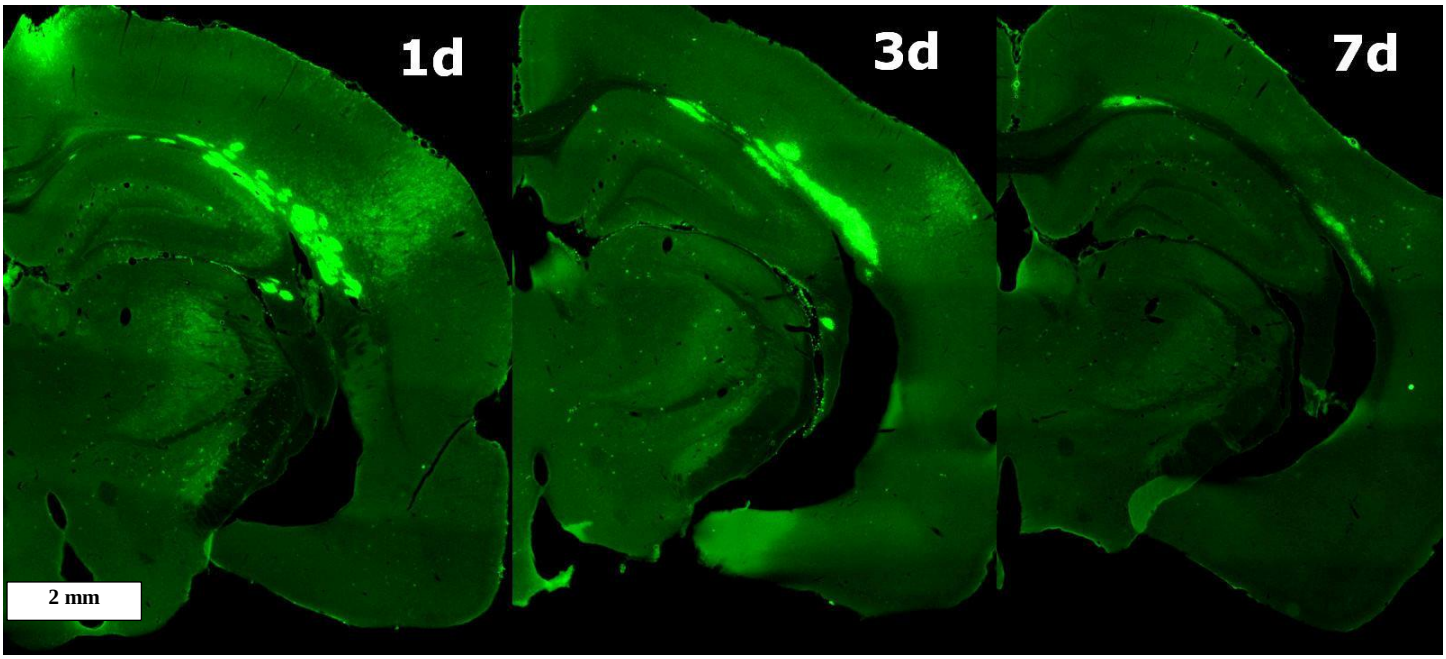

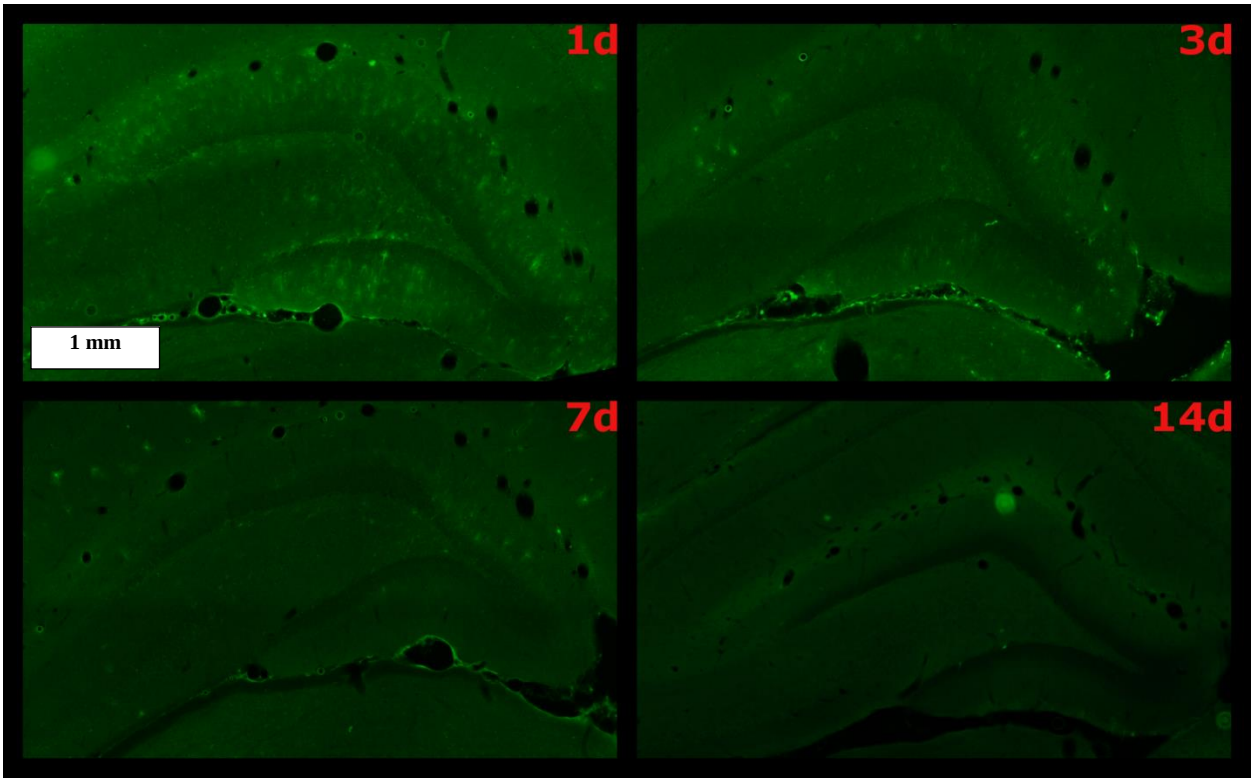

Figure 2-5: Widefield 4x (A-C) and 10x (D-G) tile scans of HO-1 progression overall (A-C) and the hippocampus (D-G) over time. Note broad expression of HO-1 near the bleed with general consolidation of signal 1-3d and signal reduction 7d+.

2.5 HO-1 Change Neocortex vs Hippocampus

We proceeded to utilize confocal microscopy at 20x to observe co-expression with other cell marker proteins (**Figure 2-6**) we observed that HO-1 was highly reactive in both the neocortex and the dentate gyrus after injury and in the concentrations of HO-1 used for staining there is nearly no signal observed in Sham animals. In both the dentate gyrus and in reactive neocortex HO-1 appears to primarily co-express with GFAP+ cells with only occasional IBA1+ crossover.

2.5.1 Figure 2-6: Acute Changes in HO-1 vs GFAP or IBA1 in Hippocampus and Neocortex

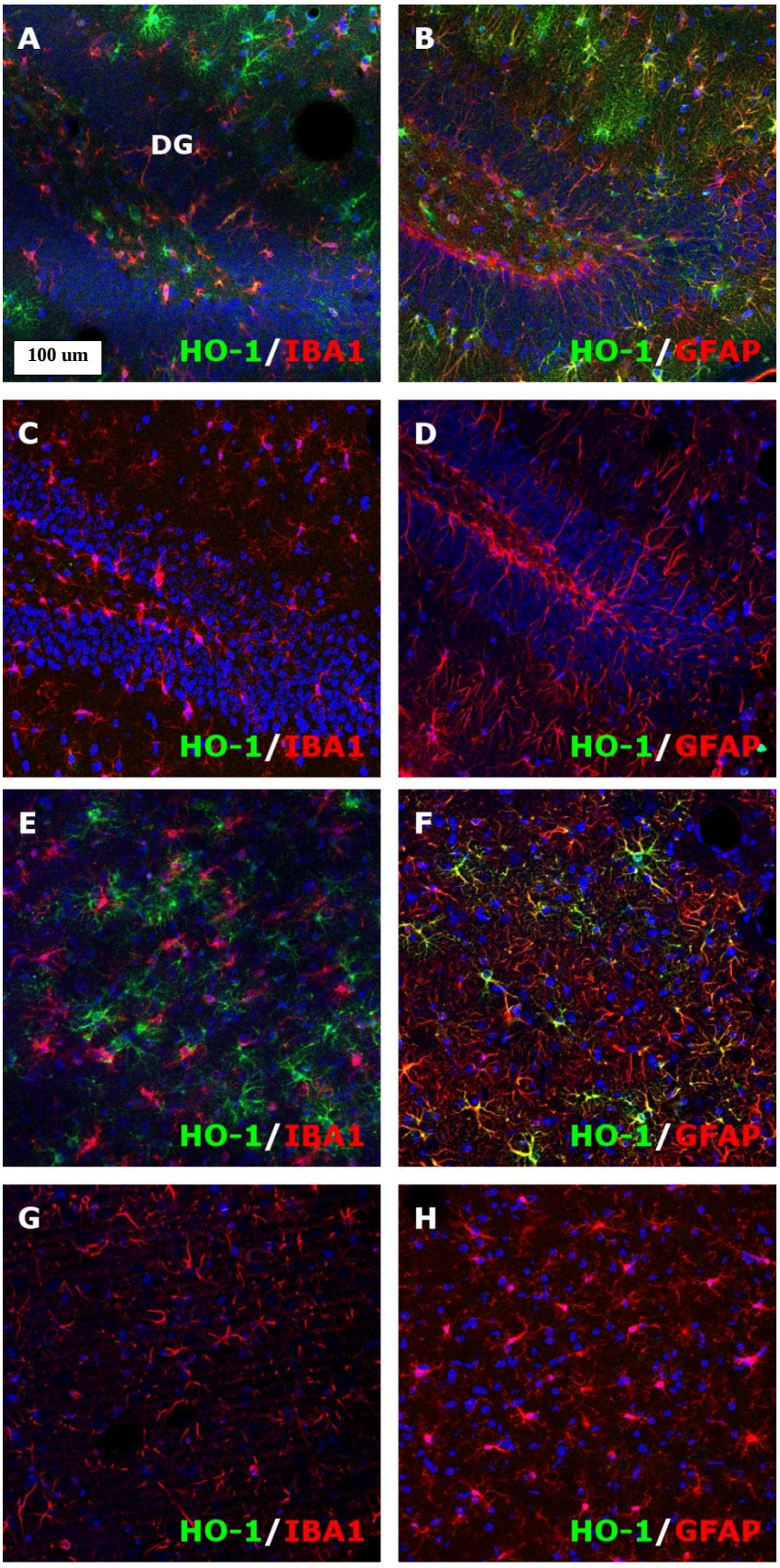

Figure 2-6: Confocal 20x 1d Injury (A-B, E-F) vs Sham (C-D, G-H) HO-1 expression paired with cell marker labels for astrocytes (GFAP) and microglia (IBA1). Note essentially no HO-1 expression in Sham animals and prominent reactivity in injured animals. Further, note that HO-1 coexpresses most frequently with GFAP.

In order to examine net changes in tissue expression of HO-1 we sampled animals 1-15d after injury at select intervals (1,3,7,15d) bilaterally taking cortical samples trimmed of white matter and any observable interface bleeds as well as whole hippocampal bulb samples.

We observed that HO-1 significantly increased in both Neocortex and Hippocampus after injury with an expression peak at 3d post-injury (**Figure 2-7**). In the neocortex ANOVA using the model $\boldsymbol{Value \sim Day * Condition}$ showed significant main effects due to Day, Condition, and their interaction (p =4.992e-07, 1.094e-07, 4.992e-07 respectively). TukeyHSD post-hoc analysis of group effects showed a TBI-Sham comparison of p < 2e-16. Pairwise Wilcoxon daily comparisons with Benjamini-Hochberg correction showed there is a significant increase in expression vs Sham by 1d (555 ± 57%, p = 0.0257), peak expression at 3d (1317± 218%, p = 0.0065), declining at 7d (237± 42%, p = 0.0556), and dropping to near Sham levels though maintaining significance at 15d (137± 11%, p = 0.0410).

In the hippocampus ANOVA using the model $\boldsymbol{Value \sim Day * Condition}$ showed significant main effects due to Day, Condition, and their interaction (p = 0.0005406, 0.0036844, 0.0005406). TukeyHSD post-hoc analysis of group effects showed a TBI-Sham comparison of p= 0.0017829. Pairwise Wilcoxon daily comparisons with Benjamini-Hochberg correction showed there is a modest increase in expression by 1d post-injury (228± 50%, Not Significant), peak expression at 3d (2037± 589%, p =0.033), declining at 7d (234± 33%, p = 0.049), and dropping to near Sham levels at 15d (141± 25%, Not Significant).

In both tissues we demonstrated increases in HO-1 peaking at 3d which is consistent with literature observations and the expected timeline of heme degradation but seems somewhat at odds with our cell staining particularly in widefield images. In large part we attribute the

perceived brighter signal in the widefield images as a partial image artifact due to widespread autofluorescence of heme in the necrotic site causing a washout effect paired with diffuse cell reactivity that condenses and organizes 1-3d post-injury.

2.5.2 Figure 2-7: HO-1 Western Blot Time Course 1-15d

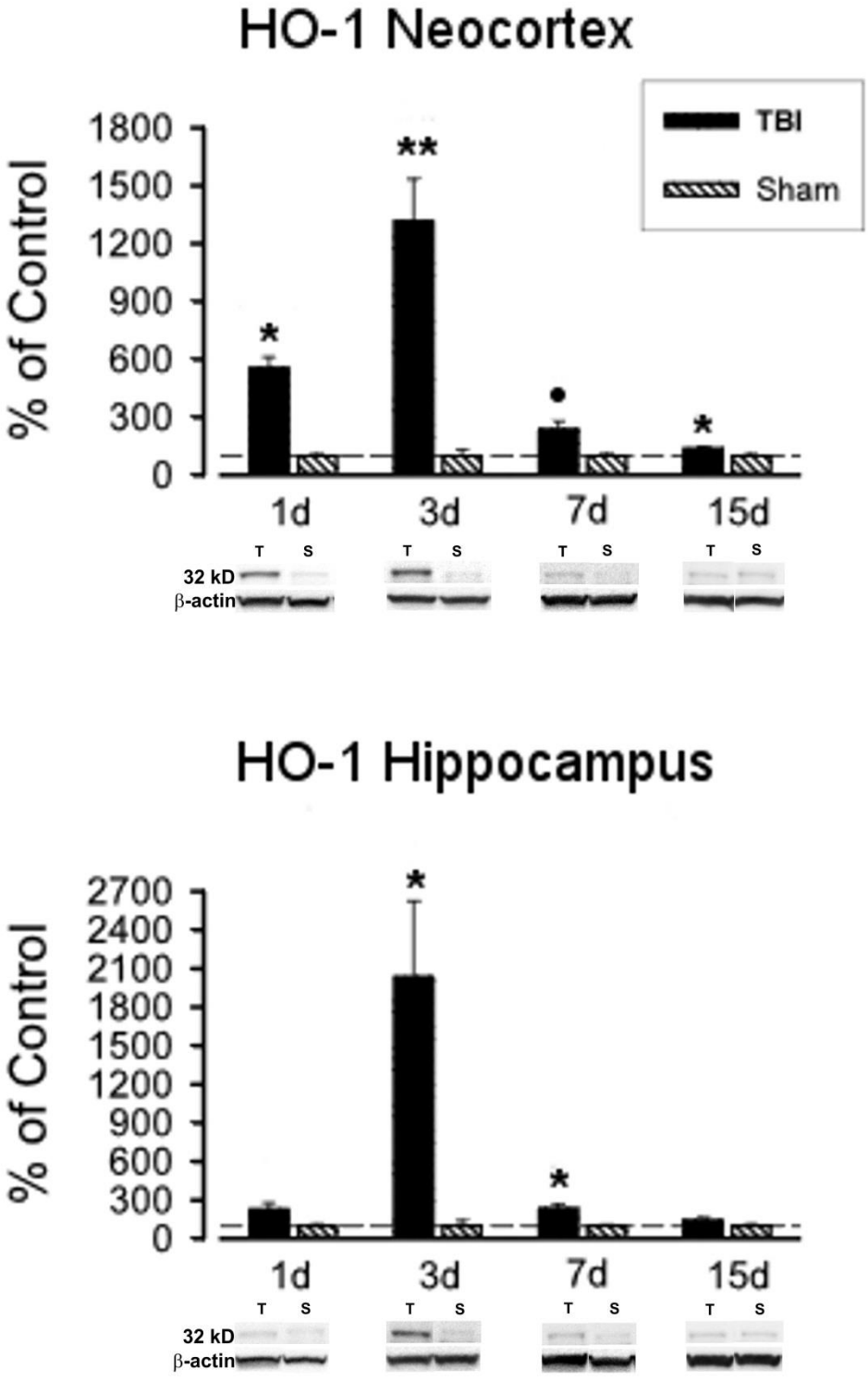

Figure 2-7: Western Blot expression of HO-1 in Sham vs TBI 1-15d post-injury. HO-1 is significantly elevated by 1d in the neocortex and peaks in expression at 3d post-injury. The hippocampus shows an early elevation at 1d which is significant and peaks at 3d. In the neocortex this elevation drops to near Sham by 15d but is still significantly elevated. In the hippocampus expression is significantly elevated through 7d and elevated but not significant at 15d. Note that 1d relative expression is higher in the neocortex but expression peaks highest in the hippocampus. (Mean ± SEM, n=5-7/group; Wilcoxon-Test with Benjamini-Hochberg correction, *, **, *** for $p < .05, .005, .0005$ respectively; ANOVA $p < 5*10^{-8}$ Neocortex, $p < 5*10^{-3}$ Hippocampus)

Having established the timeline of HO-1 expression in the tissue we next turned to looking at which cells expressed HO-1 during the progression.

We observed that in the neocortex there are two distinct regions (here described as hemorrhagic/necrotic and reactive) of HO-1 reactivity and their associated glia change depending on location. Away from bleeds the reactive neocortex shows expression of HO-1 that appears to organize and peak 1-3d post injury and is characterized by co-expression with GFAP+ cells that persists through 15d (**Figure 2-8**). There is occasional but limited co-expression observed in IBA1+ cells and these instances increase when imaging closer to the necrotic injury sites. In contrast when directly imaging near the necrotic site (**Figure 2-9**) there is extensive co-expression of HO-1 in IBA1+ cells that are both on the boundary of the injury site and pervasive through them. HO-1+ GFAP+ positive cells are observed directly backing against these HO-1+ IBA1+ cells. Of particular note is the correlation of HO-1+ IBA1+ cells with capillaries inside or near the bleed site which appears to show IBA1+ cells highly reactive for HO-1 extravasating into the tissue.

2.5.3 Figure 2-8: HO-1 and Glial Reactivity in Reactive Neocortex 1-7d Post-Injury

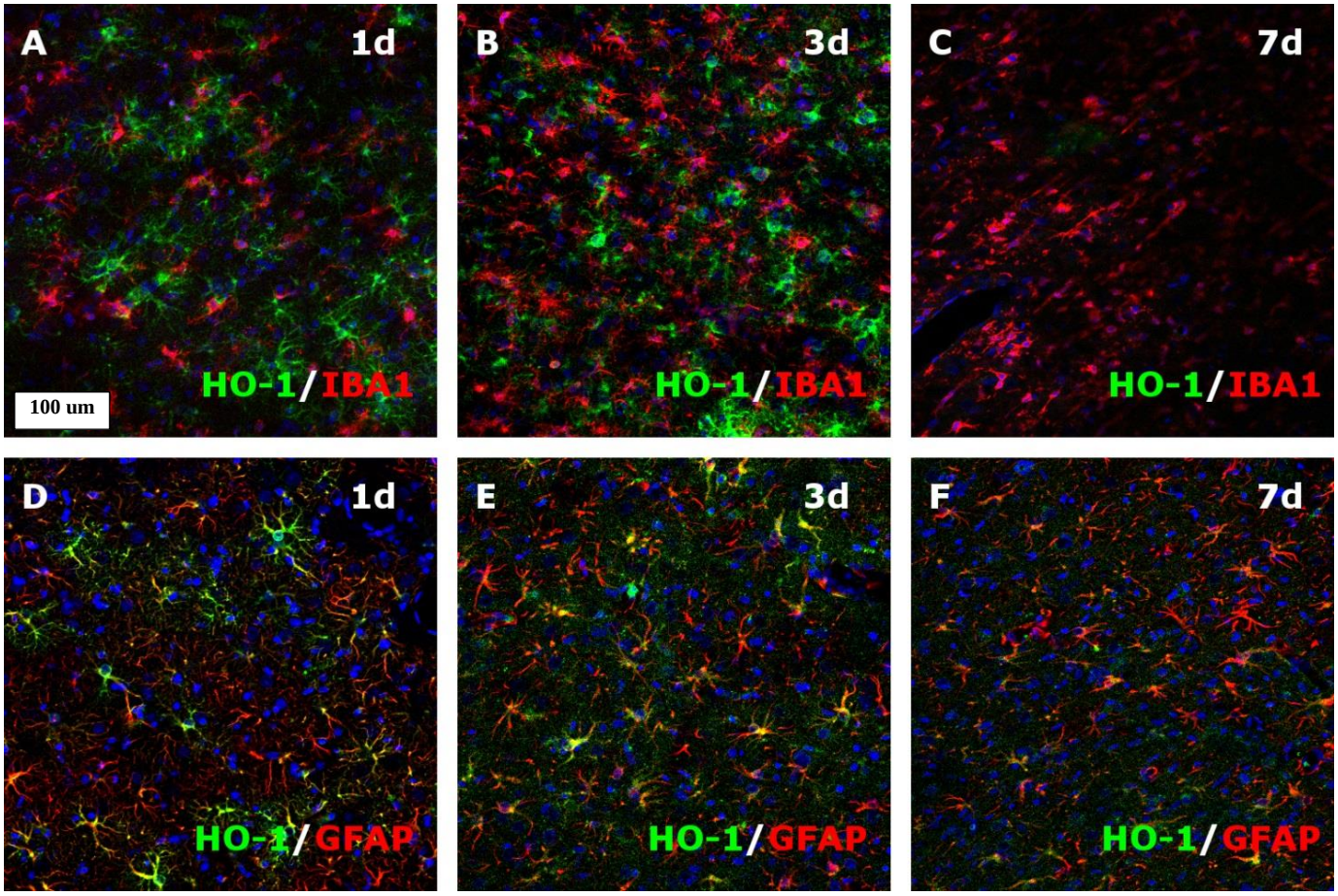

Figure 2-8: 20x Confocal images of reactive neocortex 1-7d showing expression of HO-1 with IBA1 (A-C) or GFAP (D-F). Note co-expression of HO-1+ and GFAP+ cells 1-7d and general absence of co-expression with IBA1.

2.5.4 Figure 2-9: HO-1 and Glial Reactivity in Necrotic Neocortex 3-7d

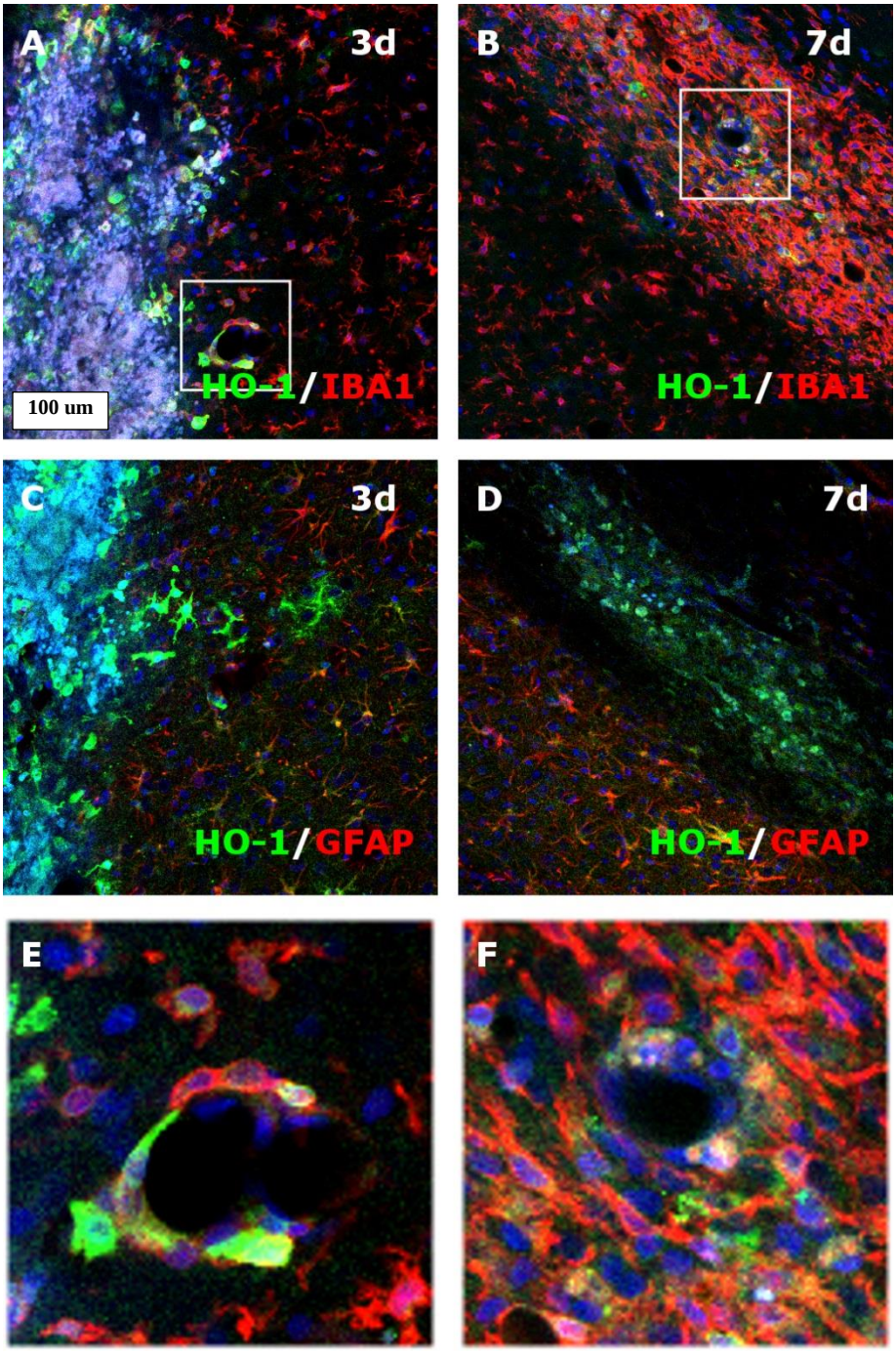

Figure 2-9: Confocal 20x images of neocortex near necrotic site 3-7d showing expression of HO-1 with IBA1 (A-B) or GFAP (C-D). Note extensive coexpression of IBA1 and HO-1 at both 3d and 7d (A,B) and only limited coexpression with GFAP (C) which appears absent at 7d. Insets (E,F) show HO-1+ IBA1+ cells with significant vessel association and possible extravasation.

We then turned to the hippocampus and particularly the dentate gyrus which is spared of any direct observable hemorrhagic injury. We observed that HO-1 shows an organizing response in the hippocampus with increased expression at 1d post injury that is bright but largely confined along the dentate gyrus polymorph layer/molecular layer boundary. At all time points HO-1 primarily co-stains with GFAP+ positive cells identified as astrocytes. As time continues at 3d and 7d expression appears to shift towards the hippocampal fissure and at 7d and 15d post injury the majority of expression is limited to the molecular layer of CA1. Throughout there appears to also be an increase in HO-1 expression associated with the vessels of the hippocampal fissure which occasionally co-stain with GFAP+ but in other instances are indeterminate in origin, morphologically most likely endothelial cells or pericytes.

2.5.5 Figure 2-10: HO-1 and Reactive Glia in Hippocampus 1-7d Post-Injury

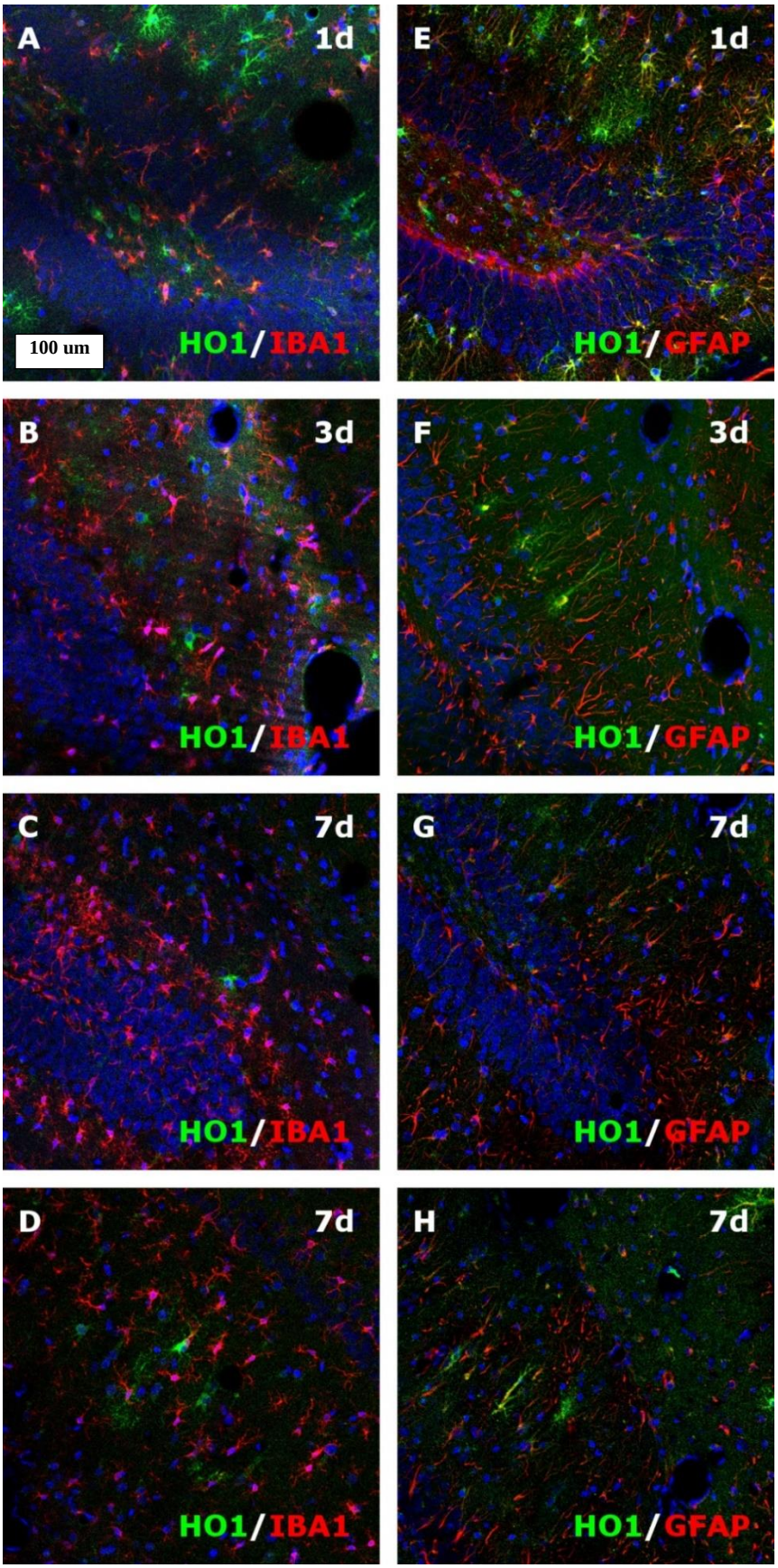

Figure 2-10: Confocal 20x images of the dentate gyrus 1-7d showing HO-1 co-expression with IBA1 (A-C) or GFAP (E-G). Note that HO-1 appears to primarily co-express with GFAP+ cells and appears over time to shift from directly adjacent to the granule cell layer outwards into the molecular layer towards the hippocampal fissure. D,H show the 7d expression in the molecular layer superior to C,G, showing that expression of HO-1 has shifted superiorly.

2.5.6 Summary of Observations in HO-1

HO-1 is significantly elevated after injury with significant elevation at 1d, peak expression at 3d, and sustained elevation through 7d or 15d (Hippocampus and Neocortex respectively). Reactivity in areas without bleeds appears to be primarily astrocytic (GFAP+) in nature while near bleeds HO-1 expression is dominantly expressed by IBA1+ positive cells and there are multiple instances of what appear to be transvasating macrophages highly expressing HO-1.

The pattern of cellular expression also shifts over time. In the hippocampus initial expression of HO-1 is largely restricted to the dentate gyrus molecular layer immediately adjacent to the granule cell layer. As time proceeds expression shifts further out into the molecular layer towards the hippocampal fissure and by 7d there is increased expression in the molecular layer of CA1. Throughout this shift in location HO-1 is dominantly expressed by GFAP+ cells.

In the neocortex there are two distinct regions of HO-1 expression: directly near bleed sites (and their associated necrotic tissue), and in the cortical layers that overlay bleeds. Directly near the bleed sites there is time dependent organization and recruitment of HO-1 expressing cells that are predominantly IBA1+ cells that strongly express HO-1. This process appears to peak at 3d and by 7d we see significant consolidation of expression and reduction in the necrotic site with very reduced DNA karyorrhexis observed (DAPI shmear). In direct contrast the cortical layers overlaying these bleeds primarily express HO-1 in astrocytes and are more uniformly dispersed throughout the reactive tissue.

2.6 FTL Change Neocortex vs Hippocampus

After establishing the time course of HO-1 after injury we proceeded to examine the effect that HO-1 driven heme processing had on the expression of the known iron storage protein FTL and its association with the iron sequestration/trafficking protein LCN2. The intent is to observe the paired responses of an acute iron sequestering protein that can be expected to be upregulated with increased heme catabolism as well as a long term marker of iron deposition associated with long term pathological damage. We observed that LCN2 peaked acutely at 1d in the tissue and that FTL appeared to lag behind HO-1 and LCN2 expression before peaking at around 7d after injury. After this point FTL declined through 15d as deposited iron is cleared. In the neocortex (**Figure 2-11**) this is clearly seen in tile scans near the necrotic site. There is a large halo of LCN2 surrounding the bleed and as time advances the periphery and then the center begins to lose autofluorescense and begin to stain for FTL. This is similarly seen in the hippocampus (**Figure 2-12, Figure 2-13**) where the 1d upregulation of LCN2 is associated with the vessels in the hippocampal fissure and as time progresses shifts towards the superior granule cell layer of the dentate gyrus concurrent with increased FTL expression.

2.6.1 Figure 2-11:FTL vs LCN2 in Neocortex 1-15d Post-Injury

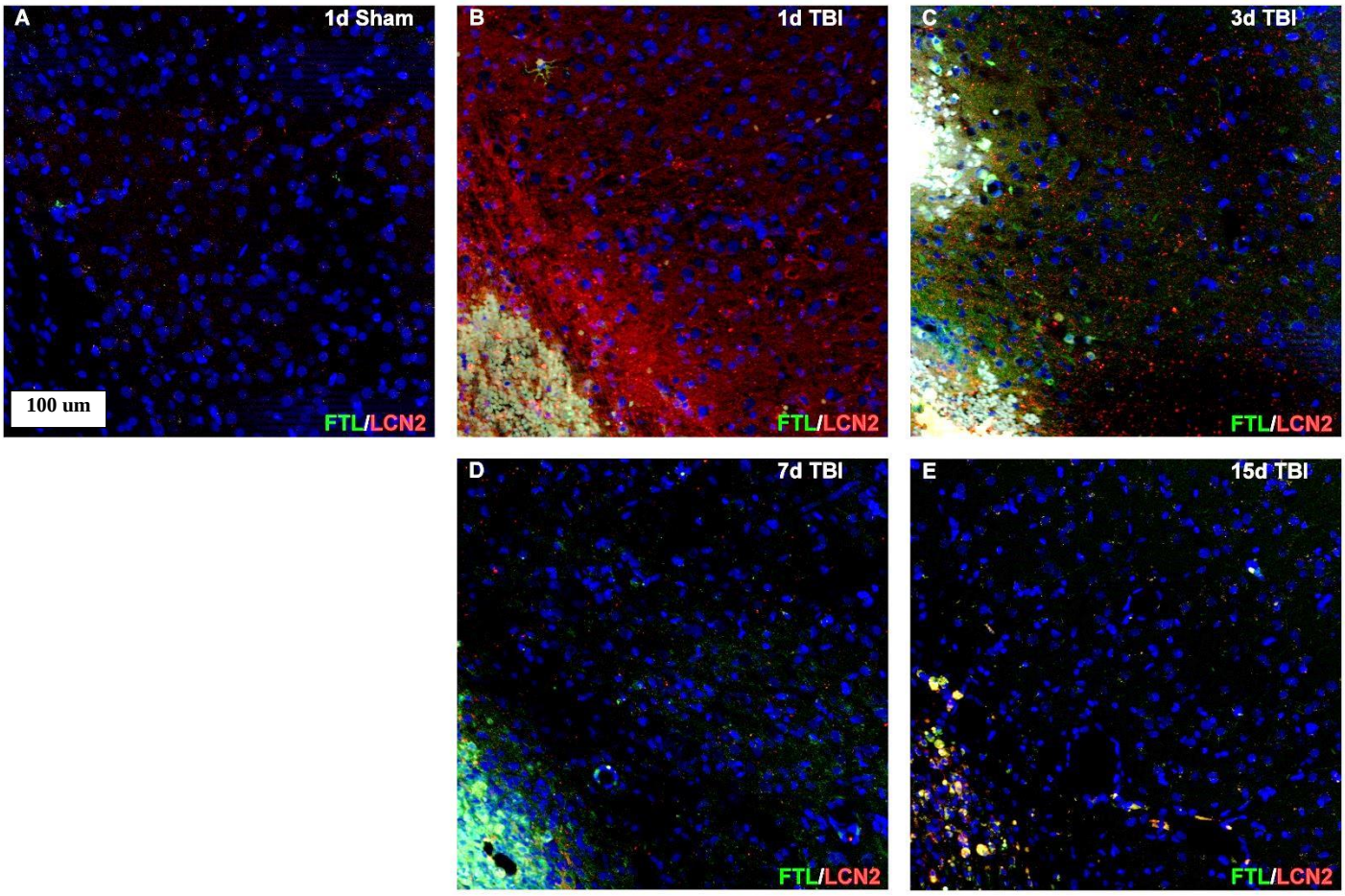

Figure 2-11: 20x Apotome tile scans of neocortex showing expression of FTL and LCN2 over time after sham surgery (A), and 1d,3d, 7d, and 15d (B-E respectively), after TBI. Note minimal expression of FTL in sham injured tissue or in 1d TBI that is markedly increased at 3d and 7d. LCN2 expression that peaks at 1d declines as FTL increases. Note that autofluorescence of erythrocytes and vessels is not out of imaging range in the 1d and 3d tissue. Further note extreme focal points of high FTL expression at 3d which consolidates through day 7 (time of WB peak expression), and declines through 15d while remaining notably elevated compared to Sham.

2.6.2 Figure 2-12:FTL vs LCN2 in Hippocampus 1-15d Post-Injury

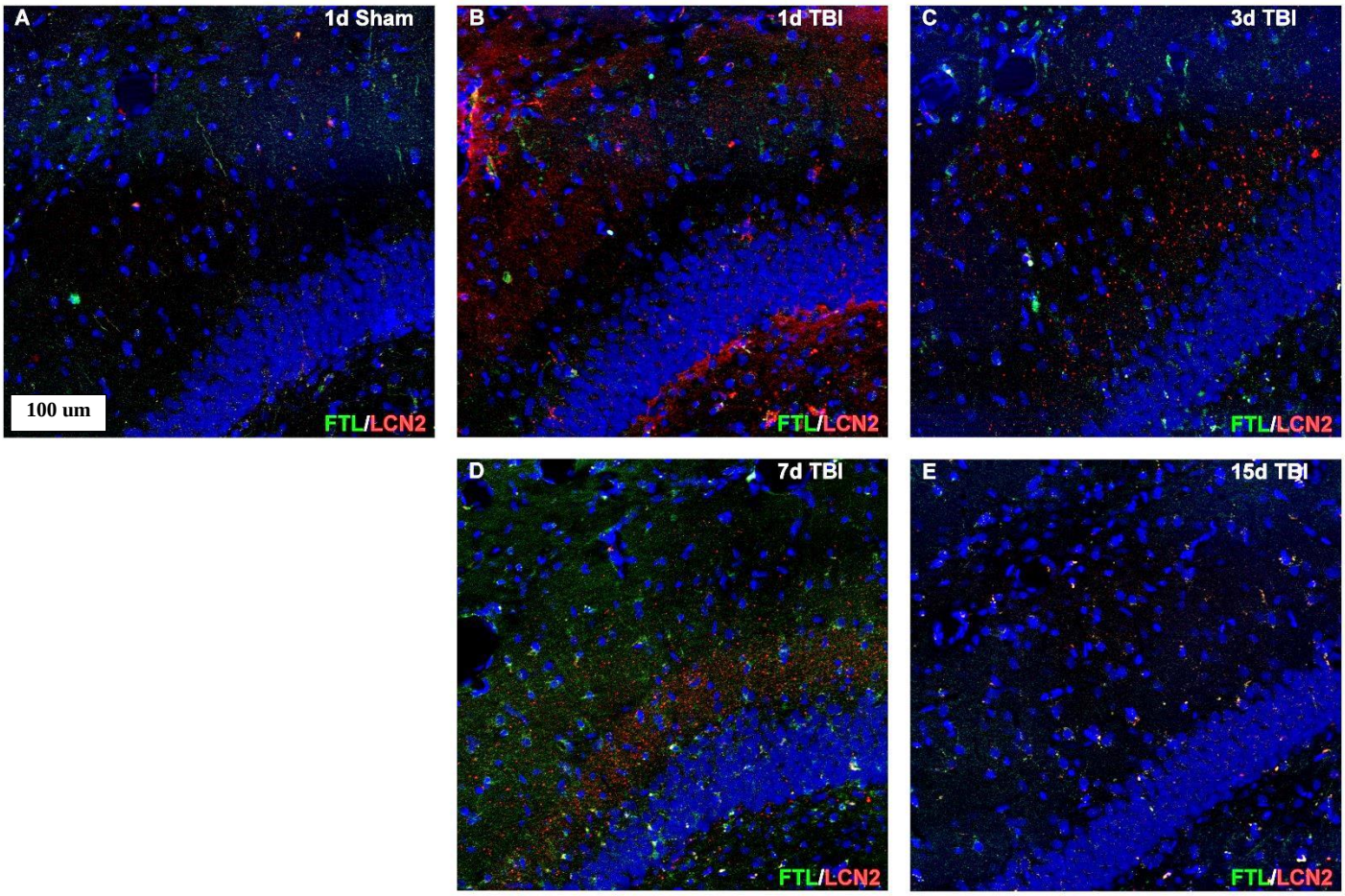

Figure 2-12: 20x Apotome tile scans of hippocampus showing expression of FTL and LCN2 over time after sham surgery (A) and 1d,3d,7d,15d TBI (B-E). Note absence of FTL or LCN2 in Sham animal with steady increases in FTL 1-7d in scattered populations. Additionally note LCN2 expression peaking at 1d in the molecular layer and then organizing along the dentate granule cell layer.

2.6.3 Figure 2-13: FTL vs LCN2 Hippocampal Fissure 1-7d Post-Injury

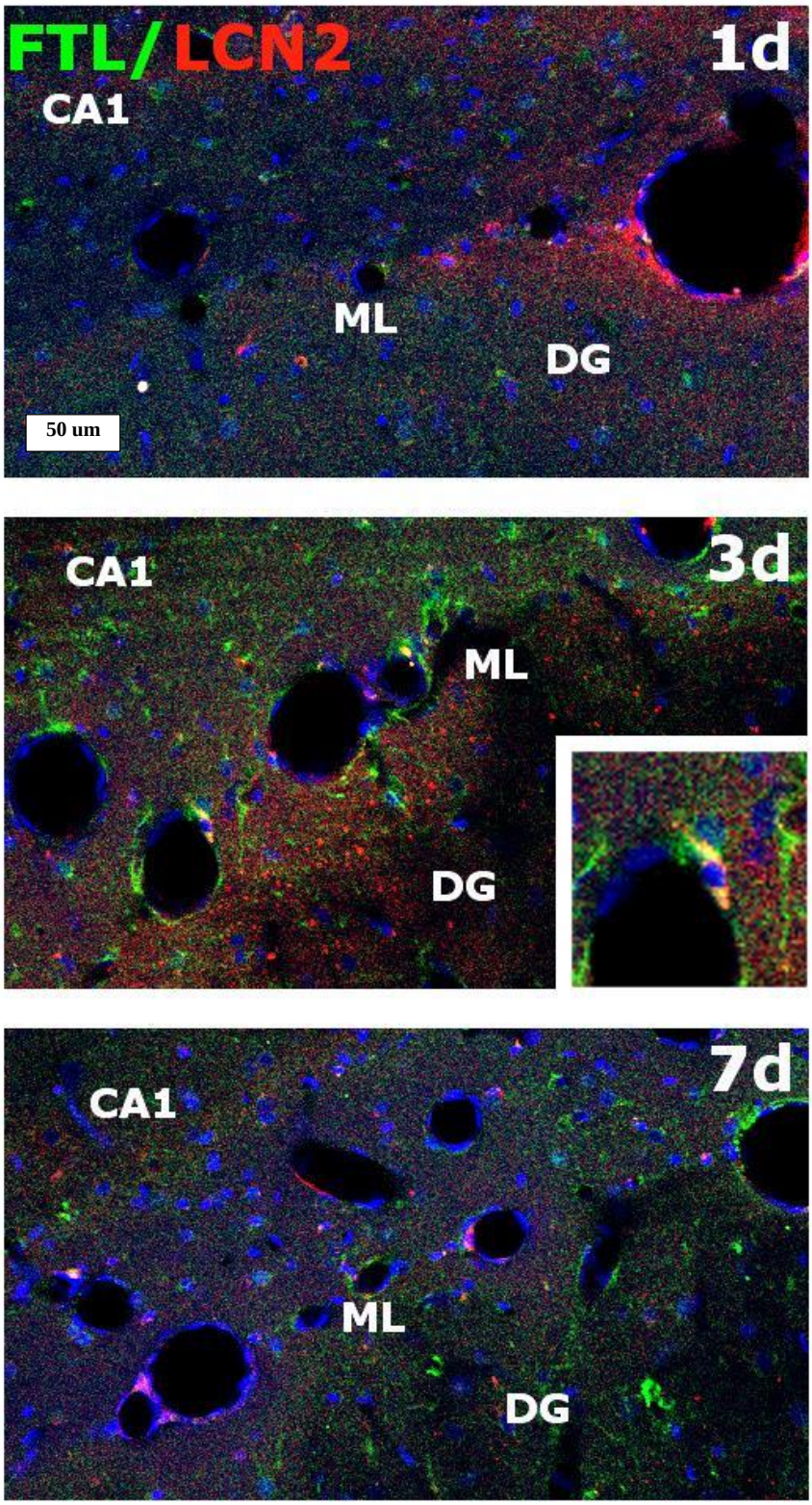

Figure 2-13: 20x Confocal images of the hippocampal fissure 1-7d showing association of vessels with FTL and LCN2 and the switchover from acute to long term iron sequestration over time.

Western blot analysis of FTL protein after injury shows a similar story. We observed that Ferritin was significantly increased vs Sham in both the neocortex and hippocampus after injury with peak expression at 7d. In the neocortex ANOVA using the model $\boldsymbol{Value \sim Day * Condition}$ showed significant main effects due to Day, Condition, and their interaction (p=0.001451, 4.062e-05, 0.001451). TukeyHSD post-hoc analysis of group effects showed a TBI-Sham comparison of p= 0.000271. Pairwise Wilcoxon daily comparisons with Benjamini-Hochberg correction showed there is no change in expression at 1d (95±20%, Not Significant), rising at 3d (206±26%, p = 0.038), peaking at 7d (377±82%, p = 0.083), and declining to near Sham levels by 15d (136±13%, p = 0.100).

In the hippocampus ANOVA using the model $\boldsymbol{Value \sim Day * Condition}$ showed significant main effect only due to Condition (p= 0.0002949). TukeyHSD post-hoc analysis of group effects showed a TBI-Sham comparison of p= 0.0002324). Compared to the neocortex there is greater diversity in the injured sampling and pairwise Wilcoxon daily comparisons with Benjamini-Hochberg correction show that by 1d after injury there is already an initial rise in expression (163±28%, p = Not Significant) which continues to rise through 3d and 7d (202±44%, p = 0.091, and 291±54%, p=0.089 respectively). Interestingly, peak expression from 7d is largely maintained through 15d in the hippocampus (237±68%, p = 0.089).

2.6.4 Figure 2-14: FTL Western Blot 1-15d Post-Injury

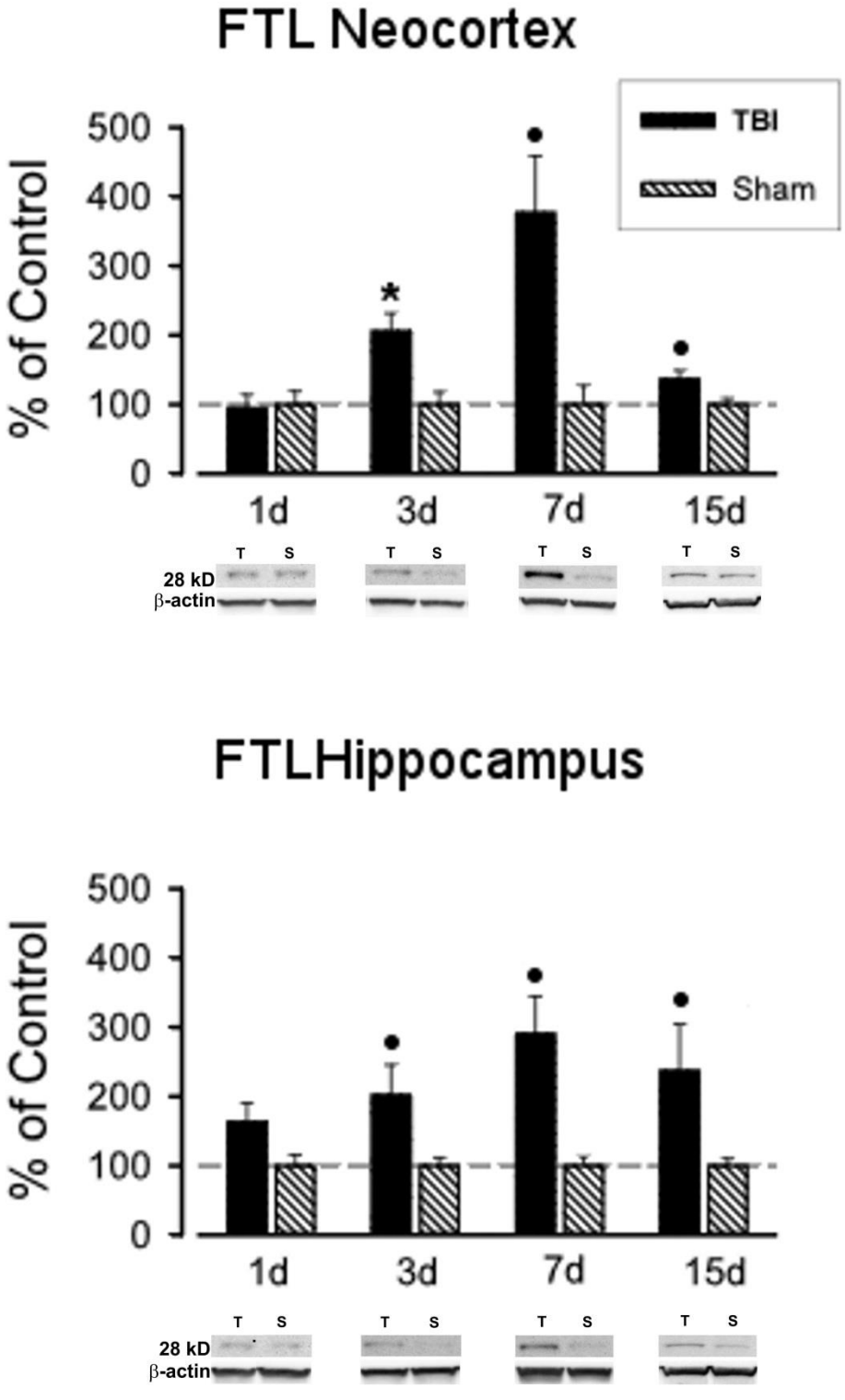

Figure 2-14: FTL is significantly elevated in the Neocortex at 3d, peaking at 7d and remaining modestly elevated through 15d. In the Hippocampus FTL at 1d is elevated and progressively increases through 7d largely maintain the 7d peak through 15d. (Mean ± SEM, n=5-7/group; Wilcoxon-Test with Benjamini-Hochberg Correction. •,*, **, *** for $p < .10, .05, .005, .0005$ respectively; ANOVA $p < 5*10^{-4}$ Neocortex, $p < 5*10^{-4}$ Hippocampus)

2.6.5 Summary of Observations in FTL

Ferritin lags behind HO-1 in increased expression which is reasonably expected since the primary driver of Ferritin expression is an increase in iron that results from HO-1 activity. In immunohistochemistry it is difficult to identify increases in FTL expression over background until significant organization of iron sequestration has been organized which is most easily seen in the neocortex that experiences *in situ* bleeds.

The neocortex responds exactly as expected, lacking a significant driver of expression at 1d there is no rise in expression. By 3d (when HO-1 activity peaks), and especially at 7d (when heme substrate has been depleted) FTL expression continues to rise before decreasing through 15d as iron is progressively cleared and consolidated in the tissue.

Rather unexpectedly we observe in western blot that FTL expression rises within 1d after injury (though without significance). Further, while peak expression of FTL is less than in the neocortex it appears to persist with greater effect through 15d. To some extent it is difficult to ascertain the meaning of this rise since the increased FTL expression is widely dispersed and not particularly remarkable histopathologically.

2.7 LCN2 Change Neocortex vs Hippocampus

Concurrent to our observations of FTL which had strong crossover with LCN2 we also looked independently at LCN2 expression in the tissue.

We observed that LCN2 is highly expressed acutely after injury and is largely expressed in the same regions as HO-1 **(Figure 2-15**). Expression of LCN2 is extraordinarily scarce in the uninjured brain and is essentially undetectable in Sham animals. The expression of LCN2 also appears to be entirely in the same set of cells that also express HO-1 at 1d after injury (**Figure 2-16**).

2.7.1 Figure 2-15: Acute HO-1 vs LCN2 Hippocampus Widefield

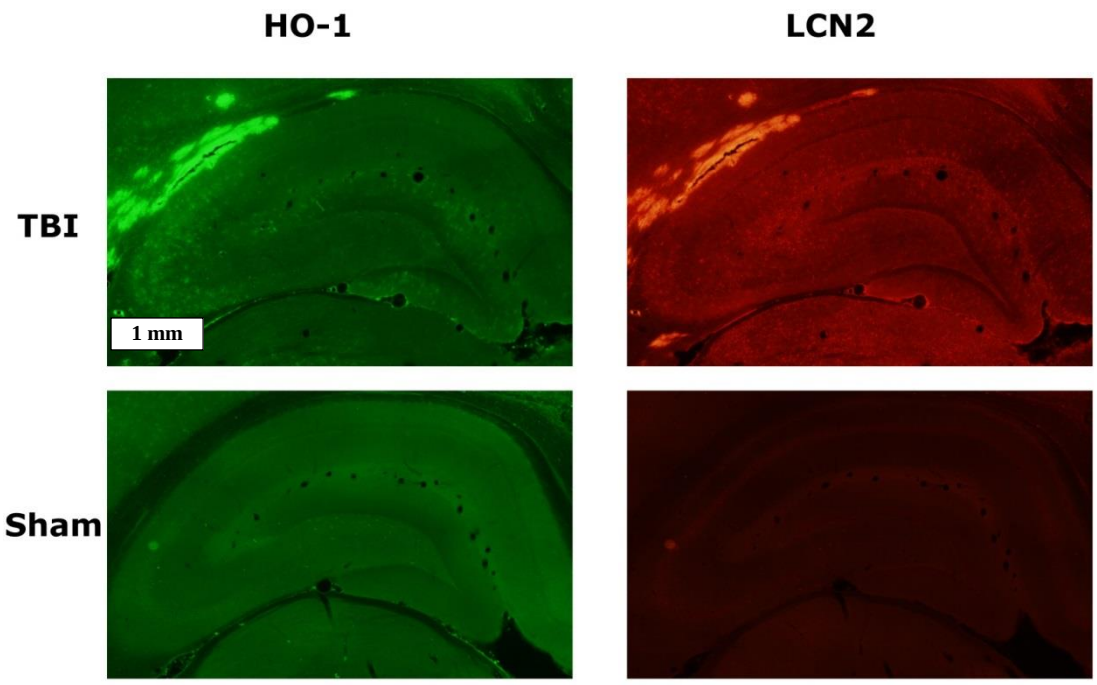

Figure 2-15: 10x widefield hippocampus tile scans of HO-1 and LCN2 in 1d TBI or Sham Animals. Note the extensive expression of HO-1 and LCN2 in the injured animal and the near absence of signal in the Sham, particularly the LCN2 Sham.

2.7.2 Figure 2-16: Acute HO-1 vs LCN2 Hippocampus and Neocortex Confocal

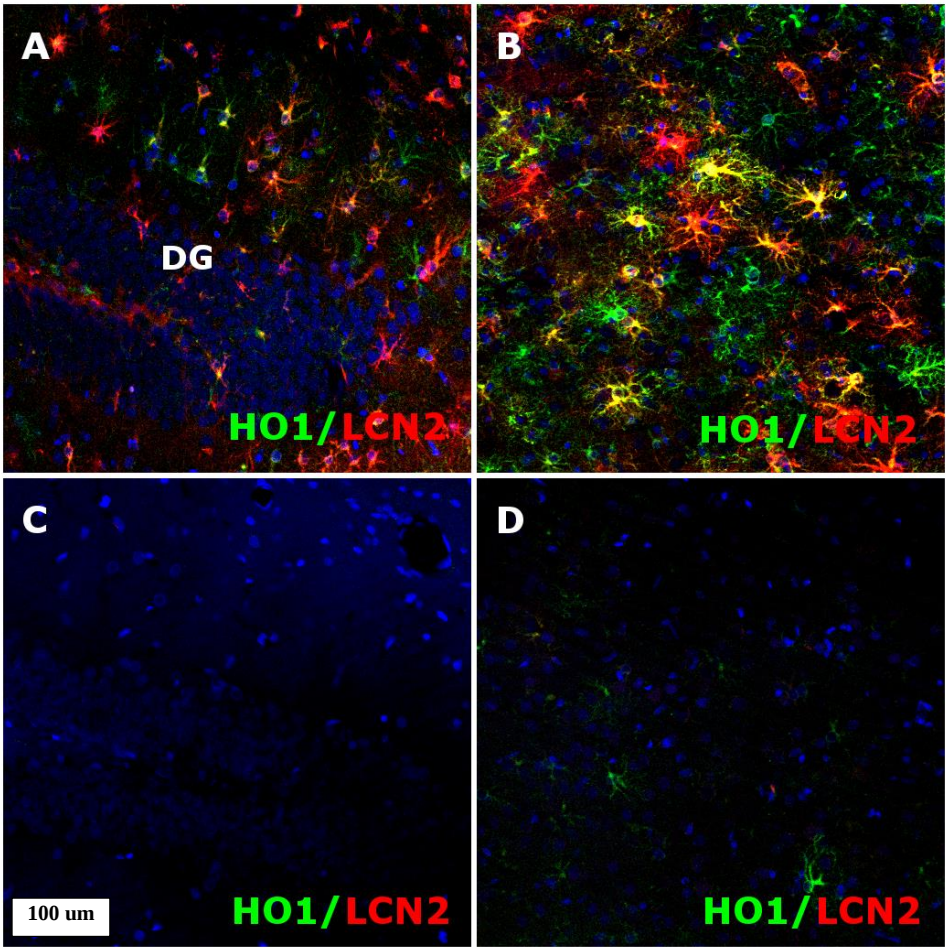

Figure 2-16: 20x confocal 1d TBI (A,B) and Sham (C,D) stained for HO-1 and LCN2. Note that in both the Hippocampus (A,C), and the Neocortex (B,D) there is a near complete absence of expression in the Sham animal while there is extensive co-localization of HO-1+ LCN2+ cells in the injured animal.

We further observed that while HO-1 appears to maintain expression 1-3d before declining 7d+, LCN2 immediately declines in expression after 1d post injury (**Figure 2-17**). By 7d post-injury LCN2 is essentially unidentifiable in the samples observed.

2.7.3 Figure 2-17: HO-1 vs LCN2 Hippocampus 1-7d Post-Injury Widefield

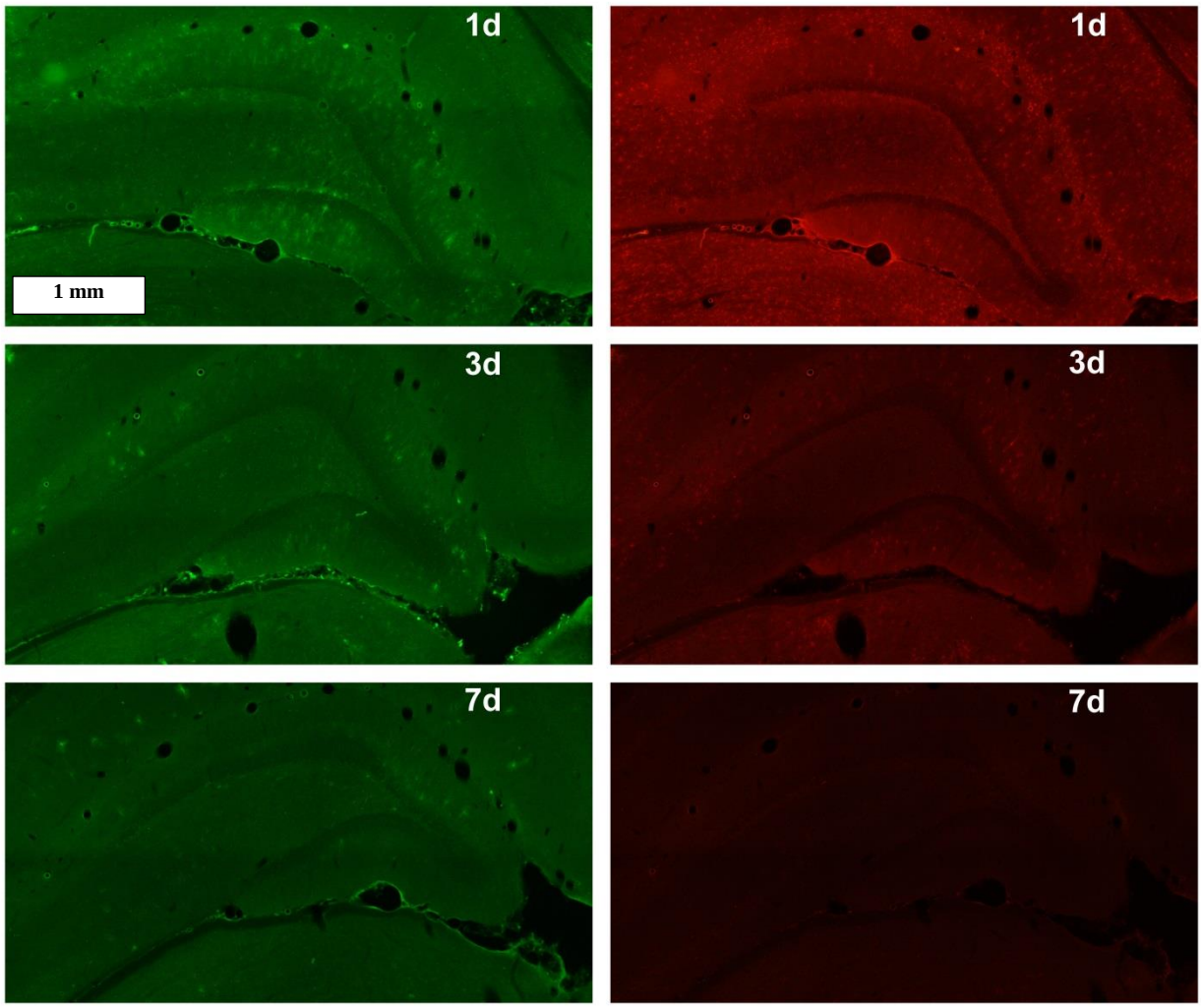

Figure 2-17: 10x widefield tile scans of HO-1 (Green) and LCN2 (Red) 1-7d post injury. Note organizing expression of HO-1 with shifts of expression from the superior dentate molecular layer into the molecular layer of CA1. Further, note the high expression of LCN2 1d post injury steadily degrades to near absent signal by 7d.

In order to confirm and strengthen the observations of the immunohistochemistry data we further examined LCN2 expression via western blot 1-7d post injury (**Figure 2-18**).

We observed that LCN2 expression vs Sham peaks by 1d after injury and declines exponentially through 7d. In the neocortex ANOVA using the model $\mathbf{log}[\boldsymbol{Value}] \sim \boldsymbol{Day} * \boldsymbol{Condition}$ showed significant main effects due to Day, Condition, and their interaction (p=0.0002544, 1.040e-08, 5.188e-07 respectively). TukeyHSD post-hoc analysis of group effects showed a TBI-Sham comparison of p<2e-16. Pairwise Wilcoxon daily comparisons with Benjamini-Hochberg correction showed that LCN2 peaks at 1d post injury (5845±1328%, p = 0.0179), declines at 3d (618±203%, p = 0.0087), and is at Sham levels by 7d (109±3%, Not Significant).

The hippocampus in contrast peaks much higher than the neocortex and persists in significant elevations through 7d. ANOVA using the model $\mathbf{log}[\boldsymbol{Value}] \sim \boldsymbol{Day} * \boldsymbol{Condition}$ showed significant main effets due to Day, Condition, and their interaction (p=4.161e-09, 2.044e-13, 1.934e-09). TukeyHSD post-hoc analysis of group effects showed a TBI-Sham comparison of p<2e-16. At 1d post injury we observed peak expression (47486±9761%, p = 0.0159), a decline at 3d (2893±976%, p = 0.0087) and approaching Sham levels at 7d (129±5%, p = 0.0238).

2.7.4 Figure 2-18: LCN2 Western Blot 1-7d Post-Injury

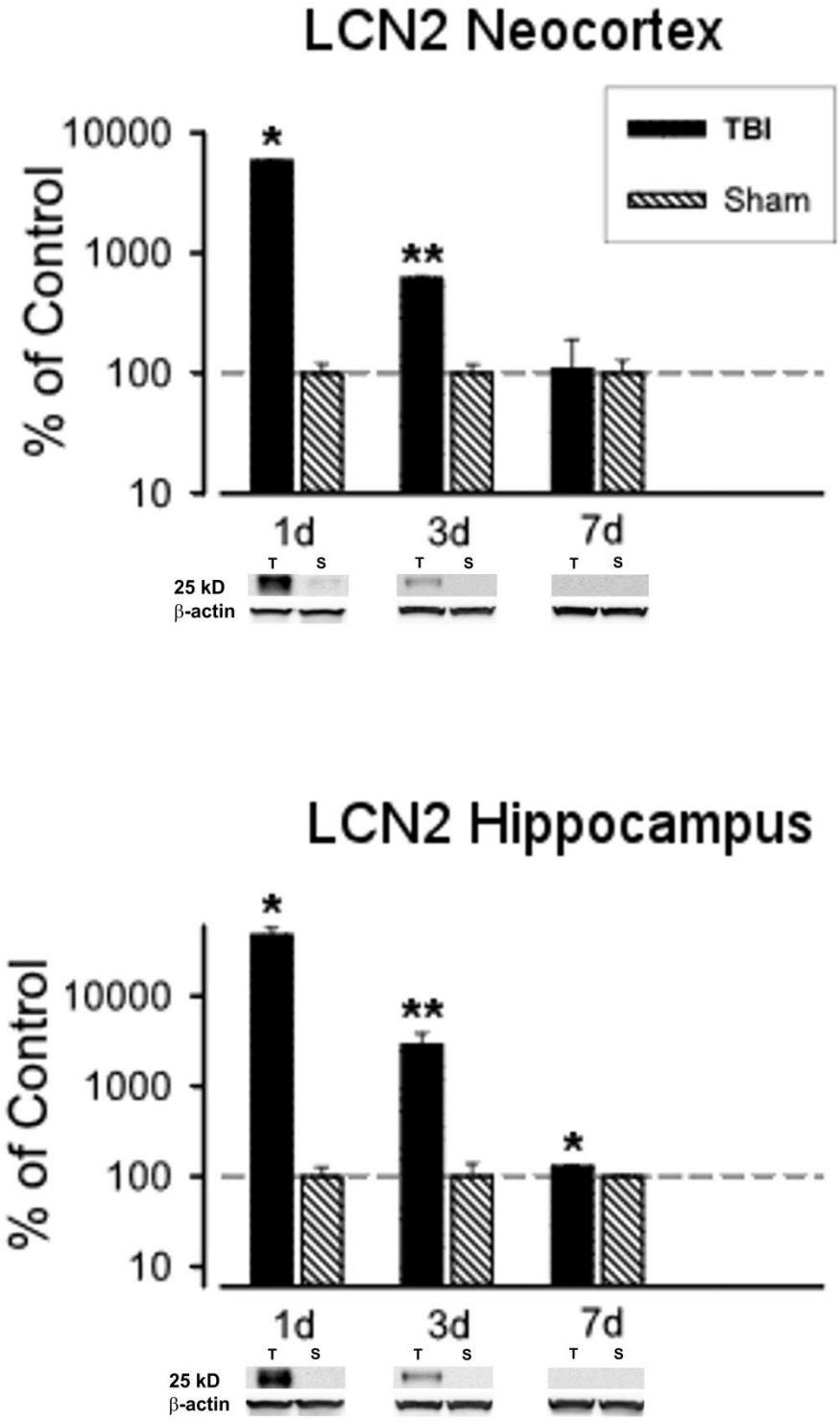

Figure 2-18: LCN2 peaks immediately after injury notable for having ~10,000% elevations 1d after injury. This peak progressively declines and is shown here in log scale. Elevation steadily declines through 3 and 7d and in the neocortex is at Sham levels by 7d, while being significantly but modestly elevated at 7d in the Hippocampus. (Mean ± SEM, n=5-7/group; Wilcoxon-Test with Benjamini-Hochberg Correction, *, **, *** for $p < .05, .005, .0005$ respectively; ANOVA $p < 5*10^{-5}$ Neocortex, $p < 5*10^{-4}$ Hippocampus).

2.7.5 Summary of Observations in LCN2

LCN2 is an acute phase protein involved in iron sequestration that is massively elevated immediately after injury. To a good degree the extreme elevations seen are to an extent trivialized due to the extreme paucity of LCN2 in Sham animals which is difficult to detect either in IHC or western blot. In both the neocortex and hippocampus LCN2 is co-expressed with HO-1 in nearly every cell that expresses either protein though this effect is more difficult to detect as LCN2 expression declines. This decline notably coincides with FTL increase which makes sense given their respective roles in iron sequestration and storage.

2.8 Gelatinase Response Neocortex vs Hippocampus

To further study the impact of injury in the two tissue regions examined we also looked at zymography of MMP2 and MMP9 which have been associated with post-TBI injury and recovery (**Figure 2-19**). It is important to note that LCN2 (discussed previously) is known to be a persistent activator of Active-MMP9 activity in both human and rodents.

We observed that in the neocortex MANOVA using the model $[\boldsymbol{ProMMP9}, \boldsymbol{ActiveMMP9}, \boldsymbol{MMP2}] \sim \boldsymbol{Day} * \boldsymbol{Condition}$ with Wilks correction showed significant main effects due to Day, Condition, and their interaction (p=1.006e-07, 4.584e-09, 1.363e-07). Derivative single enzyme ANOVA show MMP2 with a significant main effect in condition only (p= 7.616e-09) while Pro-MMP9 and Active-MMP9 have significant main effects in Day, Condition, and their interaction (Pro-MMP9: p=6.669e-09, 5.565e-07, 5.389e-09 respectively; Active-MMP9: p=9.684e-05, 2.596e-05, 8.616e-05 respectively). TukeyHSD post-hoc analysis for group effects showed TBI-Sham comparisons of p=3.96054e-07, 1.573818e-05 for Pro and Active MMP9 respectively. Pairwise Wilcoxon daily comparisons with Benjamini-Hochberg correction were then applied. The gelatinase MMP2 was upregulated vs Sham by 1d (148±2%, p = 0.0054), peaks at 3d (180±13%, p = 0.0325) and largely sustained elevation through 7d (172±7%, p = 0.0054) post injury. MMP9 in both its pro-form, and active form are elevated after injury. Pro-MMP9 peaks at 1d post injury (1305±179%, p = 0.0065) before becoming non significant at 3d and 7d (116±19% and 92±17% respectively). The Active-MMP9 lags behind the pro-form and persists in elevation longer; Active-MMP9 peaks at 1d (340±43%, p = 0.0081), declines at 3d (172±26%, p = 0.0557), and is not significant at 7d (93±24%).

2.8.1 Figure 2-19: Zymography of MMP2 and MMP9 1-7d Post-Injury in Neocortex

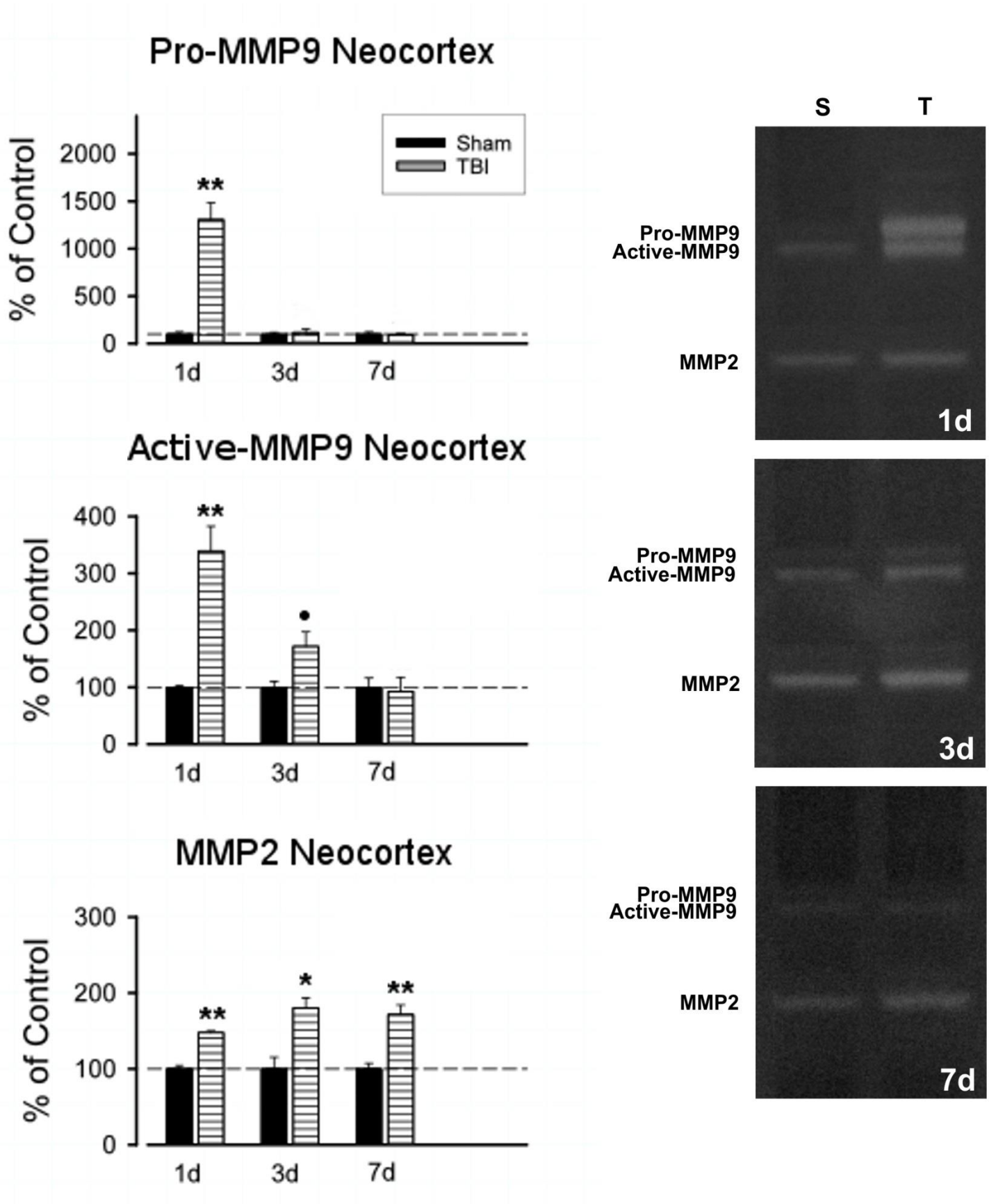

Figure 2-19: Zymogram expression of MMP2, Pro-MMP9, and Active MMP9 1-7d after injury in the neocortex. Note MMP2 peak expression at 3d and significance across entire time course. Pro-MMP9 peaks immediately at 1d before dropping to near Sham by 3d while the active form is elevated significantly through 3d. (Mean ± SEM, n=6/group; Wilcoxon-Test with Benjamini-Hochberg correction, ●,*, **, *** for p <.10, .05, .005, .0005 respectively)

Similar to the neocortex we observed that in the hippocampus (**Figure 2-20**) MANOVA using the model $[\boldsymbol{ProMMP9}, \boldsymbol{ActiveMMP9}, \boldsymbol{MMP2}] \sim \boldsymbol{Day} * \boldsymbol{Condition}$ with Wilks correction showed significant main effects due to Day, Condition, and their interaction (p=2.536e-07, 2.775e-12, 2.536e-07). Derivative single enzyme ANOVA show MMP2, Pro-MMP9, and Active-MMP9 have significant main effects in Day, Condition, and their interaction (MMP2: p=0.01424, 1.792e-13, 0.01424 respectively; Pro-MMP9: p=1.119e-08, 3.521e-07, 1.119e-08 respectively; Active-MMP9: p=0.02382, 2.64e-05, 0.02382 respectively). TukeyHSD post-hoc analysis for group effects showed TBI-Sham comparisons of p=2.297051e-13, 3.521416e-07, 2.639918e-05 for MMP2, Pro-MMP9 and Active-MMP9 respectively. Pairwise Wilcoxon daily comparisons with Benjamini-Hochberg correction were then applied.The gelatinase MMP2 was upregulated vs Sham by 1d (153±5%, p = 0.0032), peaks at 3d (201±4%, p = 0.0032) and largely sustained elevation through 7d (181±15%, p = 0.0032) post injury. MMP9 in both its pro-form and active form are elevated after injury. Pro-MMP9 peaks at 1d post-injury (1486±219%, p = 0.0065) before dropping to near Sham at 3d (194±29%, p = 0.0685) and is non-significant at 7d (84±21%). The Active-MMP9 lags behind the pro-form and persists in elevation longer; peaking at 1d (258±225%, p = 0.0081), declines at 3d (175±12%, p = 0.0649), and is not significant at 7d (133±28%).

2.8.2 Figure 2-20: Zymography of MMP2 and MMP9 1-7d Post-Injury in Hippocampus

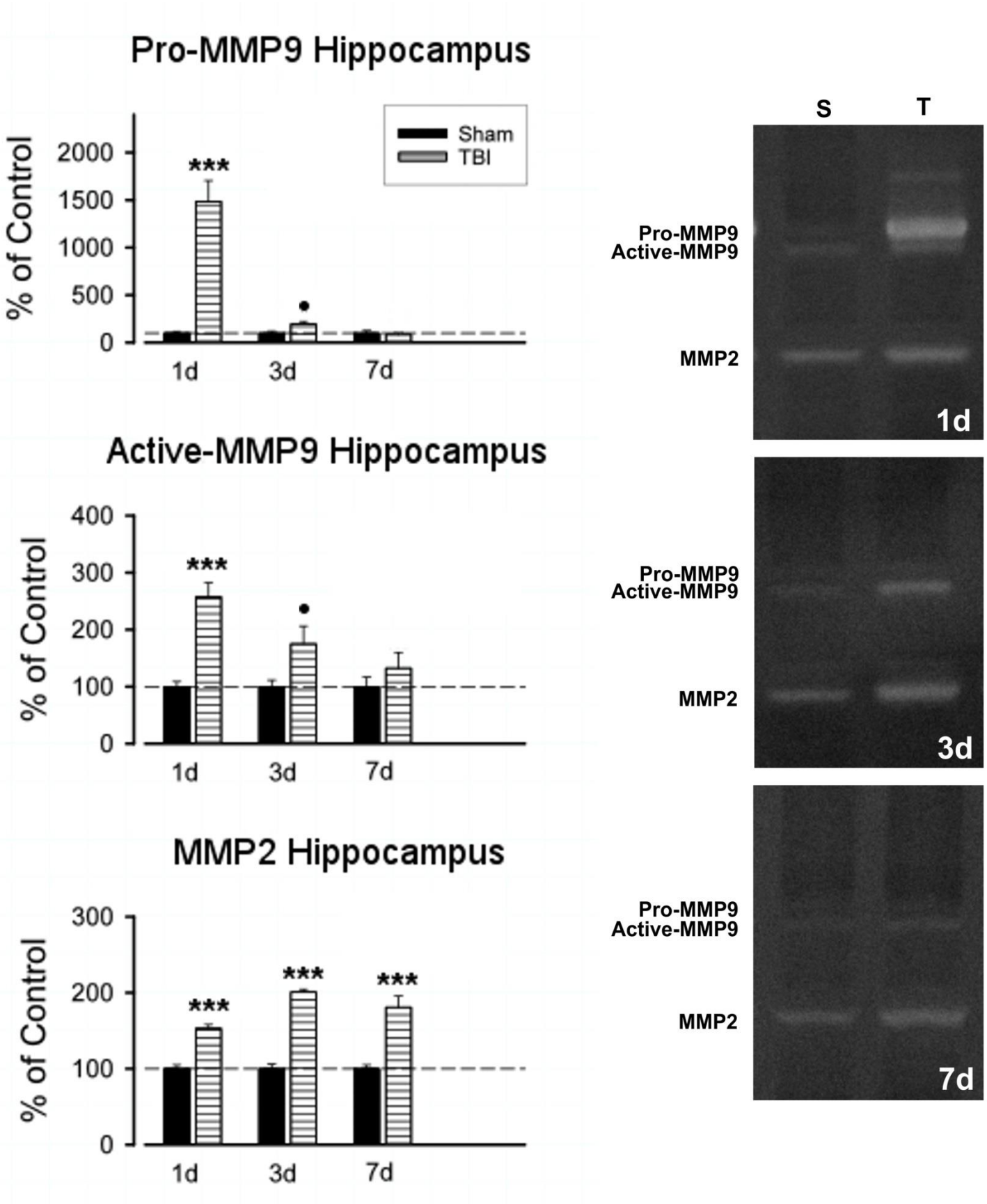

Figure 2-20: Zymogram expression of MMP2, Pro-MMP9, and Active MMP9 1-7d after injury in the hippocampus. Note MMP2 peak expression at 3d and significance across entire time course. Pro-MMP9 peaks immediately at 1d before dropping but maintains significance through 3d in a pattern identical to the active form. (Mean ± SEM, n=6/group; Wilcoxon-Test with Benjamini-Hochberg correction, ●,*, **, *** for $p < .10,.05, .005, .0005$ respectively)

2.8.3 Summary of Observations in Zymograms

MMP2 is significantly elevated after injury in both the neocortex and hippocampus within 1d after injury, peak expression at 3d, and a relatively stable plateau through 7d that remains significant. The Pro and Active forms of MMP9 similarly demonstrate matching expression in the neocortex and the hippocampus with a very high acute rise in Pro-MMP9 expression at 1d which rapidly dies to near Sham while the active form shows a more sustained expression that similarly peaks at 1d and is progressively weaker across the time course though still significant at 3d post injury.

2.9 Chapter 2 Discussion

2.9.1 Summary of Results in Chapter 2

In Chapter 2 we have identified the time course of heme processing in hemorrhagic (neocortical) and non-hemorrhagic (hippocampal) tissue after a cFPI injury. We critically identified that the expression of proteins known to be elevated in response to heme processing (HO-1, LCN2, FTL) are increased both in tissue with obvious gross hemorrhage and in a tissue which does not demonstrate apparent hemorrhage. Further, gelatinases known to interact with heme processing proteins and involved in angiogenic and synaptogenic processes also do not show marked differences in the tissue observed.

When we compare our results to what has been demonstrated in the literature we find a number of corollaries with several novel aspects of injury. Because we are examining a relatively understudied aspect of diffuse brain injury much of the relevant literature extends into other TBI injury models which are more grossly necrotic/hemorrhagic (e.g. CCI) as well as other grossly hemorrhagic CNS injuries (e.g. intracerebral hemorrhage) (Yamauchi et al., 2004; Cao et al., 2016; Alfieri et al., 2013; Lu et al., 2014; Chang et al., 2005). One of our most significant findings is that there appears to be a heme processing response, characterized by sequential elevations in LCN2, HO-1, and FTL, which occurs in non-hemorrhagic tissue and at comparable orders of magnitude to tissue known to be hemorrhagic. To further understand the nature of this finding we more closely examine the time dependent changes in heme processing proteins as well as additional markers of hemorrhagic injury.

2.9.2 Hemorrhage and HO-1 Response to mild-moderate FPI

2.9.2.1 *Extent of hemorrhage generated and sites (NVU) consistent with other reports in TBI*

The hemorrhage that we observe in our study is fairly reproducible between animals and corresponds well with literature results which show that cFPI ~2 ATM is roughly the overpressure where WM hemorrhage becomes consistently evident after injury (Dixon et al., 1987). At higher overpressures than we used there is progressively greater hemorrhage and it is known that overpressures in the 2.9-3.6 ATM range distinct hemorrhages in the hippocampus occur. This demonstrates that the hippocampus is vulnerable to hemorrhagic injury and there may be some threshold required before gross hemorrhage occurs or it may be a more gently demarcated process.

A note should be made here that by a number of definitions our injury may be classified as a purely *moderate* rather than *mild* injury because of the presence of any hemorrhage. We accept that the injury can be classed in this mild-moderate range but would observe that mice with comparable righting times do not demonstrate hemorrhage and it is likely that as an organism becomes larger and requires more force to cause a diffuse injury there is a greater propensity towards generating small hemorrhages (as might occur in the rat vs. mouse). In the case of human mild TBI for example, small microbleeds are exceedingly common and are frequently observed even in patients with no symptoms of injury (Park et al., 2009a). For a mild-moderate injury we have a notable hemorrhagic area but if we contrast this to an ICH model of hemorrhage it would be considered minor which is to say that hemorrhage is an ancillary injury in our model, though one that should be examined. As a result of this categorical debate however it appears that most research focusing on hemorrhagic outcomes in TBI has used other models,

particularly CCI models. These other models typically produce extensive focal damage and a large contusional injury which may make it difficult to assign categorically different aspects of the resulting injury (Petraglia et al., 2014).

2.9.2.2 Rapid post-injury HO-1 induction matches data for TBI, SCI and stroke/ischemia

The early induction of HO-1 observed here fits well with prior observations that have been made in other hemorrhagic injuries including CCI, SCI, ICH, H/I ((Chang et al., 2003; Yamauchi et al., 2004; Alfieri et al., 2013; Lu et al., 2014; Cao et al., 2016). In nearly all cases there is a rapid rise in HO-1 1-3d post-injury, a peak expression occurring variably between 3d and 7d, with the later periods matching injuries having correspondingly larger bleeds and thus greater quantities of HO-1's substrate heme. Frequently papers provide only a brief snapshot of HO-1 expression over time reproducing only one of the time points included in our sample period. Our observations of HO-1 increases in a non-hemorrhagic tissue, however, have not been previously reported. This is particularly interesting since the majority of models that observed HO-1 increases have involved lateral injuries and as a result have used the contralateral 'un-injured' side as a control of expression. Whether this leads to a suppression of effect is unknown but using a non-hemorrhagic matched tissue in the same animal as a control may effectively prevent the observation we have uncovered. As an example, in the circumstance of a lateral injury that acutely damages the ipsilateral neocortex and hippocampus it would be unsurprising if there was extensive hemorrhage throughout both tissues. If there is further HO-1 reactivity in the contralateral neocortex it would be expected to be significantly reduced in comparison and might reasonably appear to be sham like or absent.

2.9.2.3 *Association of HO-1 with NVU and glial response: predicted patterns reflect cell function*

When we look at the glial presentation of HO-1 we observe that there is a strong association with the primary bleed site and the cortical layers overlaying the frank hemorrhage. This component is largely expected and correlates well with previous authors' findings which have demonstrated a strong association with hemorrhage and HO-1 expression (Ryter et al., 1998; Ryter and Tyrrell, 2000; Ryter et al., 2006; Cao et al., 2016; Lu et al., 2014; Alfieri et al., 2013; Yamauchi et al., 2004; Fukuda et al., 1995). In this region we primarily see GFAP+ HO-1+ cells in the overlying neocortex and IBA1+HO-1+ cells adjacent and throughout the bleed, with expression increasing over the course of ~3d as IBA1+ cells begin to infiltrate the bleed. This general pattern of reactivity has been observed several times in other models of CNS injury (Fukuda et al., 1995; Yamauchi et al., 2004; Cao et al., 2016). Astrocyte reactivity with HO-1 has been identified both *in vitro*, and *in vivo* in animal models and the same is true for microglial reactivity (Li Volti et al., 2004; Fukuda et al., 1995; Fauconneau et al., 2002). Throughout the neocortex there appear to be associations between HO-1 reactivity and markedly dilated cortical blood vessels and in small capillaries adjacent to the bleed site which has also been previously observed (Alfieri et al., 2013; Lu et al., 2014; Lin et al., 2007b; Chang et al., 2005). Remarkably and currently unreported, we find that the hippocampus also demonstrates a profound upregulation of HO-1 even in the absence of hemorrhage which is at least partially associated with the vessels in the hippocampal fissure. It should be noted that it has been reported that HO-1 is modestly upregulated even in Sham animals in the neurons of the dentate gyrus (Vincent et al., 1994) and yet when we stained for HO-1 we did not observe any detectable HO-1 in the Sham dentate gyrus at the concentrations of antibody and laser power we used.

2.9.3 Correlated Post-injury changes in heme processing pathway molecules

2.9.3.1 *Heme pigment over time post-injury*

In the early post-injury period the most obvious gross change to the tissue is the easily identifiable hemorrhages that occur at the white matter/grey matter interface along with scattered petechial bleeds that occur throughout the neocortex and occasionally in fascial plane adjacent to the alveus/fimbria of the hippocampus (it is important to note here that in our hippocampal dissections we largely remove hemorrhagic blood from the surface fimbria). The bleeds in the early post-injury period are markedly deep red in color and over 3-7d post-injury they appear to progressively lighten and ebb as their reddish pigment heme is processed and either eliminated locally or retained as the pigment Bilirubin which has a yellowish color. This progression of pigments and gross discoloration is shared by hemorrhagic injury in essentially all tissues with the exact timeline and pigment shifts being altered by the extent of hemorrhage (e.g. large, dense, bleeds take longer to resolve than smaller dispersed bleeds, (Cao et al., 2016). It has been found by other authors that the delayed process of erythrophagocytosis and resulting heme processing may be driven by altered expression of CD47 which is progressively lost after hemorrhage, disappearing by 3d post-injury (Cao et al., 2016; Xi et al., 1998; Oldenborg et al., 2000). CD47 further has been associated with HO-1 as a regulator of erythrophagocytosis (Schallner et al., 2015).

2.9.3.2 *HO-1 expression and cell location over time post-injury*

HO-1 expression correlates directly with heme pigment progression. We observed that HO-1 was elevated by 1d after injury in hemorrhagic tissue rising to peak expression at 3d before declining through 15d. This matches numerous observations in the literature with the timeline marginally adjusted depending on the size of the bleed (Cao et al., 2016; Yamauchi et al., 2004;

Fukuda et al., 1995). It is notable again that we find a matching time course exists in the hippocampus, which does not demonstrate remarkable hemorrhage, and rather than finding an incidental increase we see a multifold elevation that similarly peaks at 3d. The underlying process that drives expression in the hippocampus is somewhat uncertain but may either rely on hemorrhage like activity that is limited to the immediate vascular wall or some form of paracrine signals delivered from cortical areas connected via the vasculature. From the initial characterization of the injury model by Dixon et al., (Dixon et al., 1987) we know that with increased overpressure we will accomplish hemorrhage in the hippocampus. This suggests that the tissue is susceptible and we are just barely on the edge of threshold for hemorrhage in our cFPI application.

There is another current point of dispute in post-injury heme processing; Chang et al., 2003 found that when they compared HO following CCI in HO-2 KO and WT mice, activity was markedly reduced one day after injury (Chang et al., 2003). They concluded that HO-2, not HO-1, was the dominant form of HO involved in processing heme after injury. While we did not assay HO-2 in our experiments its activity could be elevated at the 1d post-injury interval, prior to peak HO-1 expression and prior to erythrocyte CD47 loss. Further, HO-2 is known to be elevated in specific brain regions, particularly in the hippocampus (Vincent et al., 1994; Verma et al., 1993; Yamanaka et al., 1996) and it is possible the tissue sampled in that study had a greater proportion of HO-2 relative to HO-1.

2.9.3.3 *Ferritin expression and cell location over time post-injury*

Following the appearance of heme pigment immediately after injury, and the peak processing of heme pigment at 3d post injury, we find that ferritin expression promptly rises with a peak at 7d in both brain regions studied. This is an expected sequelae to hemorrhage recovery

that has been observed many times and in large part is due to the iron accumulation in cells that process heme (O'Shaughnessy et al., 1966; Strassmann, 1949; Wu et al., 2003). The timeline indicates that FTL becomes elevated only after there is a robust iron related signal resulting from heme processing.

Once again we observe that there is a similar matching FTL time course between the hippocampus and the neocortex, though notably the hippocampus shows a rise 1d after injury which is not observed in the neocortex. If one takes the view that there may be a widespread but limited hemorrhagic process throughout the hippocampal tissue, it is possible that even 1d after injury there may be sufficient heme accumulated and processed to the level of FTL storage such that no prominent bleed is observed. Previous authors have at times characterized HO-2 as the dominant heme processing protein in hemorrhage since it provides the bulk of heme processing activity at 1d post-injury (Yamauchi et al., 2004) and while this finding is not inconsistent with our results it may help to explain why there is early upregulation of FTL in certain tissues. Alternately, it is known that HO-1 is constituently upregulated at low levels in the neurons of the dentate gyrus (Vincent et al., 1994). These both support the idea that there is an inherent constituently expressed mechanism for widespread tissue level processing of heme as long as it is limited in quantity in any individual location. It is possible that, in circumstances of gross hemorrhage which includes necrosis of tissue, heme processing may be delayed. In this case local cell populations which might be able to process the insult in a limited fashion are unable to do so due to debilitating cellular injury and functionally impaired vascular beds.

2.9.3.4 *LCN2 expression and cell location over time post-injury*

In addition to looking at proteins and pigments more canonically associated with heme processing we also investigated Lipocalin 2 in order to understand the early iron sequestration

and trafficking that occurs after injury. LCN2 has been found in cells that express FTL and plays a known role in cellular iron trafficking (Flower, 1996; Ratledge, 2007; Nairz et al., 2007). Further we were well aware of the known interaction between LCN2 and matrix metalloproteinases, effectors of degenerative/regenerative plasticity after TBI (Phillips et al., 2014; Kjeldsen et al., 1993; Chan et al., 2014), particularly the gelatinase MMP9. LCN2 is known to persistently activate MMP9 by preventing its degradation thus leading to MMP9 accumulation and substrate proteolysiss (Kjeldsen et al., 1993). We observed that LCN2 was highly upregulated after injury with extraordinarily high expression at 1d, which is at least partially the result of near complete absence of LCN2 in Sham animals. This is expected based on a broader interpretation of the literature which has found LCN2 to be an acute phase protein highly reactive in the hours after a traumatic insult (Zhao et al., 2016b; Huang et al., 2016; Li et al., 2013; Flower, 1996). It also neatly validates the minimal influence of craniectomy surgery on the HO-1 pathway at 1d post-injury, since there is a near absence of any LCN2 protein expression in the Sham control animals.

Again we observed that both the neocortex and the hippocampus showed similar profiles of LCN2 expression, with the hippocampus marginally more elevated. Expression declines through 7d and this is expected as other iron transport and sequestering proteins become upregulated culminating in elevated FTL expression. LCN2 functions by binding small molecules that capture iron in an attempt to isolate soluble iron and these soluble iron carriers from bacteria. LCN2 in turn is able to transport iron across cell membranes sequestering it out of the interstitial fluid. We observed a pattern of expression that was highly correlated with this function, showing broad tissue level expression which became more focal and cellular as time progressed.

2.9.3.5 *Gelatinase activation (MMP2 vs MMP9) over time post-injury*

It has been previously shown that the gelatinases are upregulated after traumatic brain injury and they have been highly correlated with dysfunction after injury and with repair mechanisms associated with reactive synaptogenesis (Phillips et al., 2014; Chan et al., 2014). Since there was a convergence between these known effectors of TBI and hemorrhagic injury through LCN2, we were interested to see if gelatinase enzyme activity was correlated with the HO-1 pathway response in our cFPI model. We discovered that, similar to our previous findings, proteolysis in the post-injury neocortex and hippocampus was remarkably similar. MMP2 activity was consistent with HO-1 in that it peaked at 3d but with fewer extremes in expression, evenly elevated at both 1d and 7d suggesting kinetic activity driven response rather than one tied to hemorrhage particularly. MMP9 however showed a pattern of activity that was highly correlated with LCN2 expression. The pro-form of MMP9 showed highly inducible activity at 1d post injury as has been previously observed in a variety of CNS insults (Kyrkanides et al., 2001; Lekic et al., 2011; Rosenberg et al., 2001; Gasche et al., 1999; Szklarczyk et al., 2002b). By contrast, the active form of MMP9 more closely matches the expression profile of LCN2, suggesting that the two proteins may indeed interact during the acute post-injury cellular response to cFPI. However, to some extent this interaction effect remains unclear. For example, LCN2 has a specific binding site on human MMP9, which could explain its persistent activation of the enzyme, but in rodent models, while it has been shown that LCN2 persistently activates MMP9, the same MMP9 binding site is no longer present and no clear alternative has been established (Flower, 1996; Kjeldsen et al., 1993). Our enzyme activity findings do not agree with some studies of MMP expression after injury (Shi et al., 2017), where MMP9 mRNA was reported to peak at 3d post injury and MMP2 to peak at ~5-7d post-injury. Oddly however, this

study failed to show concurrent increases in MMP protein, where their ELISA results showed MMP9 peak at 1d and MMP2 to be stable from 1-7d. It remains unclear how to interpret such findings and whether those measures can reasonably be compared with our data.

After establishing these general baseline responses of the HO-1 pathway to cFPI, it is important to compare similarities and differences between the two brain regions examined, further considering their individual patterns in greater detail. Since analyzing response in both regions simultaneously can be complicated, we first considered each tissue individually to interpret the observed post-injury activation of heme processing proteins. The initial thesis was that two tissues known to underlie persistent TBI deficits, one of which was hemorrhagic, and one which was not, would show clear differences in the extent of HO-1 pathway activation. We did not initially expect to find that the neocortex and hippocampus would be so consistent in HO-1 pathway response to cFPI, but given these similarities, it is helpful to look at each tissue in isolation.

2.9.4 Neocortical HO-1 Response Relative to Hemorrhagic Damage at NVU

Overall, our observations of post-injury neocortical HO-1 expression are consistent with that reported for other models of TBI or CNS injury (Alfieri et al., 2013; Lu et al., 2014; Fukuda et al., 1996; Yamauchi et al., 2004; Cao et al., 2016). In grossly damaged tissue there is a clear disruption of the NVU, accompanied by an acute HO-1 upregulation that occurs 1-3d after injury, which persists through at least 7d and in numerous cases 15d+. There is a known association of this HO-1 induction with vessels likely driven by hemorrhage related triggers, in the case of TBI, the release of heme from degenerating erythrocytes. The post-injury neocortical expression of HO-1, LCN2, and FTL in our cFPI model reflects the predicted cellular response

for a moderately hemorrhagic injury. This cellular response is focused at GM/WM boundary hemorrhage and areas of NVU disruption.

2.9.4.1 GM/WM interface hemorrhage and necrosis, mixed microglia + astrocyte activation

The most notable pathological change which we observe in the neocortex is the grossly disrupted WM tract that overlays the lateral ventricles and terminates in the grey matter. This pattern has been observed since the initial characterization of the rodent cFPI model (Dixon et al., 1987). Whether it is due to an interface effect or just some compartmental path of least resistance there is considerable WM damage which enables a larger bleed to form, invading into the grey matter through Layers V and VI. The shape and direction of the bleed may be driven by the relatively fibrous wall of the lateral ventricle which constrains one boundary of the hemorrhage. On limited occasions a larger blood vessel in the cerebrum will also be involved extending hemorrhagic activity through layers IV and III but without reaching the outer surface of the tissue. This provides an interesting perspective on the resulting injury– the stress strain damage which causes gross primary tissue necrosis is relatively limited to the white matter while the expanding hemorrhage produces heme related injury over a greater tissue area and particularly in the region we examined. We can contrast this to diffuse axonal damage in the tissue which has been observed to be spread out over a larger area and affecting a greater number of tissues (Dixon et al., 1987).

In this region of primary hemorrhagic injury we see cellular necrosis and a generalized DAPI related schmear of nuclear contents which progressively disappears over 3-7 days post injury. In the cortical layers more distant from active bleed sites we see extensive GFAP+ HO-1+ reactivity which approaches quite close to the distinct hemorrhagic sites but maintains a small

perimeter. Within this perimeter and within the bleed itself we observe numerous IBA1+ HO-1+ cells, which in a number of instances appear to be transvasating out of the nearby intact capillaries. It is possible that since we are observing a snapshot in time that the GFAP+ perimeter we observe represents the maximal extent of the bleed which has been recently processed by phagocytic cells.

Throughout the neocortex in addition to the large primary bleed we also see small examples of potential petechial bleeds which show autofluoresence during imaging. While it is tempting to attribute them to a non-specific tissue signal, it is notable that they occur with greatest frequency in the tissue which is 1-3d post injury, supporting a more pathologic nature. They also have a tendency to show marked HO-1 reactivity nearby which is localized within GFAP+ rather than IBA1+ cells, further suggesting that astroglia can be effective mediators of heme processing under limited conditions. In general these petechial sites occur throughout the reactive neocortex overlaying the lateral ventricles.

2.9.4.2 Predicted intensity and location of HO-1 based on extent of NVU damage induced by injury

Disruption of the NVU is, to an extent, predictive of HO-1 expression though in the context of a gross hemorrhage this is perhaps minimalized. While we did not directly analyze specific NVU components it is notable that throughout the neocortex where we see petechial HO-1 reactivity we observe dilated blood vessels that appear aberrantly large relative to Sham controls suggestive of a vascular insult. It has been shown previously that TBI pathology produces permeable blood vessels which are much leakier than the normo-pathological non-

fenestrated vessels in the brain (DeWitt and Prough, 2003; Kenney et al., 2015; Chodobski et al., 2011). This suggests that the observed HO-1 reactivity near vessels is associated with increased permeability of the vessels and in parts of the tissue which do not show increased HO-1 reactivity we also do not see instances of enlarged lumen vessels.

As mentioned previously there is a general shift in HO-1 expression from primarily IBA1+ microglial to GFAP+ astroglial as we move further away from the center of focal bleeds. To an extent this may be explained by the relative brightness of IBA1+ glia near the bleed site, which itself is highly autofluorescent and may be obscuring reactive astrocytes. It may also be that, since microglia are generally more mobile than astroglia, they are able to accumulate in greater numbers near the bleed site and thus appear to be brighter in expression.

2.9.5 Hippocampal HO-1 Response Relative to Absence of Hemorrhagic Damage

2.9.5.1 Follows a post-injury time course and cell location similar to injured hemorrhagic neocortex

The hippocampal response after injury is particularly remarkable when contrasted to the neocortex. To our knowledge no one has attempted to examine heme processing in non-hemorrhagic tissue in the context of brain injury and in many of the other TBI models there is frequent hemorrhage into the hippocampus, particularly with lateral injury. We do see some limited hemorrhage along the surface of the fimbria and in particular animals may see some local HO-1 reactivity directly adjacent in CA3, but even in these select animals there is no evidence of hemorrhage in the dentate gyrus and CA1, where we see extensive cellular reactivity and HO-1 pathway induction. As previously noted, when the cFPI model is generated with increasing applied overpressure hemorrhages in the hippocampus do result (Dixon et al., 1987). Most

remarkable in our studies is the expression and organization of HO-1 within the dentate gyrus. At early post injury time points (1d) there is widespread, diffuse HO-1 expression which predominates directly adjacent to the granule cell layer. As post-injury time continues there is a gradual aggregation of HO-1 into more punctate cellular expression, shifting outwards into the molecular layer and towards the hippocampal fissure. By 7d, expression is largely limited to near the hippocampal fissure and into the stratum moleculare layer of CA1. Notably, HO-1 appears to be differentially expressed in microglia and astrocytes as a function of dentate subregion. The hilus of the dentate gyrus shows limited expression of HO-1, which is more highly associated with IBA1+ microglia than GFAP+ astrocytes. At the same time, in the synaptic rich dentate molecular layer, expression of HO-1+ GFAP+ cells predominates. It is uncertain why these cellular differences occur, however, one could speculate that hilar HO-1 may be induced in microglia as a response to potential CA3-4 pyramidal cell damage after cFPI, while molecular layer HO-1 response is more a result of focal NVU insult affecting associated astrocytes.

Concurrent with this process there is always an association of HO-1 with specific vessels running through the hippocampal fissure. It is not generally associated with all vessels but at all time points there are specific reactive vessels which show what appear to be astrocytic processes wrapping the vessels and expressing relatively large amounts of HO-1. The underlying mechanism for the organization of HO-1 expression or the association with vessels is at this point unknown however potential causes included damaged/permeabilized blood vessels exhibiting a slow form of hemorrhage or perhaps a loss of trophic support causing a hypoxic related response. In gene chip assays of both mice and rats subjected to cFPI, however, we were unable to identify upregulation in any hypoxia associated transcription factors known to transcriptionally regulate HO-1.

2.9.5.2 HO-1, FTL and LCN2 observed together around non-hemorrhagic vessels

It is unsurprising that the mediator of heme processing (HO-1) and both acute and long term iron storage proteins (LCN2 and FTL) are highly upregulated near focal hemorrhagic sites within the injured neocortex. It is more surprising however to observe them all co-localized around specific areas in non-hemorrhagic tissue. We observe that this association between HO-1/LCN2, which progressively evolves into HO-1/FTL co-expression, occurs primarily along select vessels in the hippocampal fissure. This is probably best explained by a tissue level attempt to secrete excess iron into the vasculature for eventual recycling in the hematopoetic tissue. This is also unlike what we see in the neocortex/white matter damage, where it appears that vessel integrity is sufficiently lost such that there are notable aggregates of iron forming in the center of the hemorrhagic bleed site.

2.9.5.3 Possible factors responsible for strong hippocampal HO-1 pathway response

Since we do not have apparent hemorrhage in the hippocampus to account for driving HO-1 expression and yet we see that HO-1 expression is highly induced in this region, both histologically and with western blot protein assay, we are forced to speculate possible causes of the strong response. It is possible that, with permeabilized vessels and a high cell vulnerability to TBI, we have identified a subthreshold, limited hemorrhagic process which is insufficiently large to produce identifiable extravasation of blood or heme-related pigments. Perhaps there is a shared mechanism with the penumbra of the cortical hemorrhagic injury, suggesting that the penumbra represents a distinct injury state with respect to HO-1 response rather than simply an injury related boundary based on tissue damage.

2.9.6 Impact of these results on post-injury management of hemorrhage

2.9.6.1 Identified vs unidentified NVU damage/hemorrhage must be considered

One of our major findings is that there appears to be a hemorrhagic or hemorrhage-like process which occurs in tissue classically observed to lack identifiable bleeds. There is a distinct timeline of HO-1 expression which is consistent in both hemorrhagic and specific non-hemorrhagic tissues. Since previous studies using other models report HO-1 response in some specific tissues and not in others, it is possible that diffuse injury generates an underlying component of the hemorrhagic process which is difficult to detect and contributes significantly to post-injury pathophysiologic cycle of damage and recovery. There has been a significant amount of work with *in vivo* models attempting to replicate the extent of post-injury hemorrhage in order to better classify incoming patients to the ED. These studies have repetitively shown that with increased magnet power, enhanced processing, or simply more careful analysis that the extent of microhemorrhage and the scope of the injury penumbra is larger than previously thought (Liu et al., 2015; Chiara Ricciardi et al., 2017). Paired histological staining of iron deposition has provided further evidence that the extent of injury far exceeds what can be feasibly obtained through imaging of living tissue as exemplified by Dr. Latour's research at NINDS recently presented at the National Neurotrauma Meeting (Abstracts from the 34(th) annual national neurotrauma symposium june 26-29, 2016 lexington, kentucky. 2016). A prerequisite to identifying pathologic iron is that significant quantities be present to overwhelm predominate innate iron recycling mechanisms under normal physiologic conditions. If this is true, then we might predict that undetected diffuse limited hemorrhage could occur throughout the injured tissue. This also suggests that it may be necessary to target underlying heme processing, even in diffuse injury, as a means of effecting improved post-injury recovery.

2.9.6.2 Manipulation of heme processing pathways feasible next step

Traditionally the focus on injury related hemorrhage and clotting has revolved around stopping active bleeds to prevent tissue trauma or degrading clots to permit tissue perfusion (Lin et al., 2017; Peres et al., 2017). More recently, however, there has been interest in examining how heme is processed after hemorrhagic stroke and how affecting heme processing can result in post-injury improvement. The rationale is fairly straightforward in models of intracerebral hemorrhage as an example where heme is a more dominant player in the post-injury tissue pathology. In our studies of diffuse cFPI it is more likely that heme related injury is an ancillary player though with significant potential to influence recovery. Since we are operating in a tissue space where injury is known to be moderately recoverable, finding areas where even limited improvement is possible may go a long way towards reducing the persistent loss of function and lower quality of life which can occur. There is already limited research ongoing in the field of hemorrhagic stroke which has been focused on modifying HO-1 through activation of its upstream transcription factor Nrf2 with various pharmacological agents. In our initial gene chip assays (see Appendix) we identified Nrf2 as the most likely transcription factor affecting HO-1 upregulation after injury. In models of stroke targeting of Nrf2, manipulation of the transcription factor is reported to reduce the total hemorrhagic area, reduce BBB disruption and improve behavioral outcome (Alfieri et al., 2013; Lu et al., 2014). While we do not expect hemorrhage focused treatments to have quite as robust an effect in a TBI model where hemorrhage is a smaller component of injury, they may provide a novel avenue of research which will help us to better understand and attenuate persistent deficits after injury. Even more promising, the later HO-1 expression (peaking at 3d) shown in our initial studies may be due to a delay in the lysis of erythrocytes, providing an extended critical window for treatment targeting HO-1. We posit that

early upregulation of heme processing proteins prior to wide substrate availability (dependent on lysis of erythrocytes) would be expected to provide more acute availability of intracellular buffering compounds and limit cytotoxicity. There has already been some promising work done in rodent models of stroke using this approach (Alfieri et al., 2013; Lu et al., 2014), demonstrating both pathological and behavioral improvement and we proffer that similar techniques may be beneficial in our model of diffuse cFPI.

3 Chapter 3

Chapter 3

Modulation of Heme Processing Response via Post-injury Induction with HO-1 Inducing Agents

3.1 Abstract Chapter 3

In order to determine if HO-1 and the HO-1/Nrf2 heme processing pathway is a viable target for post-injury therapeutic intervention we utilized a contrast dosing paradigm where we examined hemorrhagic (neocortex) and non-hemorrhagic (hippocampus) tissue 1-15d post-cFPI after 1hr post-injury treatment with either Sulforaphane, or Hemin. Both drugs are known HO-1/Nrf2 activators and the choice to use both was designed to account for the inherently broad spectrum effects that may occur since each is understood to target the pathway via a different mechanism. We observed distinct effects in protein expression, behavior, and histology in the treated vs untreated TBI animals. By 1d a significant portion of heme pigment is cleared out of the hemorrhagic injury site in the drug treated animals and both groups showed similar shifts in peak expression of HO-1 from 3d to 1d. Further, FTL, an iron storage protein and a marker of long term injury in the tissue is temporally shifted in expression and demonstrates a reduction in peak iron load in the neocortex. These changes in protein expression are matched in the histology observed in the tissue and there is a generally greater organizing effect in the drug treated animals vs the untreated animals which tend to show broader expression of all markers observed. Behaviorally the TBI+SFN showed significant acute improvement in the rotarod test, performing comparably to Sham controls by 2d post-injury. In this test the TBI+HMN group lagged behind and was closer to the TBI in performance though consistently performing slightly better. When behavior is extended out to 15d in the Morris water maze we see a profound improvement in the TBI+HMN group which appears to closely match Sham metrics and is in contrast to the TBI and TBI+SFN groups. Looking more closely however also reveals that both drug treated groups develop distinct search profiles demonstrating that a single 1hr post-injury pharmacological

manipulation has a profound effect even 15d later. The data suggest that there is a critical window after TBI which extends to at least 1hr post-injury where there is a potential window for therapeutic intervention and further demonstrates support for treating even diffusely injured patients for potential heme pathology.

3.2 Introduction Chapter 3

Heme Oxygenase 1 (HO-1) is the inducible form of the rate limiting enzyme in heme catabolism. HO-1 catabolizes heme into the potential neurotoxins carbon monoxide (CO), Iron (Fe), and Biliverdin. It does so by cleaving heme at the alpha-methene bridge which directly releases CO and removes the binding stability of Fe in the center of the Heme structure leaving behind the open metalloporphyrin Biliverdin. HO-1 has been shown to be induced by a variety of stimuli, chief amongst them heme substrate itself, and HO-1 has a high degree of specificity for heme B over other forms of heme or metalloporphyrins. HO-1 induction has been associated with injury severity and, in Chapter 2, we previously identified the time course of HO-1 expression 1-15d in both a hemorrhagic (neocortex) and non-hemorrhagic (hippocampus) tissue.

Because prior studies have suggested both positive and negative associations of HO-1 induction with injury outcome we have utilized two known inducers of HO-1 to examine if an elevation in acute post-injury HO-1might facilitate more efficient, less toxic heme processing, thereby resulting in behavioral improvement relative to untreated injured cases. The choice of the two rather broad HO-1 targeted agents was made due to the unavailability of highly selective HO-1 inducers and because our goal was to trigger a robust activation of the HO-1 heme processing response. Interestingly, there remains some uncertainty as to whether increased HO-1 will be beneficial or harmful in the FPI model. The two views are largely divide along the line of whether increasing HO-1 pharmacologically will simultaneously increase the buffering capacity of the local tissue or if the increased HO-1 activity in the absence of increased buffering capacity will overwhelm the local cells causing increased tissue necrosis. The experiments of Chapter 3

will help clarify whether acute post-injury manipulation of HO-1 qualifies as a potential neuroprotective therapy following TBI.

The two agents selected for our study are **Hemin (HMN)** and **Sulforaphane (SFN)**. Hemin is essentially the endogenous substrate of HO-1, an animal derived heme B that is stabilized with a chloride atom. Hemin induces HO-1 expression via the complete endogenous pathway. Hemin is degraded and releases Fe, which either directly or through the induction of ROS causes a conformational change in the repressor protein keap1, leading to Nef2 release, translocation to the nucleus for increased transcription of ARE consensus genes which include HO-1. Sulforaphane in contrast is a brassicaceae derived organosulfur isothiocyanate which acts as an antioxidant/weak oxidant. Sulforaphane is effective in directly inducing conformational change in keap1 and does not require digestion nor does it produce ROS or other cytotoxic species after injection. Both drugs have been used previously in animal models of stroke (Alfieri, Lu) and Sulforaphane has been used in limited trials in TBI (Dash 2005). To date they appear, while non-specific, to be among the best *in vivo* HO-1 inducers available.

The hypothesis is that early induction of HO-1 after injury via an upstream mechanism also known to increase cellular buffering capacity to HO-1 degradation products will lead to improved tissue pathology and behavioral recovery. This effect depends in part on the delay in erythrocyte lysis after injury which normally drives post-injury HO-1 upregulation. In a sense, we are providing a heme toxicity 'pre-insult' which can be given temporally after the traumatic injury has occurred but before the heme toxicity insult has resulted. Towards this end, our dosage scheme of IP 1 hour after injury is designed to mimic a best case real world paradigm where a TBI could be diagnosed and treated within hours after injury.

We expect that HO-1 induction will lead to decreased heme pigment after the injury and that overall tissue pathology will be reduced. Further, we expect both LCN2 and FTL to be upregulated early, LCN2 as part of the same transcriptional mechanism and FTL in response to the resulting available iron.

3.3 Methods Chapter 3

3.3.1 Experimental Animals

The procedures in this study met national guidelines for the care and use of laboratory animals with all experimental protocols approved by the VCU Institutional Animal Care and Use Committee (IACUC). Male Sprague-Dawley rats (290-360g, ENVIGO, Huntingdon, UK) were used in these experiments, housed in pairs when possible under a temperature (22^{o}C) and humidity (66%) controlled environment with food and water provided ad libitum and subjected to a 12 hour dark-light cycle. Rats were randomly assigned to either TBI (n=26), Sham-injured (n=21), TBI+HMN treated (n=21), or TBI+SFN treated (n=24) groups and evaluated at 1d, 3d, 7d, or 14d post injury by WB or IHC. For all analysis Sham-injured animals served as controls for the TBI animals.

3.3.2 Surgical Preparation for Rat Central Fluid Percussion Injury

24 hours prior to central fluid percussion injury animals underwent surgical preparation to mitigate acute inflammatory response confounding. Rats were anesthetized with 4% isoflurane in carrier gas (70% N_2O, 30% O_2) for 4 minutes, heads shaved, and maintained on 2% isoflurane in carrier gas delivered via nose cone for the duration of the surgery. Surgical site is cleaned with iodine solution followed by 70% ethanol and a surgical drape placed over the animal. Body temperature was maintained at 37^{o}C via heating pad (Stryker, Kalamazoo, MI), and animal vital signs (heart rate, arterial oxygen saturation, respiratory rate, pulse distention, and breath distention) monitored via pulse oximeter (MouseOX; Starr Life Sciences, Oakmont, PA). While

under anesthesia rats were secured in a stereotaxic device (Harvard Apparatus, Holliston, MA) via ear bars and a midline incision used to expose the cranium to permit a midline sagittal craniectomy midway between the lambda and bregma sutures of 4.8 mm diameter to allow visualization of intact dura mater. Two 3/16 in steel machine screws were implanted into the skull 1 cm from craniectomy center in the 1st and 3rd quadrants. The craniectomy was fitted with a modified (tapered) Luer Lock hub (2.6 mm i.d.) fixed with cyanoacrylate adhesive. Additional stability is provided using dental acrylic (Coltene/Whaledent, Inc., Cuyahoga Falls, OH) to secure screws and Luer Lock hub into a single complex. The hub was finally filled with saline to limit clotting and tissue damage prior to injury. The incision wound was sutured over the complex and treated with triple antibiotic ointment and lidocaine. Animals were monitored for post-surgical stress in a heated holding cage during the acute recovery phase prior to being returned to their home cage.

3.3.3 Central Fluid Percussion Injury

The fluid percussion injury device consists of a weighted pendulum and a 0.9% saline filled acrylic cylinder (Custom Design and Fabrication, Petersburg, VA) which is fitted with a metal pressure transducer (Entram Devices, Inc., model EPN-0300-100A). Injury is induced by releasing the weighted pendulum from a pre-determined empirically derived height which strikes a greased rubber piston on one end of the cylinder producing a pressure wave which injects a small volume of saline into the dura of the animal attached to the other end of the cylinder via the Luer Lock fitting (Figure 3-1; (Dixon et al., 1987). Height of the pendulum corresponds monotonically with injury peak pressure which in turn corresponds with injury severity. Twenty-four hours after preparative surgery, animals were anesthetized 4% isoflurane in carrier gas for 4

minutes and given a scalp incision to expose the hub complex. Animals were then attached to the fluid percussion device by filling the hub with sterile 0.9% saline to ensure a seal free of air bubbles and clots. Animals then received a mild-moderate fluid percussion injury (2.0 ± 0.1 ATM overpressure) via saline injection into the closed cranial cavity. The pressure pulse was measured by the transducer and displayed on an oscilloscope (Tektronix 1000 S, Beaverton, OR) and the peak of the pressure wave recorded. Prior to recovery of consciousness, the hub was removed and the incision sutured closed and treated with topical triple antibiotic and lidocaine. To determine and confirm injury severity, reflexes (tail, paw, ear, corneal blink) and righting times were recorded prior to acute recovery. Sham injured animals underwent the same surgical preparation and hub removal procedures but did not receive central fluid percussion injury. For Sham injured animals reflexes and righting time were not recorded as they do not differ from naïve anesthesia treated animals.

3.3.4 Protein Extraction

Rats were anesthetized with 4% isoflurane in carrier gas (70% O_2, 30% NO_2) for 4 min and sacrificed by decapitation at the appropriate experimental interval 1, 3, 7, 15d after FPI/Sham injury. Neocortex trimmed of white matter and obvious hemorrhages sampled from the central square of a 3x3 grid arranged on the surface was collected along with whole hippocampal bulbs trimmed of any extraneous tissue (n=4-7/group). Tissue samples were homogenized on ice in 250 uL of RIPA Lysis Buffer (EMD Millipore, Billerica, MA) with cOmplete protease inhibitor + EDTA (Roche Diagnostics, Mannheim, Germany) prior to separation via 14,000 g centrifugation for 20 min at 4^{o}C. Supernatant was aliquoted and stored with separated nuclear pellet at -80^{o}C. Protein concentration of extract was determined using

Pierce BCA Protein Assay Reagent kit (Thermo-Fisher, Waltham, MA) on a Fluostar Optima plate reader (BMG Labtech, Inc., Cary, NC).

3.3.5 Figure 3-1: cFPI Device

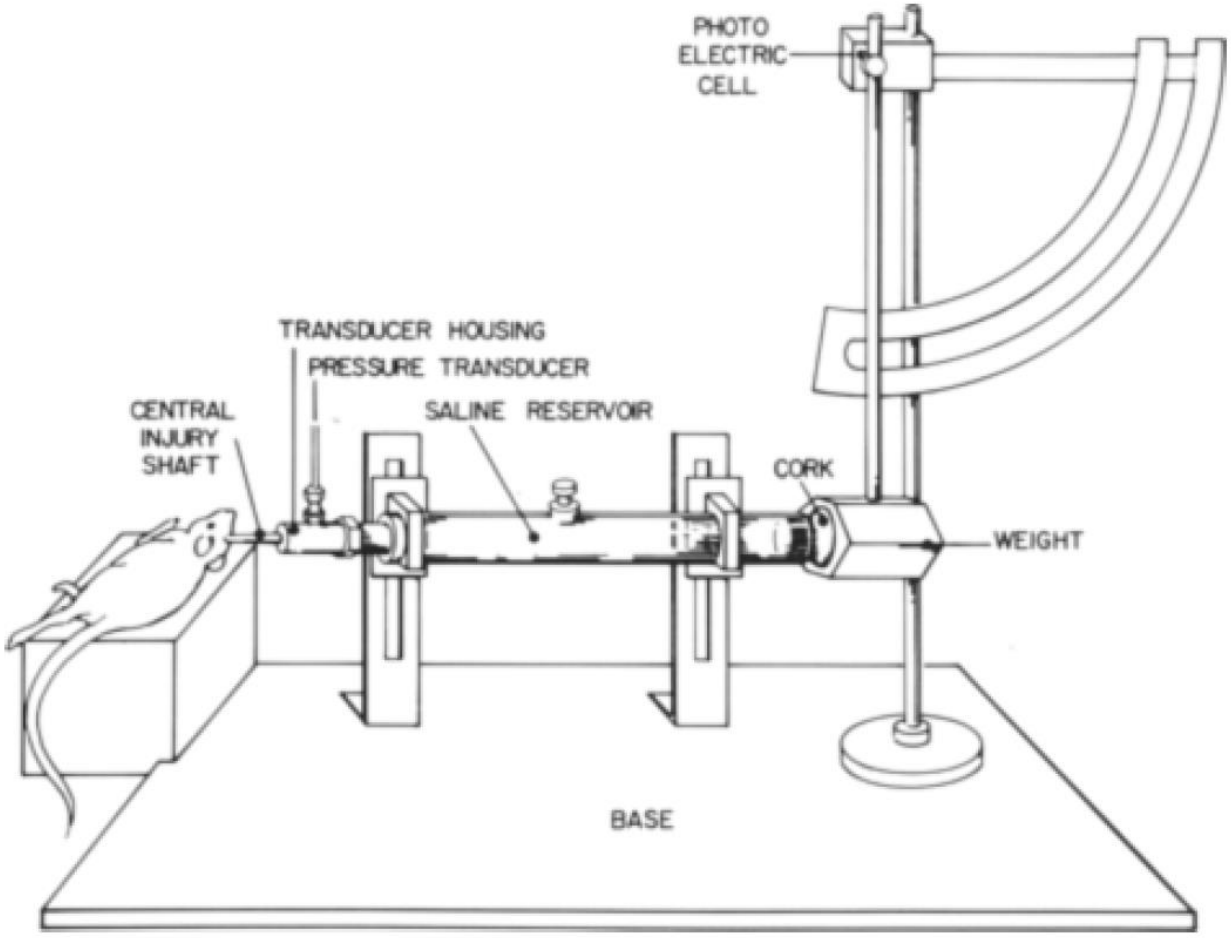

Figure 3-1**:** *Diagram of fluid percussion model of brain injury. A 4 mm central craniectomy central craniectomy is connected to one end of a Plexiglass cylinder filled with physiologic saline. At the other end in the cylinder is a Plexiglas cork mounted on O-rings. Injury is produced by striking the cork with a 4.8 kg pendulum dropped from a specific height. The pressure transient is recorded on a storage oscilloscope with an extra-cranial transducer.* Figure and text reproduced with permission from Dixon et al., 1987. In our paradigm we note several small changes including a central craniectomy 4.8 mm in diameter and the addition of a firm rubber tip on the end of the cylinder cork.

3.3.6 Western Blotting

Western Blot (WB) analysis was carried out using Bio-Rad products on their Criterion Gel system using 18 or 26 lane Criterion XT Bis-Tris Gels (Hercules, CA). 50 or 25 ug of protein were prepared in XT Sample Buffer with XT Reducing Agent and homogenized prior being denatured at 95^{o}C for 5 mins. Samples were electrophoresed on 4-12% or 12% gels in MOPS running buffer at 200v for 45 min (after 50v x 5 min stacking period) or until tracking dye approached the gel foot. Protein was transferred onto PVDF or Nitrocellulose membranes at 100v for 1 hour in a Tris-Glycine buffer with 10% methanol. Post-transfer the remaining protein on the gels was stained with 0.1% Coomassie Brilliant blue in 40% MeOH+10% glacial acetic acid overnight prior to de-stain and visualization to confirm even protein load and transfer. Meanwhile, membranes were rinsed with nano-pure deionized water before buffering with Tris-buffered saline (TBS) and blocking for 1 hour with 5% non-fat milk in TBS with 0.5% Tween (mTBST). Membranes were incubated with appropriate antibody at 1:1K or 1:2k **(see Table 3-1)** dilution overnight at 4^{o}C. After incubation, membranes were washed with mTBST and then incubated with the appropriate HRP-linked secondary for 1 hour at room temperature. Membranes were then washed in TBST to remove excess non-specific signal and finally in TBS to remove tween surfactant effects. Membranes were visualized via chemiluminescence using Super Signal West Dura Extended Duration Substrate (Thermo-Fisher, Waltham, MA). Quantitative data was collected using a Syngene G:Box with protein bands subjected to densitometric analsysis using Gene Tools software (Syngene, Frederick, MD). Protein data was expressed as fold change relative to time matched Sham control animals processed on the same

membrane. Confirmation of load control was determined using beta actin (Sigma-Aldrich, St. Louis, MO) with a known caveat that signal may modestly change during TBI.

3.3.7 Tissue Fixation

Rats were anesthetized with 4% isoflurane in carrier gas (70% O_2, 30% NO_2) for 4 min with sodium pentobarbital (400 mg/kg IP) and sacrificed via transcardial perfusion; flushed with 0.9% saline with a clamped descending aorta and snipped right atrium. When perfusion runs clear tissue is perfused with 4% paraformaldehyde in phosphate buffer (0.1 M $NaHPO_4$, pH=7.4). Once tissue was fixed whole intact brains were removed from the cranium and placed in excess tissue fixative for 24 hours prior to transfer into 0.03% NaN_3 in 1.0 M Phophate Buffered Saline (PBS) and storage at 4^o C. Prior to utilization for immunohistochemistry tissue was blocked and sectioned into 40 um coronal slices using a Leica Vibratome (VT1000S; Leica Biosystems Inc., Buffalo Grove, IL). Sections were stored separated and organized in PBS + Azide at 4^oC.

3.3.8 Immunohistochemistry

Free floating sections were selected based on rostral-caudal position and permeabilized in 5% peroxidase for 30 mins. Tissue was washed in PBS and the blocked using fish gelatin in PBS + 0.05% triton X-100. Tissue was incubated overnight with primary antibody in blocking buffer (see **Table 3-2**) at 4^oC. The following day sections were washed with PBS prior to further blocking for 30 minutes and incubated with secondary fluorescently tagged antibody in blocking buffer for 2 hours at room temperature. Sections were then washed in PBS, rinsed in Phosphate

Buffer to remove salt artifact and mounted on Superfrost Plus slides (Fisher Scientific, Pittsburgh, PA), and allowed to air dry. When dry sections were coverslipped using Vectashield + DAPI (Vector Laboratories, Burlingame, CA). Fluorescent signal was visualized on a confocal Zeiss LSM 700 (Carl Zeiss, Thornwood, NY), on an apotome Zeiss AxioImager M2 (Carl Zeiss, Thornwood, NY), or on a widefield Olympus BX51 (Olympus, Tokyo, JP).

3.3.9 Drug Injection Protocol

Certain animal cohorts were injected with either Hemin (26 mg/kg; from Bovine, Sigma-Aldrich, St. Louis, MO) or Sulforaphane (5 mg/kg; LKT Laboratories Inc., St. Paul, MN) (see appendix for further drug information). Injections were given **intraperitoneal (IP)** 1 hour post injury to briefly anesthetized rats randomly selected from TBI animals. The drugs were given in a PBS volume of 3 mL/kg body weight with 0.04% DMSO (~1 mL saline per animal). Both drugs were prepared day of in low light conditions. Sulforaphane was added to PBS in a stock solution of 400 mg/mL DMSO. Hemin was added to PBS as a powder and while Hemin effectively wets at pH 7.4 it remains a slurry. Both drugs were vortexed to break up possible clumps and mix solution. Prior to injection solutions were raised to human body temperature ~ 37^{o}C. [Note, prior attempts to use low pH to induce solubility simply resulted in the Hemin dropping out of solution when pH was raised again].

To demonstrate proof of concept we ran a limited injection protocol in naïve animals using dosages in a range that bracketed typically used values found in the literature. We demonstrated that in the setting of a naïve animal with intact BBB/NVU that we were able to detect an increase in HO-1 expression 24hr after injury using both Sulforaphane and Hemin (See

Appendix). The results demonstrate induction of HO-1 in a naïve setting. While we observed that HO-1 was induced by the agents selected we must note that the mechanism by which either drug is taken in or detected by the brain is uncertain. Further, since the barrier is grossly disrupted, or generally more permeable, after injury it is unknown if the comparison is valid and whether drug dosing in an uninjured brain is comparable. We generally proffer that given what is known about barrier disruption after injury it is most likely that the regions that experience the greatest exposure to drug are also those regions that are most damaged and thus have the least barrier integrity.

3.3.10 Figure 3-2: Rotarod Device

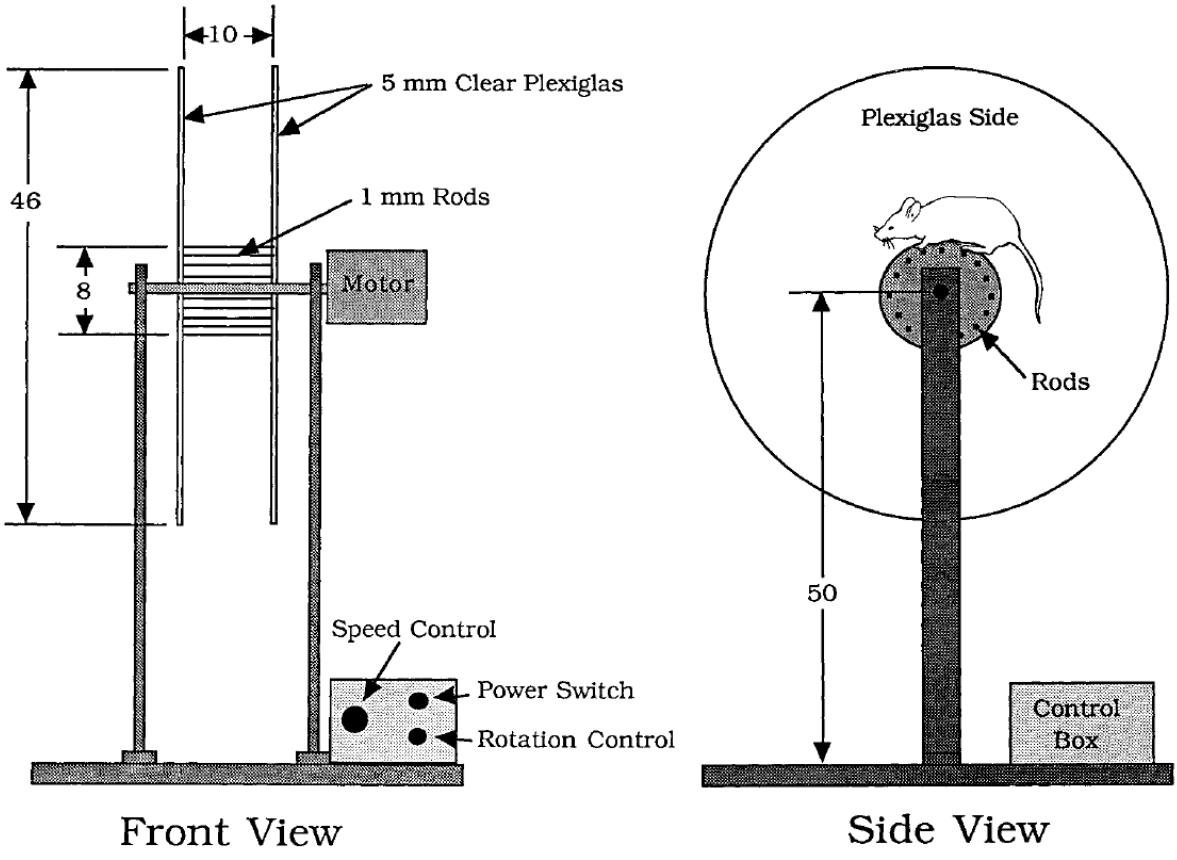

Figure 3-2: *Front and side views of the rotarod apparatus. Unless specified otherwise, all dimensions are in centimeters*. Reproduced with permission from Hamm et al., 1994. Note; it is believed experiments were run on the legacy device characterized in the original paper mentioned.

3.3.11 Rotarod

Rats were run on the rotarod apparatus 1-7d or 1-Sacrifice Day as appropriate. The device consists of two large, clear, 46 cm diameter and 5mm thick plexiglass discs spaced 10 cm apart which frame a walking area consisting of 18 1mm diameter stainless steel rods arranged in an 8 cm diameter cylinder (**Figure 3-2)**. The central pivot of the device is 50 cm above the table surface and a control box (Bodine Electric Company) adjacent to the device has controls for speed, direction of rotation, and a brake. Testing rotational velocities range from 0 rpm to a peak of 30 rpm. The test paradigm as utilized was to place the rodent on the walking area, wait 10 seconds for habituation, and then apply a rotational velocity ramp from 0 to 30 rpm gaining 3 rpm every 10 seconds until maximum velocity is reached and then maintaining this maximum for an additional 20 seconds. The test trial concludes when 1: a rat falls off the device 2: the rat is spun around the device twice 3: the rat completes the full time (see appendix for exact scoring criteria). Rats are given two trials per day with a third trial if the first two are inconsistent and there is a minimum 10 minute delay between trials. Data is recorded for time spent on the device for each trial with peak rotational speed computed from the time data. Group averages, ANOVA, and TukeyHSD are further run on the resulting data.

3.3.12 Morris Water Maze

Rats were run in the Morris Water Maze 11-15d post injury when appropriate. The device (**Figure 3-3)** consists of a 180 cm diameter, 60 cm high white plastic pool filled to a depth of 28 cm with water made opaque with non-toxic washable white paint (Crayola, Easton, PA). A clear

plexiglass platform 10 cm in diameter is fixed 2 cm below the surface as a hidden platform located midway into the 4th quadrant of the pool. The pool is located in a room with numerous extra-maze cues that remain constant throughout the experiment. In order to assess spatial memory function during the training phase (days 11-14) four trials per day are run for each animal with the animals randomly cycling through North, South, East, and West starting positions. Rats are given 120 seconds to find the platform and are manually placed on the platform if they are unable to find it. The rats remain on the platform for 30 seconds before removal to a heated incubator in between trials. The inter-trial interval was a minimum of 10 minutes. On the final day of the trial the hidden platform is removed and the rats are given 60 seconds to swim in the pool before removal. Throughout the test the rodent swim paths are recorded using video and the Water Maze package for Videomex Systems (Columbus Instrument, Columbus, OH). During the training phase swim speed, path length, and latency to the platform are observed and recorded. During the trial day swim path is observed and swim speed, quadrant time, proximity score, and relative proximity score are computed for each animal. Further subjective analysis of search patterns is conducted after constructing individual and group heat maps paired with trial path.

3.3.13 Figure 3-3: Morris Water Maze Apparatus

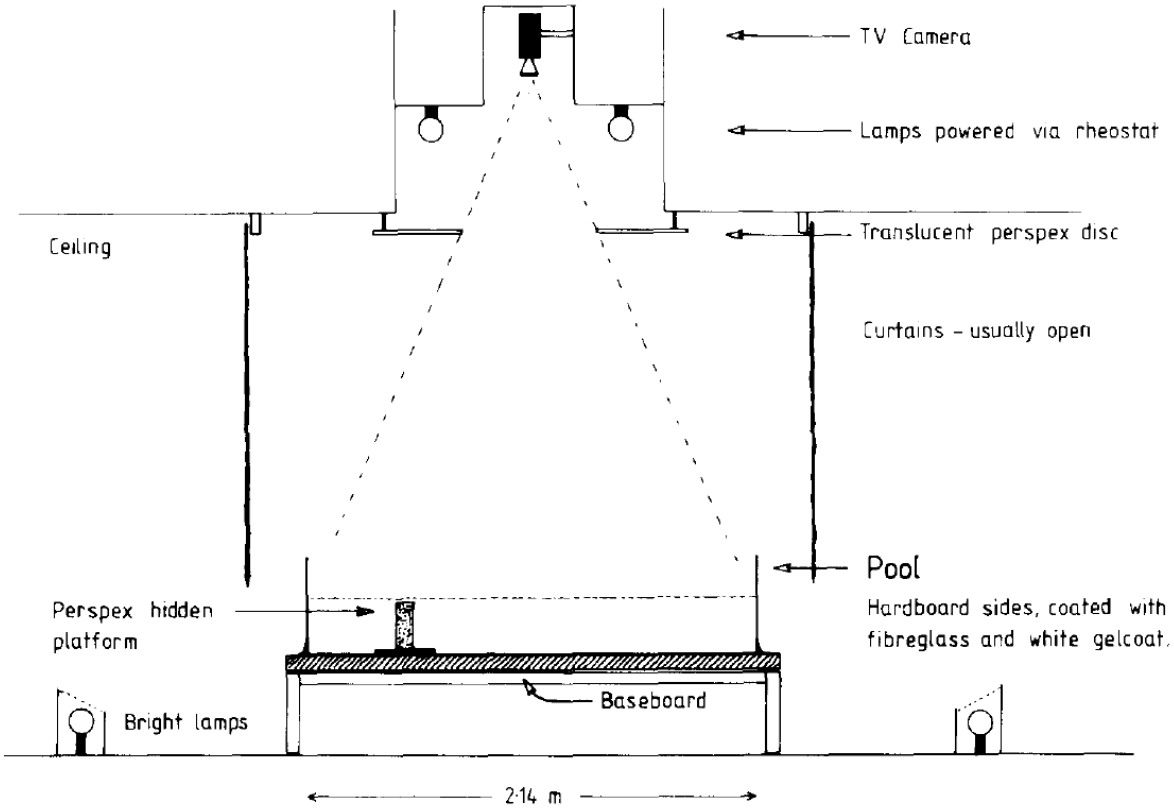

Figure 3-3: *Cross-sectional diagram of pool, and its position in the laboratory. Note support frame to ensure water level is at roughly waist height, and Perspex disc attached to laboratory ceiling to limit field of view of TV camera.* Reproduced with permission from Morris, 1984. Note that in our paradigm we use a pool that is 1.8 m in diameter made of plastic.

3.3.14 Statistics

The effects of injury condition and time post-injury were evaluated using the statistical software R using 2-way **Analysis of Variance (ANOVA)** analysis with post hoc TukeyHSD pairwise analysis of major effects. Pairwise analysis of timecourse interactions were computed using t-tests with Benjamini-Hochberg correction. I circumstances where the assumption of normality is violated, as observed via qualitative analysis Q-Q intervals and Cook's distance, data was normalized via log transform and timecourse interactions detected using Wilcoxon-Mann-Whitney tests. Western Blot and Zymography results are reported as mean ± **standard error of the mean (SEM)**. In all cases the analysis is done using two tailed tests where appropriate and with an alpha level of 0.05. Further, zymogram results involve multiple gelatinase metrics located on the same gel and are further analyzed via **Multivariate Analysis of Variance (MANOVA)** prior to subgroup ANOVA.

3.3.15 Table 3-1: Antibodies Used in Western Blot Experiments

Antibody Target	Antibody Host and Type	Antibody Source and Serial Number	Typical Secondary Used 1:15k	Typical Membrane Used	Concentration Used
HO-1	Rabbit, Polyclonal	Stressgen, ADI-OSA-150	Harlan, 611-103-122, Goat anti-Rabbit	PVDF	1:2k
FTL	Goat, Polyclonal	ABCAM AB Thermofisher	Santa Cruz, SC-2352, Bovine anti-Goat	PVDF	1:2k
LCN2	Goat, Polyclonal	R&D Systems AF3508	Santa Cruz, SC2352	Nitrocellulose	1:2k

3.3.16 Table 3-2 Antibodies Used in Immunohistochemistry Experiments

Antibody Target	Antibody Host and Type	Antibody Source and Serial Number	Typical Secondary Used 1:1k	Concentration Used
HO-1	Rabbit, Polyclonal	Stressgen, ADI-OSA-150	Alexa-488	1:300
FTL	Goat, Polyclonal	ABCAM AB Thermofisher	Alexa-488/594	1:300
LCN2	Goat, Polyclonal	R&D Systems AF3508	Alexa-594	1:200
GFAP	Chicken, Polyclonal	Encor Biotechnologies	Alexa-594	1:200
IBA1	Goat, Polyclonal	ABCAM AB5076	Alexa-594	1:300

3.4 Chapter 3 Data

After observing the time dependent processing of heme and associating it with HO-1, FTL, and LCN2 in Chapter 2 we turned towards manipulating the time course of post-injury processing by injecting to known HO-1 activating agents – Hemin, and Sulforaphane. In brief, lacking a source of a highly selective agent to target HO-1 processing and believing that the endogenous expression of HO-1 during growth, development, and injury appears to be necessary for typical rodent phenotype we attempted to influence HO-1 driven processing of Heme by targeting upstream activation of the transcription factor Nrf2. Since there are known concerns related to the variable kinetics and oxidative potential of Nrf2 activating agents (which largely affect Nrf2 by triggering various redox sensors) we used two different agents, one known to be fairly oxidative due to its release of the transition metal Fe (Hemin), and one known to be a weak electrophile (Sulforaphane).

3.5 Heme Pigment Disappearance in Drug Treated Animals

Figure 3-4 A shows a simplified cartoon of ordered heme processing. Heme B from a variety of potential sources (e.g. hemoglobin, neuroglobin) is taken up by a cell and is degraded by heme oxygenase. When present in small quantities heme is frequently processed by HO-2, the constituently present form of heme oxygenase, but in larger quantities or in the circumstance of acute trauma the inducible form, HO-1, is rapidly amplified. Either enzyme functions identically by cleaving Heme B at the alpha-methene bridge releasing 1 molecule each of Biliverdin, Fe (II), and CO with some degree of selectivity for Heme B over other Heme variants (see Appendix). In an appropriately buffered system Biliverdin is rapidly reduced to Bilirubin, conjugated, and excreted from the cell, and the body. CO diffuses out of the cell and is ultimately bound to circulating Heme B and released into the atmosphere after pulmonary gas exchange. Fe meanwhile is buffered by iron storage proteins, acutely stored locally, and over time secreted from the cell and incorporated into new metalloproteins e.g. new Heme B during erythropoiesis. In the circumstance of acute elevations of Heme B degradation Fe additionally has been shown to trigger redox sensors either directly or through reactive oxygen species that have been generated via iron mediated reactions with water (the Fenton and Haber-Weiss reactions). In this simplified cartoon, Fe affects the repressor protein keap1 which when modified releases the transcription factor Nrf2 which translocates to the nucleus and increases expression of HO-1 enhancing Heme B degradation.

This general process is somewhat altered under the circumstances of trauma as illustrated in **Figure 3-4 B**. In the situation of iron overload the buffering capacity of the cell can be overwhelmed and each of the catabolic products of Heme B degradation can induce potentially

cytotoxic damage to the cell. CO can bind indiscriminately to a large variety of metalloproteins inhibiting or modifying their normal functions and can cause lipid peroxidation in the cell membrane. Bilirubin can intercalate into the lipid bilayer inducing aberrant fluidity and can directly activate inflammatory receptors on the cell membrane. Fe(II) meanwhile behaves essentially the same as it does normally, just with excess concentrations of iron driving greater generation of reactive oxygen species than can be buffered acutely leading to extensive oxidative damage to cell contents.

3.5.1 Figure 3-4: Heme Procesing Cartoon:

A

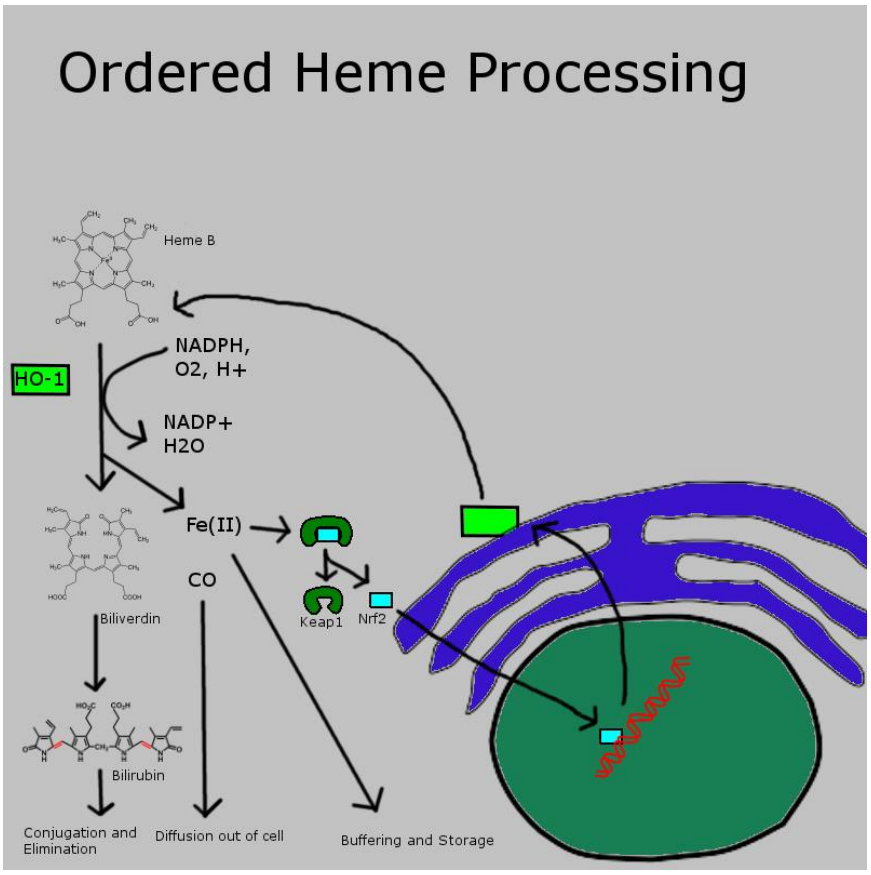

B

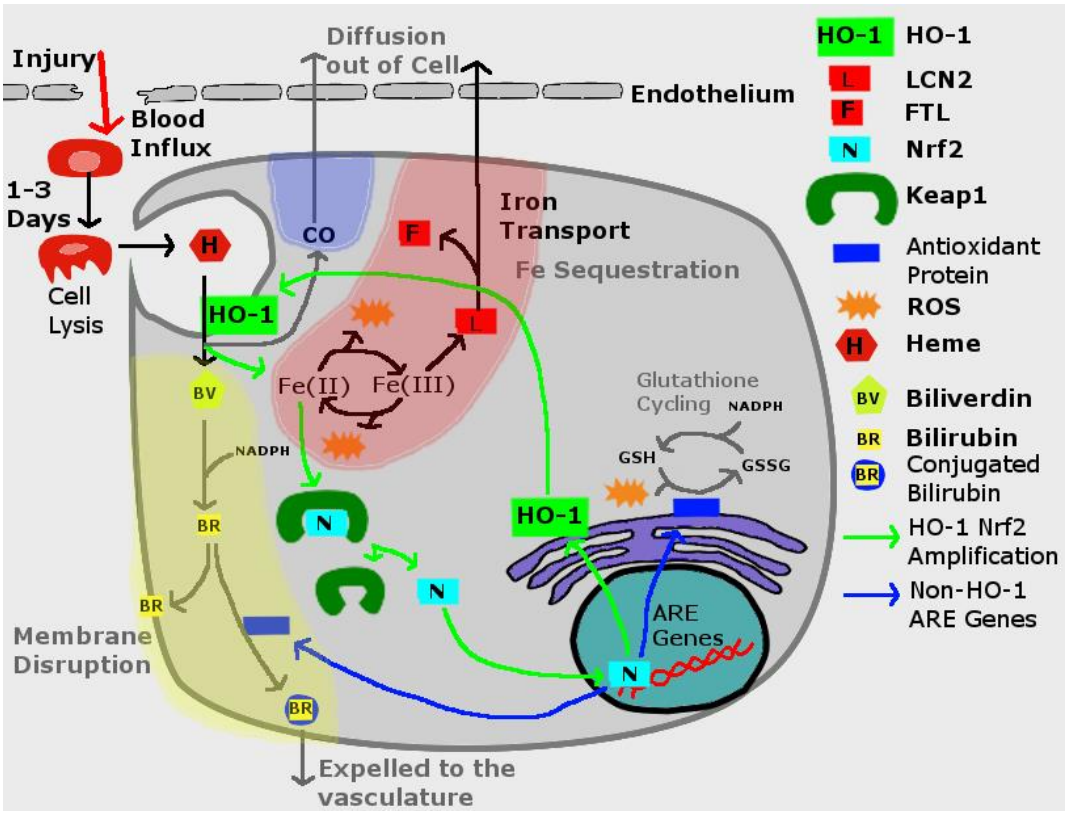

Figure 3-4: Simplified diagrams of heme processing under normal conditions (A), and after traumatic injury (B). Under normal conditions heme B is taken in by a phagocytic cell and degraded by HO-1, or constituently active HO-1 releasing Fe(II), CO, and Biliverdin/Bilirubin. If there are sufficient initial quantities of heme B being processed Fe(II) accumulates and causes Nrf2 to become released from its transcriptional repressor keap1 inducing forward feedback amplifying HO-1 expression until the signal is exhausted. After traumatic injury there is a delay of ~1-3 days before extravasated erythrocytes lyse their cell contents or undergo erythrophagocytosis causing uptake of heme B. In this circumstance almost by definition of heme excess/iron overload there are multiple additional considerations from ordered heme processing. Each of the catabolic products of Heme B have known cytotoxic effects illustrated along with their endogenous buffering mechanisms.

To establish feasibility of drug dosing paradigm we did a 1/3 log step ramp of drug doses in the ranges that have been used in the literature (See Appendix). We found that in naïve animals we saw an increase in HO-1 expression with our midrange dosage and a multifold increase at our maximum doses. Since we interpreted these results to show that the drugs were capable in influencing expression in a brain with intact barrier function, and in conjunction with literature evidence which demonstrated consistent effects, we selected 5 mg/kg Sulforaphane, and 26 mg/kg Hemin doses to use in the experiment moving forwards. In both cases we predict a modest increase in expression in naïve animals and at the start of the experiment had expected to ultimately see that HO-1 would be increased even further in barrier damaged TBI rat subjects that received an additional HO-1 activating signal (the injury). To rephrase: we expected that inducing HO-1 would cause an additive effect further increasing HO-1.

To study the effect of influencing heme processing we began by injecting 5 mg/kg of Sulforaphane or 26 mg/kg of Hemin 1 hour after injury. 1d after injury both Hemin and Sulforaphane treated animals show a remarkable reduction in heme pigment relative to TBI animals (**Figure 3-5**). This can be observed in the primary bleed site after injury in the callosum and into the grey matter in cortical layer VI. Additionally note that the tissue thinning in the overlaying neocortex appears reduced in the drug treated animals. Also note that even though the pigment is absent, there are still easily identifiable necrotic/bleed sites which contain some yellowish pigment indicative of heme catabolism.

3.5.2 Figure 3-5: Loss of Heme Pigment After Drug Treatment 1d Post-Injury

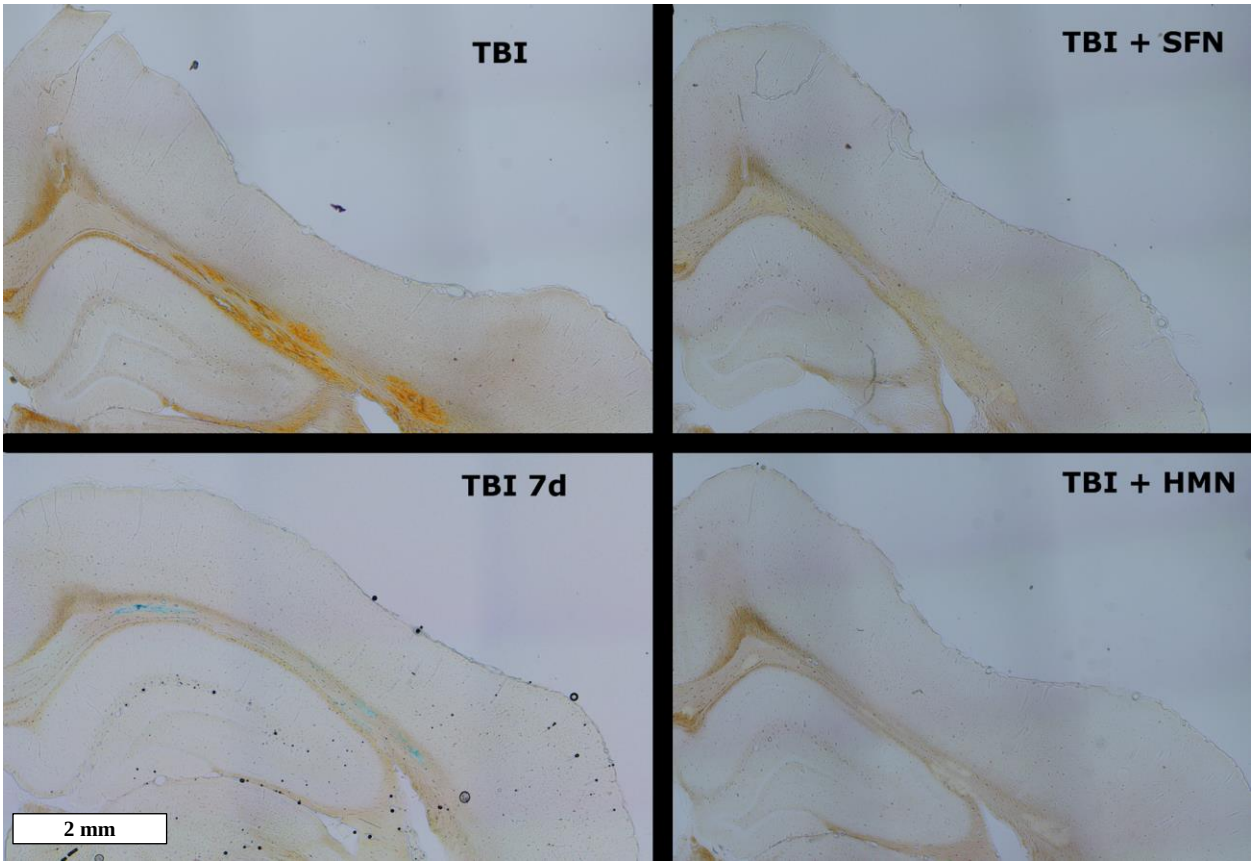

Figure 3-5: 4x Widefield Contrast images of 1d TBI and TBI+SFN/HMN Perls' Stained animals. Note presence of heme pigment (Reddish color) and cortical thinning in 1d TBI animal (A) and contrast to absence of pigment in TBI+SFN (B) and TBI+HMN (C) animals and concurrent reduction in cortical thinning. Both drug treated groups (B, C) demonstrate necrotic areas lacking heme pigment while still showing some yellowish pigment indicative of bilirubin produced from heme catabolism.

3.6 Drug Treated HO-1 Shift responding to pigment changes, LCN2 unaffected

3.6.1 HO-1 Results

We observed that drug treatment with both Hemin and Sulforaphane caused suppression of peak HO-1 expression in both the neocortex and hippocampus (**Figure 3-6**, **Table 3-3**). In all drug treated cases HO-1 expression in drug treated animals appeared to peak at 1d post injury or possibly earlier, shifting the time course of peak expression at least 2 days prior to the peak seen in untreated animals. In the neocortex, ANOVA using the model $\boldsymbol{log}[\boldsymbol{Value}]\sim\boldsymbol{Day}*\boldsymbol{Condition}$ we have significant main effects in Day, Condition, and their interaction (p=2.2e-16, 2.381e-14, 1.131e-07 respectively). TukeyHSD of group effects showed significant differences in Sham-HMN (p=0.0000007), Sham-SFN (p=0.0000003), Sham-TBI (p<2e-16), TBI-SFN (p=0.0120846), and TBI-HMN (p=0.0132195). In the hippocampus, ANOVA using the model $\boldsymbol{log}[\boldsymbol{Value}]\sim\boldsymbol{Day}*\boldsymbol{Condition}$ we have significant main effects in Day, Condition, and their interaction (p=1.313e-12, 4.154e-14, 4.154e-14 respectively). TukeyHSD of group effects showed significant differences in Sham-HMN (p<2e-16), Sham-SFN (p=0.0000008), Sham-TBI (p<2e-16), TBI-SFN (p=0.0049354), and low significance in TBI-HMN (p=0.0874031).

At 1d post injury we do not observed differences between the drug treated groups and untreated animals in HO-1 expression however by 3d the expression diverges. Longer time points demonstrate more variable effects and the effect sizes are sufficiently reduced to be less important. In the neocortex after the initial suppression at 3d the TBI+HMN treated animals are at Sham levels of expression while both the TBI and TBI+SFN groups are reduced from their

peaks but still elevated relative to Sham. By 15d the effect size is minimal and yet the variance has become so tight in the Sham and treated groups that TBI is elevated relative to Sham but the TBI+SFN group now shows significance vs the TBI group.

The hippocampus tells a similar story with significant differences between the TBI and TBI+SFN or TBI+HMN groups at 3d. At longer time points however the Sulforaphane group is more suppressed than the Hemin group and is not different from Sham at 7d or 15d while Hemin and TBI groups maintain a significant difference though with a very modest effect size.

3.6.2 Figure 3-6: HO-1 Western Blot Results Drug Treated 1-15d Post-Injury

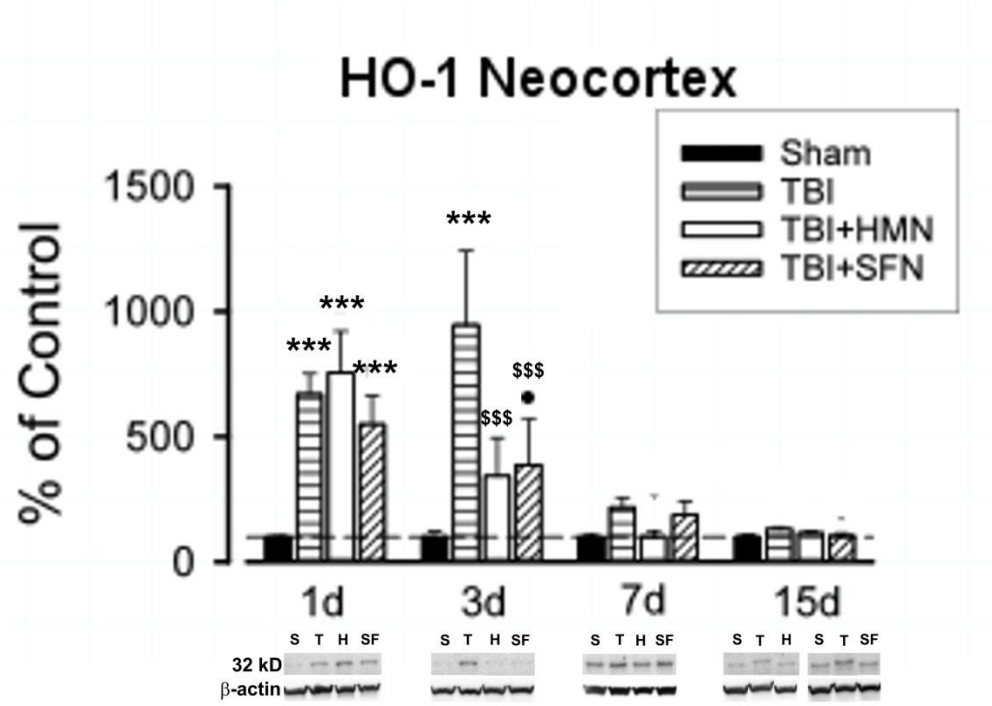

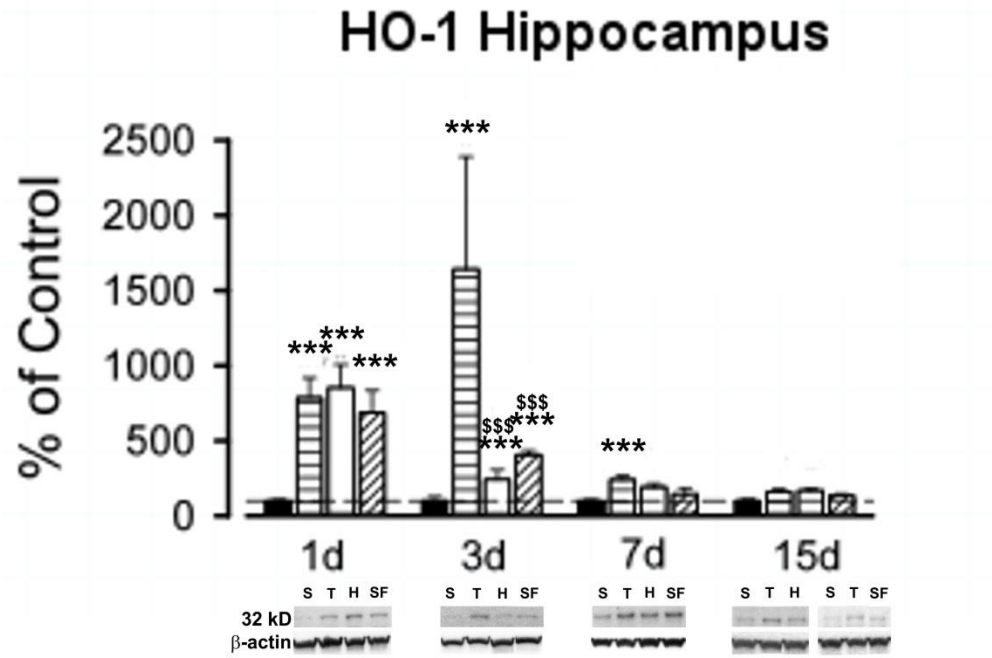

Figure 3-6: Western Blot expression of HO-1 in Sham, TBI, TBI+HMN, and TBI+SFN presented as fold of control 1-15d post-injury. HO-1 is significantly elevated in the neocortex and hippocampus following injury in both TBI and TBI+Drug treated animals. At 3d significance vs Sham is maintained in all groups except the neocortex TBI+HMN group and drug treated groups show reductions vs 1d levels and are significantly reduced relative to untreated TBI animals. At longer time points expression drops to near Sham levels in treated animals while TBI untreated animals decline but remain more elevated than treated animals through 15d post-injury. (Mean ± SEM, n=4-7/group; T-Test with Benjamini-Hochberg correction, ●,*, **, *** for $p < .10, .05, .005, .0005$ respectively vs Sham, $$$ for $p<.0005$ vs TBI).

3.6.3 Table 3-3: HO-1 Western Blot Result Table 1-15d Post-Injury

Neocortex Mean±SEM	Day 1	Day 3	Day 7	Day 15
Sham	1.00±0.14	1.00±0.23	1.00±0.12	1.00±0.08
TBI	6.70±0.82	9.46±2.96	2.18±0.40	1.32±0.08
HMN	7.57±1.65	3.43±1.52	1.01±0.23	1.15±0.07
SFN	5.50±1.14	3.88±1.84	1.88±0.56	1.04±0.10

Hippocampus Mean±SEM	Day 1	Day 3	Day 7	Day 15
Sham	1.00±0.11	1.00±0.29	1.00±0.10	1.00±0.12
TBI	7.88±1.31	16.42±7.48	2.41±0.29	1.58±0.21
HMN	8.55±1.53	2.42±0.65	1.93±0.22	1.70±0.15
SFN	6.88±1.48	4.07±0.27	1.45±0.42	1.34±0.13

Table 3-3: HO-1 mean expression over control of each condition by group and presented as Mean ± SEM in Neocortex and Hippocampus. Note 1d elevations vs Sham consistent in all groups and divergence between TBI and TBI+Drug groups at 3d with convergence of expression through 15d.

We observed substantially altered HO-1 expression in the tissue after treatment with either Hemin or Sulforaphane. At 1d post-injury treatment with either drug appeared to have a direct impact on the proximity of reactive cells to the injury, the morphology of these cells, and the fluorescent character of the bleed itself. We have previously posited that each of the agents selected would cause an induction of HO-1 when injected post-injury and the image staining in Figures 4 and 5 appear to support this theory. In figure 4 we see a substantial shift in autofluorescense within the bleed site which seems to be strongly associated with increased HO-1 expression in cells directly adjacent to the necrotic site. In the untreated animal as we have seen previously there is high reactivity of the glia with an anisotropic arrangement to their appendages which occurs some distance away from the bleed. In the TBI+SFN animal it appears that HO-1+ cells are already present throughout the bleed and directly adjacent in the injury penumbra. Further, the processes of the cells have been arranged in an isotropic form laying largely parallel to the curvature of the WM/GM interface that contains the bleed. The TBI-HMN animal appears to extend this trend with extremely focal expression of HO-1 concurrent with extensive morphological change with a loss of somatic expression of HO-1 and LCN2 instead presenting a focal process driven expression. It is helpful to note here that we have previously shown that the majority of the LCN2+ HO-1+ cells located at some distance from the bleed are largely GFAP+ positive while HO-1+ cells found inside the bleed site or directly adjacent are strongly skewed towards IBA1+ cells.

The hippocampus experiences similar changes to the neocortex but lacking a bleed lacks the same focal organization when drug treated (Figure 5). We observe that the untreated animal shows a broad expression of HO-1 concurrent with an almost uniform spread of LCN2 throughout the tissue that creates a muted appearance to the staining. In the TBI+SFN animal we

begin to see organization of the response with increased LCN2 focus in the hippocampal fissure concurrent with numerous discrete strongly HO-1+ cells in the dentate gyrus molecular layer. The 1d TBI+HMN animal seems to show the greatest extent of this organization with LCN2 expression largely limited to the hippocampal fissure and extensive highly responsive HO-1+ cells throughout the dentate gyrus in both the molecular layer and the hilus.

3.6.4 Figure 3-7: HO-1 vs LCN2 Neocortex Drug Treated 1d Post-Injury

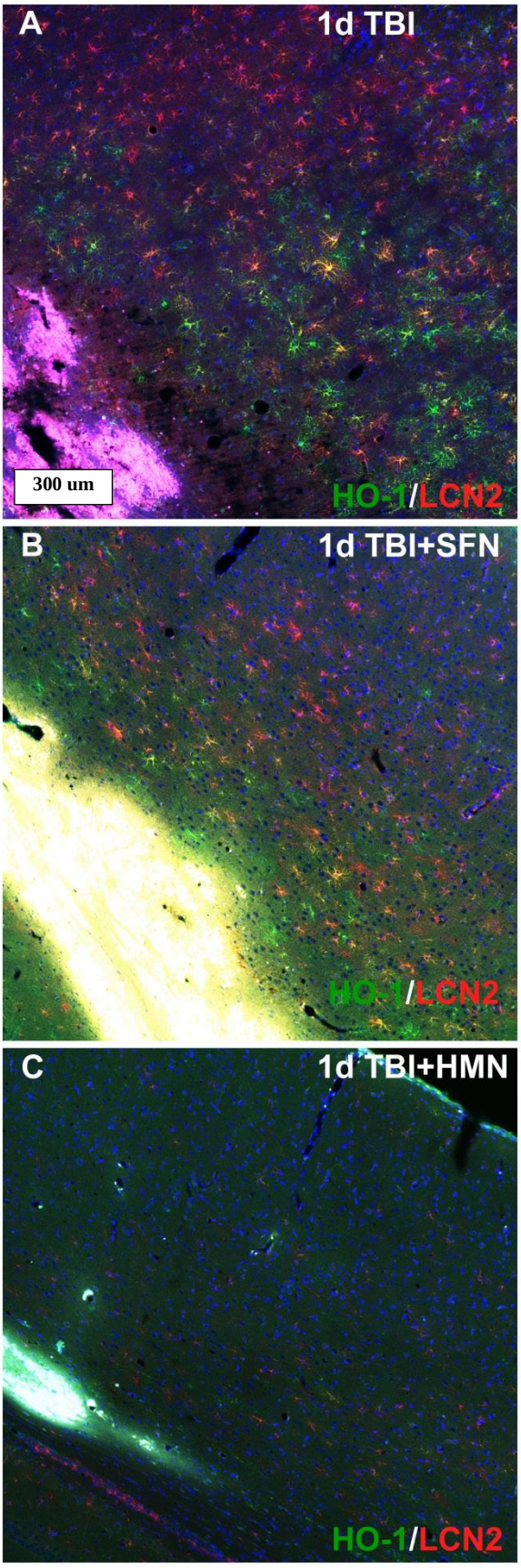

Figure 3-7: 20x Confocal tile scans showing major necrotic bleed and overlaying neocortex stained with HO-1, LCN2, and DAPI at 1d post-injury. In the untreated animal (A) note broad distribution of HO-1+ and LCN2+ cells spaced somewhat distantly from the necrotic bleed and note the grossly purple color of the bleed site due to a mixture of heme autofluorescence and DAPI staining. Reactive morphology of observed cells shows an anisotropic distribution of cellular processes. The TBI+SFN treated animal (B) shows stratification of HO-1 and LCN2 expression with HO-1 in close proximity to and throughout the injury. Further, the cell morphology has become isotropic with processes arranged tangentially to the injury. The TBI+HMN treated animal (C) shows extreme condensing of HO-1 expression into focal nodes in bleed sites. Note that red autofluorescence is lost in bleed site. Further note that while there is limited somatic staining of HO-1 and LCN2, there is a broad level of process expression which provides a relatively muted appearance of broadly responding fluorescence.

3.6.5 Figure 3-8: HO-1 vs LCN2 Hippocampus Drug Treated 1d Post-Injury

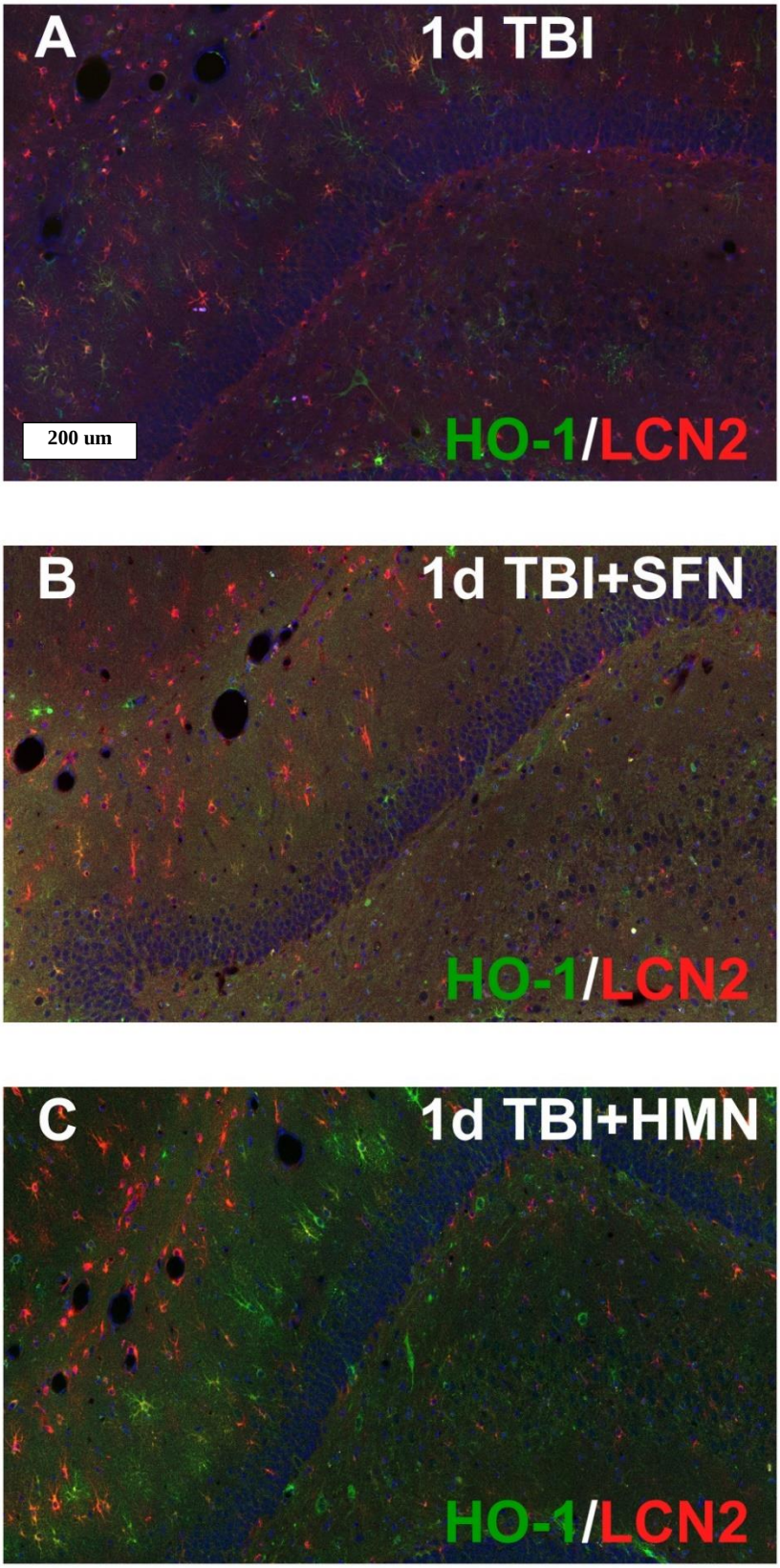

Figure 3-8**:** 20x Confocal tile scans showing the dentate gyrus of the hippocampal formation stained with HO-1, LCN2, and DAPI at 1d post-injury. In the untreated animal (A) note fairly broad expression of HO-1 and LCN2 throughout the tissue. In both the TBI+SFN and TBI+HMN animals (B,C) note increased expression of HO-1 particularly in the hilus of the dentate and expression of LCN2 which appears more restricted to the hippocampal fissure.

At later time points we continue to see an organizing process occurring in the TBI and TBI treated animals which appears to be more advanced in the drug treated animals, particularly in the TBI+HMN treated animals. This organization is best seen in the neocortex and along the WM/GM interface due to the necrotic nature of that injury providing easier to identify tissue pathology. At 7d post-injury (Figure 3-11) we observe that HO-1 expression is evident within the necrotic site particularly for the 7d TBI animals. Co-stain with GFAP reveals a general absence of co-expression between astrocytes and HO-1+ cells. We observe that in the TBI+SFN animal there is reduced HO-1 expression in the necrotic site though the total size of the area is similar. The TBI+HMN animals show further progression of observation with substantially limited HO-1 expression in the necrotic site along with reduced area.

Remarkably, even though expression of HO-1 converges to Sham levels by 15d in the neocortex IHC tile scans show dense granular expression largely restricted to the callosum and concurrent with high levels of FTL expression (Figure 3-12). Both the TBI and TBI+SFN groups seem to show larger areas and increased levels of expression compared to the TBI+HMN group which is consistent with the observations made at 1d and 7d.

3.6.6 Figure 3-9: HO-1 vs IBA1 Neocortex Drug Treated 3d Post-Injury

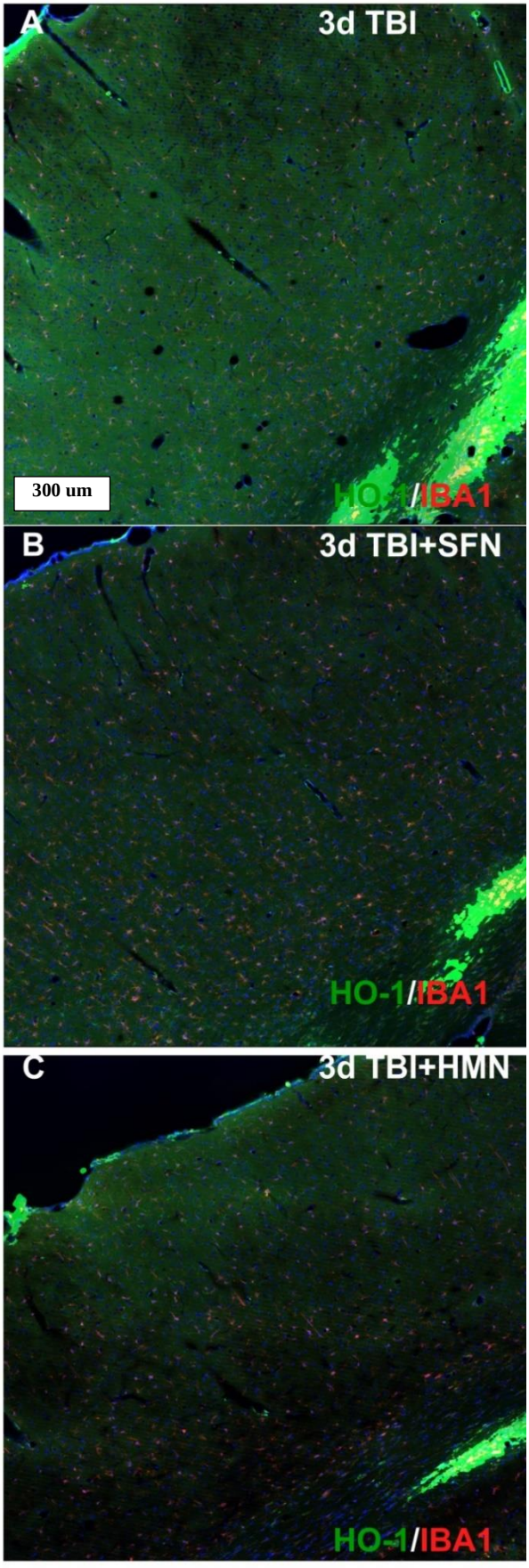

Figure 3-9: 20x Apotome tile scans showing the hemorrhagic and reactive neocortex stained with HO-1, IBA1, and DAPI at 3d post-injury. In the untreated animal (A) note significant blown out signal in the bleed site and broad expression of HO-1 throughout the tissue. Contrast in the TBI+SFN (B) and TBI+HMN (C) animals a reduction in the size of the bleed site and a global reduction in HO-1 throughout the tissue though maintaining numerous highly reactive cells.

3.6.7 Figure 3-10: HO-1 vs IBA1 Hippocampus Drug Treated 3d Post-Injury

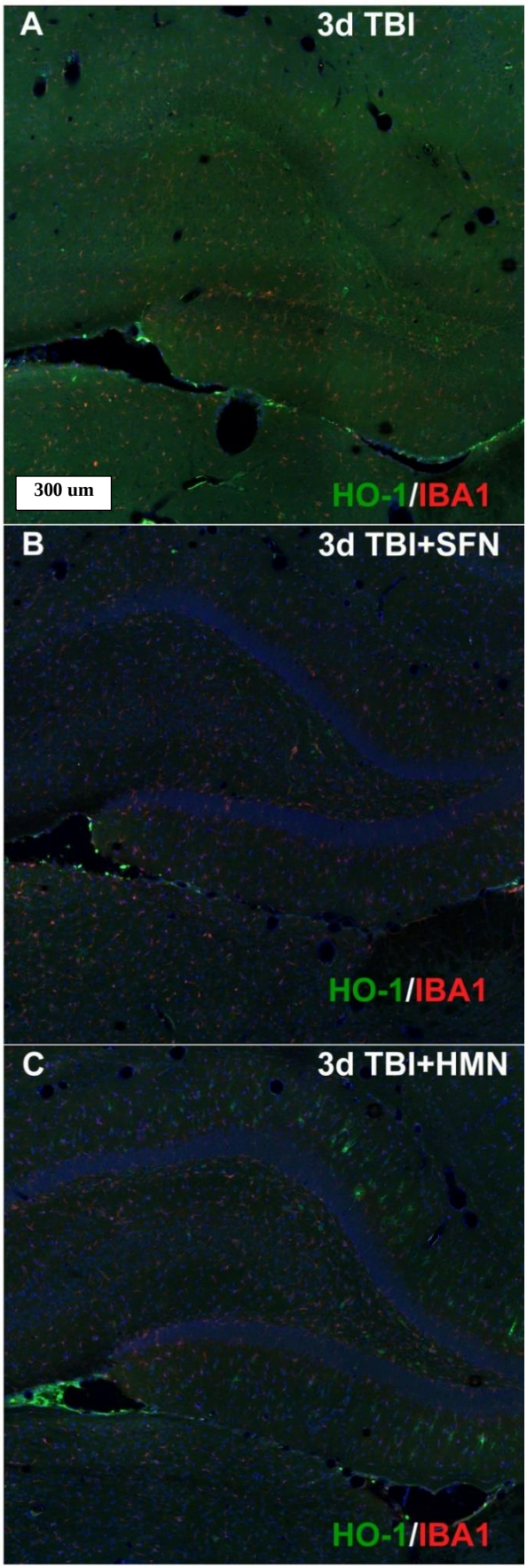

Figure 3-10: 20x Apotome tile scans showing the dentate gyrus of the hippocampal formation stained with HO-1, IBA1, and DAPI at 3d post-injury. In the untreated animal (A) note broad elevation of HO-1 throughout the tissue in addition to numerous highly reactive cells. Contrast in the TBI+SFN (B) and TBI+HMN (C) animals which show a reduction in the overall broad signal and more of an organizing response to the single cell reactivity, particularly in the TBI+HMN treated animal.

3.6.8 Figure 3-11: HO-1 vs GFAP Neocortex Drug Treated 7d Post-Injury

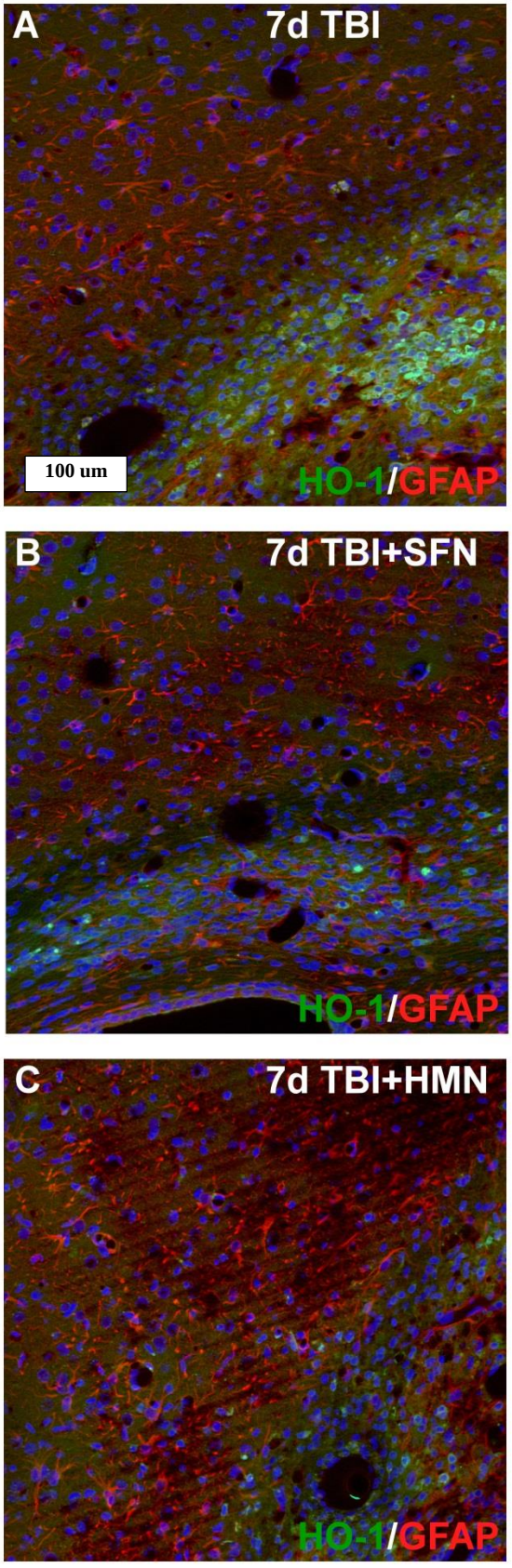

Figure 3-11: 20x Apotome tile scans showing the major necrotic injury and overlaying neocortex stained with HO-1, GFAP, and DAPI at 7d post-injury. Note absence of co-expression between HO-1 and GFAP and dense somatic staining of HO-1 largely restricted to the WM tract under the neocortex. Also note the difference in quantity of HO-1 expression which appears to be most intense and broadly expressed in the untreated animal (A), more muted/less expansive in the TBI+SFN animal (B), and most muted but with broad expression into the neocortex in the TBI+HMN animal (C).

3.6.9 Figure 3-12: HO-1 vs FTL Neocortex Drug Treated 15d Post-Injury

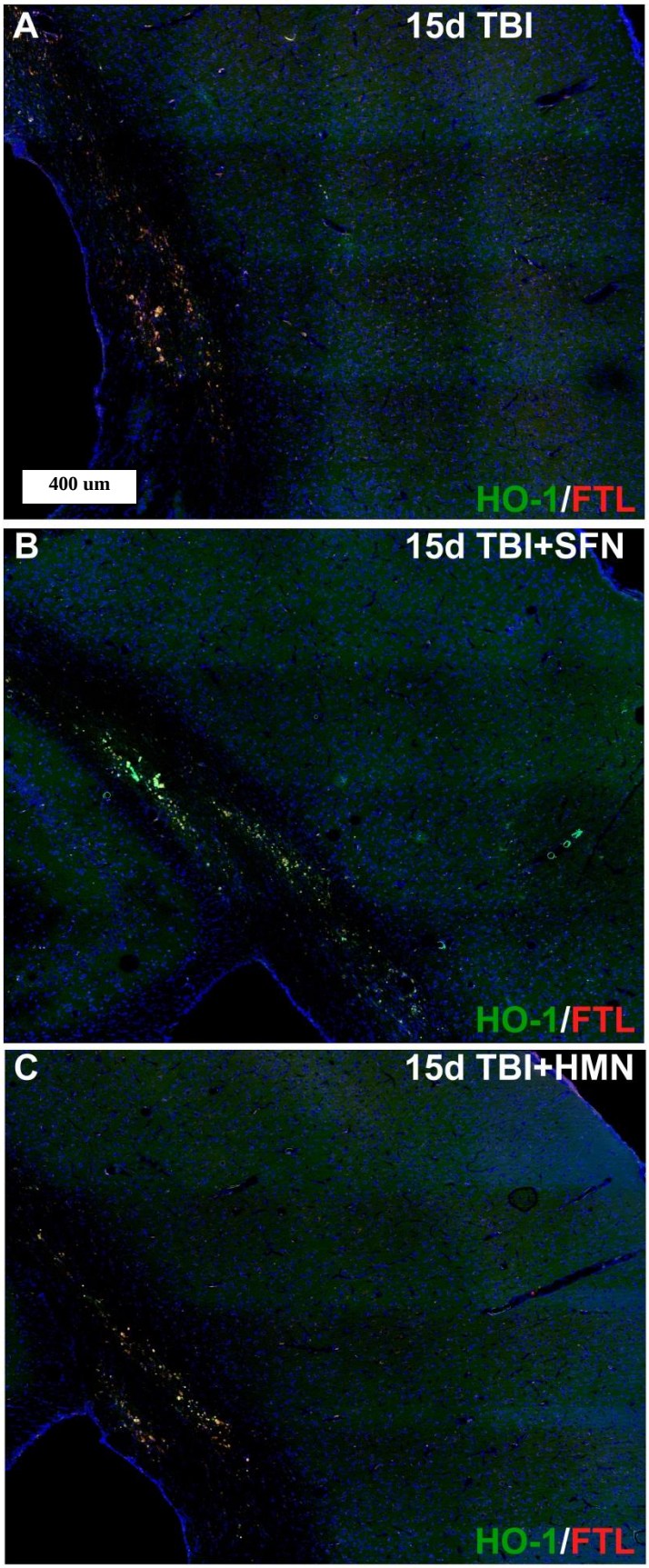

Figure 3-12: 20x Apotome tile scans showing the major necrotic injury and overlaying neocortex stained with HO-1, FTL, and DAPI at 15d post-injury. HO-1 is significantly reduced compared to previous time points but there are notable changes that occur between the TBI (A) and drug treated groups (B & C, TBI+SFN & TBI+HMN respectively). The total size of the FTL staining region is comparable in the 15d TBI and 15d TBI+SFN animals and they have similar limited expression of highly reactive cells scattered throughout the neocortex. These highly reactive cells are absent in the 15d TBI+HMN tissue and the total area of FTL reactive tissue in the callosum appears reduced compared to 15d TBI and 15d TBI+SFN animals.

3.7 Summary of Observations HO-1

In summary we have observed via contrast imaging, Perls staining, western blot, and immunohistochemistry that injection with the known HO-1/Nrf2 activators Hemin and Sulforaphane causes a shift in heme processing, and particularly a shift in HO-1 expression along with concurrent heme processing markers.

HO-1 may be modestly induced by or before 1d post-treatment but is significantly depressed by 3d relative to TBI in both the hippocampus and the neocortex with later levels of expression converging with both TBI and Sham through 15 days.

This observation is supported by the immunohistochemistry, most clearly seen in the neocortex near the necrotic site where there is obvious changes to glial morphology and expression of heme processing proteins after drug treatment.

3.8 LCN2 Results

We continued our investigation by looking at potential changes in acute iron sequestration via LCN2 expression after injury. Overall LCN2 expression is relatively unchanged between TBI and drug treatment groups from a total protein perspective (as assayed by WB). There are some differences however, in the cellularity and location of LCN2 expression, at least in part driven by differing morphology in the underlying glial cell populations which has been shown previously in **Figure 3-7** &

Figure 3-8 at 1d post-injury.

We observed in western blot that the drug treatment groups demonstrated almost no variation from the TBI only group. In the neocortex, ANOVA using the model $\boldsymbol{Value \sim Day * Condition}$ we have significant main effects due to Day, Condition, and their interaction (p =7.593e-06, 7.898e-06, 0.02369 respectively). TukeyHSD of group effects showed significant differences in Sham-HMN (p=0.0003823), Sham-SFN (p=0.0010063), Sham-TBI (p<0.0000351), and no significance in the TBI-SFN, and TBI-HMN groups. In the hippocampus, ANOVA using the model $\boldsymbol{Value \sim Day * Condition}$ we have significant main effects due to Day, Condition, and weak significance in their interaction (p =0.0004352, 2.764e-06, 0.0584626 respectively). TukeyHSD of group effects showed significant differences in Sham-HMN (p=0.0001023), Sham-SFN (p=0.0000333), Sham-TBI (p<0.0003554), and no significance in the TBI-SFN, and TBI-HMN groups.

There are only two time points where the a drug treatment differs from the TBI, at 7d in the neocortex where the drug treated groups lose significance vs Sham and appear to drop to near sham levels though they are not significantly different from the TBI group. An interesting note here is that compared to earlier in Chapter 2, all injured groups in this chapter demonstrate more sustained LCN2 expression that is still elevated through day 7. Further, the peak expression at 1d is 10-100 fold rather than 100-1000 fold which may indicate a baseline shift due to Sham stress response when being behaviorally tested. Most interesting is that the expression of LCN2 no longer peaks at 1d post injury before dropping off at 3d, but rather maintains a relatively constant expression through 3d before only modestly declining.

3.8.1 Figure 3-13: LCN2 Western Blot Results Drug Treated 1-7d Post-Injury

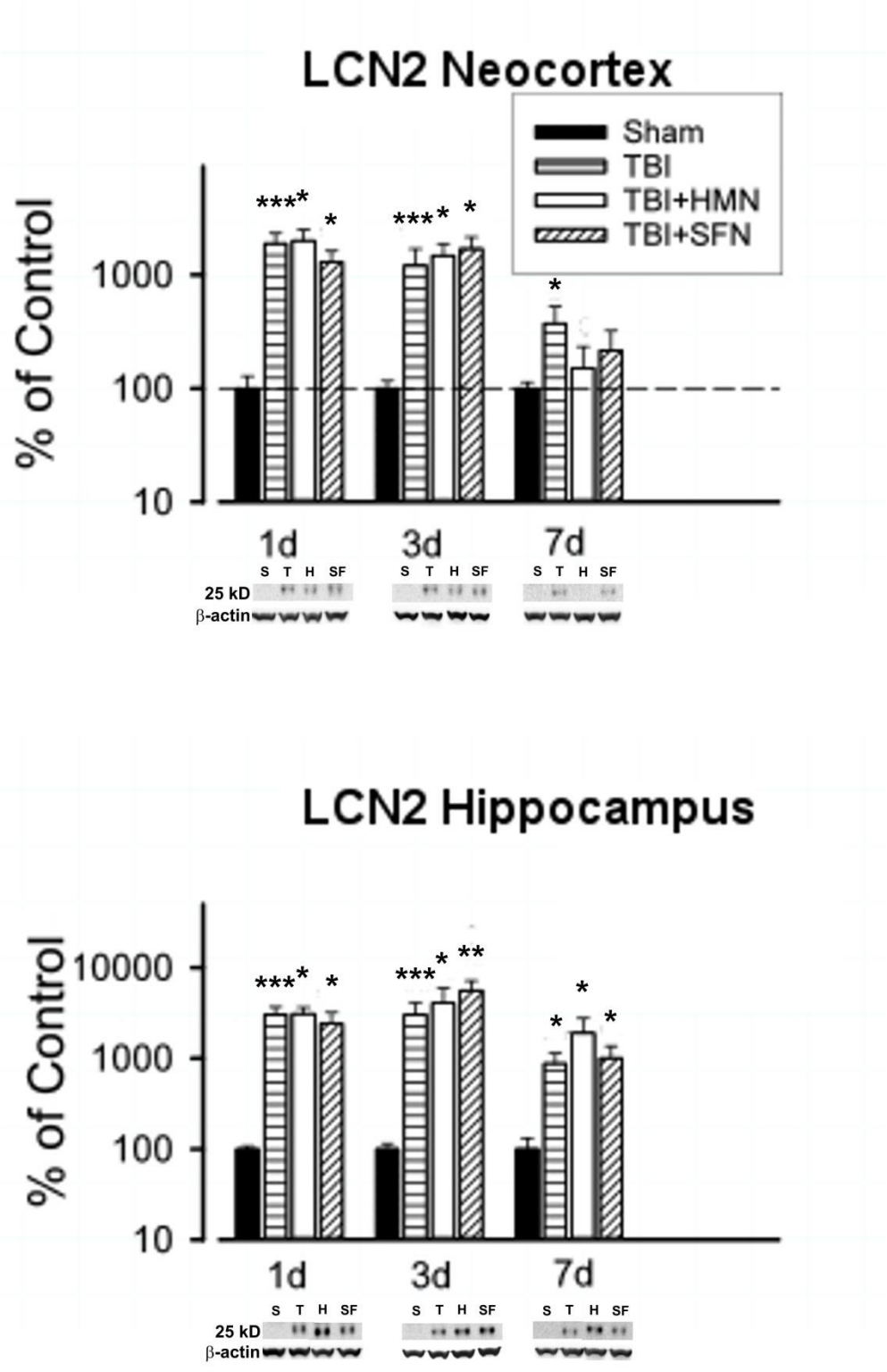

Figure 3-13: Western Blot Expression of LCN2 in Sham, TBI, TBI+HMN, and TBI+SFN presented as fold of control with log scale 1-7d post-injury. LCN2 expression appears largely unchanged regardless of treatment group. LCN2 expression in all groups peaks 1-3d post-injury and has decreased towards Sham levels by 7d post-injury in both the neocortex and the hippocampus. The few specific values to note are drops to non-significnce relative to sham in the drug treated neocortical samples. (Mean ± SEM, n=4-7/group; Wilcoxon-Test with Benjamini-Hochberg correction, *, **, *** for $p < .05, .005, .0005$ respectively vs Sham, $ for $p<.05$ vs TBI).

3.8.2 Table 3-4: LCN2 Western Blot Result Table 1-7d

Neocortex Mean±SEM	Day 1	Day 3	Day 7
Sham	1.00±0.28	1.00±0.17	1.00±0.13
TBI	18.88±4.37	12.09±4.82	3.73±1.52
HMN	19.98±4.92	14.74±4.08	1.51±0.82
SFN	13.00±3.21	16.93±4.55	2.15±1.06

Hippocampus Mean±SEM	Day 1	Day 3	Day 7
Sham	1.00±0.08	1.00±0.15	1.00±0.32
TBI	30.50±6.39	30.36±10.62	8.77±2.63
HMN	30.97±5.56	40.49±19.44	19.08±8.56
SFN	24.11±8.03	56.09±15.23	10.11±3.55

Table 3-4: LCN2 mean expression over control of each condition by group and presented as Mean ± SEM in Neocortex and Hippocampus. Note fairly constant expression between treatment groups and sustained elevation of LCN2 1d-3d before declining at 7d.

3.9 Rotarod Behavioral Results

In order to study potential behavioral outcomes of HO-1 induction with Hemin or Sulforaphane we chose an acute metric of cortical function that has been shown to be inhibited by traumatic brain injury. The test provides a well characterized measure of balance/coordination and motor-planning. In our paradigm we used a velocity ramp which after a 10s habituation delay increases at a rate of 0.3 RPM/s with a maximum velocity of 30 RPM held until a total trial time of 130 seconds is reached (120 seconds of rotation). We recorded group differences in device contact time or max rotational velocity before an animal fell, completed the test, or spun around twice.

Rotarod Naïve animals were placed on the rotarod device and their performance tracked over the next 7 days with daily trials conducted. The initial day 1 ability of the animals was stratified by condition with the Sham animals performing best, the TBI animals performing the worst, and both drug treated groups midway between the two untreated conditions (Figure 3-14 & Figure 3-15, Table 3-5 & Table 3-6). Largely as expected the Sham animals performed best out of all groups, quickly learning the task with the majority of animals running the test to completion by the third day (a special note must be mentioned however that a subset of animals after learning the task then proceeded to attempt to escape the task; as a result the Sham scores actually reduced after day 4). The TBI+SFN group performed next best overall, quickly reaching performance ability that matched the Sham animal group and modestly outperforming the Sham group by day 7 (due to the aforementioned escape attempts). The TBI+HMN group lagged a little behind the TBI+SFN and Sham groups, more closely matching the TBI group until day 4 when it began to pull away. There are a couple of interesting points of stratification between the

various animals. The drug treated animals in both the TBI+SFN and TBI+HMN group had day1 performance that was roughly midway between the Sham and TBI groups. The TBI+SFN group then proceeded to have an accelerated learning curve while the Hemin learning curve lagged. By day 7 when the majority of the animals had successfully learned the task all groups except the TBI+SFN group included animals that attempted to avoid the test. ANOVA results demonstrated that across the full trial both the Sham and TBI-SFN groups were significantly different from the TBI and TBI+HMN groups.

3.9.1 Figure 3-14: Rotarod Contact Time 1-7d Post-Injury

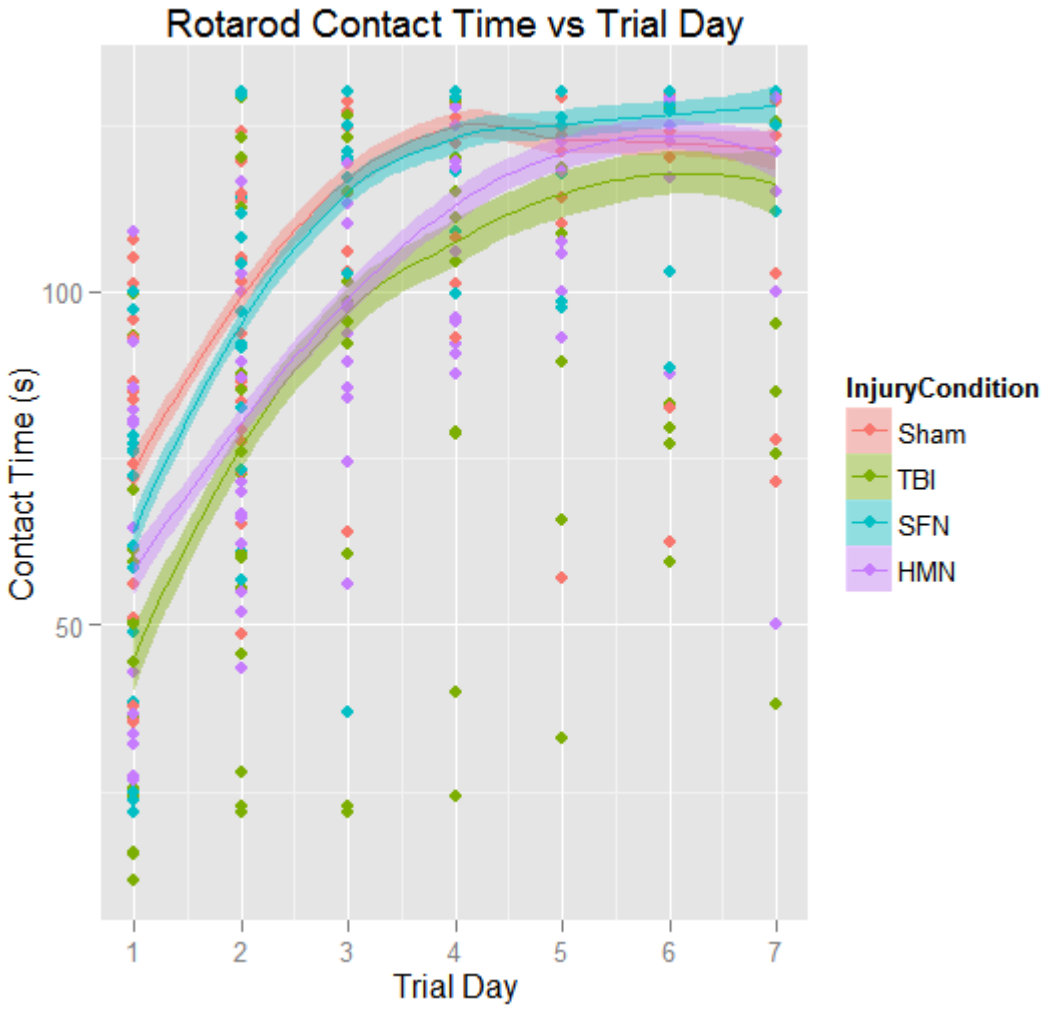

Figure 3-14: Rotarod Contact Time vs Trial Day. 50% Confidence Interval shown along with mean values and individual data points for each animal by group. Of particular interest: note the start position shift from TBI to Sham treated animal with both TBI+SFN and TBI+HMN treated animals performing better at 1d post injury. TBI+SFN treated animals rapidly catch up to Sham treated animals within 2-3 days of training while TBI+HMN treated animals show improvement but lag. Of special note, there is a decline in Sham animal performance after 4d which largely coincides with a subset of animals who became bored and attempted to escape or avoid the task.

3.9.2 Table 3-5: Rotarod ANOVA Model

Rotarod Contact Time							
Model:							
Time ~Condition*Day							
	Df	Sum of Sq	RSS	AIC	F Value	Pr(>F)	
<none>	216380	2788.3					
Condition	3	8313	224693	2798.9	5.2892	0.001376	**
Day	6	37517	253897	2846.8	11.9347	2.29E-12	***
Condition:Day	18	7774	224154	2767.9	0.8244	0.671663	

Table 3-5 A: Rotarod Contact Time ANOVA type III SS & F tests. Note Condition and Day both show significance however there is no interaction effect.

TukeyHSD					
$Condition					
	diff	lwr	upr	P adj	
TBI-Sham	-14.7941	-22.448566	-7.13967	5.42E-06	***
SFN-Sham	-0.42035	-8.325835	7.485125	9.99E-01	NS
HMN-Sham	-9.2402	-17.294272	-1.18612	1.71E-02	*
SFN-TBI	14.37376	6.468283	22.27924	2.20E-05	***
HMN-TBI	5.553922	-2.500154	13.608	2.85E-01	NS
HMN-SFN	-8.81984	-17.112861	-0.52682	3.21E-02	*

Table 3-5 B: Tukey HSD results from Table 3B fit for Condition showing pairwise differences between treatment groups. Note that TBI-Sham, and SFN-TBI pairs are significantly different while SFN-Sham is NS. Further, HMN is significant vs SFN or Sham but is not significant vs TBI. This shows grouping of the data where SFN and Sham treated animals have similar behavioral outcome while HMN and TBI is more similar.

3.9.3 Figure 3-15: Rotarod Max RPM 1-7d Post-Injury

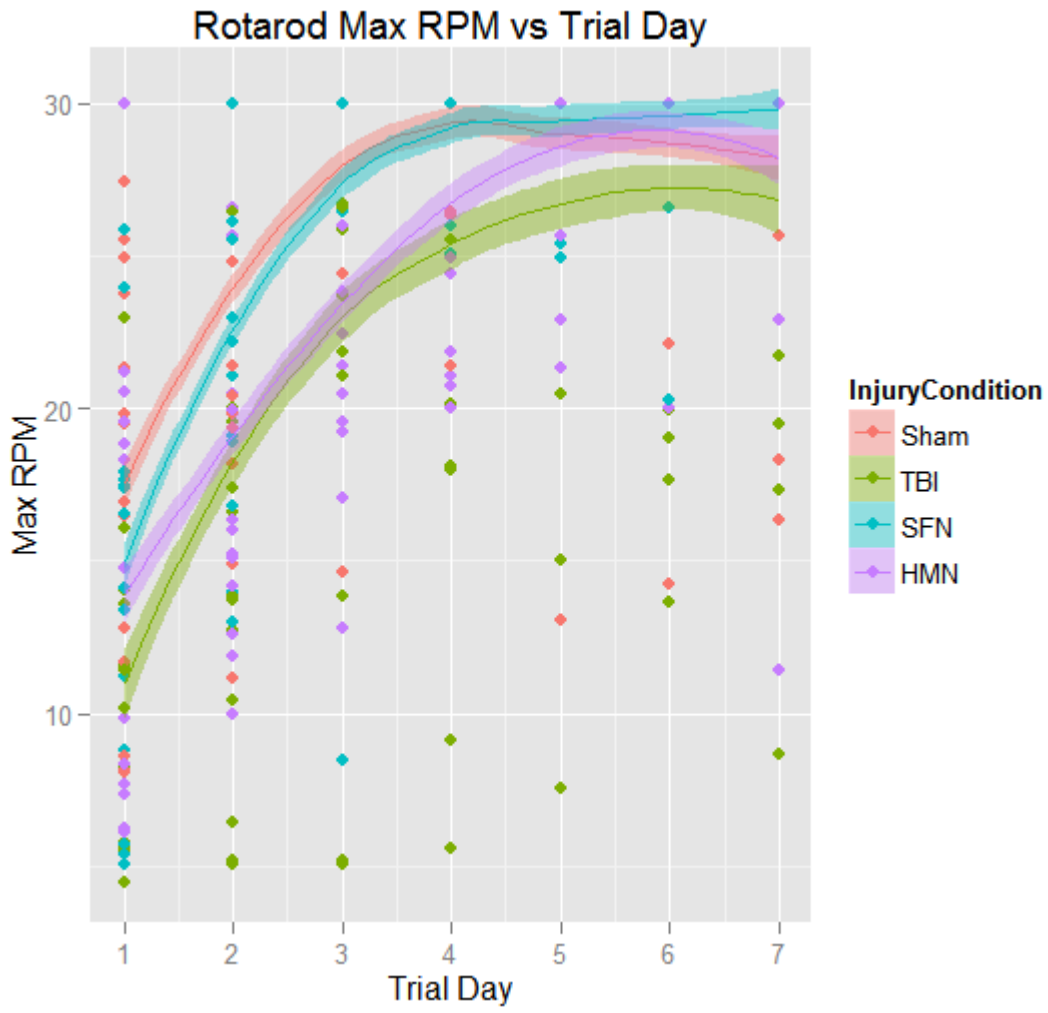

Figure 3-15: Rotarod Max RPM vs Trial Day. 50% Confidence Interval shown along with mean values and individual data points for each animal by group. Very similar to the results shown previously but there is slightly greater partition between the HMN and TBI animal results. This test is different from previous in that the max RPM is held constant for the final 30 seconds of the trial so some animals will hit the max RPM and still not hit the max time.

3.9.4 Table 3-6: Rotarod Max RPM ANOVA Model

Rotarod Max Velocity							
Model:							
Velocity ~Condition*Day							
	Df	Sum of Sq	RSS	AIC	F Value	Pr(>F)	
<none>	12589	1534					
Condition	3	402.09	12991	1541.9	4.397	0.004636	**
Day	6	1896.55	14486	1583.9	10.3698	1.03E-10	***
Condition:Day	18	402.65	12992	1511.9	0.7339	0.776342	

Table 3-6 A: Rotarod Contact Time ANOVA type III SS & F tests. Note Condition and Day both show significance however there is no interaction effect.

TukeyHSD					
$Condition					
	diff	lwr	upr	P adj	
TBI-Sham	-3.72348	-5.5697798	-1.87718	1.85E-06	***
SFN-Sham	-0.254	-2.1608539	1.652846	9.86E-01	NS
HMN-Sham	-2.2249	-4.1675898	-0.28221	1.74E-02	*
SFN-TBI	3.469476	1.5626264	5.376326	2.17E-05	***
HMN-TBI	1.498583	-0.4441096	3.441275	1.93E-01	NS
HMN-SFN	-1.97089	-3.9712206	0.029433	5.52E-02	.

Table 3-6 B: Tukey HSD results from Table 4A fit for Condition showing pairwise differences between treatment groups. Note that TBI-Sham, and SFN-TBI pairs are significantly different while SFN-Sham is NS. Further, HMN is significant vs Sham and near significant vs SFN but is not significant vs TBI. This shows grouping of the data where SFN and Sham treated animals have similar behavioral outcome while HMN and TBI is more similar.

A number of additional metrics were calculated for the Rotarod to identify underlying shifts in animal behavior at different time points and overall. In Figure 3-16 we calculated the individual group box plots along with their means at 1,3,5, and 7d. We observed that at day 1 each of the groups demonstrates a fairly similar spread of variance between animals but by 3d post-injury there is an impressive shift in behavior with the Sham and TBI+SFN groups simultaneously improving while the TBI and Hemin groups similarly lag. By 5d we begin to see major convergence of the groups that continues through 7d when all medians are the peak test time and is a major artifact of having a hard cap on trial time/speed. Note that no group is devoid of outliers at day 7 and yet the difference in the Sham/SFN and TBI/HMN group pairings is still heavily influenced by the IQR.

We further looked at some cumulative measures of performance which provide neat insights into the changes in animal performance over time (Figure 3-17). Cumulative rotarod time which comprises the sum of each daily trial mean results in near identical construction of plots for the Sham and TBI+SFN groups which are distinct from both the TBI and TBI+HMN groups. In contrast, it is interesting in examining the time delta between day 1 and day 7 that each of the groups have an almost identical spread of improvement suggesting that day 1 performance is characteristic of day 7. Since this would appear to be at odds with intuitive observation of Figure 3-14 & Figure 3-15, we extended the analysis by looking at the delta between the best and worst performance in each animals trials. This better accounts for animals which begin to decline in performance at later time intervals as well as for animals that demonstrated aberrant day 1 performance. The result is a clear shift in group IQR which suggests that a large part of the performance lag in the TBI+HMN treated group may be due to more variable animal performance compared to the other groups.

3.9.5 Figure 3-16: Rotarod Contact Time Box Plots 1,3,5,7d Post-Injury

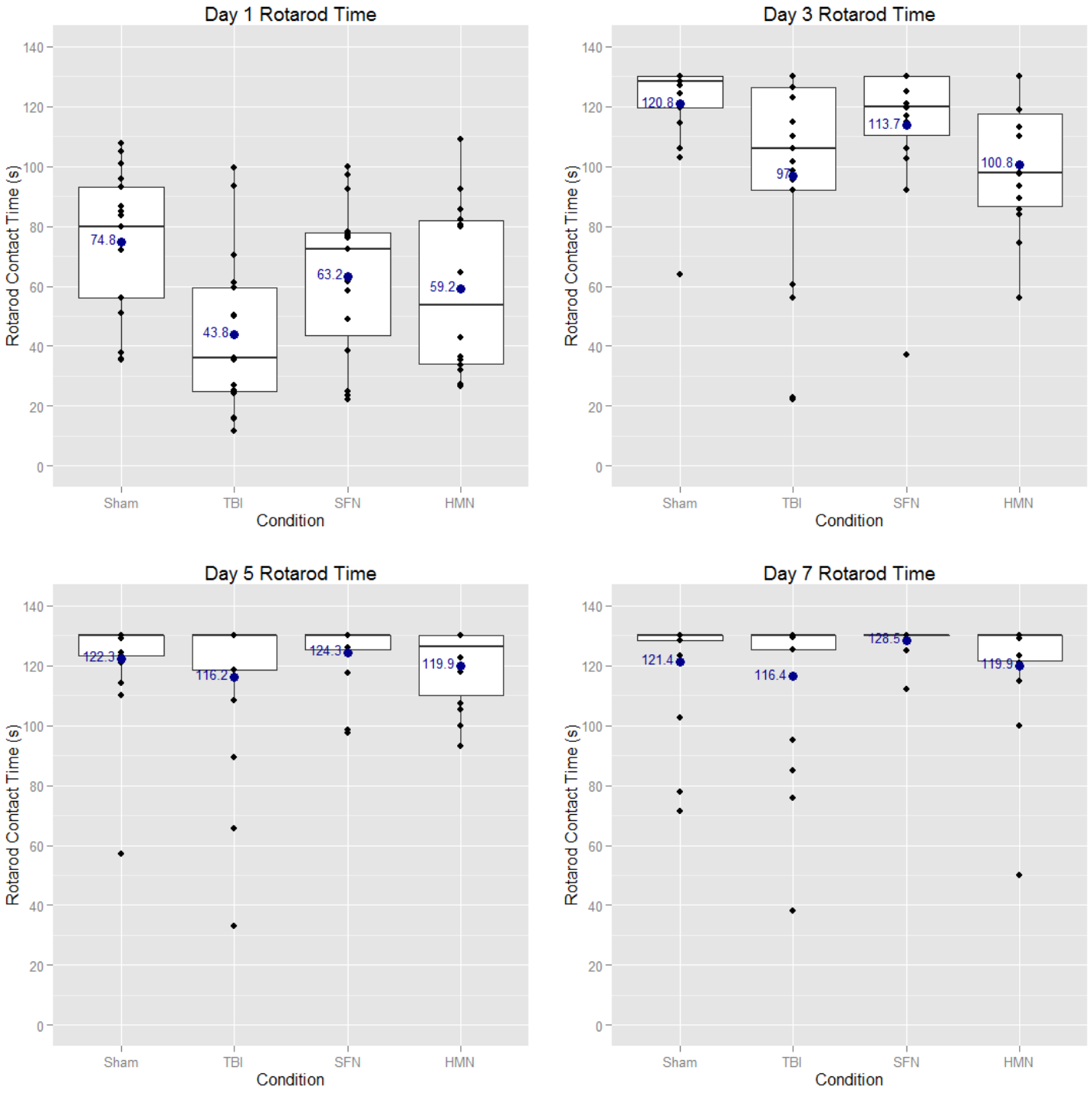

Figure 3-16: Boxplots of Rotarod Contact Time at 1,3,5,7d intervals with group means highlighted in blue. It is clear that at all time points the range in behavior is fairly overlapping, at 1d there are notable differences in the means of the various treatment groups but in all cases the IQR of any two overlap and this persists with the sole possible exception of Sham-HMN at 3d where the overlap is minimal. As time moves forward the means of all groups increase and due to the hard cap on performance (130 seconds is the maximum regardless of ability to continue further) there is a steady increase in outliers as time continues and the means of all groups condense towards the same value of just under 130s.

3.9.6 Figure 3-17: Cumulative Rotarod Metrics

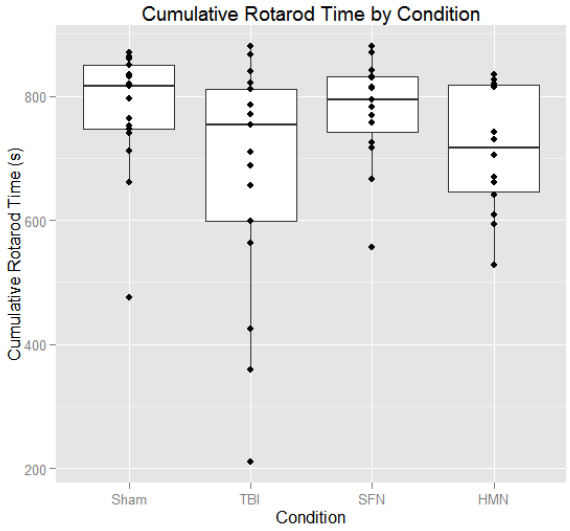

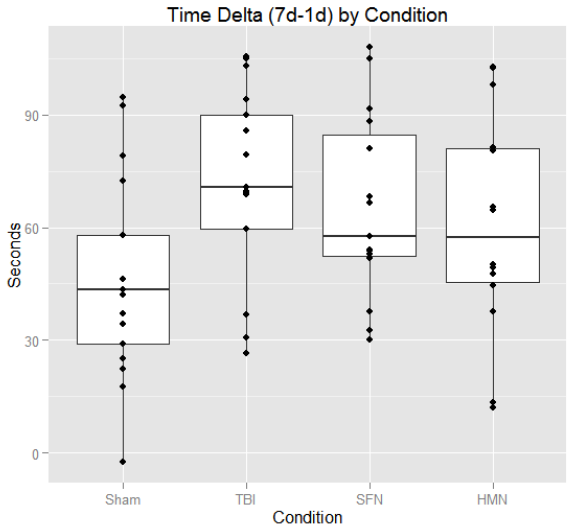

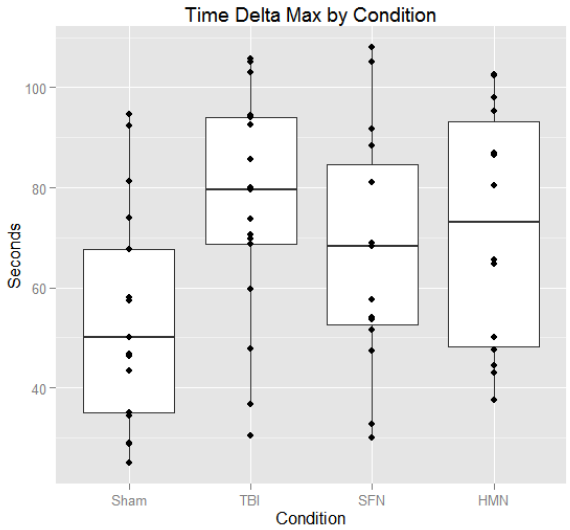

Figure 3-17: Boxplots of Cumulative Rotarod Performance Contact Time Metrics. (A) shows Cumulative Rotarod Time by group condition demonstrating that the aggregate time spent on the device diverges as expected into two similar sets of SHM-SFN and HMN-TBI. (B) shows the improvement from Day 1 to Day 7. Note that the SHM group does not improve as strongly as the other groups in part because the 1d performance is higher. (C) shows the difference between the maximum and minimum performance of each animal by group. This is similar to (B) but better accounts for animals that have variable early or late performance. The result is shows that all TBI and TBI-Drug groups have similar performance improvements while the SHM group has limited improvement to high 1d performance.

3.9.7 Summary of Observations Rotarod

The major observation of our Rotarod analysis appears to be a stratification of the different groups into Sham/SFN and TBI/HMN pairs where the Sulforaphane treatment appears to have a robust behavioral effect that improves performance within a few days of initiating the trial. It is interesting that both groups showed an initial 1d improvement vs TBI and yet only the TBI+SFN group showed a robust improvement in the following days with the TBI+HMN group possibly showing an effect at later times that is largely washed out by too many animals hitting the peak test performance. It is possible that initiating the rotarod later in the post-injury period would show greater discrimination between the TBI and TBI+HMN groups if the lag in performance is interpreted to be due to a lack of drug availability since Hemin is relatively insoluble but this would be unexpected given the robust HO-1 and heme blanching effect observed previously.

3.10 Zymogram changes and long term sequelae of tissue damage (FTL)

3.10.1 Zymogram Results

Drug treated groups show consistent depression of gelatinase activity with varying degrees of significance. We observed that in the neocortex HMN and SFN samples were run separately and MANOVA using the model $[\boldsymbol{ProMMP9}, \boldsymbol{ActiveMMP9}, \boldsymbol{MMP2}] \sim \boldsymbol{Day} * \boldsymbol{Condition}$ with wilks correction showed significant main effects in the HMN samples due to Day and Condition (p=2.165e-06, 0.03758 respectively). The derivative ANOVAs for each enzyme show significance in Pro-MMP9 for Day (p= 9.178e-08) and in Active-MMP9 in Day and Condition (p=3.338e-07, 0.01435 respectively). In the SFN samples using the same model we observed that there were significant main effects due to Day and Condition (p=2.165e-06, 0.0351 respectively). The derivative ANOVAs for each enzyme show significance in MMP2 for Day and Condition (p=0.01990, 0.04495). Pro-MMP9 for Day (p= 1.781e-11), in Active-MMP9 in Day (p=3.149e-06). Isolating the MANOVA in the neocortex to just the TBI-Drug comparisons we observed that TBI-HMN had significant main effects due to Day and Condition (p=0.0004223, 0.0375755 respectively), the derivative ANOVAs showed Conditional significance only in Active-MMP9 (p= 0.01435). TBI-SFN had significant main effects due to Day and Condition (p= 3.968e-10, 0.0351 respectively), the derivative ANOVAs showed Conditional significance only in MMP2 (p= 0.04495).

We observed that in the hippocampus HMN and SFN samples were run separately and MANOVA using the model $[\boldsymbol{ProMMP9}, \boldsymbol{ActiveMMP9}, \boldsymbol{MMP2}] \sim \boldsymbol{Day} * \boldsymbol{Condition}$ with wilks correction showed significant main effects in the HMN samples due to Day only

(p=2.594e-12). The derivative ANOVAs for each enzyme show significance in MMP2 for Day (p=1.202e-05), Pro-MMP9 for Day (p= 2.782e-09) and in Active-MMP9 in Day (p=0.0004085). In the SFN samples using the same model we observed that there were significant main effects due to Day and weak significance in Condition (p=1.967e-07, 0.05275 respectively). The derivative ANOVAs for each enzyme show significance in MMP2 for Day and Condition (p=2.496e-05, 0.01162). Pro-MMP9 for Day (p= 9.948e-06), in Active-MMP9 in Day (p=0.0001648). Isolating the MANOVA in the hippocampus to just the TBI-Drug comparisons we observed that TBI-HMN had significant main effects due to Day only (p= 2.594e-12), the derivative ANOVAs do not show Conditional significance in any enzyme. TBI-SFN had significant main effects due to Day and weak significance in Condition (p= 1.967e-07, 0.05275 respectively), the derivative ANOVAs showed Conditional significance only in MMP2 (p= 0.01162).

In the neocortex the hemin treated group shows weak significant depression from TBI in MMP2 activity at 7d. In the MMP9 metric there is significant depression by 3d to Sham levels in the active form while the pro-form is depressed but not significantly.

The TBI+SFN treated group shows a very similar general trend though with different points of significance. At 3d post injury MMP2 activity is weak-significantly reduced vs Sham though this does not continue through 7d. More oddly, while there is reduction in Pro-MMP9 expression to Sham levels at 3d, there was anomalously high expression of Pro-MMP9 at 7d . The active MMP9 form does not show significance vs TBI but nonetheless appears depressed at 3d post injury, midway between Sham and TBI expression.

The hippocampus demonstrates a similar pattern of gelatinase expression compared to the neocortex – the major pattern difference is that the pro form of MMP9 does not peak nearly as high in expression. Nonetheless a similar pattern of drug expression effects is seen with generalized depression compared to TBI in the majority of metrics. Notably the TBI+SFN group has significantly reduced MMP2 expression at 1d and 3d post injury compared to the TBI group.

3.10.2 Figure 3-18: Zymography for MMP2, MMP9 in Drug Treated Neocortex

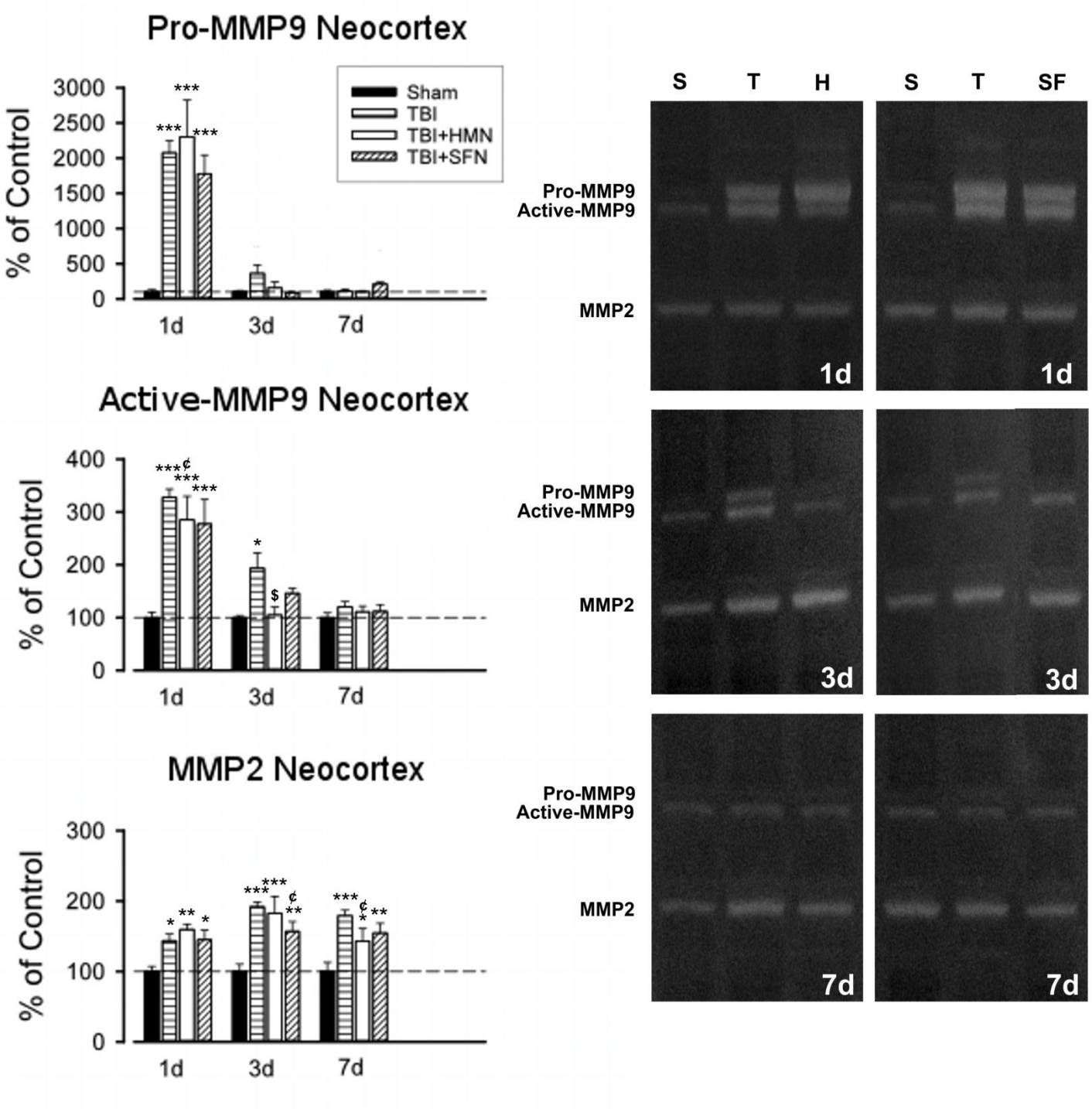

Figure 3-18: Neocortical expression of the gelatinases MMP2 and MMP9 (Pro and Active forms) 1d-7d post injury in TBI and TBI+HMN/SFN animals compared to Sham. Note similarities in expression between TBI and TBI-Drug groups with generalized depression in most metrics. (Mean ± SEM, n=4/group; T-Test with Benjamini-Hochberg correction, ●, *, **, *** for p < .10, .05, .005, .0005 respectively vs Sham, ₡, $, for p<.10, .05 vs TBI).

3.10.3 Figure 3-19: Zymography for MMP2, MMP9 in Drug Treated Hippocampus

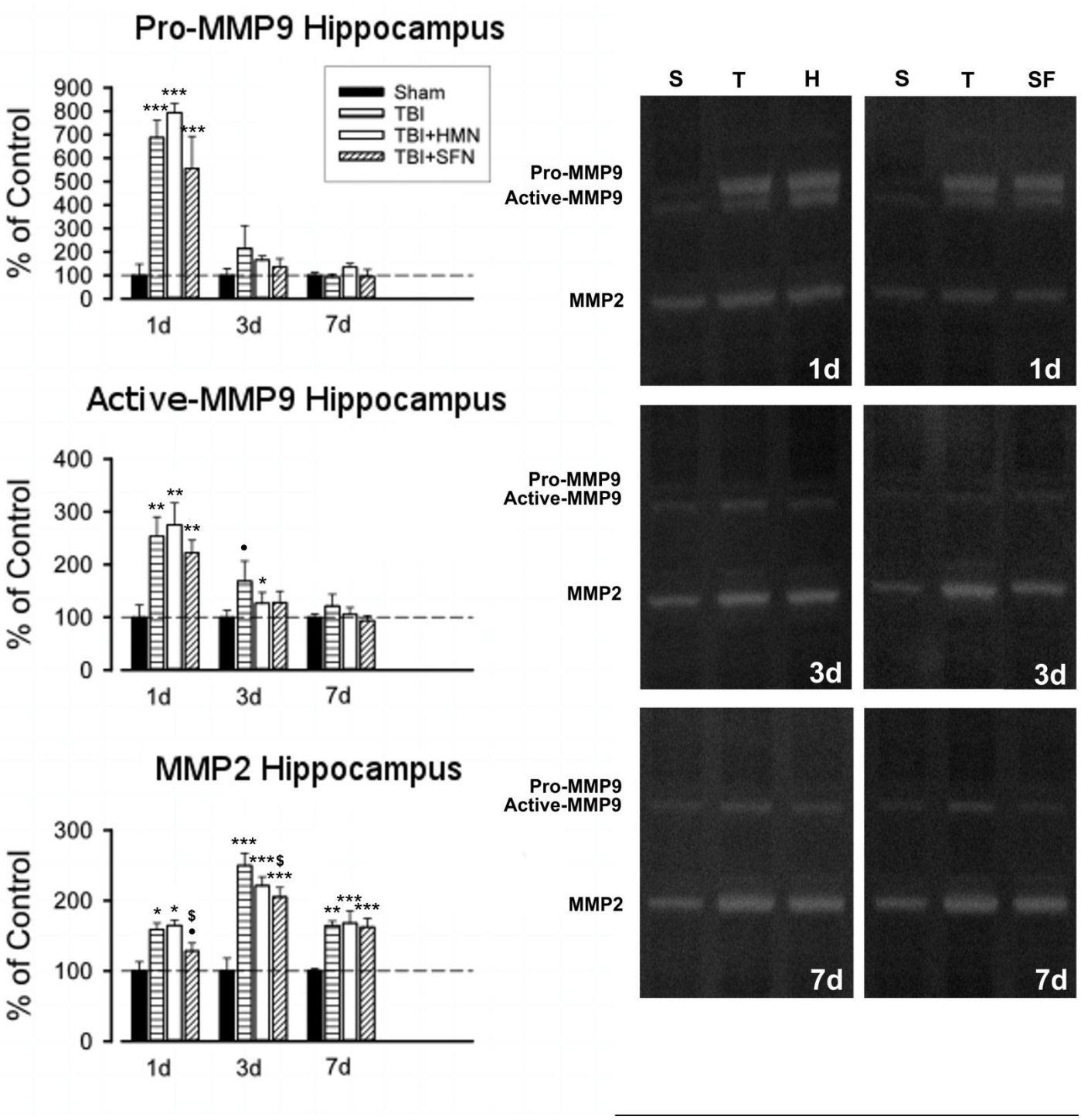

Figure 3-19: Hippocampal expression of the gelatinases MMP2 and MMP9 (Pro and Active forms) 1d-7d post injury in TBI and TBI+HMN/SFN animals compared to Sham. Note similarities in expression between TBI and TBI-Drug groups with generalized depression in most metrics. (Mean ± SEM, n=4/group; T-Test with Benjamini-Hochberg correction, ●, *, **, *** for $p < .10, .05, .005, .0005$ respectively vs Sham, $ for $p<.05$ vs TBI).

3.10.4 Summary of Observations Zymography

In the zymograms we observe that there seems to be a general suppression of expression during drug treatment but that this is only rarely significant at any time point. In all cases the expression of MMP2, and both Pro-MMP9 and Active-MMP9 appear to follow a similar time dependent profile as the TBI group. The grouped comparisons via MANOVA however reveal that there appear to be drug effects when considering the whole set of results and that these effects appear to be different depending on the drug applied – Sulforaphane appears to have a consistent effect on MMP2 in both the neocortex and the hippocampus while the effect of Hemin appears to be more restricted to the active form of MMP9 and only found significant in the neocortex.

3.10.5 FTL Results

In our FTL results we see that there are modest shifts in the neocortical which is expected based on our previous HO-1 results and minimal shifts in our hippocampal measures. In the neocortex, ANOVA using the model $\boldsymbol{Value \sim Day * Condition}$ we have significant main effects in Day, Condition, and their interaction (p=1.514e-05, 6.477e-07, 0.0003856 respectively). TukeyHSD of group effects showed significant differences in Sham-HMN (p=0.0142169), Sham-SFN (p=0.0174498), Sham-TBI (p<0.0000005), and near but no significance in TBI-SFN (p=0.1211002), and TBI-HMN (p=0.1659528). In the hippocampus, ANOVA using the model $\boldsymbol{Value \sim Day * Condition}$ we have significant main effects in Day, Condition, but not their interaction (p=0.0001035, 6.571e-06, 0.1004482 respectively). TukeyHSD of group effects showed significant differences in Sham-HMN (p=0.0002607), Sham-TBI (p<0.0000119), weak significance in Sham-SFN (p=0.0716488), near but non significance in TBI-SFN (p=0.1780772), and no significance in TBI-HMN (p=0.9981158).

FTL is significantly elevated in the drug treated neocortex 1d post injury while the TBI group is not elevated. By 3d however this significance has disappeared in the drug groups and both appear suppressed relative to the TBI which is significantly elevated vs Sham. The TBI+SFN group is significantly different from the TBI at this time point. All groups peak in expression at 7d post injury, with TBI peaking substantially higher than the TBI+Drug groups, ~50% higher, and by day 15 all TBI/TBI+Drug groups converge as expression declines. Significance vs sham is lost in all groups except the TBI+SFN group but all the TBI groups are similar in expression. In the Hippocampus FTL is unaffected at day 1 and is increased in all groups at day 3, with weak significance in the TBI group, and significance occurs in all TBI groups relative to sham by 7d which is largely maintained through day 15 with sustained

elevation of FTL compared to the neocortex. It is notable that the TBI+SFN group shows an early modest increase in FTL compared to other TBI groups at 1d and from that point consistently lags behind the other groups through 15d.

3.10.6 Figure 3-20: FTL Western Blot Results Drug Treated 1-15d Post-Injury

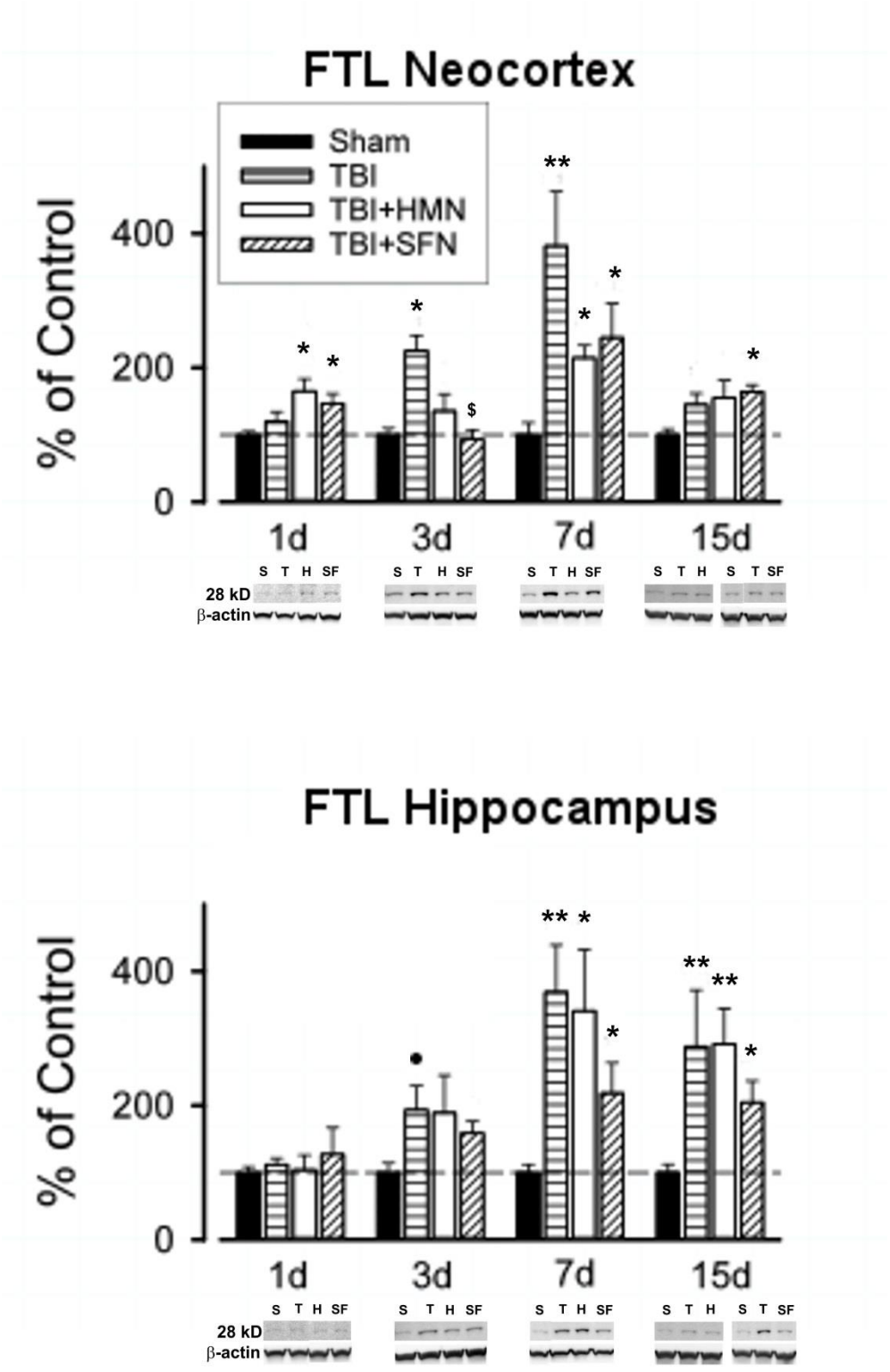

Figure 3-20: Western Blot expression of the iron storage protein Ferritin (FTL) in TBI, TBI+HMN, and TBI+SFN animals compared to Sham 1-15d post-injury. Note similarities in expression between TBI and TBI+Drug groups with acute depression at 3d in the neocortex and at 7d in the TBI+SFN hippocampus. (Mean ± SEM, n=4-7/group; Wilcoxon-Test with Benjamini-Hochberg correction, ●,*, **, *** for $p < .10, .05, .005, .0005$ respectively vs Sham, $ for $p<.05$ vs TBI).

3.10.7 Table 3-7: FTL Western Blot ANOVA Model

Neocortex Mean±SEM	Day 1	Day 3	Day 7	Day 15
Sham	1.00±0.06	1.00±0.10	1.00±0.18	1.00±0.08
TBI	1.20±0.14	2.25±0.23	3.81±0.81	1.45±0.16
HMN	1.65±0.18	1.35±0.25	2.15±0.19	1.55±0.26
SFN	1.47±0.14	0.93±0.14	2.45±0.51	1.65±0.10

Hippocampus Mean±SEM	Day 1	Day 3	Day 7	Day 15
Sham	1.00±0.08	1.00±0.15	1.00±0.12	1.00±0.12
TBI	1.12±0.09	1.93±0.36	3.69±0.70	2.88±0.84
HMN	1.04±0.22	1.89±0.56	3.41±0.0.91	2.91±0.53
SFN	1.28±0.40	1.59±0.18	2.19±0.45	2.05±0.31

Table 3-7: FTL mean expression over control of each condition by group 1-15d and presented as Mean ± SEM in Neocortex and Hippocampus. Note peak expression of FTL at 7d post injuryand conversion of drug treated groups with TBI at at 15d.

3.11 Long Term Behavioral Shifts

3.11.1 Morris Water Maze

In order to study longer term behavioral effects of injury and HO-1 targeted pharmacotherapy we utilized the Morris Water Maze as a metric of largely hippocampal function which has been well characterized in a variety of rodent paradigms including traumatic brain injury models. The Morris water maze is primarily a test focused on learning, memory, and spatial awareness though there are minor crossovers with cortical motor function as is typical of most physical tests.

In our paradigm we used a 1.8 m diameter pool with 60 cm high side walls filled with opaque water ~28 cm deep which hides a 10cm diameter clear plexiglass platform 2 cm below the surface in the south eastern quadrant of the pool. During 4 training days each animal is randomly without duplication placed sequentially in each ordinal starting position and allowed to search for the platform for 120s. After training, on the fifth testing day a probe trial is performed where each animal is placed in an identical starting position and allowed for 60s to search for the platform which has been removed. We recorded the latency of the animals to the platform as well as their search patterns and after subsequently derived numerous derivative properties including swim speed, quadrant time, platform proximity, and relative platform proximity and contrasted the groups via ANOVA and post-hoc parametric tests.

We initially begin by characterizing the animals during their training phase, focusing in on Path Length, Platform Latency, and Swim Speed. It should be noted that these metrics are interrelated since ending the test necessarily truncates both the Path Length and Platform

Latency metrics while Swim Speed is directly calculated from dividing distance traveled by the time. Path Length and Platform Latency provide a metric of whether the animals are successfully mastering the test while Swim Speed is a screening metric to establish if there are any confounds driven by something that impairs motor function.

During the Morris water maze training phase the general metrics of performance show that the groups all appear to behave largely as expected. The interrelated measurements of Path Length and Platform Latency show that the Sham group quickly learns the task by about day 2 and the injured groups lag behind with notably impaired performance on day 1. Interestingly, both drug treated groups appear to have a similar 1d-2d performance improvement compared to the Sham group though they start from an inferior performance. Further, both the Hemin and Sulforaphane treated groups appear to have matching performance until day 4 when they diverge with the TBI+HMN group improving further to near Sham metrics while the TBI+SFN treated group oddly decreases in performance and has a final training day mean almost identical to the TBI group. The swim speed metric shows that there are no significant motor differences between the groups and swim speed is largely constant after a slight day 1 elevation.

3.12 General Metrics: Path Length, Platform Latency, Swim Speed

3.12.1 Figure 3-21: Morris Water Maze Path Length during Training 11-14d Post-Injury

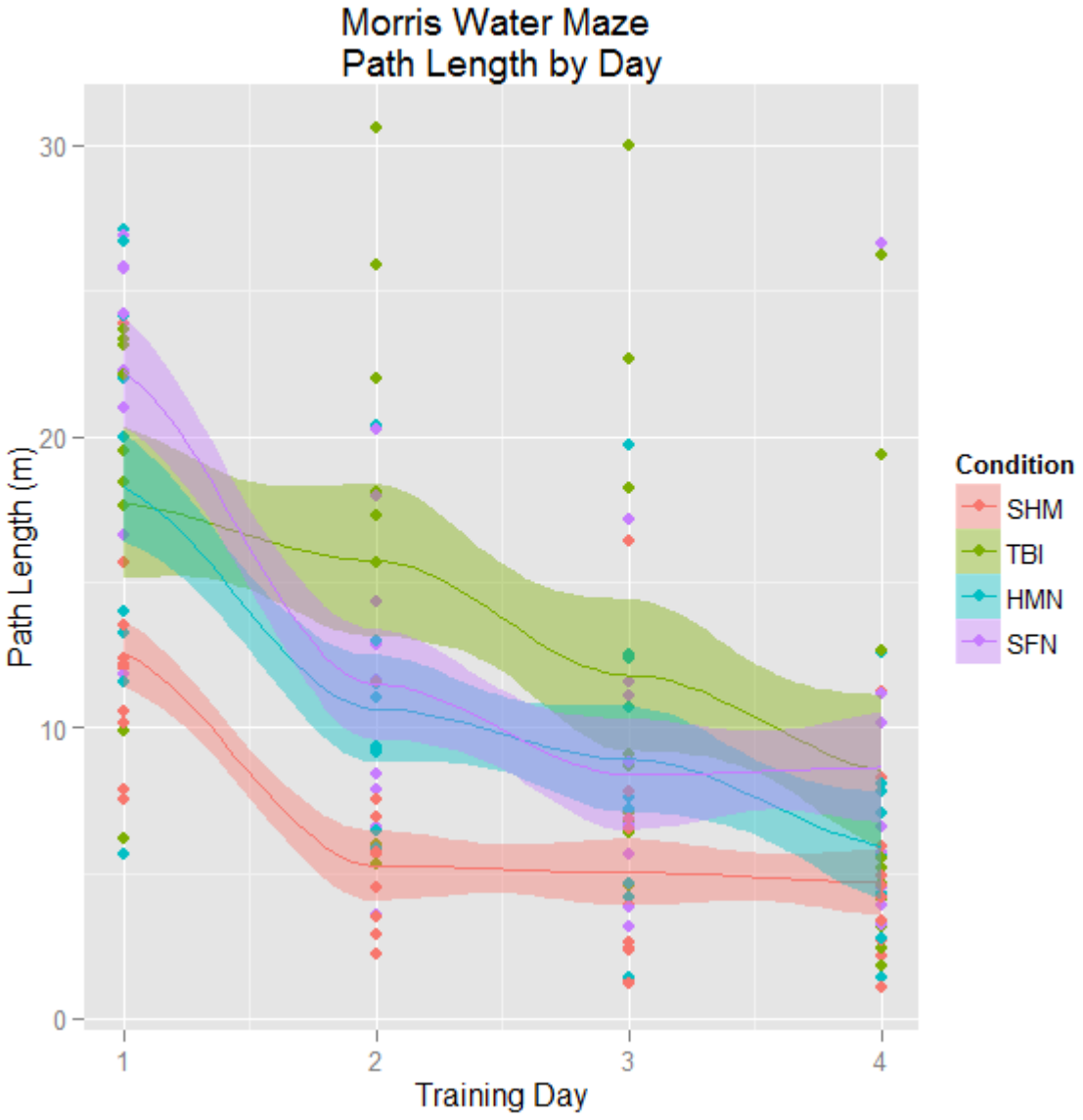

Figure 3-21: Morris Water Maze Path Length by Day during training phase of testing contrasting group behavior. Mean performance within 1 SEM is shown as well as individual animal performance scores. Note Sham path length is relatively constant after day 2 while other groups continue to improve through the end of the training phase. Additionally note that the 1d-2d improvement delta is comparable between Sham and both the TBI+HMN and TBI+SFN groups while being different from the TBI group. Observe convergence towards 1m at day 4.

3.12.2 Figure 3-22: Morris Water Maze Latency to Platform Post-Injury 11-14d

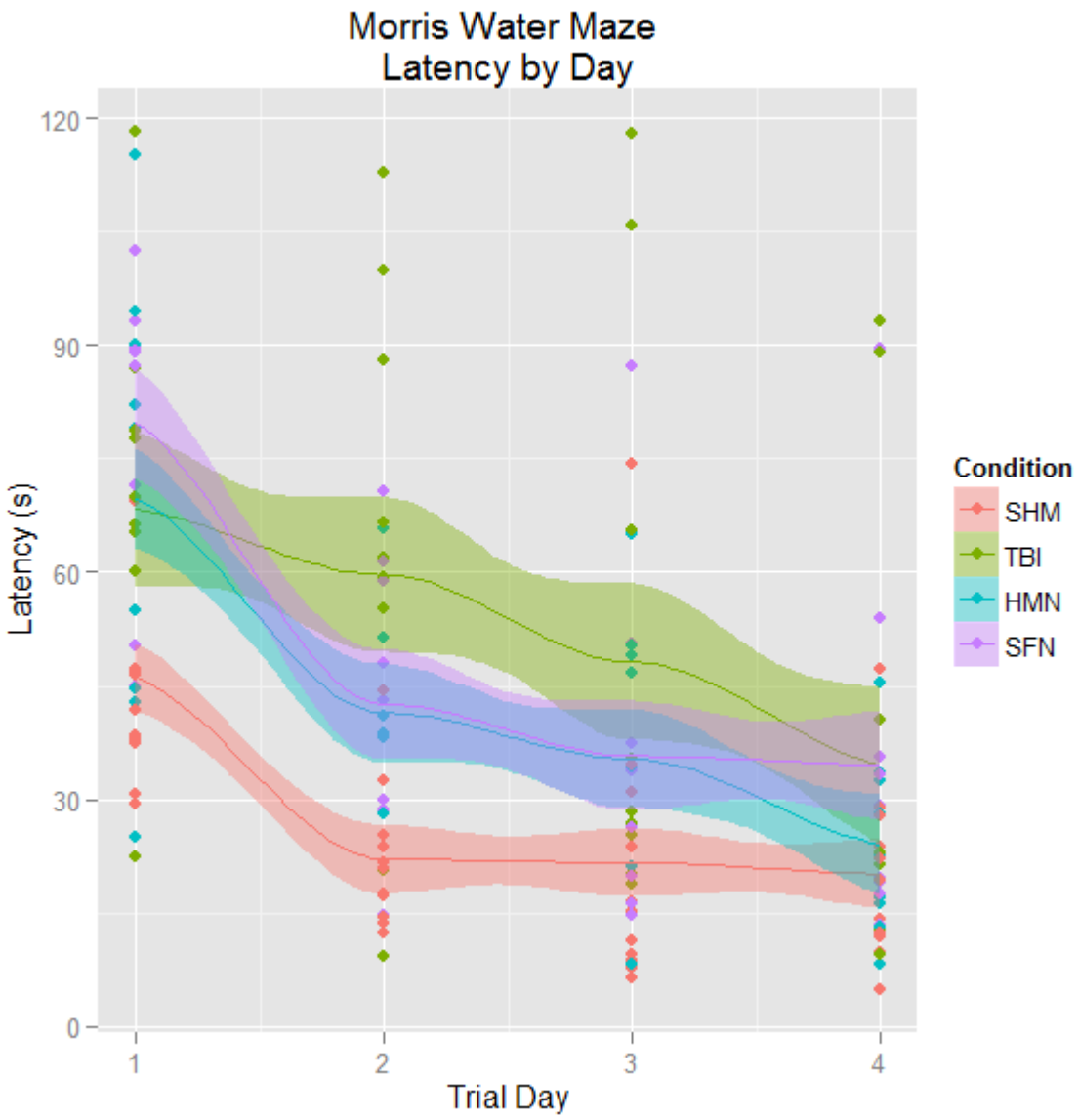

Figure 3-22: Morris Water Maze Latency by Day during training phase of testing contrasting group behavior. Mean performance within 1 SEM is shown as well as individual animal performance scores. Note Sham latency is relatively constant after day 2 while other groups continue to improve through the end of the training phase. This value is highly correlative to path length and note convergence towards ~15 s at day 4.

3.12.3 Figure 3-23: Morris Water Maze Swim Speed 11-14d Post-Injury

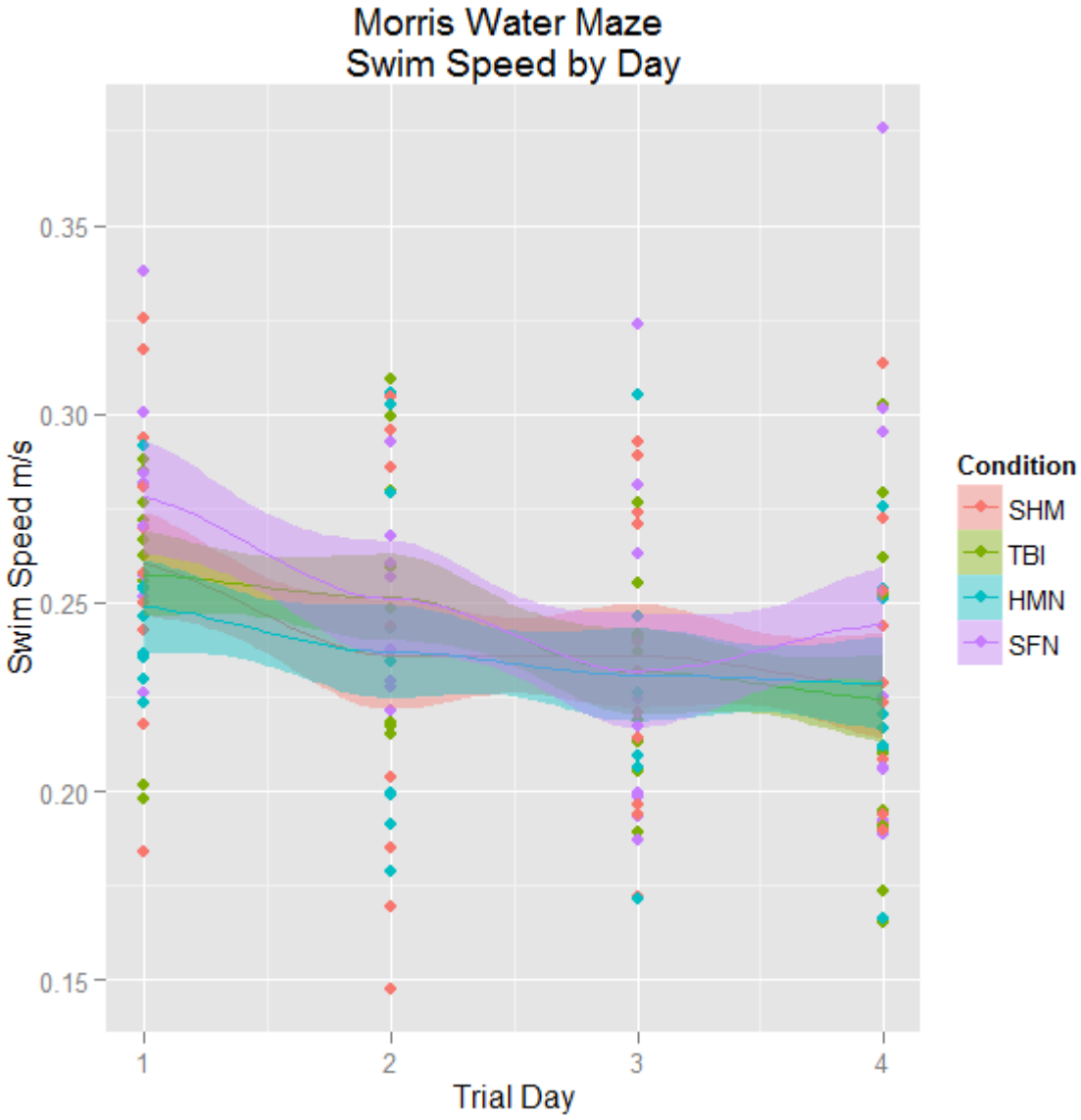

Figure 3-23: Morris Water Maze Swim Speed by Day during training phase testing contrasting group behavior. Mean performance within 1 SEM is shown as well as individual animal performance scores. Note that swim speed is relatively constant among all groups with a modest elevation during the first trial day which stabilizes 2-4 days.

3.12.4 Water Maze Heat Maps for Individual Groups

After noting the initial performance metrics for the training phase of the Morris water maze test, we next moved on to examining the probe trial data. Since we no longer have a latency score to compare animals by and given that relatively constant swim speed previously identified suggests that path length is not a meaningful measure we used derivative metrics obtained from the animal paths to distinguish between the overall profiles of their behavior. First however, we looked at the individual tracks of the animals in the different groups noting general behavioral trends as well as occasional extreme outliers.

We see in the Sham group (Figure 3-24) that the majority of animals appear to demonstrate an intense focal search near the platform which largely consists of target scanning behavior with a mixture of scanning surroundings and periodic wall touches. The animals uniformly search the south eastern quadrant where the platform was previously located and all animals quickly cross over the platform site before proceeding towards focal or moderately expansive search patterns.

We see in the TBI group (Figure 3-25) that the majority but not all animals cross the platform and the searches are remarkably different from the Sham group. There is still a small subset of animals that engage in a target scanning behavior but more typically they demonstrate a random focused search or a mixture of thigmotaxis (wall hugging) or incursion (wall bouncing) behavior. In the majority of cases these behaviors still result in crossing the platform location but it was observed that it seemed to take longer before this occurred relative to the Sham group.

The TBI+HMN (Figure 3-26) group shows a general reversal of TBI behavior which appears much more closely related to Sham. All animals cross the platform site and the majority engage in target scanning and scanning of surroundings with occasional deviation towards focal scanning a moderate distance away from the platform. There is a general absence of thigmotaxis with a single exception and only a moderate amount of incursion with an apparent preference for broad scanning searches.

The TBI+SFN (Figure 3-27) group in contrast shows similar behavior to the TBI group. All animals cross the platform but it takes them a while. Only 1/9 animals show any semblance of a targeted search and only 2/9 (including previous) showed any focused search pattern. Instead the animals strongly tended towards thigmotaxis, incursion, and chaining (concentric paths a set distance from the walls) which show a distinct search pattern.

These heat maps demonstrate that not only do the animals have different success rates at getting to the platform and learning the test as identified in the training phase, they also have different behavior in how they attempt to search for the platform that appear to be influenced by 1d induction of HO-1.

3.12.5 Figure 3-24: Morris Water Maze Probe Trials for Individual Sham Animals

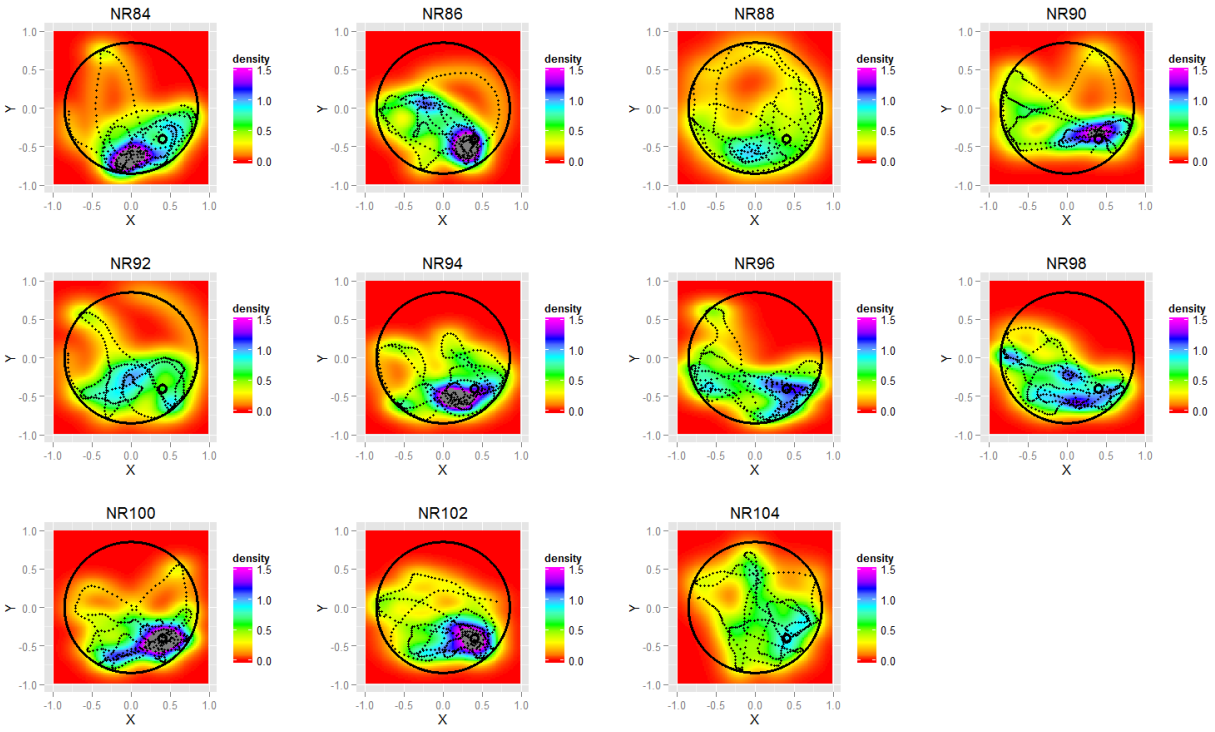

Figure 3-24: Heat Maps of Probe Trials for individual Sham animals showing general pattern of behavior. Note that all animals search near the platform with some variance in how widely the animals search. All animals concentrate their search patterns in the south eastern (lower right) corner of the maze.

3.12.6 Figure 3-25Morris Water Maze Probe Trials for Individual TBI Animals

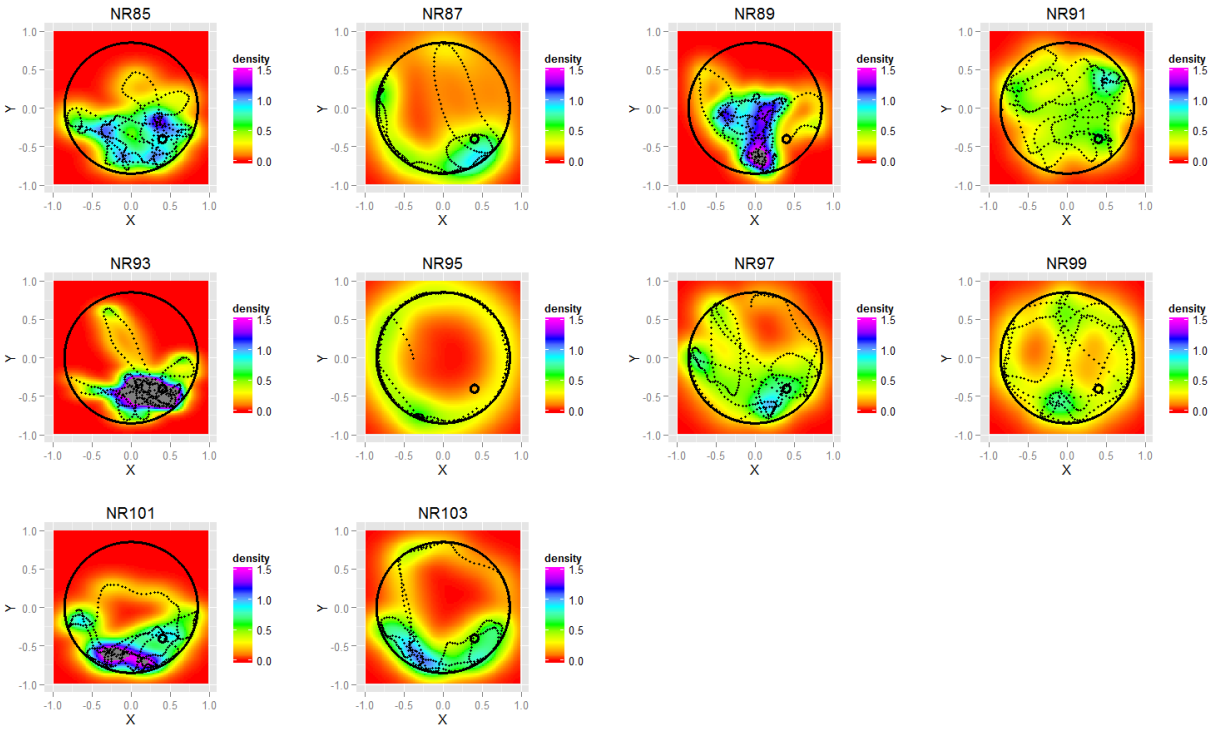

Figure 3-25: Heat Maps of Probe Trials for individual TBI animals showing general pattern of behavior. Performance is markedly worse compared to the Sham group. Note that not all animals cross the platform, unlike other groups shown and many of the search patterns are focused on the center of the pool though in aggregate they tend towards the south and eastern edges. Further note two identified outliers of NR95 which only exhibited wall searching behavior and avoided the center of the pool, and NR93 who repetitively crossed the platform in a very constrained search aberrant for the group.

3.12.7 Figure 3-26Morris Water Maze Probe Trials for Individual TBI+HMN Animals

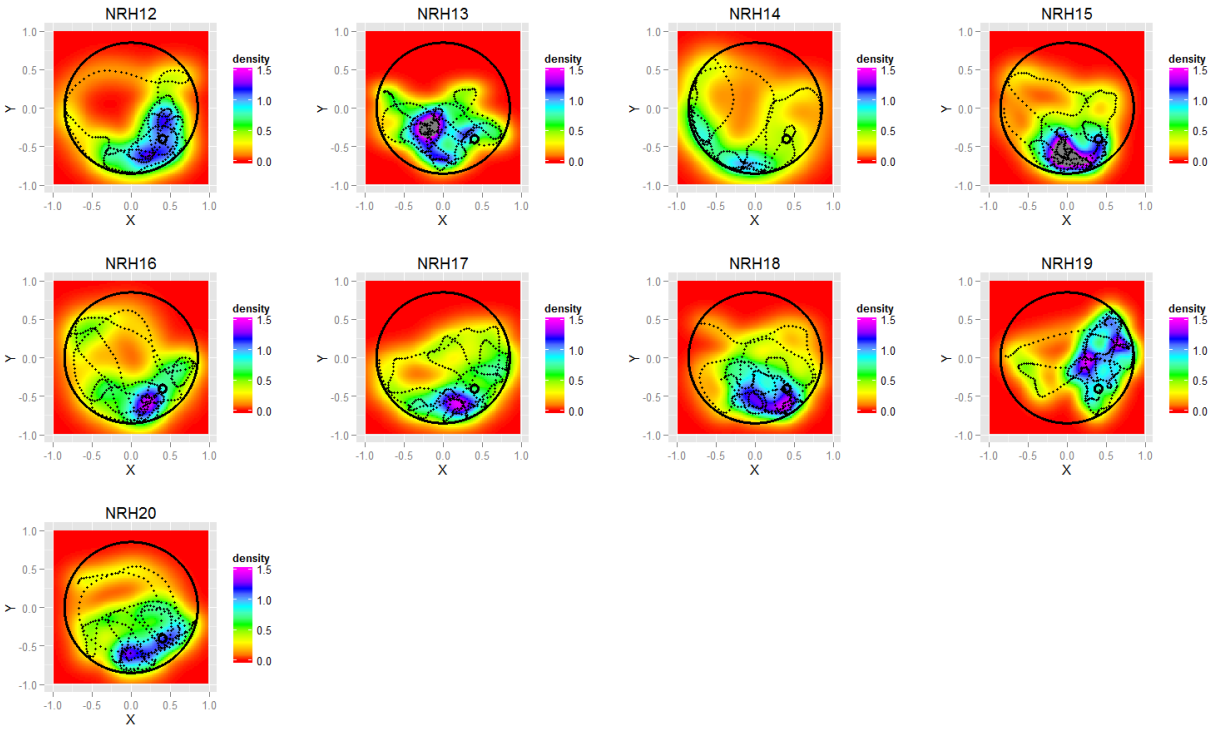

Figure 3-26: Heat Maps of Probe Trials for individual TBI+HMN animals showing general pattern of behavior. Performance is comparable to Sham performance with concentrated searches in the south eastern corner of the maze. Note that the majority of animals search in a fairly confined area near the platform location with the notable outlier of NRH14 which crosses the platform but does not generally search near its location.

3.12.8 Figure 3-27Morris Water Maze Probe Trials for Individual TBI+SFN Animals

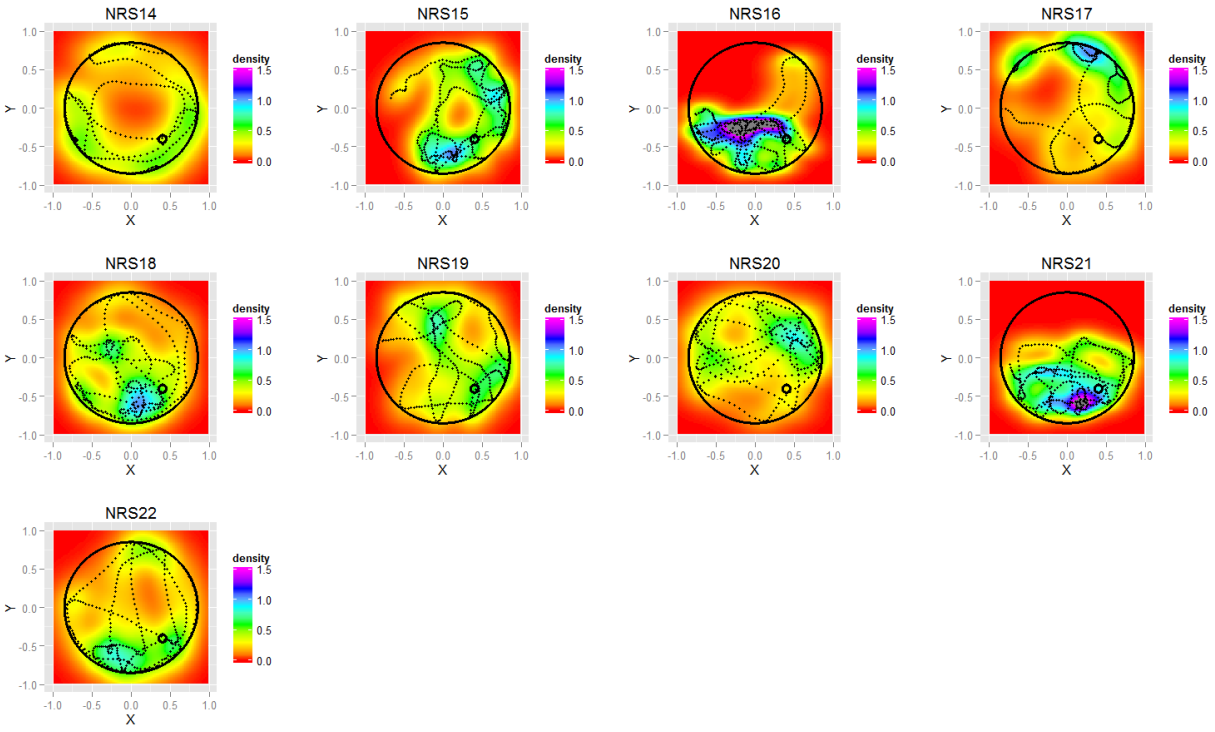

Figure 3-27: Heat Maps of Probe Trials for individual TBI+SFN animals showing general pattern of behavior. Performance is markedly different from Sham and appears most similar to TBI. Note that all animals appear to cross the platform at some point during their search but also that they tend to search very broadly throughout the pool and in general show the broadest search patterns of any group.

3.12.9 MWM Summaries and Analysis

After examining the individual behavior of the animals by condition in the Morris water maze test we then moved from subjective observations of search patterns into derived numerical scores of their search patterns. As our first step we generated a combined heat map that condenses the performance of each group into a more easily digestible form (Figure 3-28). The similarities between the Sham and TBI+HMN groups are apparent in the figure as well as the contrasting similarities between the TBI and TBI+SFN groups. In all cases there is a general focused search into the south eastern quadrant of the pool with a slight bias towards the southern position which may be an artifact of all probe trial animals starting in the identical west position. It is also quite clear that the Sham and TBI+HMN groups largely avoid the northern edge of the pool while the TBI and TBI+SFN frequently pass through.

Converting this data into a numerical form we investigated the group differences in the Quadrant Score (time spent in the south eastern quadrant, Figure 3-29), the Proximity Score (average distance from the platform during the test, Figure 3-30), and the Relative Proximity Score (a dimensionless inverse measure of proximity score divided by the line length from the platform to the wall that lies through the given animal position, Figure 3-31). We see from the quadrant score that there is a clear split between the Sham and TBI+HMN groups vs the TBI and TBI+SFN groups which is largely expected from our previous observations. In the quadrant score the Sham has the best performance with the TBI+HMN group close behind and both the TBI and TBI+SFN group lagging substantially. The proximity scores show a similar story although in this measure of proximity to the platform the TBI+HMN group appears moderately better than the Sham group as a result of the TBI+HMN tendency to search from the center of the

pool rather than the wall. Both the TBI and TBI+SFN continue to lag in this metric. Finally, the relative proximity score shows similar results to the proximity score with slightly modified means and interquartile ranges.

We continued the analysis by running the ANOVA and TukeyHSD analysis on the group data against the training phase and the probe trial individually and against the full time course. Note that as the metrics chosen are all averages they are dependent on the test latency. The Quadrant Score during the training phase (Table 3-8) shows that the Sham group is statistically significant from all other groups while the other groups were all non significant. The stratification during training was exactly along whether the animal received a TBI initially.

During the probe trial in contrast (Table 3-9), stratification appears to occur similar to what would be expected from our observations in Figure 3-28. The Sham group is significant vs TBI and TBI+SFN but not TBI+HMN while the TBI group is weakly significant vs the TBI+HMN group and not different from the TBI+SFN group.

Here we find a bit of an interesting story – if analyzing the probe trial using relative proximity we find the same pattern of significant and non-significant as the Quadrant Score with the exception that the TBI-Sham group is now weakly significant while the TBI+HMN group is significantly different. Further, analysis of the whole time course using the relative proximity score shows the expected stratification with the TBI group different from all others except TBI+SFN significantly and the Sham group different from all others except the TBI+HMN group.

3.12.10 Figure 3-28: Morris Water Maze Probe Trial Heat Maps by Condition

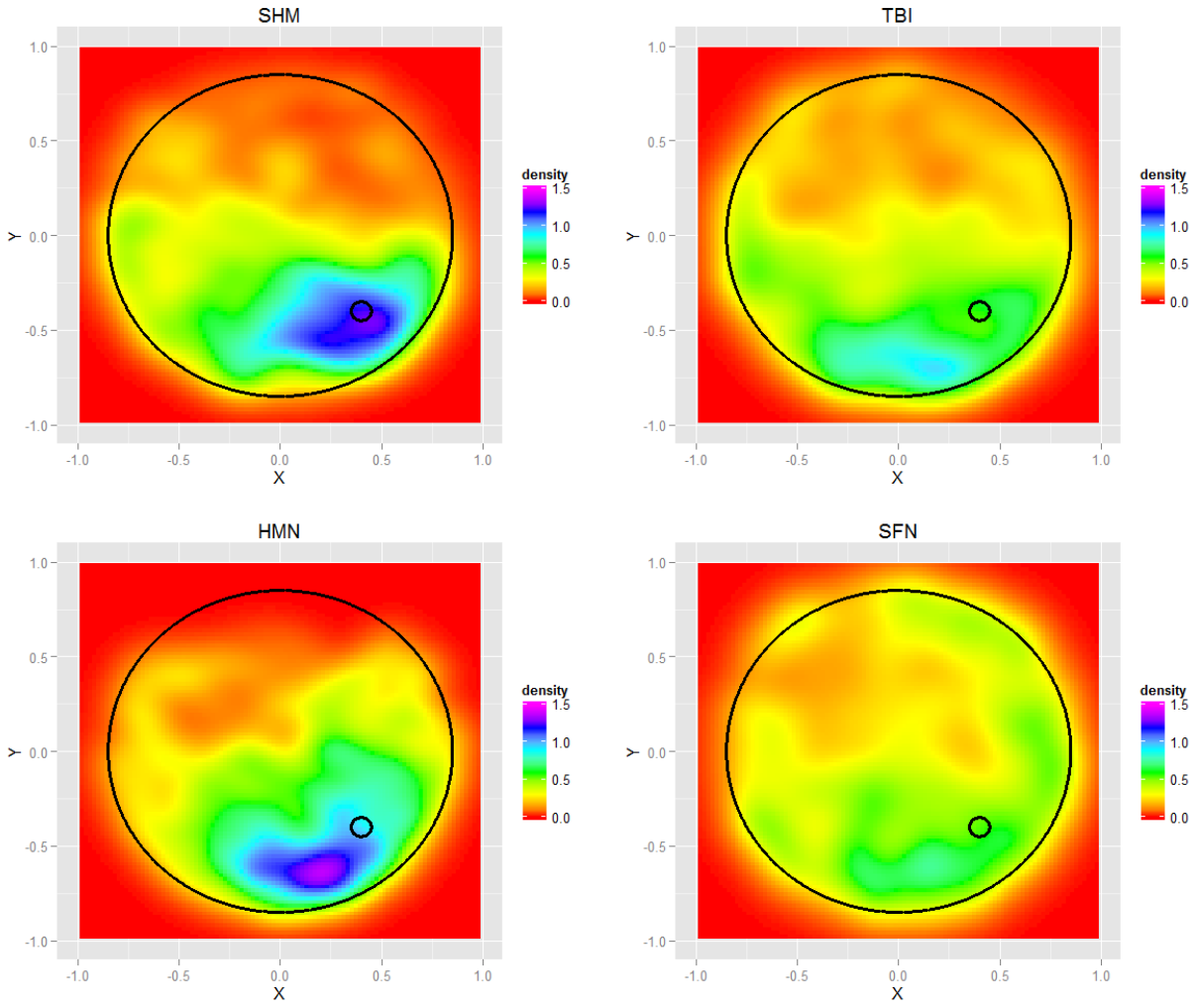

Figure 3-28: Aggregate Heat Maps of Probe Trials by condition for Sham, TBI, TBI+HMN, and TBI+SFN animal groups. Paths have been removed to allow for better interpretation of data and the similarities between the SHM/HMN and TBI/SFN groups are easily apparent based on search density. All groups in aggregate show a similar general search direction towards the south eastern corner of the maze and note that all animals were started in the east (left side) position. This data set has removed the outliers previously identified in the water maze tracks.

3.12.11 Figure 3-29: Morris Water Maze Probe Trial Quadrant Score by Group

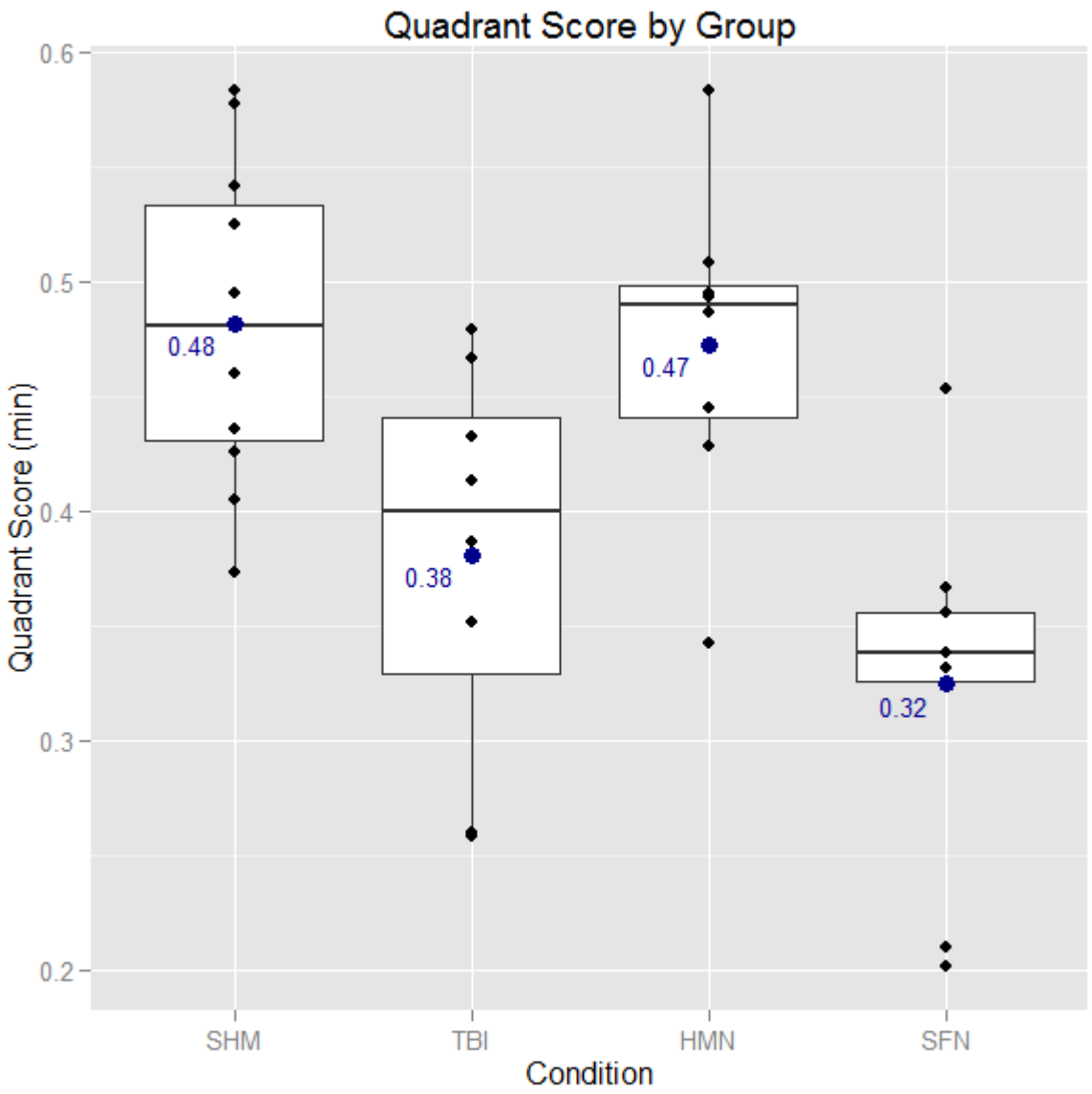

Figure 3-29: Box Plot Comparisons of Quadrant Score by Condition during day 5 probe trial. Note similarities between the SHM and HMN groups vs SFN and TBI groups. Note Normality of SHM group. Since dropping outliers in HMN and SFN artificially restricted variance they were maintained in the set.

3.12.12 Figure 3-30: Morris Water Maze Proximity Score by Group

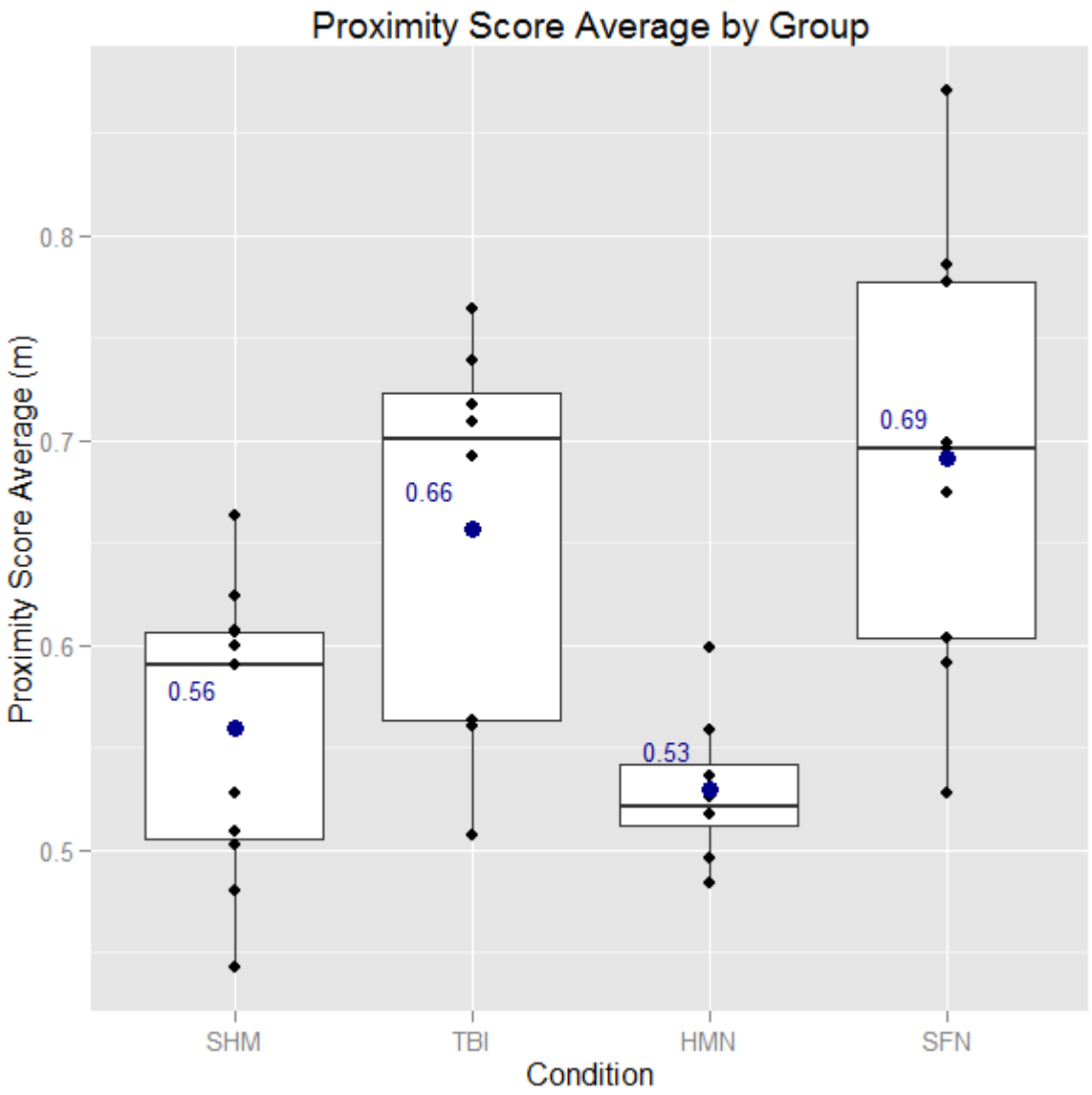

Figure 3-30: Box Plot Comparisons of Proximity Score by Condition during day 5 probe trial. Note similarities between the SHM and HMN groups vs SFN and TBI groups.

3.12.13 Figure 3-31: Morris Water Maze Relative Proximity Score by Group

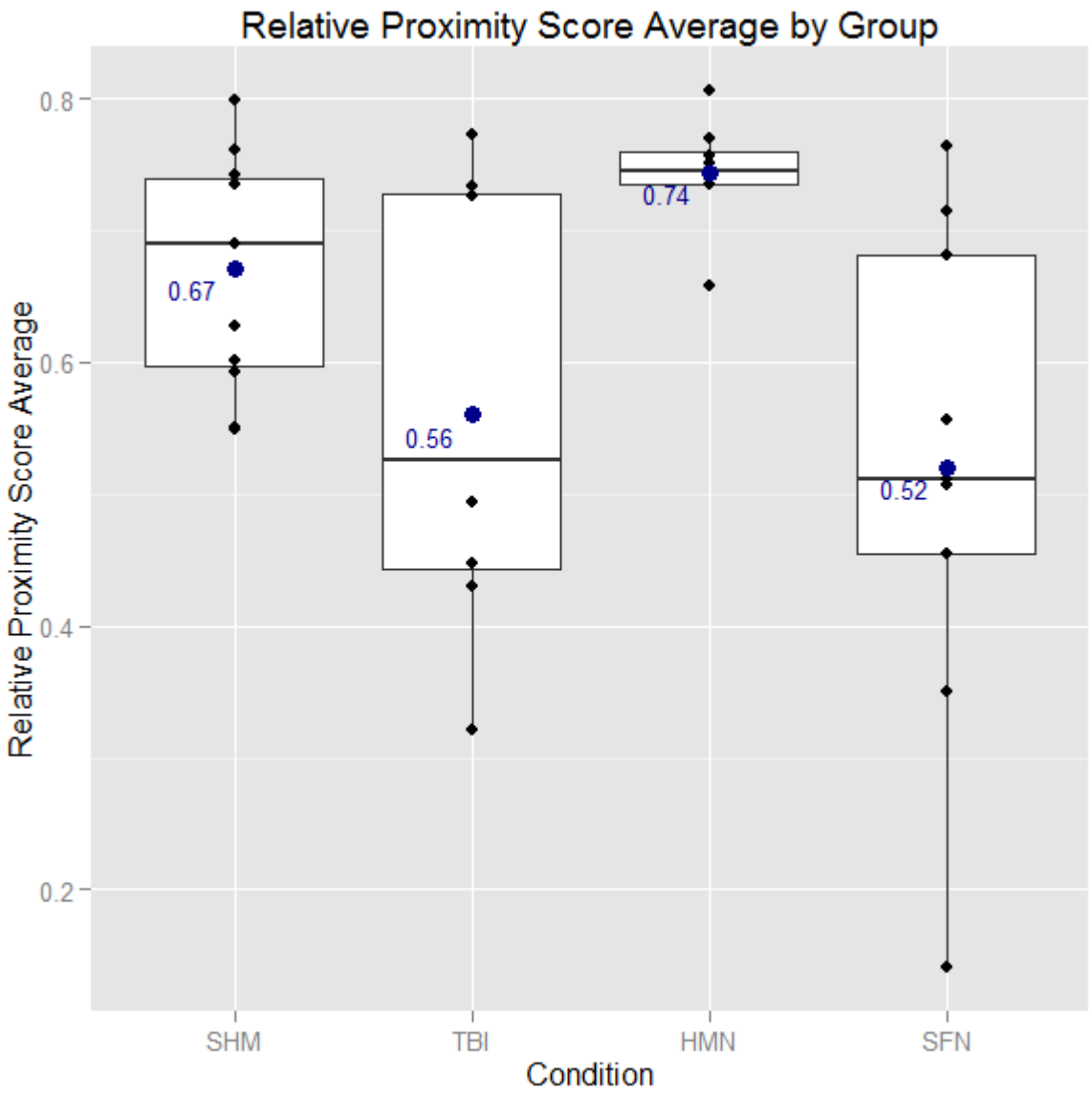

Figure 3-31: Box Plot Comparisons of Relative Proximity Score by Condition during day 5 probe trial. Note similarities between the SHM and HMN groups vs SFN and TBI groups.

3.12.14 Table 3-8: Morris Water Maze Training Quadrant Score ANOVA Model

TukeyHSD QSAve Training					
$Condition					
	diff	lwr	upr	p	
TBI-SHM	-0.07548	-0.14618	-0.00477	0.031491	*
HMN-SHM	-0.07192	-0.14262	-0.00121	0.044586	*
SFN-SHM	-0.10115	-0.16955	-0.03276	0.001054	***
HMN-TBI	0.003562	-0.07252	0.079643	0.99935	NS
SFN-TBI	-0.02568	-0.09961	0.048259	0.802708	NS
SFN-HMN	-0.02924	-0.10318	0.044697	0.732513	NS

Table 3-8: Training Phase Morris Water Maze TukeyHSD from ANOVA Quadrant Score QSAve ~Day*Condition. Note that during training Sham is different from all other groups significantly, but there are no other pairwise significant results. To some extent this is unsurprising since the TBI and TBI-Drug groups all originate with a similar impediment that strongly influences their ability to master the task.

3.12.15 Table 3-9: Morris Water Maze Probe Trial Proximity Score

TukeyHSD PSAve Probe Trial Day					
$Condition					
	diff	lwr	upr	p	
TBI-SHM	-0.10087	-0.19579	-0.00596	0.033826	*
HMN-SHM	-0.00929	-0.1042	0.08563	0.993348	NS
SFN-SHM	-0.15736	-0.24917	-0.06555	0.000312	***
HMN-TBI	0.091587	-0.01055	0.193722	0.091669	.
SFN-TBI	-0.05649	-0.15574	0.042772	0.425325	NS
SFN-HMN	-0.14807	-0.24733	-0.04881	0.001689	***

Table 3-9: Probe Trial Phase TukeyHSD from ANOVA Proximity Score PSAve ~Condition. Note that HMN is different from SFN and from TBI group. SHM is different from SFN but only weakly significant vs TBI which is interesting but due to the large spread in values.

3.12.16 Table 3-10: Morris Water Maze All Days Relative Proximity Score

$Condition PHPAve All days					
	diff	lwr	upr	p	
SFN-HMN	-0.10414	-0.17831	-0.02997	2.03E-03	**
SHM-HMN	0.015193	-0.05573	0.08612	9.45E-01	NS
TBI-HMN	-0.08391	-0.16023	-0.00759	2.49E-02	*
SHM-SFN	0.119333	0.050725	0.18794	7.15E-05	***
TBI-SFN	0.020228	-0.05394	0.094399	8.94E-01	NS
TBI-SHM	-0.09911	-0.17003	-0.02818	2.16E-03	**

Table 3-10: All Days TukeyHSD from ANOVA Relative Proximity Score PHPAve~Condition*Day. Note that SHM-HMN and TBI-SFN are the only non significant pairs. SHM and HMN essentially are the same, TBI-SFN are the same. This gives probably the best score, is essentially a proximity score that has a modified back end.

3.12.16.1 Summary of MWM observations

We observe that there are multiple points where the Morris water maze behavior of the animals tested appears to stratify along one or another factorial condition. During training it is clear that TBI regardless of drug treatment causes impaired day 1 performance which has a lasting impact throughout the test. Drug treated animals demonstrate a similar day 1-2 improvement in performance as the Sham and generally show a similar profile of improvement. This may indicate that the animals were capable of learning the location of the platform effectively but experienced some other non-motor inhibition to completing the task. As a partial explanation – it was frequently observed, especially in the TBI+SFN animals, that some of the drug treated animals would complete the test by reaching the platform, and then would promptly jump off and continue swimming; which is to say that the animals learned to complete the task but did not appropriately finish it.

When looking at the swim paths during their probe trials it is similarly clear that the animal groups (and individually) develop different search pattern techniques. On aggregate they are with only a single exception all successful patterns for finding the platform though some are more effective than others. Why specific drug treated groups tended towards search patterns aberrant from either the TBI or Sham search patterns is unknown. By the time we come to calculating metrics it is abundantly obvious that there are two distinct groupings of TBI/TBI+SFN and Sham/TBI+HMN but depending on which metric is used and the relative weighting of the particular search pattern determines whether the TBI-Sham or TBI-TBI+HMN comparisons are significant $p < 0.05$ or significant $p < 0.10$ via post-hoc TukeyHSD.

3.13 Discussion Chapter 3

3.13.1 Summary Chapter 3

In Chapter 3 we have identified the effects of pharmacologically upregulating Nrf2/HO-1 with either Hemin or Sulforaphane in a critical window after TBI. We found both treatment paradigms produced robust changes in histology, protein expression, and behavioral outcomes. Treatment appeared to shift the heme processing response to an earlier time course with net reductions in heme processing protein expression generally observed at later time points. While both drugs had highly similar effects on a number of critical measures, there were also numerous cases where the two drugs demonstrated divergent outcomes suggesting that the causal relationship between Nrf2/HO-1 induction and desirable outcomes is complex.

It is particularly interesting that throughout the time course we see changes in histology, protein expression, and behavioral outcomes after a single 1hr post-injury dose with two different Nrf2/HO-1 activating agents. To an extent this may be complicated in the Hemin treated case since it persists in the peritoneal cavity through 15d. However, the robust 1d effect in clearing the heme from the injury site indicates that there is an acute day 1 effect from the drug. Further, the observation of long term behavioral changes in the Sulforaphane treated animals demonstrates that there is an acute window where pharmacologic manipulation is capable of producing change in long term outcome, even with an agent that is rapidly metabolized.

3.13.2 Discussion Chapter 3

3.13.2.1 Targeted HO-1 Induction Premise

In this study we examined the temporal and spatial response of HO-1 and heme processing when the Nrf2/HO-1 pathway is induced pharmacologically during the early post-injury period. An underlying premise to this work is the delayed lysis and erythrophagocytosis that occurs after a hemorrhagic injury, which in bulk occurs 48+ hours after in the initial loss of vascular integrity (Cao et al., 2016; Lu et al., 2014; Xi et al., 1998). In this context early post-injury dosing functions largely in a pre-conditioning role during what is posited as a critical window of HO-1 activation. It has been well established in TBI and many other traumatic injuries that a wide variety of pre-conditioning treatments are effective at mitigating post-injury pathology (Yokobori et al., 2013). The fundamental problem has always been that predicting a traumatic event is difficult and a fairly low effective yield proposition. In circumstances of well-established etiologies such treatments have shown population wide effectiveness (e.g. low dose aspirin) but such disease conditions are relatively rare to come by. In this circumstance, with a known delayed pathological event that occurs a specific time after injury, there is the opportunity to apply a pre-conditioning paradigm to a post-injury treatment since the insult being affected (heme release) is delayed after the initial injury.

We have selected two somewhat broad range agents to induce this pre-conditioning, Hemin and Sulforaphane, because there is a lack of highly specific agents that target Nrf2/HO-1 (Ryter et al., 2006). Development of such agents is currently a hot topic in research, and notably, most Nrf2 activators are currently measured as a percentage of Sulforaphane effectiveness (Kuo et al., 2016; Ahuja et al., 2016; Carreno-Velazquez et al., 2016). Each of the drugs targets HO-1 induction in a slightly different way. Sulforaphane is known to directly interact with the Nrf2

repressor protein Keap1, causing a conformational change and releasing Nrf2 to affect downstream transcription (Ryter et al., 2006). Sulforaphane is highly soluble and readily taken up by cells systemically. Hemin mechanism, in contrast, is less certain. It has been suggested that hemin works by degrading circulating heme binding proteins, thus attenuating the expansion of heme signals after traumatic insult to cause a limited local injury (Regan and Panter, 1996; Lu et al., 2014). In this process locally generated heme acts on nearby cells and induces Nrf2/HO-1 via the endogenous pathway. It has alternately been suggested that heme binding to hemopexin rather than simply occupying circulating heme binding proteins instead acts to solubilize heme allowing it to be distributed systemically (Mehta and Reddy, 2015).

It is important to note several distinctions between the data presented in this chapter and that of Chapter 2. Here the animals were all exposed to behavioral testing of some kind prior to tissue sampling. All animals were exposed to the rotarod until their protein extraction or perfusion date and all animals that survived to 15d were run both on the rotarod and in the Morris water maze. We expect that the addition of behavioral testing and stress will have a modest effect on the resulting molecular measures due to an active learning process that occurs in conjunction with required physical activity, both of which are known to affect recovery after injury (Vanderbeken and Kerckhofs, 2017; Morris et al., 2016).

3.13.2.2 Drug Treated Heme Processing

We see a robust, immediate effect in our 1d contrast images of heme pigment in the tissue. There is remarkable blanching of the necrotic site seen in both the TBI+SFN and TBI+HMN animals and it is also easy to see the necrotic vacuolization that occurs after injury and which normally contains significant heme pigment. In place of the normally reddish heme pigment we instead see a pale yellow color indicative of residual bilirubin. In the sections shown

there is more yellow pigment in the TBI+SFN animals and a more translucent appearance in the TBI+HMN animals. This suggests that either heme has been locally consumed/expelled from the erythrocytes or erythrophagocytosis has been shifted to earlier to an earlier post-injury interval. These results are consistent with images shown by Lu et al., in their Hemin treatment of the ICH paradigm though they did not directly address heme pigment shifts in their paper (Lu et al., 2014). Several authors have noted an association between HO-1 and erythrophagocytosis both as the effector of ultimate processing of heme and also as a potential driver of increased erythrocyte degradation (Cao et al., 2016; Alfieri et al., 2013; Lu et al., 2014).

3.13.2.3 Drug Treated HO-1 Expression

When we then look at the western blot time course of HO-1 expression 1-15d after injury we see a similar story. 1d expression of HO-1 is similar in both the TBI and TBI+HMN/SFN groups, however, there is a significant reduction in HO-1 in treatment groups at 3d post-injury which demonstrates that peak expression of HO-1 has shifted in the drug treatment groups to ~1d post-injury. Further, we see that the HO-1 expression in the TBI+HMN group is modestly higher than TBI at 1d but is lower than even the TBI+SFN group by 3d further supporting the idea that increased early HO-1 leads to decreased long term HO-1 level. TBI+SFN, in contrast, has a gentler decline over time. Even with these decreases it should be noted that through 15d, even when we lose significance vs the Sham, the TBI+HMN and TBI+SFN groups continue to show modest increases in expression. This demonstrates that injured-treated animals continue to show some HO-1 response, even if a significant portion of the heme-related injury process has been preferentially cleared.

Interestingly, when we look at the peak cortical expression of HO-1 compared to the hippocampus at 3d post-injury we see an effect similar to that reported in Chapter 2, where peak

expression of HO-1 is higher in the hippocampus than in the neocortex (16.42x in the hippocampus, 9.46x in the neocortex). However, this is not observed in the drug treated groups at 3d where nearly identical values are reported for the two regions in the TBI+SFN animals (3.88x in neocortex, 4.07 in hippocampus) and the reverse pattern is seen in the TBI+HMN group (3.43x neocortex, 2.42x hippocampus). Interestingly, if we make the same comparison at 1d post-injury we revert to the previous pattern with higher elevations in Hippocampal expression compared to the neocortex. It appears that regardless of treatment peak HO-1 expression is consistently higher in the hippocampus.

We note the contrast between our results and those obtained by Alfieri et al in their Sulforaphane treated paradigm of I/R in stroke (Alfieri et al., 2013). While we only have a snapshot of their findings they identified a significant increase in HO-1 as a percentage of ipsilateral hemispheric control at 1d post-injury vs untreated animals. Unfortunately we do not have a good data comparison since they used a measure of HO-1 induction area rather than a western blot analysis of HO-1 protein. Thus, it is unknown if there was an upregulation in protein expression or a just broadening of HO-1 area. We have previously observed in Chapter 2 that there is wide dispersion of HO-1 expression during the immediate post-injury period, which becomes more focal and organized over time. In IHC images we also observe that TBI+SFN treated animals frequently show a broad degree of HO-1 background staining which is distinct from both the TBI and TBI+HMN tissues.

We also note a few differences between the TBI/Sham data set in this chapter and that previously described in Chapter 2. In this data set we see modestly lower 3d HO-1 expression and higher 1d HO-1 expression in the hippocampus which more closely matched the cortical time course. Further, we found persistent elevation through 15d in both the neocortex and

hippocampus. These shifts may be explained, in part, by additional stress of behavioral testing in these animals. Moreover, the choice to employ data analysis with non-parametric tests, as the reduced number of samples permitted single blot multi-group comparisons, created a less than normally distributed data set with heavy tails due to central limit theorem considerations. If we focus on the interpretation that behavioral stress was a factor, it can be noted that increased blood pressure is known to have an effect on leakage of intravascular constituents into the parenchyma simply due to fluid dynamics. As such, we may have effectively utilized a pump to increase net perfusion into the tissue.

IHC of HO-1 supported our previous observation of blanching in the 1d drug treated tissue. Notably, there is a clear pigment shift in the cortical necrotic site as we lose autofluorescence in the red channel indicating a loss of heme or erythrocyte pigment at the necrotic site. Further, this shift is sequential, with the TBI group showing extensive reddish pigment, the TBI+SFN group showing some, and the TBI+HMN group showing essentially none. In paired staining with LCN2 we also see that the morphology of the astrocytes (previously identified via GFAP reactivity) has shifted from an anisotropic reactive appearance to a progressively isotropic organization. Their processes extended parallel to the pial surface with a shift in expression of both HO-1 and LCN2 from largely somatic to more process oriented profiles. In general there appears to be more cellular organization of the HO-1 response in the drug treated groups and the bleeds appear more resolved. In the hippocampus, where we do not see necrosis, there is also a more organized response. In drug treated tissue it is notable that HO-1 and LCN2 appear in more distinct laminar profiles, while expression appears broader across the dentate gyrus in the 1d untreated animals. These observations continue through 3d post-injury where in the neocortex we see a substantial reduction in bleed/necrotic site area and

concurrent reduction in general HO-1 reactivity. The hippocampus shows a similar shift though we lack a direct comparison of a major hemorrhagic site.

By 7d, when we look at HO-1 vs GFAP near the necrotic site, there is loss of co-expression, which we have seen previously, and the remaining HO-1 which is highly expressed in the center of the bleed site, is much reduced in both the TBI+SFN and the TBI+HMN groups. Further, there appear to be HO-1 halos that form around small vessels which are not cell localized, suggesting an enhanced vascular or iron trafficking response in the drug treated tissue. At 15d when we contrast HO-1 with FTL after the different treatments we see clear change from TBI cases which show high expression of both HO-1 and FTL in cells scattered throughout the damaged tissue. The TBI+HMN group seems particularly reduced in area and intensity vs the TBI and the 15d TBI+SFN animal seems similar to TBI but with a greater shift towards HO-1 vs FTL. In summary, the HO-1 data appears to show differences between the treated and untreated animals, observed in both the quantitative measures of protein expression and in the IHC tissue distribution.

3.13.2.4 Affected Iron Sequestration and Storage Proteins

When we look at LCN2, however, we see essentially no difference in total expression between the TBI and TBI treated groups. There are a few modest points of significance in the drug treated groups vs Sham but the effect size is low in those circumstances and inconsistent across the time course. In general LCN2 is up by 1d, persists through 3d, and is still fairly elevated at 7d post-injury. This pattern of expression is in contrast with the LCN2 data reported in Chapter 2. While we still see that LCN2 expression in the hippocampus is roughly 10 fold higher than the neocortex, the expression vs Sham in both tissues appears roughly 10 fold lower, largely due to effects at the 1d post-injury period. Further, we see relatively constant expression

of LCN2 from 1-3d and sustained expression through 7d. A persistent 7d elevation suggests that the stress of the behavioral testing may have altered LCN2 response. This could be explained by increased LCN2 expression in the Sham animals, causing a upward shift in baseline protein level, which manifests as sustained expression in the injured animals. At least two factors might contribute to this LCN2 elevation. Given the increased cardiovascular requirements of running the rotarod and Morris water maze, the animals may experience a greater amount of vascular leak after injury, as the stressful requirements of activity lead to increased systemic blood pressure. It is also possible that LCN2 expression has been shifted due to the induction of task learning, starting when the animals are first exposed to the rotarod. LCN2 is associated with dendritic spine plasticity and may be expected under the circumstances (Ferreira et al., 2013; Skrzypiec et al., 2013; Mucha et al., 2011; Chattarji, 2011). We can contrast these measures of acute iron sequestration (LCN2), where we saw minimal treatment effects, with our measure of long term iron deposition (FTL), which demonstrates a clear shift after drug treatment.

The results observed for FTL are interesting in that they present the only major contrast between neocortex and hippocampus observed. In our measures of HO-1, LCN2 and gelatinase activity we regularly see similar results in terms of expression profile. This does not extend to the results in the neocortex and hippocampus for FTL. In this metric, we see that by 1d post-injury there are significant cortical increases of FTL expression in the TBI+drug groups compared to Sham, and the TBI+HMN group is significantly higher vs the modest rise in TBI. By 3d, however, we have a net FTL reduction in both drug treated groups and neither is different from Sham while being significantly suppressed compared to the TBI. By 7d the suppression continues although all TBI groups are elevated vs Sham and by 15d they are all declining in lock step.

The hippocampal response is different. There is essentially no change in expression at 1d following drug treatment. The metrics largely fluctuate in lockstep with a consistent pattern of little to no rise at 1d, rising through 7d and then declining. The only outlier to this pattern is the TBI+SFN group which both shows a modest but not significant increase in expression at 1d which in turn leads to a consistent modest suppression of expression 3-15d with the decrease significant vs TBI at 7d. It is uncertain why these differences exist but one possibility is the disruption of the NVU being greater in the neocortex than the hippocampus. This line of thinking concerns both the absorption and uptake of the drugs, and their potential effect. If we consider Hemin to be a more insoluble compound that is poorly transported it may be unsurprising that a less damaged barrier would fail to produce significant effect (hippocampus vs neocortex). In this circumstance we would see a minor effect in the hippocampus with the Sulforaphane treated group only, and that is what we see, a modest early rise which is not significant, followed by suppression through 15d. This is in contrast to the neocortex, where a more grossly degraded barrier is associated with significant rises in expression at 1d for both drugs. A greater enhancement vs the hippocampal tissue suggests that the drugs are more capable of having an effect due to the loss of barrier function. The following roller coaster of reduced cortical expression at 3d followed by a rise at 7d is probably explained by early upregulation of FTL helping to effectively clear the iron response element signal normally required for increasing FTL expression. At later time points this effect may be lost but the persistent reduction may be due to the prevention of protein expression overshoot during the initial forward amplification cycle of FTL.

If we hold FTL as an indicator of long term damage, we would expect the hippocampus to perform preferentially better at longer time behavioral tests while both drugs would perform

similarly at short time points. Interestingly, this is at odds with some of the other metrics examined and ultimately at odds both with the rotarod and the Morris water maze data presented below. As another point of interest – it is somewhat perplexing that FTL remains more upregulated relative to Sham in the hippocampus than in the neocortex, when we know that there is hemorrhagic injury associated with the neocortex. Further, while we have previously observed Perls stain both inside the previous hemorrhagic injury and scattered in the neocortex, we have not made the same observations within the hippocampus.

3.13.2.5 Early Behavioral Outcomes Post-Injury Assayed by Rotarod

Shifting to look at the results of early behavioral data via the rotarod test we observe that there are distinct drug effects over the post-injury period. We designed our test protocol based on the paradigm described by Hamm et al., (Hamm et al., 1994). Rotarod naïve animals are placed on the device for the first time 1d after injury and as such the test functions as a combined metric of cortical and hippocampal function. The animals both have to be able to successfully run the test, requiring some degree of motor function ability, and must be able to learn and remember how to run the test day to day. We observe that over the course of 7d after injury the animals stratify into two distinct groups – a high performing Sham/TBI+SFN group, and a lower performing TBI/TBI+HMN group. At 1d the treated TBI groups have an initial performance that is roughly halfway between the TBI and Sham performance. This is probably a reasonable data point for the day 1 motor function differences across groups. By day 2 and ongoing, the TBI+SFN group almost exactly matches the Sham, while the trajectory of the TBI+HMN group is flatter and looks very similar to the TBI group. The greatest difference between the TBI and TBI+HMN groups occurs only when looking at the max RPM achieved, which shows some separation at 5-6d post injury. It is possible that if animals were tested longer and at higher

rotational speed we could discern a difference between the TBI and TBI+HMN groups. By the end of the test there is a suggestion of modest improved performance in the TBI+HMN group, but the hard cap on performance due to testing limits ultimately causes a compression of the data set by 7d. An important note here is that there is an anomalous decrease in performance for the Sham controls after 4d. Some animals which performed very well on the test 1-4d post-injury appeared to become bored by the test and began to develop techniques to avoid the test, including jumping off the device or, in one case, wrapping his whole body around the rotating rod and letting it slide under him without moving. Other authors looking at hemorrhage models and using these drugs have demonstrated acute behavioral improvements though they did not use this specific behavioral paradigm (Alfieri et al., 2013; Lu et al., 2014). Expanding the literature search finds several authors who applied a form of the rotarod and showed behavioral improvement using both Sulforaphane and Hemin in models of Parkinson's disease (Morroni et al., 2013) and Huntington's disease (Khan et al., 2011). While the literature is sparse there are consistent reports of Hemin and Sulforaphane causing improved outcomes in behavioral testing over the acute post-injury period which is largely consistent with our observations; we find significant improvement with Sulforaphane and suggestive, but not definitive, acute post-injury improvement with the Hemin treated animals.

To some extent the behavioral data appears to contrast with what we saw in the histological data; it appeared that HO-1 and heme were more cleared in the Hemin treated group compared to the Sulforaphane treated group and yet in this early post-injury performance metric it appears that the Sulforaphane treated animals performs better. The day 1 improvement suggests that both drugs had an initial effect but the divergence at 2d onwards suggests there may be another underlying process that has been affected. One possibility is that the blood brain

barrier and NVU are more stable in the Sulforaphane treated animals vs the Hemin treated animals. This may explain why the Hemin performance lagged, particularly if this aspect of TBI pathology remains for a longer period of time relative to the Sulforaphane group. It is also possible that there is some effect on iron trafficking or glutathione generation which is different between the groups. The observations also seem to better fit with the known kinetics of the drugs, where Sulforaphane is rapidly absorbed and metabolized by the body, while Hemin processing lags for multiple days, slowly being released into the body. There is also the possibility that the mechanism of heme clearance causes the difference in effect. As an example, the 1d post-injury improved performance could be directly related to initial heme clearance, while longer term post-injury performance is more dependent on evolving iron load and regulation. Interestingly, the neocortex and hippocampus show the TBI+HMN group as having elevated FTL relative to the TBI+SFN group, possibly indicating alterations in iron homeostasis.

3.13.2.6 Drug Attenuated Gelatinase Activity

In order to further understand the pathology that develops after injury we observed the activity of the gelatinases MMP2 and MMP9, each known to be upregulated after TBI. These enzymes are important to consider since their activity is interrelated with some of the HO-1 pathway proteins. LCN2 is known to persistently activate MMP9 by preventing degradation of its active form and leading to sustained proteolytic activity (Flower, 1996; Kjeldsen et al., 1993; Yan et al., 2001). Additionally, both drugs used, Hemin and Sulforaphane have been associated with alterations in gelatinase expression, most frequently MMP9. Hemin has been shown to increase the shift of Pro-MMP9 to the active form via interaction with the hemopexin binding domain (Geurts et al., 2008) and has been used in models of HO-1 knockdown to establish that decreased HO-1 leads to increased MMP9 activity (Yu et al., 2013; Chen et al., 2013).

Sulforaphane meanwhile has been shown to suppress MMP9 activity in a number of different models including SCI and Breast Cancer (Mao et al., 2010; Rose et al., 2005) and in an *in vitro* tumor model was shown to inhibit secretion of MMP9 while not affecting MMP2 secretion (Annabi et al., 2008). We see some similarities and some differences relative to these published findings for both the neocortex and hippocampus when we review our zymography data 1-7d post-injury and we will address each in turn.

Hemin and sulforaphane appear to affect post-injury gelatinase activity in the neocortex and the hippocampus, but do so selectively, as a function of both of brain region and post-injury interval. Overall, we observe a generalized suppression of enzymatic activity, with several instances of non-significant elevations at 1d post-injury, which may indicate an earlier onset of gelatinase expression/activity. To present our interpretation of these results, we will consider each of the drug manipulations separately. With Hemin, treated animals show a generalized suppression in activity except at 1d after injury, yet there are relatively infrequent instances of significant change vs the TBI untreated. We see that the primary effects in neocortex after TBI+HMN are significant reduction in 7d measurements of MMP2 versus TBI alone and in the active form of MMP9 at 3d post-injury. In our hippocampal measurements we do not observe a significant reduction of the gelatinases at any time point, placing this region in direct contrast to the neocortex. Based on MMP literature we would have expected a greater activity of these MMPs in the hemin treated animals with regions containing hemorrhagic tissue (neocortex). Indeed, there is evidence that hemin via the hemopexin binding domain coordinates cleavage of the propetide block to promote activation of Pro-MMP9. As a result of this process, we expected to see reduced Pro-MMP9 activity, with concurrent increases in active lysis, yet we observed the opposite (Geurts et al., 2008). Discriminating the details of Pro to active MMP9 transition

following injury and drug treatment would require additional studies with controlled analysis of activation rate, which was not feasible in the present study.

We can better understand HO-1 pathway relationship to MMP activation by contrasting hemin treatment to the sulforaphane treated animals. TBI+SFN again demonstrates a generalized suppression of activity, but shows more frequent instances of significant effect vs TBI untreated cases. In the neocortex we see significant reductions in both MMP2 and Pro-MMP9 activity at 3d after TBI, along with an unusual significant elevation at 7d. In the hippocampus we further observe that the Sulforaphane treated animals show significant depression at 1d and 3d in measurements of MMP2. It should be noted that we may have expected more instances of significant drug effects in our hippocampal measurements for both pro and active MMP9, however, the Chapter 3 data set had an aberrantly high 3d variance in the TBI alone group, which precluded statistical significance. This is perhaps best observed when contrasting the gelatinase activity here with that seen in Chapter 2, and noting that while activity progressively declines in the active MMP9 form we only are able to show significance vs Sham at 1d and 7d. We would note that if the 3d TBI sample had been more tightly grouped we would likely demonstrate a highly correlated pattern between the time course of drug affected HO-1expression and early shift in MMP activity, resulting in a decreased expression/activity pairing by 3d post-injury.

In summary, we have identified that both Hemin and Sulforaphane cause a consistent generalized suppression in MMP2 and MMP9 1d+ after injury with significance identified at numerous time points. The variance in certain sample groups suggests that increased sample size might further elucidate differences between the TBI and TBI+Drug treated animals. We can speculate that at least some portion of the divergence in drug treated activity is due to the

mechanistic differences between Hemin and Sulforaphane treatment. Since Hemin is the endogenous substrate of HO-1 and can function both as an activator of Pro-MMP9 and an effector of hemorrhage like injury we would expect that Hemin might cause an increase in gelatinase activity at 1d which would be ameliorated as post-injury time continued. In general this is what we observe with 1d activity in the Hemin group, with elevated in several metrics for both tissues. We can contrast this mechanism with Sulforaphane, a non-ROS producing agent, which is not associated with a direct MMP binding/activation site. We would expect Sulforaphane instead to induce a generalized suppression and this is what we observe with the notable aberrant elevated 7d Pro-MMP9 activity in the Neocortex. Interestingly, this modest induction of Pro-MMP9 could be the result of indirect Sulforaphane action on gene expression through increased Nrf2 accessibility to the nucleus.

3.13.2.7 Long Term Behavioral Outcomes Post-Injury Assayed by Morris Water Maze

Having tracked the expression of hemorrhage related protein expression, early behavioral outcomes, and gelatinase activity post-injury we next shifted to observing long term behavioral outcomes utilizing the Morris water maze paradigm first developed by Morris (Morris, 1984). In brief our paradigm utilizes a training period of 4 days starting 11 days post-injury with a variable start position and a final probe trial on day 5 with the platform removed. The Morris water maze is a frequently used behavioral assessment for TBI and has previously been employed to assess the cognitive effects of Sulforaphane and Hemin treatment in models of CCI, diabetes, okadaic acid induced impairment, Alzheimer's disease, and Scopolamine induced neurotoxicity (Wang et al., 2016; Dwivedi et al., 2016; Zhang et al., 2015; Lee et al., 2014; Bhardwaj et al., 2016; Dash et al., 2009). In each case the treated rats showed some degree of behavioral improvement after injury though occasionally requiring an altered dosing paradigm. Interestingly, while hemin has

been more rarely applied in water maze studies, its use in an Alzheimer's model demonstrated a restoration of working memory (Bhardwaj et al., 2016).

In the Morris water maze we see clear delineations between the groups both during the training phase (11-14d post injury → 1-4d training) and the probe trial run on the final day (15d post-injury → 5d testing). We see during the training phase that the TBI and TBI+Drug animals show similar performance deficits compared to the Sham. However, both drug treatment groups show a similar 1-2d improvement delta in path length and latency to the platform. From this point the TBI+SFN group largely plateaus while the TBI+HMN group continues to slowly improve. The TBI group also improves over time, though at a slower rate than the drug treated groups. By the end of training, the means of the TBI and TBI+SFN groups converge in contrast to the merging means of the Sham and TBI+HMN groups. When we look at the possible interrelated confound of swim speed we find that the rats do not demonstrate any significant differences in swimming ability. It is notable however, that while swim speed converges through 3 days post-injury, in all groups at day 4 we see a noticeable uptick in swim speed in the TBI+SFN group with multiple animals swimming faster than previously observed.

The paired group effect is similarly seen when we look at the aggregate heat maps of position in the probe trials where it is clear that the Sham and the TBI+HMN groups show concentrated search patterns that focus on or near the platform, while the TBI and TBI+SFN groups show similar profiles of a general search in the direction of the platform but significant exploration outside of the platform area. When we look at the results of quadrant score by ANOVA we see that these same paired groups are also significantly different.

The observation that the groups show this paired response in the Morris water maze probe trial is reasonable from the aggregate data but has important caveats when we examine the individual tracks. While overall data within groups looks similar, the actual search patterns of individual animals reveal distinct treatment related behavioral modalities. In the Sham treated group we see that the majority of animals are involved in a focal target scanning search where they identify the platform position and hover over it, repetitively searching. A small number of animals also demonstrate a broader search pattern but still with a continually crossing of the previous platform site. The TBI group shows a very different mix of patterns. Three of the animals show some semblance of a search pattern though only one actually focuses on the site of the platform. The rest of the animals show either heavy thigmotaxis (wall hugging), wall bouncing, or random search behavior. Not all of the animals find the platform during the time provided and some only find it at the very end of the trial period.

The TBI+HMN group, which previously paired well with the Sham, reveals that while their search patterns are very similar and are highly focused, they frequently are focused some distance away from the platform rather than directly over it. Animals move into the correct general vicinity but they do not generally identify the correct exact position. On aggregate this results in a search pattern slightly west of the true position but a number of animals also search north, south, and even east of the platform.

These patterns are also all in contrast to those of the TBI+SFN group. These animals repetitively search the pool. They frequently cross the platform position, and do so fairly early in the testing paradigm but they do not persist in searching a focal area. It should be noted that even in prior metrics, the TBI+SFN group did tend to have a modestly higher swim speed than the other groups. Further, it was noted several times during testing that subjects in this group had a

tendency to find the platform (ending the test) and then spontaneously jump off and continue to swim. It appears that while they can locate the platform they are less interested in escaping the test or at least are more interested in searching their surroundings.

With the water maze data it appears that differentiating between the effects of drug treatment depends, to some extent, upon the selection of outcome metric. It is fairly clear that the TBI+HMN treated group demonstrates an improved search performance vs the TBI group but the distinction between the TBI and TBI+SFN group performances is less clear. Further, it is apparent that even at 15d post injury each drug exhibits a long lasting effect on cognitive behavior. This is not surprising in the TBI+HMN group given that even at 15d post injury a recognizable amount of heme persists in the peritoneal site of injection, whereas a long term effect is surprising in the TBI+SFN treated animals since the molecule is relatively rapidly processed. Describing behaviors as 'better' or 'worse' should be done with caution, since they are inherently dependent upon the selected component of the behavioral test. If instead of quadrant score we look at alternative metrics such as proximity score or relative proximity score we see that the same effects largely persist, although greater or lesser differences between groups might be revealed. In contrast, truncating the trial to 30 seconds rather than 60 or eliminating the first 5 seconds to give the rodents time to orient themselves has a tendency to induce alternate stratification of the data. For example, the TBI+SFN treated groups tend to show higher numerical scores relative to the TBI group because they focus on the platform earlier in the probe trial even if they do not persist in their interest.

Finally, our results show that not only choice of test metric, but also test design can influence detection of Sulforaphane treatment effects on cognition. There has been some work in TBI utilizing Nrf2 targeting agents, most notably by Dr. Dash at UT Houston. His group utilized

Sulforaphane in a number of different CNS injury paradigms and at one point studied the effects of the drug on Morris water maze performance in a CCI model of injury. They found that with a repeat dosing paradigm they were able to successfully induce behavioral improvement compared to TBI during an extended training phase that occurred 14-22 days after injury. While we did not see strong differentiation between the TBI and TBI+SFN groups during our training phase, we did find that they are not identical and additionally that the resulting probe trial search patterns are distinct even if they are not, on average, numerically separable. Since we used different behavioral and dosing paradigms it is difficult to directly compare our results, however, it seems clear that Sulforaphane delivered during the early post injury period is capable of producing sustained changes in cognitive behavior. Moreover, several other authors have examined Sulforaphane in models of diabetes, okadaic acid injury, Alzheimer's Disease, and Scopolamine induced neurotoxicity, and have consistently reported that Sulforaphane treatment produces behavioral improvements (Wang et al., 2016; Dwivedi et al., 2016; Zhang et al., 2015; Lee et al., 2014; Dash et al., 2009).

4 Chapter 4: Discussion

4.1 Summary of Results

In Chapter 2 we examined a number of elements of HO-1 and Nrf2 heme processing pathway and contrasted their response to TBI in a tissue with a known large hemorrhagic influence (neocortex), and a tissue with no overt hemorrhage (hippocampus). Two main findings were reported: 1.) identification of the timeline for heme processing after cFPI and how it was correlated with known timelines of hemorrhagic processing and synaptic recovery, and 2.) demonstration that the tissue level response of HO-1 pathway proteins in both the neocortex and hippocampus is remarkably similar, even when the amount of accumulated heme in the tissue differs dramatically. To our knowledge this is the first time that heme processing has been shown to be so highly activated in non-hemorrhagic tissue of a diffuse injury model.

In Chapter 3 we continued our contrast of hemorrhagic/non-hemorrhagic heme processing response in the neocortex and hippocampus but also added the intervention of two known HO-1 pathway inducers in a therapeutic window of 1 hour after injury. A couple of real world limitations necessitated this multi-metric approach – there are to date a very limited number of good Nrf2 activators and none of them are highly selective. Further, we first sought to test interventional effect through an acute, single dose paradigm, using two unique agents with differing kinetics but sharing a common pathway target. Towards this end, we repeated the molecular measurements of Chapter 2 as metrics, adding a set of animals that were also subjected to two behavioral outcome assays – the rotarod, an acute measure of largely cortical recovery/deficit, and the Morris water maze, a longer term measure of largely hippocampal recovery/deficit.

We found both treatment paradigms produced robust changes in histology, protein expression, and behavioral outcomes. Treatment appeared to shift the heme processing response to an earlier time course with net reductions in heme processing protein expression generally observed at later time points. While both drugs had highly similar effects on a number of critical measures, there were also numerous cases where the two drugs demonstrated divergent outcomes suggesting that the causal relationship between Nrf2/HO-1 induction and desirable outcomes is complex.

4.2 Post-Injury Heme Processing

Heme processing in our model fits well into the literature reports of small bleed resolution (Cao et al., 2016; Chang et al., 2003; Yamauchi et al., 2004; Alfieri et al., 2013; Lu et al., 2014; Regan and Panter, 1996). We see a steady progression of an evolving bleed which reaches maximal size between 1-3d post-injury and is substantially reduced by 7d and absent by 15d. By 3d post-injury we begin to see the yellow pigment of Bilirubin (indicative of heme catabolism) along the outer edges of the bleed as well as loose formation of Fe(II,III) hexacyanoferrate (II,III) (Perls' Prussian Blue) indicative of iron deposition and aggregation. By 7d and especially by 15d any remaining pigment is seen in dense sporadic cells that heavily dye with Prussians blue indicating significant aggregation of any remaining heme as well as iron. It is somewhat important to note here that pigments are only easily visualized when they form aggregates. In low concentrations of Fe, Perls stain does not produce a remarkable effect, e.g. we do not see universal evidence of Perls stain from normal cytochrome heme staining, we only see the blue aggregates when there are larger densities of Fe.

A number of different models looking at hematoma in larger animals or small bleeds have identified that HO-1 is significantly elevated by 3d post injury and peaks either at around

3d in the circumstance of smaller bleeds, or at 7d+ in larger hematomas where a large portion of the erythrocyte mass is physically remote from phagocytic cells (Cao et al., 2016). It is likely that this process is mediated by CD47 which is normally found on circulating erythrocytes and which regulates target cell phagocytosis (Oldenborg et al., 2000). In fact, it has been shown that the rate of erythrocyte phagocytosis is significantly increased when CD47 is lost, an experiment which has been somewhat elegantly done via the injection of transgenic CD47 KO erythrocytes (Ni et al., 2016). CD47 has in turn been associated with HO-1 which was identified as a modulator of erythrophagocytosis (Schallner et al., 2015). It has been shown that erythrocyte diameter decreases 4h-7days post injury, with a minimal diameter achieved by 3d, the same time that CD47 is lost and HO-1 expression is elevated.

Interestingly, Dr. Cao et al., have noted that treatment with deferoxamine helped to maintain CD47, hemoglobin, and decreased HO-1. They identified this as a positive response but there may be some suggestion that by preventing HO-1 amplification they may acutely demonstrate improved outcomes which later fail when the clot is eventually processed. This speaks to a chicken or egg problem when it comes to heme processing. Heme itself can be cytotoxic and damaging to the surrounding tissue, but at the same time the catabolic products of heme can also be cytotoxic, or alternatively cytoprotective depending on concentration. Hemin itself has been used as a model of intracerebral hemorrhage when injected locally or *in vitro* and as a protective pre-treatment in ICH when applied systemically (Chen-Roetling et al., 2015). This strongly suggests that a combination of time-dependent processing rate and ability to buffer the resulting products is likely to be critical towards preventing cellular injury.

It should be noted that there is some controversy over whether or not heme is predominantly processed by HO-1 or HO-2 after a traumatic injury. Dr. Noble-Haeusslein's

group measured HO activity in a CCI model using HO-2 KO mice and noted that activity was reduced one day after injury compared to wild type (WT) mice and thus, concludes HO-2 is likely the dominant form of HO which processes heme (Chang et al., 2003). This is likely true at the 1d post-injury interval, but our results suggest that HO-1 does not peak until several days later and it is not unreasonable to suggest that prior to HO-1 elevation HO-2 plays a larger role. Further, if the 1d HO-2 response is present in our cFPI model, it would occur at a time point prior to CD47 loss on erythrocytes, and largely exists before the strong pro erythrophagocytotic signals to release heme develop and prior to peak HO-1 induction.

4.3 Hemorrhagic Processing in the Neocortex vs Hippocampus

We see the induction of similar expression profiles of proteins known to be involved in heme processing within both hemorrhagic and non-hemorrhagic tissue and at comparable levels. It appears that the cFPI introduces a heme processing response even if there is limited heme present in the tissue. We have noted previously that for FPI there is a gradation of severity with increasing overpressures inducing ever increasing hemorrhagic injury (Dixon et al., 1987). Thus, it is possible that we have introduced an injury in a specific non-hemorrhagic tissue (the hippocampus) which is right at the edge of a hemorrhagic threshold with increased local signaling a result of more limited vascular disruption or constituent leak into the surrounding parenchyma. It is tempting to consider the hippocampus as an entirely non-hemorrhagic tissue and thus likely to be driven by a non-hemorrhagic trigger e.g. hypoxia and there are certainly known hypoxia induced transcription factors which upregulate HO-1 expression. However, we did not observe any of these transcription factors being upregulated when we ran our initial gene chip assays (see Appendix). Nor are they frequently identified as drivers of HO-1 expression, even in ischemic models of stroke which is peculiar but may be primarily driven by later

reperfusion injury. It is also possible that the limited hemorrhage seen in the fimbria of the hippocampus provides a more generalizable signal, but most importantly the initial expression of HO-1 observed in molecular layer of the dentate gyrus adjacent to the granule cell layer is spatially distant from any observed hemorrhagic site.

4.4 HO-1 Expression/Evidence of Bleeds

Outside of the visually identifiable bleed site, which extends from the lateral grey/white matter interface into the neocortical layers, we see significant increases in HO-1 expression as well as LCN2 and FTL even without any observable frank bleed. Indeed, expression in multiple cases is even more elevated in the hippocampal tissue than in the cortical tissue.

There are several possible explanations for the observed these protein expression profiles. The pattern and combination of acute iron sequestering protein, heme processing protein, and iron storage protein in sequential succession is highly suggestive that they are involved with and responding to local heme processing in the tissue. Further, while HO-1 and LCN2 can both be amplified by Nrf2 driven transcription, FTL is not responsive to Nrf2 but rather to iron response elements indicating the presence of free iron in the tissue. This suggests that heme may be processed in the tissue even though it is not identifiable with standard histological techniques.

Currently there are a number of ways of identifying bleeds in tissue. In vivo methods include CT and MRI techniques such as SWIM (Liu et al., 2016; Chiara Ricciardi et al., 2017; Wintermark et al., 2013). These techniques tend to produce a relatively large voxel compared to histological studies but are excellent at identifying moderately sized microbleeds. Dr. Latour's group demonstrated that in paired cadaveric experiments the bleed signatures identified via MRI

are substantially enlarged when the tissue is stained with Perls' stain suggesting an imaging limitation to only bleeds of sufficient size (Dr. Latour, NINDS, (Abstracts from the 34(th) annual national neurotrauma symposium june 26-29, 2016 lexington, kentucky. 2016). It should be noted here, that this enlarged tissue penumbra is the affected area where there is still sufficient iron deposition/aggregation to cause an easily observable excess which can be stained. Smaller quantities of iron or iron that is effectively trafficked out of the tissue would not demonstrate Prussian blue formation. This speaks to a potential problem in trying to identify if there are 'nano' bleeds throughout the tissue, in circumstances where erythrocyte integrity is suspect we may lack cell markers and simultaneously lack large aggregate pigments or signatures. If we contrast the molecular weights of hemoglobin (~65 kilodaltons; kDa) with the molecular weights of IgG (~150 kDa) we can see that in circumstances where there is free hemoglobin in the vasculature (or bound via hemopexin ~63 kDa) it is likely to leak into the parenchyma after TBI. While we see little evidence of direct bleeds in the hippocampus what we do see is large amounts of iron trafficking proteins, heme processing proteins, and iron sequestering proteins. We may also speculate that with increased image processing and tissue staining techniques it appears we are ever expanding and more carefully delineating the parenchyma surrounding injured tissue. It is always possible these molecules are responding to a more generalized signal but the specificity of temporal expression to certain tissue locations and a tendency to occur near blood vessels suggests an ongoing hemorrhagic or hemorrhage like process.

4.5 Lipocalin 2 and Gelatinase Role in Heme Processing and Recovery

4.5.1 Lipocalin 2 is a known effector of Angiogenesis and Dendritic Spine Remodeling

We have primarily focused on HO-1 as a driver of recovery after traumatic injury, utilizing agents known to preferentially target HO-1, including the application of its endogenous substrate. From this perspective we posited LCN2 and the gelatinases MMP2 and MMP9 as ancillary effectors of hemorrhagic processing driven by HO-1. Their role in the post-injury response may be independent or interactive, and was predicted to be driven by upstream changes in HO-1 activation. We did find that TBI increases both LCN2 expression and gelatinase activity in a time-dependent manner which correlates with HO-1 induction. Interestingly, we also found that drugs altering HO-1 induction do not profoundly change LCN2 expression and only moderately affect gelatinase activity, suggesting that their response to injury in our model may be less dependent on HO-1 or each other. While these results might be surprising, it is important to note that LCN2 and the gelatinases each have known effects on the vascular system that could alter post-injury response regardless of hemorrhage. Nevertheless, it remains possible that LCN2 and these MMPs are highly interdependent during the evolution of TBI pathophysiology, perhaps by sharing common stimulatory pathways and directly targeting injury tissue at numerous levels.

In addition to its role as an acute iron sequestering protein LCN2 has also more recently been identified as a significant player in angiogenesis, critical to post-injury vascular stabilization and repair. We will again note here that we observe essentially no LCN2 in our Sham animals by either western blot or IHC, thus making our observed 1-7d post-injury increases in LCN2 extraordinarily easy to identify. The research group headed by Dr. Eng Lo at

Harvard has recently published several papers looking at the role of LCN2 during angiogenesis and how it might serve as a secreted signaling factor to facilitate communication between neurons and glia (Wu et al., 2015; Xing et al., 2014). In the paper by Xing they noted that LCN2 is secreted by neurons and appeared to activate reactive glia into pro-recovery phenotypes. They found LCN2 expression was increased both in the forebrain of their rat ischemia injury model and in human stroke tissue samples. It was also noted that LCN2 enhanced angiogenesis *in vitro* via a mechanism that required increased iron and ROS (both byproducts of HO-1 heme breakdown); interestingly, chelation or reduction of either reduced angiogenesis. They further associated these findings with previous research that reporting LCN2 upregulation after CNS injury (Jin et al., 2014; Rathore et al., 2011; Xing et al., 2014) and showing that the MMPs associated with LCN2 appeared to be necessary for both neural and vascular remodeling (Yang et al., 2011). To an extent some of these effects are unsurprising and even the nomenclature of LCN2's primary alternate name, NGAL (Neutrophil Gelatinase Associated Lipocalin), speaks to its early identified role as a gelatinase associated protein. Recent publications on LCN2 have also found angiogenic associations in both CNS and non-CNS tissue (Yang et al., 2013; Wu et al., 2015). Thus, it is possible that a portion of the acute/subacute LCN2 and gelatinase elevation we observed could serve to support the onset of angiogenesis for vascular recovery from TBI.

The LCN2 findings in our study can also be compared to a series of papers showing a strong association between LCN2 and synaptic plasticity via regulation of dendritic spine formation and maturation in the hippocampus and amygdala (Ferreira et al., 2013; Skrzypiec et al., 2013; Mucha et al., 2011; Chattarji, 2011). Notably, we found maximal LCN2 response within the non-hemorrhagic hippocampus, suggesting that plasticity induced by TBI synaptic disruption might also contribute to post-injury elevation of the protein. In restraint models of

stress LCN2 increase was concurrent with higher dendritic spine density, however, *in vitro* exposure of hippocampal neurons to LCN2 showed a paradoxical decrease in spine density, suggesting that LCN2 supports a homeostatic mechanism for stabilizing synapses during periods of neuronal stress (Skrzypiec et al., 2013; Chattarji, 2011; Mucha et al., 2011). Particularly interestingly for our paradigm, Mucha and colleagues found that it was an iron free form of LCN2 associated with dendritic spine formation and maturation in the hippocampus (Mucha et al., 2011). When we compare our results with these findings it is important to consider the injury and behavioral assessment paradigms used. We injure the rats via cFPI with an overpressure known to induce hemorrhage and resulting iron overload. We then proceed to run the animals on new behavioral tasks which they are incapable of mastering during the first testing day, generating some degree of stress. As such we have a combined diffuse axonal injury, hemorrhage, iron overload and acute stress in a model of CNS insult, all initiated by a single fluid pulse across the intact dura. Thus, it might be predicted that TBI animals behaviorally assessed in Chapter 3 would demonstrate an extended post-injury LCN2 upregulation, likely related to synaptic plasticity induced by injury pathology, stress of behavioral testing and learning.

Overall, if we consider our results against the work of previous authors we would expect LCN2 induction during the acute post-injury intervals to not only serve as an iron buffering mechanism, but also play an angiogenic and gelatinolytic role. In contrast to Dr. Lo's studies, we find that post-injury LCN2 is primarily expressed by glia rather than neurons, which would support both roles. However, we do find a strong association of LCN2 induction with cortical hemorrhagic injury, which is consistent with prior studies employing the lateral FPI model (Zhao et al., 2016b; Zhao et al., 2016a), and supports the interpretation that acute LCN2 upregulation is

a hemorrhage driven, HO-1 correlated process in the cFPI model. Further, LCN2 induction occurs during the early stages of iron overload, which may limit its role in the context of dendritic spine management. Interestingly, IHC shows that the widespread dispersal of LCN2 signal at 1d post-injury progressively shifts to a more punctate and cellular-associated pattern by 3d, perhaps marking a change in LCN2 role from buffering of iron produced by heme processing toward regulation of adaptive synaptic plasticity over time. Although we failed to detect LCN2 in our Sham animals, this could be a function of the reagents used and does not necessarily negate the potential for a LCN2 role in maintaining baseline homeostasis of spine plasticity. Again, it is important to note just how extraordinarily high the level of LCN2 induction was during the early post-injury period.

4.5.2 Gelatinases as effective targets for both synaptic and vascular remodeling

Similar to the multiple roles which are possible for LCN2, the gelatinases MMP2, 9 are known to affect cell function in multiple ways, all driven by temporo-spatial patterns of proteolytic activity as reviewed by Phillips and colleagues (Phillips et al., 2014). It has been known for some time that MMPs are associated with synapse formation (Ethell and Ethell, 2007). They appear to function in this role by preferentially breaking down ECM and inducing stability in new favored neuronal connections (Reiss et al., 2005; Warren et al., 2012). MMPs have been associated with various neurodegenerative conditions including Alzheimer's disease and Huntington's disease (Asahina et al., 2001; Safciuc et al., 2007). Further, their activity has been shown to influence the pathology/recovery cycles in stroke and ischemia models, as well as SCI and traumatic brain injury (Rosenberg, 1995; Rosenberg and Navratil, 1997; Rosenberg, 2009; Asahi et al., 2000a; Zhang et al., 2010). In many cases only a small subset of MMPs are identified, most typically MMP2,3,9, and MT-5 but it should be noted that these specific MMPs

are more conveniently assayed and may be more broadly represented in the literature. MMP9 in particular has been highly studied and is associated with response to cortical stab wound and hippocampal neuroexcitatory insult (Kyrkanides et al., 2001; Szklarczyk et al., 2002a), as well as ICH (Lekic et al., 2011) SCI (Hsu et al., 2008; Zhang et al., 2011) and TBI (Kim et al., 2005; Falo et al., 2006; Ding et al., 2009; Li et al., 2009). MMP9 is frequently identified as being highly upregulated in the first 24 hours after injury or insult is applied. MMP2 is also associated with numerous injuries including ICH (Lekic et al., 2011), SCI (Hsu et al., 2006), and TBI (Truettner et al., 2005; Phillips et al., 2014). In addition to their known roles in synaptic plasticity gelatinases have also been associated with the breakdown of the blood brain barrier and appear to exacerbate hemorrhage (Montaner et al., 2001). Attenuation of expression and activity appears to limit further hemorrhagic injury (Lo 04) and is associated with reduction of functional deficits after brain injury (Lo et al., 2004).

While increased MMP expression and activity during a myriad of CNS injuries and neurodegenerative conditions might suggest that these enzymes function in a largely destructive manner it is important to note that they can also act in constructive roles. For example, they appear to be critical for normal neurogenesis during gestation and postnatal neurodevelopment and act as mediators of reactive synaptogenesis and in cortical circuit recovery after ipsilateral stroke (Liu et al., 2011; Vaillant, 2003; Luo, 2005; Phillips and Reeves, 2001; Phillips et al., 2014). A number of authors have attempted to reverse MMP mediated degradative processes and produce neuroprotection by effectively knocking down expression of the various enzymes. However, it is important to note that in our targeted treatment paradigm we probed for whether manipulation of HO-1 can indirectly affect gelatinase response to NVU disruption, perhaps through altering enzyme interaction with upregulated LCN2. While we found Hemin and

Sulforaphane efficacious in protecting tissue structure and improving behavioral outcome, there was only modest reduction in gelatinase activity at selective time points and a general profile more suggestive of shifting peak activity than necessarily reducing overall activity. Since we found improved behavioral outcomes after treatment with each drug, we posit that even this low level reduction in MMP activity at critical post-injury intervals might contribute to neuroprotection.

In our current data set, definitive statements about the link between HO-1, LCN2 and gelatinase activation were not warranted, however, the results did reveal some interesting points about this interaction. We originally posited that LCN2 activation of MMP9 contributed to vascular injury/expanded hemorrhage after TBI. While the post-injury time course of MMP9 activity does closely match acute increase in expression of LCN2, supporting the potential for LCN2 activation of MMP9 with HO-1 upregulation, post-injury treatment with either Hemin or Sulforaphane did not show correlated change in LCN2 expression and MMP9 activity. However, unstressed animal data in Chapter 2 contrasted with stressed animal data in Chapter 3 may provide insight into the dual role of LCN2 in the early post-injury period; we see a flattened expression of LCN2 in the stressed animals concurrent with a reduction in heme substrate by 1d post-injury and this may directly correlate with the reduction of active-MMP9 at 3d to near Sham levels via loss of hemopexin coordinated MMP9 activation.

At least one positive correlation between HO-1 reduction, attenuated LCN2 expression and depressed gelatinase activity was found in the 7d post-injury neocortex. There Hemin treatment essentially reversed injury-induced elevation of HO-1 and LCN2, accompanied by a significant reduction in MMP2 enzyme activity. Interestingly, there also appears to be paired MMP2 and HO-1 response in untreated TBI animals, both peaking at the 3d post-injury time

point, but this may simply represent a correlation of the zenith of catalytic processing in hemorrhagic recovery and onset of extracellular remodeling. Clearly this potential correlation between HO-1, LCN2 and MMP2 response must be further explored, however, it remains possible that adjusting the net activity of the gelatinases or shifting the time course of their activity might be accomplished by manipulation of the HO-1 pathway. Given that we acknowledge throughout this document the multi-factorial, multi-modal nature of TBI injury, our zymography results further support targeting of MMP activity as a possible effector of improved recovery from both hemorrhagic and non-hemorrhagic vascular damage.

4.5.3 Mechanisms of Select Agents

Overall it appears that targeting HO-1 with either Hemin or Sulforaphane has a positive net effect on behavior. Importantly, in no circumstance do we see any metric of injury deficit increase after application of either agent. The two drugs do, however, work via distinct mechanisms which are intended to more fully address the impact of targeting HO-1/Nrf2 when there is a lack of highly specific agents. Sulforaphane is a highly soluble compound which is applied in a carrier of DMSO and PBS via IP injection at 5 mg/kg. Prior evidence has shown that it is rapidly taken up by cells and circulates systemically readily crossing the BBB and affecting transcriptional change at just about every step along the way. Sulforaphane has been shown to directly interact with the Nrf2 repressor binding protein Keap1 inducing a conformational change and allowing Nrf2 translocation to the nucleus. At no point during this process is ROS generated nor any catalytic heme products generated. Sulforaphane functions as a non-hemorrhagic pre-conditioning agent and acts quickly upon injection. Hemin, in contrast, is a largely insoluble compound injected IP as a slurry at 26 mg/kg. Through 15d post-injury there is still observable hemin pigment in the peritoneal cavity, which shows progressive reduction over

time. Hemin ostensibly works via solubilization with hemopexin or other heme binding proteins and is slowly absorbed into the blood stream and circulated systemically. Hemopexin and other trafficking agents allow small quantities of heme to be deposited inside specific cells and it functions as the endogenous substrate for HO-1, or with constitutive HO-2 as an initial pathway trigger. During this process hemin acts like any peripherally deposited heme aggregate and generates ROS and heme breakdown products both locally and wherever it is transited. It is notable that Hemin itself is used occasionally as a model of ICH via direct intracerebral injection and in excess can be cytotoxic.

It is quite possible that more selective agents or genetic manipulations may be more effective in elucidating the underlying mechanism of hemorrhagic injury. Nevertheless, it is important to note that single factorial genetic manipulations have so far not produced useful therapies for human patients. With a multi-modal, multi-factorial injury it is quite possible that 'messier' agents are more effective on account of ancillary effects which play roles in alternative pathways. Towards this end it is very useful to contrast multiple agents that ostensibly target the same pathway but via modestly or entirely different mechanisms.

4.6 Behavioral outcomes after Treatment

After treatment with both Sulforaphane and Hemin we observed behavioral changes that appeared to be induced by the applied pharmacologic agent. In the short 1-7d time course we saw a robust improvement in the rotarod performance after 1hr post-injury dosing with Sulforaphane at 5 mg/kg and at 11-15d we saw behavioral changes in the Morris water maze that showed altered platform search behavior. Some improvements with Sulforaphane have been

reported previously, notable by Dash et al., 2009, where they demonstrated improved search patterns in the Morris water maze though only after a specific dosing paradigm (1+24 hour dosing but not 6 hour not 6+24 hour; Dash et al., 2009). A number of differences exist between their model and ours, including the use of CCI vs cFPI and a different post-injury testing interval (11-15d vs 14-22d). It is possible that with our Sulforaphane dosing paradigm we were able to induce a short term protective effect that is lost over time or was an insufficiently large signal to cause long term improvement. Our hemin treated group provides an essential contrast both in the drug kinetics and the behavioral results. The rotarod appears to show no real improvement (though the Hemin animals always out perform the TBI) and yet by 15d we see a robust improvement and alteration in the Morris water maze search pattern of TBI+HMN animals contrasting with the search patterns of the TBI animals. To date no studies have been published on the effects of hemin therapy following traumatic brain injury so we lack any even partially applicable model for contrast. Instead we can look at various studies focused on intracerebral hemorrhage, although they tend not to focus on Morris water maze as an outcome metric.

4.7 HO-1 as a Therapeutic Target

HO-1 and the products of its heme metabolism have long been considered as therapeutic targets in a variety of hemorrhagic and ischemic injuries including stroke, lung, and acute kidney injuries (Ryter et al., 2006; Bolisetty et al., 2017). Ryter in particular has been quite effective in linking the effects of heme metabolites to potential HO therapeutic utility. Rather unfortunately, his closing statements noting the need for better pharma agents or gene therapy approaches have, more than 10 years later, been unrealized. A brief sampling of abstracts from the most recent Society for Neuroscience conference in 2016 revealed a number of papers commenting on Nrf2 function, but the majority use measurements of HO-1 to identify activity. Only two groups were

seeking development of Nrf2 targeting molecules, one group (Carreno-Velazquez et al., 2016) was focused on finding non-oxidative molecules that had activity 15-100% of that of Sulforaphane, while the other group (Ahuja et al., 2016) gave up on activating Nrf2 directly and instead focused on disrupting Keap1.

One of the significant problems in working with HO-1 is the ability to identify transcription factor upregulation via Nrf2. Many of the antibodies raised against Nrf2 have been purified based on expected column migration and this has led, in many cases, to antibodies that are non-specific (Lau et al., 2013). The result is a myriad of possibly erroneous data that has likely hampered research in the area. Numerous researchers have solved this problem by simply ignoring Nrf2 except to reference as the mechanism for how their pharmacologic manipulation functions. In these cases outcome measures including HO-1, NQO1 and (glutathione synthase) are used frequently as easily identifiable readouts of ARE transcriptional activation. This in fact may not be a bad way to easily measure Nrf2 activity – in studies utilizing Nrf2 KO it has been shown that protective effects otherwise observed and increases in protein expression of downstream targets are eliminated (Zhao et al., 2007). It seems that our use of Sulforaphane and Hemin is appropriate given the tools available but it is unfortunate that a more specific Nrf2 activator is not available and that there are no spectacular Nrf2 antibodies. Despite these problems, modern lab on a chip screening of small molecules will likely cause a revolution in the field of Nrf2 activated targets. Further, recent development of upstream alternative regulators (e.g. via bach 1 or keap1 targeting) should provide an alternative method to activate HO-1/Nrf2 more selectively (Carreno-Velazquez et al., 2016; Ahuja et al., 2016).

To date, numerous animal studies in acute kidney injury, acute lung ischemia, and stroke have demonstrated reductions in tissue pathology associated with pharma upregulation of HO-1

though the evidence becomes significantly more complex once the various metalloporphyrins used as HO-1 inhibitors are considered. The difficulty is that the various substrate inhibitors (e.g. ZnPPIX, CoPPIX) each release different metallic specie which can independently play a role in cell signaling or development of pathology and in all cases still result in the release of both CO and biliverdin. The result is a confusing challenge of trying to interpret just how oxidative Zn or Co are relative to Fe and whether they sufficiently reduce ROS generation or if they are just preventing or prolonging heme processing.

Our data suggests that early induction of HO-1 causes a suppression of the normally evolving post-injury HO-1 peak and results in early processing of heme and erythrocytes after injury, effectively clearing the presence of heme. Behavioral outcomes at both 1-7d and 11-15d show functional improvement though there is some difference in the nature of behavioral protection depending on the drug used while the clearance of heme appeared to occur regardless.

We have mentioned previously that there have been a small number of studies utilizing Sulforaphane and TBI, particularly in CCI models (Dash et al., 2009). In general these studies have employed CCI as an extension of ICH research and observe relatively similar metrics in terms of lesion size and gross tissue loss. The one behavioral study was done by Dr. Dash's group and looked at latency to platform 14-22 days using a repeat dosing paradigm. They showed that dosage at 6hr post injury and repeat dosing at 6 hrs and 24 hrs post injury had no effect while dosing at 1hr and repeating at 24hr had an observable effect. It should be noted that this was in a CCI model and extended for a longer period of time than our study in an injury with worse motor function outcomes. Further, they did not provide a Sham comparison with the data and it is somewhat difficult to interpret how significant an improvement occurred. This is important since it introduces the question about whether Sulforaphane needs to be dosed ultra-

acutely after the injury. Our perspective of a 24-48 hour lag in erythrocyte degradation would suggest that a window of ~24 hours may exist but the failure to find effect after a delay of 6 hours is concerning. That being said, it is still important to acknowledge that they used a different model. We did not find a difference in latency in our TBI and TBI+SFN groups though we started assessment earlier, and the major distinctions come in the search patterns that result. The best quantitative discrimination behaviorally between the two groups was seen in the rotarod. Thus, it is possible that our data is in agreement with what was previously found in a different model of TBI with the added interpretation of comparative search patterns and acute behavioral improvement. Further it appears that there is the suggestion that the available treatment window may be reduced from a full 24 hours and may be limited to the ~1-6 hour range after injury.

In contrast to the limited behavioral data which is available for Sulforaphane treatment in TBI, we were unable to find any studies that looked at systemic hemin treatment after brain injury. There are a small number of papers looking at SCI injury and systemic hemin therapy but the majority of neural injury and hemin papers are focused on intracerebral hemorrhage where locally applied hemin is a model of induced injury while hemin applied systemically is a protective model of pre-treatment. Rather amazingly, there is even a paper looking at *in vitro* neuronal death which found that Sulforaphane was protective against applied hemin (Soane et al., 2010). With that said, there has been extensive research by Dr. Regan and colleagues focused on intracerebral hemorrhage and hemin therapies. In these studies they largely focus on pre-treatment but more recently several post injury applications have been studied (Lu et al., 2014). Hemin appears to be excluded from most organs due to binding to hemopexin or albumin (Linden et al., 1987) and as a result acts primarily on the microvasculature and has been

observed to attenuate blood spinal cord barrier permeability and CNS permeability (Lu et al., 2014; Yamauchi et al., 2004).

4.8 Differential Drug Treatment Effects

Our initial hypothesis was that early induction of Nrf2/HO-1 via pharmacological means would produce a net benefit by limiting heme toxicity after TBI. Somewhat implicit in this hypothesis is that heme resolution would also have an effect on other recovery pathways that act to recover cell and tissue function after injury by limiting added cell stress and by potentially increasing cell vigor. Somewhat as expected, we found that the drugs we used produced profound targeted effects on HO-1, and on heme pigment while generating more varied effects on metrics which are progressively further away from the critical catabolic event targeted. Both drugs caused a shift in HO-1 time course coincident with loss of heme pigment. In hemorrhagic tissue (the neocortex) this appeared to have direct effects on the production of FTL which was expected. A more variable result occurred in the hippocampus with divergence in drug behavior suggesting that it is not just the drug which is required for altered FTL expression. There must be some other co-signal which acts to affect transcription. We had limited expectations for the gelatinase results due to conflicting theories on expression driven by heme substrate/injury and known activation by the drugs applied. Only the MANOVA for SFN showed an effect on the drugs suggesting that SFN more than HMN had a greater effect on gelatinase reduction which may in part be driven by reduced oxidative cell damage.

Hemin and Sulforaphane are fundamentally different drugs and were expected to intersect solely at their function on activating HO-1 via Nrf2. We see that both drugs have extremely similar effects in shifting the time course of HO-1 expression, and in inducing heme pigment loss. After that point it appears that there may be co-signals and alternate pathways

activated by the drugs which are different and numerous independent functions of each drug have been identified by various authors. From the strictest sense we can note that in the dosing paradigm used for each drug there did not appear to be a material difference in kinetics on a timescale of days – both drugs were capable of inducing HO-1 expression shifts by 3d. With that said we could observe HMN pigment in the peritoneal cavity for weeks after injury suggesting that the drugs acts as a depot injection. We may thus expect that HMN has a continuous dosing paradigm which continues throughout the time course of our study while SFN has only acute effect. This may explain some of the differences between the observed results but even if we had maintained a constant level of SFN in the tissue throughout the time course we suggest the outcome would still vary. The drugs cross the barrier in different ways and it would be expected that as barrier function recovers HMN would have greater difficulty in crossing the barrier.

More critically, the way that the drugs target the Nrf2/HO-1 pathway is different. SFN is relatively more targeted – it is known to affect specific cysteine residues on a specific repressor protein of Nrf2 though it admittedly has some general antioxidant activity. In marked contrast HMN itself is cytotoxic and pro-oxidant and affects the expression of Nrf2 via mild oxidative damage in an iron driven mechanism. We do not expect that our application of HMN is in itself grossly cytotoxic but it is nonetheless remarkable that the two molecules themselves differ in their oxidative/reductive potential. This may suggest that there are other mechanisms outside of heme processing which play a role. Perhaps the grossly oxidative state of HMN causes increased production of antioxidant buffering compounds (e.g. glutathione), or alterations to caspases and cell cycle proteins. The ARE which is activated by Nrf2 is known to activate a number of antioxidant response molecules but it has also been well established that transcription factors are heavily influenced by co-signals and co-factors which more selectively activate specific targets.

If one takes the position that the long term behavioral outcome presented is that HMN has a greater beneficial effect it may be reasonable to attribute this to the longer term dosing behavior of HMN. Perhaps after loss of local heme pigment Nrf2 alters its transcriptional targeting from HO-1 to a more glutathione synthase oriented axis. SFN treated animals may lack this effect and have reduced long term benefits after the initial heme clearance.

The SFN treated animals however due appear to have an anxiogenic effect – they do better on the acute motor behavior metric but the rotarod is essentially a running away task. They swim well in the MWM pool 11 days after injury but they also seem to swim a little faster, and they have a greater tendency to jump off the platform after finding it and continuing to swim. This suggests that there may be a stabilized anxiogenic memory or response that has persisted across the experimental period.

It is also possible that the early kinetics of heme processing play a strong role in later outcomes though we find this idea somewhat suspect. The question revolves around the critical window of processing and whether processing early or quickly is desirable. We can see from our 1d IHC results that the bleed looks more effectively processed in the HMN treated animals which would be expected to possibly also generate an acutely toxic bolus of heme degradative products, driving more efficient enzymatic processing. We expect our HMN induced mechanism to produce concurrent buffering effects but it is always possible in the acute post-injury period that these have had insufficient time to build in the acute post-injury period. Further, the drugs are both known to have roles in the activation or expression of the gelatinases we studied though differential comparisons are somewhat difficult in a time-dependent injury affected paradigm.

4.9 Future Directions

HO-1 and its Nrf2 activation axis are promising molecules for treating heme related pathologies, including TBI, and currently exist in an un-targeted space. There are presently no drugs FDA approved for targeting HO-1/Nrf2. Early HO-1 induction appears to reduce heme related pathology and improves behavioral outcomes in the injury paradigm utilized in our study but there are several avenues that should be examined moving forward. There are several directions for future work which will help to better understand the pathway mechanism, the pathway manipulation, and behavioral outcomes after treatement.

4.9.1 Pathway Mechanism Experiments

We focused on a fairly confined portion of the HO-1/Nrf2 heme processing pathway and there are several experiments which would help to further elucidate the underlying processing response. One of the major interperative concerns with our results is the appearance of heme processing in a tissue that does not have apparent hemorrhage. We note that it is possible that in circumstances where insufficient pigment has been deposited that you could have widespread slow leakage and deposition of heme into the tissue but definitive evidence is currently lacking. To our knowledge no one as of yet has used radiolabeled heme to identify maximal extent of heme tissue deposition and this experiment may provide definitive proof of whether HO-1 in non-hemorrhagic tissues is involved in heme processing or if there is an alternative process that occurs. We suspect that there may be limited diffuse deposition of heme throughout the hippocampus. Further, we have largely focused on the heme processing aspect of HO-1/Nrf2 activation but there are also a whole host of antioxidant proteins that can also be expressed via the ARE sequence and understanding the oxidative buffering capacity of the tissue after injury is likely to be important when considering possible treatment modalities. We expect, for example,

that glutathione synthase and glutathione will both be elevated after injury and that both of the drugs we use will cause additional increases early post-injury.

We have also noted that there are concerns with genetic manipulation and antibody blockade of the HO-1/Nrf2 pathway and that we chose multiple drugs to gain the most information feasible in a translational paradigm. However, we acknowledge that it is important to further elucidate the exact pathway mechanisms that occur after injury. Both Sulforaphane and Hemin have potential confounds with triggering alternative redox sensors or producing reactive oxygen species during their metabolism. The exact mechanism of drug targeting on Nrf2 is poorly understood and it would be helpful to track the translocation of Nrf2 into the nucleus both in TBI and in drug treated TBI. Further, the causative benefit of Nrf2 amplification may be better elucidated through the targeting of Keap1 or the transcriptional repressor Bach1 through alternative means and we are aware that recent effort has been made towards the development of selective Bach1 repressor agents (Gazaryan and Thomas, 2016).

When the project was started there were no other pharma agents identified as being more selective but recent presentations at the Society for Neuroscience national meeting have identified multiple groups interested in developing Nrf2 selective agents. This recent interest in Nrf2 agent development helps to explain why Nrf2 and HO-1 have lagged as potential therapeutic avenues compared to other transcription factors more heavily researched in TBI – that is to say, with no widely accepted selective agents currently available, rationalizing and securing heavy investment in projects focused on the topic has failed to materialize.

4.9.2 Pathway Manipulation Experiments

The current study examined a single dosing paradigm in order to contrast two drugs with drastically different kinetic profiles and metabolic properties. Future work should examine whether more aggressive dosing protocols would produce better outcomes and whether Hemin, or one of its metabolites, is responsible for increased HO-1 activation. Experiments performed by Dr. Dash have previously looked at Sulforaphane dosage schemes in a study of glutathione mediated TBI outcome effects and showed that a specific repeat dosing paradigm where animals were dosed 1 hour after injury and then repeat dosed 24 hours after injury resulted in behavioral improvements in the Morris water maze not seen with single dose paradigms at 6 or 24 hours singly (Dash et al., 2009). In our study, it appears that IP Hemin resulted in a dosing model with continued slow degradation of the largely insoluble compound, such that large, easily observed quantities were retained within the peritoneal cavity. This suggests that Hemin itself may not be entirely responsible for signaling in the brain – either an intermediary has been upregulated and altered brain gene expression or a more soluble form of Hemin or one of its metabolites might be responsible. This brings up an interesting question about the role of low molar concentrations of systemic bilirubin after injury.

4.9.3 Behavioral Outcomes

We used only a small number of behavioral tests and found that there were interesting results with both pharmacologic agents used. Behavioral recovery after TBI, however, has can be assessed with a wide range of possible tests, each of which can be used to better elucidate specific functional changes during the recovery process. The current study only examined rats through 15d post injury and it is possible that, while heme pathology plays a role in reducing

rodent behavioral outcomes during this time, it may not continue to be effective at longer post-injury time points. The underlying premise is that early treatment and resolution of a critical aspect of injury pathobiology (heme accumulation) will result in long term outcome benefits. This was examined here only through 15d. The current data shows that many of the metrics directly tied to heme processing have converged to control levels by day 15 post-injury so the expectation would be that any improvement achieved by that point would persist through longer survival periods.

It is also possible that our behavioral testing onset at 1d post-injury induced early stress in the animals, exacerbating heme-related injury via increased blood pressure and/or anxiety. Testing the animals after a day or two delay post-injury might ameliorate these effects. Alternatively, pre-training the animals on the behavioral tests may remove the 'test-learning' aspect of the assay making the rotarod and Morris water maze metrics a better measure of long-term memory and long-term cortical function. Further, expanding the assessment of drug effects on memory could include reversal goal testing in the water maze, which would determine the effects of heme pathway manipulation on the process of extinguishing memory and re-learning the task. Lastly, it may be of interest to include a behavioral measurement of anxiety during testing. It was observed several times that the SFN treated animals occasionally exhibited behavior that could be associated with increased anxiety and it would be helpful to know if there has been some anxiogenic effect or if the observations are driven by slightly altered functional recovery.

4.10 Final Remarks

Traumatic brain injury has long resisted effective post-injury treatment paradigms. As a result of being a constellation of tissue pathology that is produced by dissipation of energy inside the cranium, from seemingly any source, it is a widely multimodal injury that can take innumerous forms. In the course of this thesis we have attempted to carve out greater knowledge in a narrowly defined paradigm that allows for effective experimentation with the hope that some of the information may prove to be generalizable for a heterogeneous population of TBI victims. It appears from our findings that the hemorrhagic injury response occurring after TBI may be generalizable to classically non-hemorrhagic tissues, and it appears that treating this response can be beneficial for behavioral outcome, even in tests that assay protection linked to these same injured tissues that typically lack hemorrhage. This suggests that further studies of the underlying heme degradation process response or therapeutic intervention targeting HO-1/Nrf2 appear to be warranted. The evidence shows that it may be possible to enact a treatment protocol in a critical window that exists at least through 1 hour post-injury.

5 List of References

Abstracts from the 34(th) annual national neurotrauma symposium june 26-29, 2016 lexington, kentucky. (2016) J Neurotrauma (United States) 33:A1-A139.

Adams JH, Graham DI, Gennarelli TA, Maxwell WL (1991) Diffuse axonal injury in non-missile head injury. J Neurol Neurosurg Psychiatry (ENGLAND) 54:481-483.

Adams JH, Graham DI, Murray LS, Scott G (1982) Diffuse axonal injury due to nonmissile head injury in humans: An analysis of 45 cases. Ann Neurol (UNITED STATES) 12:557-563.

Adams JH, Doyle D, Ford I, Gennarelli TA, Graham DI, McLellan DR (1989) Diffuse axonal injury in head injury: Definition, diagnosis and grading. Histopathology (ENGLAND) 15:49-59.

Adams JH, Doyle D, Graham DI, Lawrence AE, McLellan DR, Gennarelli TA, Pastuszko M, Sakamoto T (1985) The contusion index: A reappraisal in human and experimental non-missile head injury. Neuropathol Appl Neurobiol (ENGLAND) 11:299-308.

Ahuja M, Ammal-Kaidery N, Morgan J, Igarashi K, Attucks OC (2016) Preclinical validation of Bach1 inhibition for the development of parkinson's disease therapy.

Alam J (1994) Multiple elements within the 5' distal enhancer of the mouse heme oxygenase-1 gene mediate induction by heavy metals. J Biol Chem (UNITED STATES) 269:25049-25056.

Alam J, Cook JL (2003) Transcriptional regulation of the heme oxygenase-1 gene via the stress response element pathway. Curr Pharm Des (Netherlands) 9:2499-2511.

Alam J, Den Z (1992) Distal AP-1 binding sites mediate basal level enhancement and TPA induction of the mouse heme oxygenase-1 gene. J Biol Chem (UNITED STATES) 267:21894-21900.

Alam J, Camhi S, Choi AM (1995) Identification of a second region upstream of the mouse heme oxygenase-1 gene that functions as a basal level and inducer-dependent transcription enhancer. J Biol Chem (UNITED STATES) 270:11977-11984.

Alam J, Cai J, Smith A (1994) Isolation and characterization of the mouse heme oxygenase-1 gene. distal 5' sequences are required for induction by heme or heavy metals. J Biol Chem (UNITED STATES) 269:1001-1009.

Alam J, Shibahara S, Smith A (1989) Transcriptional activation of the heme oxygenase gene by heme and cadmium in mouse hepatoma cells. J Biol Chem (UNITED STATES) 264:6371-6375.

Alam J, Wicks C, Stewart D, Gong P, Touchard C, Otterbein S, Choi AM, Burow ME, Tou J (2000) Mechanism of heme oxygenase-1 gene activation by cadmium in MCF-7 mammary

epithelial cells. role of p38 kinase and Nrf2 transcription factor. J Biol Chem (UNITED STATES) 275:27694-27702.

Albert-Weissenberger C, Siren AL (2010) Experimental traumatic brain injury. Exp Transl Stroke Med (England) 2:16-7378-2-16.

Alfieri A, Srivastava S, Siow RC, Cash D, Modo M, Duchen MR, Fraser PA, Williams SC, Mann GE (2013) Sulforaphane preconditioning of the Nrf2/HO-1 defense pathway protects the cerebral vasculature against blood-brain barrier disruption and neurological deficits in stroke. Free Radic Biol Med (United States) 65:1012-1022.

Andriessen TMJC, Jacobs B, Vos PE (2010) Clinical characteristics and pathophysiological mechanisms of focal and diffuse traumatic brain injury. 14:2381-2392.

Annabi B, Rojas-Sutterlin S, Laroche M, Lachambre MP, Moumdjian R, Beliveau R (2008) The diet-derived sulforaphane inhibits matrix metalloproteinase-9-activated human brain microvascular endothelial cell migration and tubulogenesis. Mol Nutr Food Res (Germany) 52:692-700.

Annegers JF, Hauser WA, Coan SP, Rocca WA (1998) A population-based study of seizures after traumatic brain injuries. 338:20-24.

Asahi M, Asahi K, Jung JC, del Zoppo GJ, Fini ME, Lo EH (2000a) Role for matrix metalloproteinase 9 after focal cerebral ischemia: Effects of gene knockout and enzyme inhibition with BB-94. J Cereb Blood Flow Metab (United States) 20:1681-1689.

Asahi M, Sumii T, Fini ME, Itohara S, Lo EH (2001) Matrix metalloproteinase 2 gene knockout has no effect on acute brain injury after focal ischemia. 12:3003-3007.

Asahi M, Asahi K, Jung J, del Zoppo GJ, Fini ME, Lo EH (2000b) Role for matrix metalloproteinase 9 after focal cerebral ischemia: Effects of gene knockout and enzyme inhibition with BB-94. 1681-1689.

Asahina M, Yoshiyama Y, Hattori T (2001) Expression of matrix metalloproteinase-9 and urinary-type plasminogen activator in alzheimer's disease brain. Clin Neuropathol (Germany) 20:60-63.

Asikainen I, Kaste M, Sarna S (1998) Predicting late outcome for patients with traumatic brain injury referred to a rehabilitation programme: A study of 508 finnish patients 5 years or more after injury. 12:95-107.

Ayoub AE, Cai TQ, Kaplan RA, Luo J (2005) Developmental expression of matrix metalloproteinases 2 and 9 and their potential role in the histogenesis of the cerebellar cortex. J Comp Neurol (United States) 481:403-415.

Baker AH (2002) Metalloproteinase inhibitors: Biological actions and therapeutic opportunities. 115:3719-3727.

Bales JW, Wagner AK, Kline AE, Dixon CE (2009) Persistent cognitive dysfunction after traumatic brain injury: A dopamine hypothesis. Neuroscience & Biobehavioral Reviews 33:981-1003.

Balogun E, Hoque M, Gong P, Killeen E, Green CJ, Foresti R, Alam J, Motterlini R (2003) Curcumin activates the haem oxygenase-1 gene via regulation of Nrf2 and the antioxidant-responsive element. Biochem J (England) 371:887-895.

Baranova AI, Wei EP, Ueda Y, Sholley MM, Kontos HA, Povlishock JT (2008) Cerebral vascular responsiveness after experimental traumatic brain injury: The beneficial effects of delayed hypothermia combined with superoxide dismutase administration. J Neurosurg (United States) 109:502-509.

Barnett SC (2004) Olfactory ensheathing cells: Unique glial cell types? 21:375-382.

Barone E, Di Domenico F, Butterfield DA (2014) Statins more than cholesterol lowering agents in alzheimer disease: Their pleiotropic functions as potential therapeutic targets. Biochem Pharmacol (England) 88:605-616.

Barros CS, Franco SJ, Muller U (2011) Extracellular matrix: Functions in the nervous system. Cold Spring Harb Perspect Biol (United States) 3:a005108.

Bartfai T, Sanchez-Alavez M, Andell-Jonsson S, Schultzberg M, Vezzani A, Danielsson E, Conti B (2007) Interleukin-1 system in CNS stress: Seizures, fever, and neurotrauma. Ann N Y Acad Sci (United States) 1113:173-177.

Bartnik-Olson BL, Holshouser B, Wang H, Grube M, Tong K, Wong V, Ashwal S (2014) Impaired neurovascular unit function contributes to persistent symptoms after concussion: A pilot study. J Neurotrauma (United States) 31:1497-1506.

Bashir S, Vernet M, Yoo WK, Mizrahi I, Theoret H, Pascual-Leone A (2012) Changes in cortical plasticity after mild traumatic brain injury. Restor Neurol Neurosci (Netherlands) 30:277-282.

Becker JW, Marcy AI, Rokosz LL, Axel MG, Burbaum JJ, Fitzgerald PMD, Cameron PM, Esser CK, Hagmann WK, Hermes JD, Springer JP (1995) Stromelysin-1: Three-dimensional structure of the inhibited catalytic domain and of the C-truncated proenzyme. 4:1966-1976.

Bellander BM, Singhrao SK, Ohlsson M, Mattsson P, Svensson M (2001) Complement activation in the human brain after traumatic head injury. J Neurotrauma (United States) 18:1295-1311.

Benedictus MR, Spikman JM, van der Naalt J (2010) Cognitive and behavioral impairment in traumatic brain injury related to outcome and return to work. 91:1436-1441.

Bessis A, Bechade C, Bernard D, Roumier A (2007) Microglial control of neuronal death and synaptic properties. Glia (United States) 55:233-238.

Bhardwaj M, Deshmukh R, Kaundal M, Krishna Reddy BV (2016) Pharmacological induction of hemeoxygenase-1 activity attenuates intracerebroventricular streptozotocin induced neurocognitive deficit and oxidative stress in rats. Eur J Pharmacol (Netherlands) 772:43-50.

Bhardwaj RD, Curtis MA, Spalding KL, Buchholz BA, Fink D, Bjork-Eriksson T, Nordborg C, Gage FH, Druid H, Eriksson PS, Frisen J (2006) Neocortical neurogenesis in humans is restricted to development. Proc Natl Acad Sci U S A (United States) 103:12564-12568.

Bilimoria PM, Stevens B (2015) Microglia function during brain development: New insights from animal models. Brain Res 1617:7-17.

Blinzinger K, Kreutzberg G (1968) Displacement of synaptic terminals from regenerating motoneurons by microglial cells. Cell Tissue Res 85:145-157.

Bliss TV, Lomo T (1973) Long-lasting potentiation of synaptic transmission in the dentate area of the anaesthetized rabbit following stimulation of the perforant path. J Physiol (England) 232:331-356.

Block ML, Hong JS (2007) Chronic microglial activation and progressive dopaminergic neurotoxicity. Biochem Soc Trans (England) 35:1127-1132.

Block ML, Hong JS (2005) Microglia and inflammation-mediated neurodegeneration: Multiple triggers with a common mechanism. Prog Neurobiol (England) 76:77-98.

Bolisetty S, Zarjou A, Agarwal A (2017) Heme oxygenase 1 as a therapeutic target in acute kidney injury. Am J Kidney Dis (United States) 69:531-545.

Borger DR, Essig DA (1998) Induction of HSP 32 gene in hypoxic cardiomyocytes is attenuated by treatment with N-acetyl-L-cysteine. Am J Physiol (UNITED STATES) 274:H965-73.

Bower JH, Maraganore DM, Peterson BJ, McDonnell SK, Ahlskog JE, Rocca WA (2003) Head trauma preceding PD: A case-control study. Neurology (United States) 60:1610-1615.

Bozdagi O, Nagy V, Kwei KT, Huntley GW (2007) In vivo roles for matrix metalloproteinase-9 in mature hippocampal synaptic physiology and plasticity. 98:334-344.

Breder C, Dinarello C, Saper C (1988) Interleukin-1 immunoreactive innervation of the human hypothalamus. 240:321-324.

Browne KD, Chen X, Meaney DF, Smith DH (2011) Mild traumatic brain injury and diffuse axonal injury in swine. 28:1747-1755.

Büki A, Povlishock J (2006) All roads lead to disconnection?–Traumatic axonal injury revisited. Acta Neurochir 148:181-194.

Buki A, Okonkwo DO, Wang KK, Povlishock JT (2000) Cytochrome c release and caspase activation in traumatic axonal injury. J Neurosci (United States) 20:2825-2834.

Buki A, Siman R, Trojanowski JQ, Povlishock JT (1999) The role of calpain-mediated spectrin proteolysis in traumatically induced axonal injury. J Neuropathol Exp Neurol (England) 58:365-375.

Bullock R, Zauner A, Woodward JJ, Myseros J, Choi SC, Ward JD, Marmarou A, Young HF (1998) Factors affecting excitatory amino acid release following severe human head injury. 89:507-518.

Bye N, Carron S, Han X, Agyapomaa D, Ng SY, Yan E, Rosenfeld JV, Morganti-Kossmann MC (2011) Neurogenesis and glial proliferation are stimulated following diffuse traumatic brain injury in adult rats. 89:986-1000.

Camhi SL, Alam J, Otterbein L, Sylvester SL, Choi AM (1995) Induction of heme oxygenase-1 gene expression by lipopolysaccharide is mediated by AP-1 activation. Am J Respir Cell Mol Biol (UNITED STATES) 13:387-398.

Cao S, Zheng M, Hua Y, Chen G, Keep RF, Xi G (2016) Hematoma changes during clot resolution after experimental intracerebral hemorrhage. Stroke (United States) 47:1626-1631.

Carreno-Velazquez T, Beswick P, Wahab B, Atack J (2016) A structure-based approach to identifying novel modulators of the Nrf2 transcription pathway.

Castellani R, Smith MA, Richey PL, Perry G (1996) Glycoxidation and oxidative stress in parkinson disease and diffuse lewy body disease. Brain Res (NETHERLANDS) 737:195-200.

Cederberg D, SiesjÃ¶ P (2009) What has inflammation to do with traumatic brain injury? 26:221-226.

Chakraborti S, Mandal M, Das S, Mandal A, Chakraborti T (2003) Regulation of matrix metalloproteinases: An overview. Mol Cell Biochem (Netherlands) 253:269-285.

Chamak B, Dobbertin A, Mallat M (1995) Immunohistochemical detection of thrombospondin in microglia in the developing rat brain. 69:177-187.

Chan JL, Reeves TM, Phillips LL (2014) Osteopontin expression in acute immune response mediates hippocampal synaptogenesis and adaptive outcome following cortical brain injury. Exp Neurol (United States) 261:757-771.

Chang EF, Claus CP, Vreman HJ, Wong RJ, Noble-Haeusslein LJ (2005) Heme regulation in traumatic brain injury: Relevance to the adult and developing brain. J Cereb Blood Flow Metab (United States) 25:1401-1417.

Chang EF, Wong RJ, Vreman HJ, Igarashi T, Galo E, Sharp FR, Stevenson DK, Noble-Haeusslein LJ (2003) Heme oxygenase-2 protects against lipid peroxidation-mediated cell loss and impaired motor recovery after traumatic brain injury. J Neurosci (United States) 23:3689-3696.

Chao CC, Hu S, Molitor TW, Shaskan EG, Peterson PK (1992) Activated microglia mediate neuronal cell injury via a nitric oxide mechanism. J Immunol (United States) 149:2736-2741.

Chattarji S (2011) Lipocalin comes callin' on the hippocampus. Proc Natl Acad Sci U S A (United States) 108:18197-18198.

Chen HW, Chao CY, Lin LL, Lu CY, Liu KL, Lii CK, Li CC (2013) Inhibition of matrix metalloproteinase-9 expression by docosahexaenoic acid mediated by heme oxygenase 1 in 12-O-tetradecanoylphorbol-13-acetate-induced MCF-7 human breast cancer cells. Arch Toxicol (Germany) 87:857-869.

Cheng JP, Hoffman AN, Zafonte RD, Kline AE (2008) A delayed and chronic treatment regimen with the 5-HT1A receptor agonist 8-OH-DPAT after cortical impact injury facilitates motor recovery and acquisition of spatial learning. Behav Brain Res (Netherlands) 194:79-85.

Chen-Roetling J, Lu X, Regan RF (2015) Targeting heme oxygenase after intracerebral hemorrhage. Ther Targets Neurol Dis (United States) 2:474.

Cherian L, Goodman JC, Robertson C (2011) Improved cerebrovascular function and reduced histological damage with darbepoietin alfa administration after cortical impact injury in rats. J Pharmacol Exp Ther (United States) 337:451-456.

Chiara Ricciardi M, Bokkers RP, Butman JA, Hammoud DA, Pham DL, Warach S, Latour LL (2017) Trauma-specific brain abnormalities in suspected mild traumatic brain injury patients identified in the first 48 hours after injury: A blinded magnetic resonance imaging comparative study including suspected acute minor stroke patients. J Neurotrauma (United States) 34:23-30.

Chodobski A, Zink BJ, Szmydynger-Chodobska J (2011) Blood-brain barrier pathophysiology in traumatic brain injury. Transl Stroke Res (United States) 2:492-516.

Christman CW, Salvant Jr. JB, Walker SA, Povlishock JT (1997) Characterization of a prolonged regenerative attempt by diffusely injured axons following traumatic brain injury in adult cat: A light and electron microscopic immunocytochemical study. 94:329-337.

Christopherson KS, Ullian EM, Stokes CCA, Mullowney CE, Hell JW, Agah A, Lawler J, Mosher DF, Bornstein P, Barres BA (2005) Thrombospondins are astrocyte-secreted proteins that promote CNS synaptogenesis. 120:421-433.

Cirstea MC, Levin MF (2000) Compensatory strategies for reaching in stroke. Brain (England) 123 (Pt 5):940-953.

Clark AW, Krekoski CA, Bou S, Chapman KR, Edwards DR (1997) Increased gelatinase A (MMP-2) and gelatinase B (MMP-9) activities in human brain after focal ischemia. 238:53-56.

Cobbs CS, Fenoy A, Bredt DS, Noble LJ (1997) Expression of nitric oxide synthase in the cerebral microvasculature after traumatic brain injury in the rat. 751:336-338.

Coburn K (1992) Traumatic brain injury: The silent epidemic. AACN Clin Issues Crit Care Nurs (United States) 3:9-18.

Colton CA, Wilcock DM (2010) Assessing activation states in microglia. CNS & Neurological Disorders-Drug Targets (Formerly Current Drug Targets-CNS & Neurological Disorders) 9:174-191.

Colton CA (2009) Heterogeneity of microglial activation in the innate immune response in the brain. J Neuroimmune Pharmacol (United States) 4:399-418.

Conant K, Gottschall PE (2005) Matrix metalloproteinases in the central nervous system.

Conti AC, Raghupathi R, Trojanowski JQ, McIntosh TK (1998) Experimental brain injury induces regionally distinct apoptosis during the acute and delayed post-traumatic period. J Neurosci (United States) 18:5663-5672.

Coronado VG, Xu L, Basavaraju SV, McGuire LC, Wald MM, Faul MD, Guzman BR, Hemphill JD, Centers for Disease Control and Prevention (CDC) (2011) Surveillance for traumatic brain injury-related deaths--united states, 1997-2007. MMWR Surveill Summ (United States) 60:1-32.

Coronado VG, McGuire LC, Sarmiento K, Bell J, Lionbarger MR, Jones CD, Geller AI, Khoury N, Xu L (2014) Corrigendum to â€œTrends in traumatic brain injury in the U.S. and the public health response: 1995â€“2009 â˜†â€• [J. saf. res. 43 (2012) 299-307]. 48:117.

Correale J (2014) The role of microglial activation in disease progression. Mult Scler (England) 20:1288-1295.

Correale J, Villa A (2004) The neuroprotective role of inflammation in nervous system injuries. 251:1304-1316.

Cotman C (1999) Axon sprouting and regeneration. In: Basic neurochemistry: Molecular, cellular and medical aspects (Siegel G, Agranoff B, Albers R, eds), ppChapter 29. Philadelphia: Lippincott-Raven.

Cotman C, Gentry C, Steward O (1977) Synaptic replacement in the dentate gyrus after unilateral entorhinal lesion: Electron microscopic analysis of the extent of replacement of synapses by the remaining entorhinal cortex. 6:455-464.

Cramer SC, Nelles G, Benson RR, Kaplan JD, Parker RA, Kwong KK, Kennedy DN, Finklestein SP, Rosen BR (1997) A functional MRI study of subjects recovered from hemiparetic stroke. Stroke (United States) 28:2518-2527.

Cruse I, Maines MD (1988) Evidence suggesting that the two forms of heme oxygenase are products of different genes. J Biol Chem (UNITED STATES) 263:3348-3353.

Cuadrado A, Rojo AI (2008) Heme oxygenase-1 as a therapeutic target in neurodegenerative diseases and brain infections. Curr Pharm Des (Netherlands) 14:429-442.

D'Amato CJ, Hicks SP (1978) Normal development and post-traumatic plasticity of corticospinal neurons in rats. Exp Neurol (United States) 60:557-569.

Dash PK, Mach SA, Moore AN (2001) Enhanced neurogenesis in the rodent hippocampus following traumatic brain injury. 63:313-319.

Dash PK, Zhao J, Orsi SA, Zhang M, Moore AN (2009) Sulforaphane improves cognitive function administered following traumatic brain injury. Neurosci Lett (Ireland) 460:103-107.

del Zoppo GJ, Hallenbeck JM (2000) Advances in the vascular pathophysiology of ischemic stroke. Thromb Res (UNITED STATES) 98:73-81.

Deller T, Del Turco D, Rappert A, Bechmann I (2007) Structural reorganization of the dentate gyrus following entorhinal denervation: Species differences between rat and mouse. 501-528.

Demestre M, Wells GM, Miller KM, Smith KJ, Hughes RAC, Gearing AJ, Gregson NA (2004) Characterisation of matrix metalloproteinases and the effects of a broad-spectrum inhibitor (BB-1101) in peripheral nerve regeneration. 124:767-779.

DeWitt DS, Prough DS (2003) Traumatic cerebral vascular injury: The effects of concussive brain injury on the cerebral vasculature. J Neurotrauma (United States) 20:795-825.

Dietrich WD, Alonso O, Halley M (1994) Early microvascular and neuronal consequences of traumatic brain injury: A light and electron microscopic study in rats. 11:289-301.

Ding JY, Kreipke CW, Schafer P, Schafer S, Speirs SL, Rafols JA (2009) Synapse loss regulated by matrix metalloproteinases in traumatic brain injury is associated with hypoxia inducible factor-1alpha expression. Brain Res (Netherlands) 1268:125-134.

Dinkova-Kostova AT, Holtzclaw WD, Cole RN, Itoh K, Wakabayashi N, Katoh Y, Yamamoto M, Talalay P (2002) Direct evidence that sulfhydryl groups of Keap1 are the sensors regulating induction of phase 2 enzymes that protect against carcinogens and oxidants. Proc Natl Acad Sci U S A (United States) 99:11908-11913.

Dityatev A, Schachner M (2003) Extracellular matrix molecules and synaptic plasticity. 4:456-468.

Dixon CE, Clifton GL, Lighthall JW, Yaghmai AA, Hayes RL (1991) A controlled cortical impact model of traumatic brain injury in the rat. J Neurosci Methods (Netherlands) 39:253-262.

Dixon CE, Kraus MF, Kline AE, Ma X, Yan HQ, Griffith RG, Wolfson BM, Marion DW (1999) Amantadine improves water maze performance without affecting motor behavior following traumatic brain injury in rats. Restor Neurol Neurosci (Netherlands) 14:285-294.

Dixon CE, Lyeth BG, Povlishock JT, Findling RL, Hamm RJ, Marmarou A, Young HF, Hayes RL (1987) A fluid percussion model of experimental brain injury in the rat. J Neurosurg (UNITED STATES) 67:110-119.

Du C, Hu R, Csernansky CA, Hsu CY, Choi DW (1996) Very delayed infarction after mild focal cerebral ischemia: A role for apoptosis? 195-201.

Duong TD, Erickson CA (2003) MMP-2 plays an essential role in producing epithelial-mesenchymal transformations in the avian embryo. 229:42-53.

Durante W, Peyton KJ, Schafer AI (1999) Platelet-derived growth factor stimulates heme oxygenase-1 gene expression and carbon monoxide production in vascular smooth muscle cells. Arterioscler Thromb Vasc Biol (UNITED STATES) 19:2666-2672.

Dwivedi S, Rajasekar N, Hanif K, Nath C, Shukla R (2016) Sulforaphane ameliorates okadaic acid-induced memory impairment in rats by activating the Nrf2/HO-1 antioxidant pathway. Mol Neurobiol (United States) 53:5310-5323.

Dziembowska M, Wlodarczyk J (2012) MMP9: A novel function in synaptic plasticity. 44:709-713.

Eichenbaum H, Yonelinas AP, Ranganath C (2007) The medial temporal lobe and recognition memory. Annu Rev Neurosci (United States) 30:123-152.

Ek CJ, Dziegielewska KM, Stolp H, Saunders NR (2006) Functional effectiveness of the blood-brain barrier to small water-soluble molecules in developing and adult opossum (monodelphis domestica). 496:13-26.

Ek CJ, Habgood MD, Dziegielewska KM, Saunders NR (2003) Structural characteristics and barrier properties of the choroid plexuses in developing brain of the opossum (monodelphis domestica). 460:451-464.

Ekdahl CT, Kokaia Z, Lindvall O (2009) Brain inflammation and adult neurogenesis: The dual role of microglia. 158:1021-1029.

Elbirt KK, Whitmarsh AJ, Davis RJ, Bonkovsky HL (1998) Mechanism of sodium arsenite-mediated induction of heme oxygenase-1 in hepatoma cells. role of mitogen-activated protein kinases. J Biol Chem (UNITED STATES) 273:8922-8931.

Emery DL, Fulp CT, Saatman KE, SchÃ¼tz C, Neugebauer E, McIntosh TK (2005) Newly born granule cells in the dentate gyrus rapidly extend axons into the hippocampal CA3 region following experimental brain injury. 22:978-988.

Erb DE, Povlishock JT (1991) Neuroplasticity following traumatic brain injury: A study of GABAergic terminal loss and recovery in the cat dorsal lateral vestibular nucleus. 83:.

Ethell IM, Ethell DW (2007) Matrix metalloproteinases in brain development and remodeling: Synaptic functions and targets. 85:2813-2823.

Ewing JF, Maines MD (1993) Glutathione depletion induces heme oxygenase-1 (HSP32) mRNA and protein in rat brain. J Neurochem (UNITED STATES) 60:1512-1519.

Faden A, Demediuk P, Panter S, Vink R (1989) The role of excitatory amino acids and NMDA receptors in traumatic brain injury. 244:798-800.

Falo MC, Fillmore HL, Reeves TM, Phillips LL (2006) Matrix metalloproteinase-3 expression profile differentiates adaptive and maladaptive synaptic plasticity induced by traumatic brain injury. 84:768-781.

Falo MC, Reeves TM, Phillips LL (2008) Agrin expression during synaptogenesis induced by traumatic brain injury. 25:769-783.

Farkas O, Povlishock JT (2007) Cellular and subcellular change evoked by diffuse traumatic brain injury: A complex web of change extending far beyond focal damage. Prog Brain Res 161:43-59.

Farkas O (2006) Mechanoporation induced by diffuse traumatic brain injury: An irreversible or reversible response to injury? 26:3130-3140.

Fauconneau B, Petegnief V, Sanfeliu C, Piriou A, Planas AM (2002) Induction of heat shock proteins (HSPs) by sodium arsenite in cultured astrocytes and reduction of hydrogen peroxide-induced cell death. J Neurochem (England) 83:1338-1348.

Faul MD, Xu L, Wald MM, Coronado VG (2010) Traumatic brain injury in the united states: Emergency department visits, hospitalizations and deaths 2002-2006. (Atlanta,(GA)) .

Favatier F, Polla BS (2001) Tobacco-smoke-inducible human haem oxygenase-1 gene expression: Role of distinct transcription factors and reactive oxygen intermediates. Biochem J (England) 353:475-482.

Ferguson PL, Smith GM, Wannamaker BB, Thurman DJ, Pickelsimer EE, Selassie AW (2009) A population-based study of risk of epilepsy after hospitalization for traumatic brain injury. 51:891-898.

Ferreira AC, Pinto V, Da Mesquita S, Novais A, Sousa JC, Correia-Neves M, Sousa N, Palha JA, Marques F (2013) Lipocalin-2 is involved in emotional behaviors and cognitive function. Front Cell Neurosci (Switzerland) 7:122.

Finkelstein EA, Corso PS, Miller TR (2006) The burden of injuries. 160-174.

Fiske B, Brunjes P (2000) Microglial activation in the developing rat olfactory bulb. Neuroscience 96:807-815.

Fleminger S (2003) Head injury as a risk factor for alzheimer's disease: The evidence 10 years on; a partial replication. 74:857-862.

Flower DR (1996) The lipocalin protein family: Structure and function. Biochem J (ENGLAND) 318 (Pt 1):1-14.

Fluiter K, Opperhuizen AL, Morgan BP, Baas F, Ramaglia V (2014) Inhibition of the membrane attack complex of the complement system reduces secondary neuroaxonal loss and promotes neurologic recovery after traumatic brain injury in mice. J Immunol (United States) 192:2339-2348.

Foda MA, Marmarou A (1994) A new model of diffuse brain injury in rats. part II: Morphological characterization. J Neurosurg (United States) 80:301-313.

Foresti R, Clark JE, Green CJ, Motterlini R (1997) Thiol compounds interact with nitric oxide in regulating heme oxygenase-1 induction in endothelial cells. involvement of superoxide and peroxynitrite anions. J Biol Chem (UNITED STATES) 272:18411-18417.

Foresti R, Sarathchandra P, Clark JE, Green CJ, Motterlini R (1999) Peroxynitrite induces haem oxygenase-1 in vascular endothelial cells: A link to apoptosis. Biochem J (ENGLAND) 339 (Pt 3):729-736.

Fredrich M, Illing R (2010) MMP-2 is involved in synaptic remodeling after cochlear lesion. 21:324-327.

Frey LC (2003) Epidemiology of posttraumatic epilepsy: A critical review. 44:11-17.

Frotscher M, Heimrich B, Deller T (1997) Sprouting in the hippocampus is layer-specific. 20:218-223.

Frugier T, Morganti-Kossmann MC, O'Reilly D, McLean CA (2010) In situ detection of inflammatory mediators in post mortem human brain tissue after traumatic injury. 27:497-507.

Fukuda K, Panter SS, Sharp FR, Noble LJ (1995) Induction of heme oxygenase-1 (HO-1) after traumatic brain injury in the rat. Neurosci Lett (IRELAND) 199:127-130.

Fukuda K, Richmon JD, Sato M, Sharp FR, Panter SS, Noble LJ (1996) Induction of heme oxygenase-1 (HO-1) in glia after traumatic brain injury. Brain Res (NETHERLANDS) 736:68-75.

Gao G, Oda Y, Wei EP, Povlishock JT (2010) The adverse pial arteriolar and axonal consequences of traumatic brain injury complicated by hypoxia and their therapeutic modulation with hypothermia in rat. J Cereb Blood Flow Metab (United States) 30:628-637.

Gasche Y, Fujimura M, Morita-Fujimura Y, Copin J, Kawase M, Massengale J, Chan PH (1999) Early appearance of activated matrix metalloproteinase-9 after focal cerebral ischemia in mice: A possible role in blood-brain barrier dysfunction. 1020-1028.

Gazaryan IG, Thomas B (2016) The status of Nrf2-based therapeutics: Current perspectives and future prospects. Neural Regen Res (India) 11:1708-1711.

Gennarelli TA, Thibault LE, Adams JH, Graham DI, Thompson CJ, Marcincin RP (1982) Diffuse axonal injury and traumatic coma in the primate. 12:564-574.

Geurts N, Martens E, Van Aelst I, Proost P, Opdenakker G, Van den Steen PE (2008) Beta-hematin interaction with the hemopexin domain of gelatinase B/MMP-9 provokes autocatalytic processing of the propeptide, thereby priming activation by MMP-3. Biochemistry (United States) 47:2689-2699.

Gidday JM (2005) Leukocyte-derived matrix metalloproteinase-9 mediates blood-brain barrier breakdown and is proinflammatory after transient focal cerebral ischemia. 289:H558-H568.

Giraudon P, Buart S, Bernard A, Belin M (1997) Cytokines secreted by glial cells infected with HTLV-I modulate the expression of matrix metalloproteinases (MMPs) and their natural inhibitor (TIMPs): Possible involvement in neurodegenerative processes. 2:107-110.

Girolamo F, Virgintino D, Errede M, Capobianco C, Bernardini N, Bertossi M, Roncali L (2004) Involvement of metalloprotease-2 in the development of human brain microvessels. 122:261-270.

Giulian D, Chen J, Ingeman JE, George JK, Noponen M (1989) The role of mononuclear phagocytes in wound healing after traumatic injury to adult mammalian brain. J Neurosci (United States) 9:4416-4429.

Goldman SM, Tanner CM, Oakes D, Bhudhikanok GS, Gupta A, Langston JW (2006) Head injury and parkinson's disease risk in twins. Ann Neurol (United States) 60:65-72.

Goldstein LE, McKee AC (2012) Response to comment on "chronic traumatic encephalopathy in blast-exposed military veterans and a blast neurotrauma mouse model". 4:157lr5-157lr5.

Goldstein M (1990) Traumatic brain injury: A silent epidemic. 27:327-327.

Gong Q, Hart BA (1997) Effect of thiols on cadmium-induced expression of metallothionein and other oxidant stress genes in rat lung epithelial cells. Toxicology (IRELAND) 119:179-191.

Gonthier B, Koncina E, Satkauskas S, Perraut M, Roussel G, Aunis D, Kapfhammer JP, Bagnard D (2009) A PKC-dependent recruitment of MMP-2 controls semaphorin-3A growth-promoting effect in cortical dendrites. 4:e5099.

Goodman DC, Horel JA (1966) Sprouting of optic tract projections in the brain stem of the rat. 127:71-88.

Gorman L, Fu K, Hovda D, Becker D, Katayama Y (1989) Analysis of acetylcholine release following concussive brain injury in the rat. J Neurotrauma 6:1-2.

Goss JR, O'Malley ME, Zou L, Styren SD, Kochanek PM, DeKosky ST (1998) Astrocytes are the major source of nerve growth factor upregulation following traumatic brain injury in the rat. 149:301-309.

Gottschall PE, Yu X, Bing B (1995) Increased production of gelatinase B (matrix metalloproteinase-9) and interleukin-6 by activated rat microglia in culture. 42:335-342.

Gottschall PE, Yu X (1995) Cytokines regulate gelatinase A and B (matrix metalloproteinase 2 and 9) activity in cultured rat astrocytes. 64:1513-1520.

Gould E (2007) How widespread is adult neurogenesis in mammals? 8:481-488.

Grady MS, Jane JA, Steward O (1989) Synaptic reorganization within the human central nervous system following injury. 71:534-537.

Graham DI, Adams JH, Nicoll JAR, Maxwell WL, Gennarelli TA (1995) The nature, distribution and causes of traumatic brain injury. 5:397-406.

Granacher RP (2008) Traumatic brain injury: Methods for clinical and forensic neuropsychiatric assessment. (FL, USA) .

Graves AB, White E, Koepsell TD, Reifler BV, Van Belle G, Larson EB, Raskind M (1990) A case-control study of alzheimer's disease. 28:766-774.

Gray J, McNaughton N (2003) The neuropsychology of anxiety: An enquiry into the function of the septo-hippocampal system. OUP Oxford.

Graziadei PP, Levine RR, Monti Graziadei GA (1979) Plasticity of connections of the olfactory sensory neuron: Regeneration into the forebrain following bulbectomy in the neonatal mouse. Neuroscience (United States) 4:713-727.

Graziadei PP, Levine RR, Graziadei GA (1978) Regeneration of olfactory axons and synapse formation in the forebrain after bulbectomy in neonatal mice. Proc Natl Acad Sci U S A (United States) 75:5230-5234.

Greco T, Fiskum G (2010) Brain mitochondria from rats treated with sulforaphane are resistant to redox-regulated permeability transition. J Bioenerg Biomembr (United States) 42:491-497.

Greenwald BD, Kapoor N, Singh AD (2012) Visual impairments in the first year after traumatic brain injury. 26:1338-1359.

Gultekin SH, Smith TW (1994) Diffuse axonal injury in craniocerebral trauma. A comparative histologic and immunohistochemical study. Arch Pathol Lab Med (United States) 118:168-171.

Gursoy-Ozdemir Y, Qiu J, Matsuoka N, Bolay H, Bermpohl D, Jin H, Wang X, Rosenberg GA, Lo EH, Moskowitz MA (2004) Cortical spreading depression activates and upregulates MMP-9. 113:1447-1455.

Habgood MD, Bye N, Dziegielewska KM, Ek CJ, Lane MA, Potter A, Morganti-Kossmann C, Saunders NR (2007) Changes in blood-brain barrier permeability to large and small molecules following traumatic brain injury in mice. 25:231-238.

Halliwell B, Gutteridge JMC (1999) *Free radicals in biology and medicine*. Oxford, UK: Oxford Univ. Press.

Hamm RJ, O'Dell DM, Pike BR, Lyeth BG (1993) Cognitive impairment following traumatic brain injury: The effect of pre-and post-injury administration of scopolamine and MK-801. Cognitive Brain Research 1:223-226.

Hamm RJ, Pike BR, O'Dell DM, Lyeth BG, Jenkins LW (1994) The rotarod test: An evaluation of its effectiveness in assessing motor deficits following traumatic brain injury. J Neurotrauma (UNITED STATES) 11:187-196.

Handsley MM, Cross J, Gaviloric J, Edwards DR (2005) The matrix metalloproteinases and their inhibitors. In: Matrix metalloproteinases in the central nervous system (Conant K, Gottschall PE, eds), pp3. London: Imperial College Press.

Hanisch U (2002) Microglia as a source and target of cytokines. 40:140-155.

Harris JL, Reeves TM, Phillips LL (2011) Phosphacan and receptor protein tyrosine phosphatase beta expression mediates deafferentation-induced synaptogenesis. Hippocampus (United States) 21:81-92.

Harris NG, Mironova YA, Hovda DA, Sutton RL (2010) Chondroitinase ABC enhances pericontusion axonal sprouting but does not confer robust improvements in behavioral recovery. 27:1971-1982.

Hartsfield CL, Alam J, Cook JL, Choi AM (1997) Regulation of heme oxygenase-1 gene expression in vascular smooth muscle cells by nitric oxide. Am J Physiol (UNITED STATES) 273:L980-8.

Hayes RL, Jenkins LW, Lyeth BG (1992) Neurotransmitter-mediated mechanisms of traumatic brain injury: Acetylcholine and excitatory amino acids. J Neurotrauma (United States) 9 Suppl 1:S173-87.

Hayes RL, Stonnington HH, Lyeth BG, Dixon CE, Yamamoto T (1986) Metabolic and neurophysiologic sequelae of brain injury: A cholinergic hypothesis. Cent Nerv Syst Trauma (United States) 3:163-173.

He AW, Yang T, Chen SQ, Li ZP, Li HP, Huang WJ, Cheng JY, Zhang J, Yang P, Wang WT (2011) Effects of hemin on neuroglobin expression after cardiopulmonary resuscitation in rats. World J Emerg Med (China) 2:54-58.

Hebb DO (1950) Organization of behavior. new york: Wiley, 6:307-307.

Heo JH, Lucero J, Abumiya T, Koziol JA, Copeland BR, del Zoppo GJ (1999) Matrix metalloproteinases increase very early during experimental focal cerebral ischemia. 624-633.

Hernandez-Ontiveros DG, Tajiri N, Acosta S, Giunta B, Tan J, Borlongan CV (2013) Microglia activation as a biomarker for traumatic brain injury. Front Neurol (Switzerland) 4:30.

Herrmann JE, Imura T, Song B, Qi J, Ao Y, Nguyen TK, Korsak RA, Takeda K, Akira S, Sofroniew MV (2008) STAT3 is a critical regulator of astrogliosis and scar formation after spinal cord injury. J Neurosci (United States) 28:7231-7243.

Hicks R, Soares H, Smith D, McIntosh T (1996) Temporal and spatial characterization of neuronal injury following lateral fluid-percussion brain injury in the rat. 91:236-246.

Hill-Kapturczak N, Voakes C, Garcia J, Visner G, Nick HS, Agarwal A (2003) A cis-acting region regulates oxidized lipid-mediated induction of the human heme oxygenase-1 gene in endothelial cells. Arterioscler Thromb Vasc Biol (United States) 23:1416-1422.

Hofman FM (1989) Tumor necrosis factor identified in multiple sclerosis brain. 170:607-612.

Holmin S, Mathiesen T (1999) Long-term intracerebral inflammatory response after experimental focal brain injury in rat. Neuroreport (England) 10:1889-1891.

Hsu JY, McKeon R, Goussev S, Werb Z, Lee JU, Trivedi A, Noble-Haeusslein LJ (2006) Matrix metalloproteinase-2 facilitates wound healing events that promote functional recovery after spinal cord injury. J Neurosci (United States) 26:9841-9850.

Hsu JY, Bourguignon LY, Adams CM, Peyrollier K, Zhang H, Fandel T, Cun CL, Werb Z, Noble-Haeusslein LJ (2008) Matrix metalloproteinase-9 facilitates glial scar formation in the injured spinal cord. J Neurosci (United States) 28:13467-13477.

Hu C, Eggler AL, Mesecar AD, van Breemen RB (2011) Modification of keap1 cysteine residues by sulforaphane. Chem Res Toxicol (United States) 24:515-521.

Huang C, Sakry D, Menzel L, Dangel L, Sebastiani A, Kramer T, Karram K, Engelhard K, Trotter J, Schafer MK (2016) Lack of NG2 exacerbates neurological outcome and modulates glial responses after traumatic brain injury. Glia (United States) 64:507-523.

Huang FP, Xi G, Keep RF, Hua Y, Nemoianu A, Hoff JT (2002) Brain edema after experimental intracerebral hemorrhage: Role of hemoglobin degradation products. J Neurosurg (United States) 96:287-293.

Hughes EG, Elmariah SB, Balice-Gordon RJ (2010) Astrocyte secreted proteins selectively increase hippocampal GABAergic axon length, branching, and synaptogenesis. Molecular and Cellular Neuroscience 43:136-145.

Hulsebosch CE, DeWitt DS, Jenkins LW, Prough DS (1998) Traumatic brain injury in rats results in increased expression of gap-43 that correlates with behavioral recovery. 255:83-86.

Hyder AA, Wunderlich CA, Puvanachandra P, Gururaj G, Kobusingye OC (2007) The impact of traumatic brain injuries: A global perspective. NeuroRehabilitation (Netherlands) 22:341-353.

Hynes RO (1992) Integrins: Versatility, modulation, and signaling in cell adhesion. 69:11-25.

Ingraham CA, Park GC, Makarenkova HP, Crossin KL (2011) Matrix metalloproteinase (MMP)-9 induced by wnt signaling increases the proliferation and migration of embryonic neural stem cells at low O2 levels. 286:17649-17657.

Ishikawa K, Sato M, Yoshida T (1991) Expression of rat heme oxygenase in escherichia coli as a catalytically active, full-length form that binds to bacterial membranes. Eur J Biochem (GERMANY) 202:161-165.

Jaillard A, Martin CD, Garambois K, Lebas JF, Hommel M (2005) Vicarious function within the human primary motor cortex? A longitudinal fMRI stroke study. Brain (England) 128:1122-1138.

Janigro D, West GA, Nguyen TS, Winn HR (1994) Regulation of blood-brain barrier endothelial cells by nitric oxide. 75:528-538.

Jiang W, Desjardins P, Butterworth RF (2009) Minocycline attenuates oxidative/nitrosative stress and cerebral complications of acute liver failure in rats. Neurochem Int (England) 55:601-605.

Jin M, Kim JH, Jang E, Lee YM, Soo Han H, Woo DK, Park DH, Kook H, Suk K (2014) Lipocalin-2 deficiency attenuates neuroinflammation and brain injury after transient middle cerebral artery occlusion in mice. J Cereb Blood Flow Metab (United States) 34:1306-1314.

John GR, Lee SC, Brosnan CF (2003) Cytokines: Powerful regulators of glial cell activation. 9:10-22.

Jones LS (1996) Integrins: Possible functions in the adult CNS. 19:68-72.

Juliet PAR, Mao X, Del Bigio MR (2008) Proinflammatory cytokine production by cultured neonatal rat microglia after exposure to blood products. 1210:230-239.

Kandel E, Schwartz J, Jessell T, Siegelbaum S, Hudspeth A (2013) Principles of neural science. (USA) .

Katayama Y, Becker DP, Tamura T, Ikezaki K (1990) Early cellular swelling in experimental traumatic brain injury: A phenomenon mediated by excitatory amino acids. 271-273.

Katayama Y, Cheung MK, Alves A, Becker DP (1989) Ion fluxes and cell swelling in experimental traumatic brain injury: The role of excitatory amino acids. 584-588.

Kawashima A, Oda Y, Yachie A, Koizumi S, Nakanishi I (2002) Heme oxygenase-1 deficiency: The first autopsy case. Hum Pathol (United States) 33:125-130.

Kazanis I, ffrench-Constant C (2011) Extracellular matrix and the neural stem cell niche. Dev Neurobiol (United States) 71:1006-1017.

Kelley BJ, Farkas O, Lifshitz J, Povlishock JT (2006) Traumatic axonal injury in the perisomatic domain triggers ultrarapid secondary axotomy and wallerian degeneration. Exp Neurol 198:350-360.

Kelley BJ, Lifshitz J, Povlishock JT (2007) Neuroinflammatory responses after experimental diffuse traumatic brain injury. 66:989-1001.

Kenney K, Amyot F, Haber M, Pronger A, Bogoslovsky T, Moore C, Diaz-Arrastia R (2016) Cerebral vascular injury in traumatic brain injury. Exp Neurol 275:353-366.

Kenney K, Amyot F, Haber M, Pronger A, Bogoslovsky T, Moore C, Diaz-Arrastia R (2015) Cerebral vascular injury in traumatic brain injury. Exp Neurol .

Kernie SG, Erwin TM, Parada LF (2001) Brain remodeling due to neuronal and astrocytic proliferation after controlled cortical injury in mice. 66:317-326.

Kettenmann H, Kirchhoff F, Verkhratsky A (2013) Microglia: New roles for the synaptic stripper. Neuron 77:10-18.

Keyse SM, Applegate LA, Tromvoukis Y, Tyrrell RM (1990) Oxidant stress leads to transcriptional activation of the human heme oxygenase gene in cultured skin fibroblasts. Mol Cell Biol (UNITED STATES) 10:4967-4969.

Keyvani K, Schallert T (2002) Plasticity-associated molecular and structural events in the injured brain. J Neuropathol Exp Neurol (England) 61:831-840.

Khan M, Sakakima H, Dhammu TS, Shunmugavel A, Im Y, Gilg AG, Singh AK, Singh I (2011) S-nitrosoglutathione reduces oxidative injury and promotes mechanisms of neurorepair following traumatic brain injury in rats. 8:78.

Kiemer AK, Bildner N, Weber NC, Vollmar AM (2003) Characterization of heme oxygenase 1 (heat shock protein 32) induction by atrial natriuretic peptide in human endothelial cells. Endocrinology (United States) 144:802-812.

Kietzmann T, Samoylenko A, Immenschuh S (2003) Transcriptional regulation of heme oxygenase-1 gene expression by MAP kinases of the JNK and p38 pathways in primary cultures of rat hepatocytes. J Biol Chem (United States) 278:17927-17936.

Kikuchi G, Yoshida T (1983) Function and induction of the microsomal heme oxygenase. Mol Cell Biochem (NETHERLANDS) 53-54:163-183.

Kim HJ, Fillmore HL, Reeves TM, Phillips LL (2005) Elevation of hippocampal MMP-3 expression and activity during trauma-induced synaptogenesis. Exp Neurol (United States) 192:60-72.

Kim HP, Wang X, Galbiati F, Ryter SW, Choi AM (2004) Caveolae compartmentalization of heme oxygenase-1 in endothelial cells. FASEB J (United States) 18:1080-1089.

Kjeldsen L, Johnsen AH, Sengelov H, Borregaard N (1993) Isolation and primary structure of NGAL, a novel protein associated with human neutrophil gelatinase. J Biol Chem (United States) 268:10425-10432.

Klein T, Bischoff R (2010) Physiology and pathophysiology of matrix metalloproteases. 41:271-290.

Kline AE, Massucci JL, Ma X, Zafonte RD, Dixon CE (2004) Bromocriptine reduces lipid peroxidation and enhances spatial learning and hippocampal neuron survival in a rodent model of focal brain trauma. J Neurotrauma (United States) 21:1712-1722.

Knoblach SM, Faden AI (1998) Interleukin-10 improves outcome and alters proinflammatory cytokine expression after experimental traumatic brain injury. 153:143-151.

Kobari M, Fukuuchi Y, Tomita M, Tanahashi N, Konno S, Takeda H (1994) Dilatation of cerebral microvessels mediated by endothelin ETB receptor and nitric oxide in cats. 176:157-160.

Kotapka MJ, Graham DI, Adams JH, Gennarelli TA (1992) Hippocampal pathology in fatal non-missile human head injury. 83:530-534.

Kremlev SG, Palmer C (2005) Interleukin-10 inhibits endotoxin-induced pro-inflammatory cytokines in microglial cell cultures. 162:71-80.

Kronke G, Bochkov VN, Huber J, Gruber F, Bluml S, Furnkranz A, Kadl A, Binder BR, Leitinger N (2003) Oxidized phospholipids induce expression of human heme oxygenase-1 involving activation of cAMP-responsive element-binding protein. J Biol Chem (United States) 278:51006-51014.

Kumar A, Loane DJ (2012) Neuroinflammation after traumatic brain injury: Opportunities for therapeutic intervention. Brain Behav Immun (Netherlands) 26:1191-1201.

Kuo P, Scofield BA, Brown DA, Yen J (2016) Amelioration of cerebral ischemic stroke by induction of Nrf2/HO-1 pathway.

Kutty RK, Maines MD (1982) Oxidation of heme c derivatives by purified heme oxygenase. evidence for the presence of one molecular species of heme oxygenase in the rat liver. J Biol Chem (United States) 257:9944-9952.

Kyrkanides S, O'Banion MK, Whiteley PE, Daeschner JC, Olschowka JA (2001) Enhanced glial activation and expression of specific CNS inflammation-related molecules in aged versus young rats following cortical stab injury. J Neuroimmunol (Netherlands) 119:269-277.

Lad L, Schuller DJ, Shimizu H, Friedman J, Li H, Ortiz de Montellano PR, Poulos TL (2003) Comparison of the heme-free and -bound crystal structures of human heme oxygenase-1. J Biol Chem (United States) 278:7834-7843.

Langlois JA, Rutland-Brown W, Wald MM (2006) The epidemiology and impact of traumatic brain injury. 21:375-378.

Lau A, Tian W, Whitman SA, Zhang DD (2013) The predicted molecular weight of Nrf2: It is what it is not. Antioxid Redox Signal (United States) 18:91-93.

Lautier D, Luscher P, Tyrrell RM (1992) Endogenous glutathione levels modulate both constitutive and UVA radiation/hydrogen peroxide inducible expression of the human heme oxygenase gene. Carcinogenesis (UNITED STATES) 13:227-232.

Lazarini F, Gabellec MM, Torquet N, Lledo PM (2012) Early activation of microglia triggers long-lasting impairment of adult neurogenesis in the olfactory bulb. J Neurosci (United States) 32:3652-3664.

Lee S, Kim J, Seo SG, Choi BR, Han JS, Lee KW, Kim J (2014) Sulforaphane alleviates scopolamine-induced memory impairment in mice. Pharmacol Res (Netherlands) 85:23-32.

Lekic T, Rolland W, Hartman R, Kamper J, Suzuki H, Tang J, Zhang JH (2011) Characterization of the brain injury, neurobehavioral profiles, and histopathology in a rat model of cerebellar hemorrhage. Exp Neurol (United States) 227:96-103.

Levin HS, Diaz-Arrastia RR (2015) Diagnosis, prognosis, and clinical management of mild traumatic brain injury. The Lancet Neurology 14:506-517.

Levin BE, Pan S, Dunn-Meynell A (1994) Chronic alterations in rat brain alpha-adrenoceptors following traumatic brain injury. Restor Neurol Neurosci (Netherlands) 7:5-12.

Levin HS (1995) Prediction of recovery from traumatic brain injury. J Neurotrauma (United States) 12:913-922.

Levonen AL, Landar A, Ramachandran A, Ceaser EK, Dickinson DA, Zanoni G, Morrow JD, Darley-Usmar VM (2004) Cellular mechanisms of redox cell signalling: Role of cysteine modification in controlling antioxidant defences in response to electrophilic lipid oxidation products. Biochem J (England) 378:373-382.

Levy AD, Omar MH, Koleske AJ (2014) Extracellular matrix control of dendritic spine and synapse structure and plasticity in adulthood. Front Neuroanat (Switzerland) 8:116.

Li Volti G, Ientile R, Abraham NG, Vanella A, Cannavo G, Mazza F, Curro M, Raciti G, Avola R, Campisi A (2004) Immunocytochemical localization and expression of heme oxygenase-1 in primary astroglial cell cultures during differentiation: Effect of glutamate. Biochem Biophys Res Commun (United States) 315:517-524.

Li N, Zhao WG, Xu FL, Zhang WF, Gu WT (2013) Neutrophil gelatinase-associated lipocalin as an early marker of acute kidney injury in patients with traumatic brain injury. J Nephrol (Italy) 26:1083-1088.

Li QQ, Qiao GQ, Ma J, Fan HW, Li YB (2015) Cortical neurogenesis in adult rats after ischemic brain injury: Most new neurons fail to mature. Neural Regen Res (India) 10:277-285.

Li RB, Guo XC, Liang HX, Wang FY, Zhu BL (2009) Study on changes of MMP-3 expression after brain contusion in rats. Leg Med (Tokyo) (Ireland) 11 Suppl 1:S176-9.

Lim GP, Chu T, Yang F, Beech W, Frautschy SA, Cole GM (2001) The curry spice curcumin reduces oxidative damage and amyloid pathology in an alzheimer transgenic mouse. J Neurosci (United States) 21:8370-8377.

Lin B, Ginsberg MD, Zhao W, Alonso OF, Belayev L, Busto R (2001) Quantitative analysis of microvascular alterations in traumatic brain injury by endothelial barrier antigen immunohistochemistry. J Neurotrauma (United States) 18:389-397.

Lin JH, Villalon P, Martasek P, Abraham NG (1990) Regulation of heme oxygenase gene expression by cobalt in rat liver and kidney. Eur J Biochem (GERMANY) 192:577-582.

Lin K-, Sloniowski S, Ethell DW, Ethell IM (2008) Ephrin-B2-induced cleavage of EphB2 receptor is mediated by matrix metalloproteinases to trigger cell repulsion. 283:28969-28979.

Lin TN, He YY, Wu G, Khan M, Hsu CY (1993) Effect of brain edema on infarct volume in a focal cerebral ischemia model in rats. 24:117-121.

Lin WS, Lin TC, Hung Y, Lin WY, Lin CS, Lin CL, Cheng SM, Kao CH (2017) Traumatic intracranial haemorrhage is in association with an increased risk of subsequent atrial fibrillation. Heart (England) .

Lin Y, Vreman HJ, Wong RJ, Tjoa T, Yamauchi T, Noble-Haeusslein LJ (2007a) Heme oxygenase-1 stabilizes the blood-spinal cord barrier and limits oxidative stress and white matter damage in the acutely injured murine spinal cord. J Cereb Blood Flow Metab (United States) 27:1010-1021.

Lin Y, Vreman HJ, Wong RJ, Tjoa T, Yamauchi T, Noble-Haeusslein LJ (2007b) Heme oxygenase-1 stabilizes the blood-spinal cord barrier and limits oxidative stress and white matter damage in the acutely injured murine spinal cord. J Cereb Blood Flow Metab (United States) 27:1010-1021.

Linden IB, Tokola O, Karlsson M, Tenhunen R (1987) Fate of haem after parenteral administration of haem arginate to rabbits. J Pharm Pharmacol (England) 39:96-102.

Liu C (1958) Intraspinal sprouting of dorsal root axons. 79:46.

Liu HS, Shen H, Harvey BK, Castillo P, Lu H, Yang Y, Wang Y (2011) Post-treatment with amphetamine enhances reinnervation of the ipsilateral side cortex in stroke rats. Neuroimage (United States) 56:280-289.

Liu J, Xia S, Hanks R, Wiseman N, Peng C, Zhou S, Haacke EM, Kou Z (2016) Susceptibility weighted imaging and mapping of micro-hemorrhages and major deep veins after traumatic brain injury. J Neurotrauma (United States) 33:10-21.

Liu J, Xia S, Hanks RA, Wiseman NM, Peng C, Zhou S, Haacke EM, Kou Z (2015) Susceptibility weighted imaging and mapping of micro-hemorrhages and major deep veins after traumatic brain injury. J Neurotrauma .

Liu JD, Tsai SH, Lin SY, Ho YS, Hung LF, Pan S, Ho FM, Lin CM, Liang YC (2004) Thiol antioxidant and thiol-reducing agents attenuate 15-deoxy-delta 12,14-prostaglandin J2-induced heme oxygenase-1 expression. Life Sci (England) 74:2451-2463.

Lo EH, Broderick JP, Moskowitz MA (2004) tPA and proteolysis in the neurovascular unit. Stroke (United States) 35:354-356.

Lo EH, Wang X, Cuzner ML (2002) Extracellular proteolysis in brain injury and inflammation: Role for plasminogen activators and matrix metalloproteinases. 69:1-9.

Loddick SA, Rothwell NJ (1996) Neuroprotective effects of human recombinant interleukin-1 receptor antagonist in focal cerebral ischaemia in the rat. 932-940.

Loesche J, Steward O (1977) Behavioral correlates of denervation and reinnervation of the hippocampal formation of the rat: Recovery of alternation performance following unilateral entorhinal cortex lesions. 2:31-39.

Lovell M, Franzen M, Silver JM, Yudofsky S, Hales RE (1994) Neuropsychiatry of traumatic brain injury. American Psychiatric Press 133-160.

Lozano D, Gonzales-Portillo GS, Acosta S, de la Pena I, Tajiri N, Kaneko Y, Borlongan CV (2015) Neuroinflammatory responses to traumatic brain injury: Etiology, clinical consequences, and therapeutic opportunities. Neuropsychiatr Dis Treat (New Zealand) 11:97-106.

Lu J, Moochhala S, Kaur C, Ling E (2001) Cellular inflammatory response associated with breakdown of the blood-brain barrier after closed head injury in rats. 18:399-408.

Lu X, Chen-Roetling J, Regan RF (2014) Systemic hemin therapy attenuates blood-brain barrier disruption after intracerebral hemorrhage. Neurobiol Dis (United States) 70:245-251.

Lucas S, Rothwell NJ, Gibson RM (2006) The role of inflammation in CNS injury and disease. 147:S232-S240.

Lund RD, Lund JS (1971) Synaptic adjustment after deafferentation of the superior colliculus of the rat. 171:804-807.

Luo J (2005) The role of matrix metalloproteinases in the morphogenesis of the cerebellar cortex. Cerebellum (United States) 4:239-245.

Lyeth BG, Dixon CE, Hamm RJ, Jenkins LW, Young HF, Stonnington HH, Hayes RL (1988) Effects of anticholinergic treatment on transient behavioral suppression and physiological responses following concussive brain injury to the rat. 448:88-97.

Lynch G, Gall C, Rose G, Cotman C (1976) Changes in the distribution of the dentate gyrus associational system following unilateral or bilateral entorhinal lesions in the adult rat. 110:57-71.

Madathil SK, Carlson SW, Brelsfoard JM, Ye P, Dâ€™Ercole AJ, Saatman KE (2013) Astrocyte-specific overexpression of insulin-like growth factor-1 protects hippocampal neurons and reduces behavioral deficits following traumatic brain injury in mice. 8:e67204.

Magavi SS, Leavitt BR, Macklis JD (2000) Induction of neurogenesis in the neocortex of adult mice. Nature (England) 405:951-955.

Maines MD (1992) *Heme oxygenase: Clinical applications and functions.*. Boca Raton, FL: CRC.

Maines MD (1988) Heme oxygenase: Function, multiplicity, regulatory mechanisms, and clinical applications. FASEB J (United States) 2:2557-2568.

Maines MD, Trakshel GM (1993) Purification and characterization of human biliverdin reductase. Arch Biochem Biophys (UNITED STATES) 300:320-326.

Maines MD, Trakshel GM, Kutty RK (1986) Characterization of two constitutive forms of rat liver microsomal heme oxygenase. only one molecular species of the enzyme is inducible. J Biol Chem (UNITED STATES) 261:411-419.

Maines MD, Ewing JF, Huang TJ, Panahian N (2001) Nuclear localization of biliverdin reductase in the rat kidney: Response to nephrotoxins that induce heme oxygenase-1. J Pharmacol Exp Ther (United States) 296:1091-1097.

Malec JF, Brown AW, Leibson CL, Flaada JT, Mandrekar JN, Diehl NN, Perkins PK (2007) The mayo classification system for traumatic brain injury severity. J Neurotrauma (United States) 24:1417-1424.

Mao L, Wang HD, Wang XL, Qiao L, Yin HX (2010) Sulforaphane attenuates matrix metalloproteinase-9 expression following spinal cord injury in mice. Ann Clin Lab Sci (United States) 40:354-360.

Mark KS, Davis TP (2002) Cerebral microvascular changes in permeability and tight junctions induced by hypoxia-reoxygenation. Am J Physiol Heart Circ Physiol (United States) 282:H1485-94.

Marmarou A, Foda MA, van den Brink W, Campbell J, Kita H, Demetriadou K (1994) A new model of diffuse brain injury in rats. part I: Pathophysiology and biomechanics. J Neurosurg (United States) 80:291-300.

Massucci JL, Kline AE, Ma X, Zafonte RD, Dixon CE (2004) Time dependent alterations in dopamine tissue levels and metabolism after experimental traumatic brain injury in rats. Neurosci Lett 372:127-131.

Mautes AE, Bergeron M, Sharp FR, Panter SS, Weinzierl M, Guenther K, Noble LJ (2000) Sustained induction of heme oxygenase-1 in the traumatized spinal cord. Exp Neurol (UNITED STATES) 166:254-265.

Maxwell WL, Povlishock JT, Graham DL (1997) A mechanistic analysis of nondisruptive axonal injury: A review. J Neurotrauma (United States) 14:419-440.

McCoubrey WK,Jr, Maines MD (1994) The structure, organization and differential expression of the gene encoding rat heme oxygenase-2. Gene (NETHERLANDS) 139:155-161.

McIntosh TK (1994) Neurochemical sequelae of traumatic brain injury: Therapeutic implications. Cerebrovasc Brain Metab Rev (United States) 6:109-162.

McKee AC, Cantu RC, Nowinski CJ, Hedley-Whyte ET, Gavett BE, Budson AE, Santini VE, Lee H, Kubilus CA, Stern RA (2009) Chronic traumatic encephalopathy in athletes. 68:709-735.

Meaney DF, Smith DH, Shreiber DI, Bain AC, Miller RT, Ross DT, Gennarelli TA (1995) Biomechanical analysis of experimental diffuse axonal injury. 12:689-694.

Mehta NU, Reddy ST (2015) Role of hemoglobin/heme scavenger protein hemopexin in atherosclerosis and inflammatory diseases. Curr Opin Lipidol (England) 26:384-387.

Meighan SE, Meighan PC, Choudhury P, Davis CJ, Olson ML, Zornes PA, Wright JW, Harding JW (2006) Effects of extracellular matrix-degrading proteases matrix metalloproteinases 3 and 9 on spatial learning and synaptic plasticity. 96:1227-1241.

Menet V, Prieto M, Privat A, Gimenez y Ribotta M (2003) Axonal plasticity and functional recovery after spinal cord injury in mice deficient in both glial fibrillary acidic protein and vimentin genes. Proc Natl Acad Sci U S A (United States) 100:8999-9004.

Michaluk P, Kaczmarek L (2007) Matrix metalloproteinase-9 in glutamate-dependent adult brain function and dysfunction. 14:1255-1258.

Michaluk P, Mikasova L, Groc L, Frischknecht R, Choquet D, Kaczmarek L (2009) Matrix metalloproteinase-9 controls NMDA receptor surface diffusion through integrin Â 1 signaling. 29:6007-6012.

Milner R, Campbell IL (2002) The integrin family of cell adhesion molecules has multiple functions within the CNS. 69:286-291.

Mitani K, Fujita H, Kappas A, Sassa S (1992) Heme oxygenase is a positive acute-phase reactant in human Hep3B hepatoma cells. Blood (UNITED STATES) 79:1255-1259.

Mitani K, Fujita H, Fukuda Y, Kappas A, Sassa S (1993) The role of inorganic metals and metalloporphyrins in the induction of haem oxygenase and heat-shock protein 70 in human hepatoma cells. Biochem J (ENGLAND) 290 (Pt 3):819-825.

Miyazaki S, Katayama Y, Lyeth BG, Jenkins LW, DeWitt DS, Goldberg SJ, Newlon PG, Hayes RL (1992) Enduring suppression of hippocampal long-term potentiation following traumatic brain injury in rat. Brain Res (Netherlands) 585:335-339.

Molgaard CA, Stanford EP, Morton DJ, Ryden LA, Schubert KR, Golbeck AL (1990) Epidemiology of head trauma and neurocognitive impairment in a multi-ethnic population. 9:233-242.

Moller JC, Klein MA, Haas S, Jones LL, Kreutzberg GW, Raivich G (1996) Regulation of thrombospondin in the regenerating mouse facial motor nucleus. Glia (United States) 17:121-132.

Montaner J, Alvarez-Sabin J, Molina C, Angles A, Abilleira S, Arenillas J, Gonzalez MA, Monasterio J (2001) Matrix metalloproteinase expression after human cardioembolic stroke: Temporal profile and relation to neurological impairment. Stroke (United States) 32:1759-1766.

Morganti-Kossmann MC, Rancan M, Stahel PF, Kossmann T (2002) Inflammatory response in acute traumatic brain injury: A double-edged sword. Curr Opin Crit Care (United States) 8:101-105.

Morganti-Kossmann MC, Satgunaseelan L, Bye N, Kossmann T (2007) Modulation of immune response by head injury. 38:1392-1400.

Morganti-Kossmann MC, Rancan M, Otto VI, Stahel PF, Kossmann T (2001) ROLE OF CEREBRAL INFLAMMATION AFTER TRAUMATIC BRAIN INJURY: A REVISITED CONCEPT. 16:165-177.

Morris R (1984) Developments of a water-maze procedure for studying spatial learning in the rat. J Neurosci Methods (Netherlands) 11:47-60.

Morris T, Gomes Osman J, Tormos Munoz JM, Costa Miserachs D, Pascual Leone A (2016) The role of physical exercise in cognitive recovery after traumatic brain injury: A systematic review. Restor Neurol Neurosci (Netherlands) 34:977-988.

Morroni F, Tarozzi A, Sita G, Bolondi C, Zolezzi Moraga JM, Cantelli-Forti G, Hrelia P (2013) Neuroprotective effect of sulforaphane in 6-hydroxydopamine-lesioned mouse model of parkinson's disease. Neurotoxicology (Netherlands) 36:63-71.

Mortimer JA, French LR, Hutton JT, Schuman LM (1985) Head injury as a risk factor for alzheimer's disease. 35:264-264.

Motterlini R, Foresti R, Bassi R, Green CJ (2000) Curcumin, an antioxidant and anti-inflammatory agent, induces heme oxygenase-1 and protects endothelial cells against oxidative stress. Free Radic Biol Med (UNITED STATES) 28:1303-1312.

Mucha M, Skrzypiec AE, Schiavon E, Attwood BK, Kucerova E, Pawlak R (2011) Lipocalin-2 controls neuronal excitability and anxiety by regulating dendritic spine formation and maturation. Proc Natl Acad Sci U S A (United States) 108:18436-18441.

Muir EM, Adcock KH, Morgenstern DA, Clayton R, von Stillfried N, Rhodes K, Ellis C, Fawcett JW, Rogers JH (2002) Matrix metalloproteases and their inhibitors are produced by overlapping populations of activated astrocytes. 100:103-117.

Muir KW (2006) Glutamate-based therapeutic approaches: Clinical trials with NMDA antagonists. Curr Opin Pharmacol (England) 6:53-60.

Myer DJ, Gurkoff GG, Lee SM, Hovda DA, Sofroniew MV (2006) Essential protective roles of reactive astrocytes in traumatic brain injury. Brain (England) 129:2761-2772.

Nadel L, O'Keefe J, Black A (1975) Slam on the brakes: A critique of altman, brunner, and bayer's response-inhibition model of hippocampal function. Behav Biol (United States) 14:151-162.

Nadler JV, Cotman CW (1978) Interactions between afferents to the dentate gyrus after entorhinal lesion during development: Long-term regulation of choline acetyl-transferase activity. Brain Res (Netherlands) 142:174-181.

NAGASE H, VISSE R, MURPHY G (2006) Structure and function of matrix metalloproteinases and TIMPs. 69:562-573.

Nagy V (2006) Matrix metalloproteinase-9 is required for hippocampal late-phase long-term potentiation and memory. 26:1923-1934.

Nairz M, Theurl I, Ludwiczek S, Theurl M, Mair SM, Fritsche G, Weiss G (2007) The co-ordinated regulation of iron homeostasis in murine macrophages limits the availability of iron for intracellular salmonella typhimurium. Cell Microbiol (England) 9:2126-2140.

Naughton P, Foresti R, Bains SK, Hoque M, Green CJ, Motterlini R (2002) Induction of heme oxygenase 1 by nitrosative stress. A role for nitroxyl anion. J Biol Chem (United States) 277:40666-40674.

Newcomb JK, Pike BR, Zhao X, Banik NL, Hayes RL (1999a) Altered calpastatin protein levels following traumatic brain injury in rat. J Neurotrauma 16:1-11.

Newcomb JK, Zhao X, Pike BR, Hayes RL (1999b) Temporal profile of apoptotic-like changes in neurons and astrocytes following controlled cortical impact injury in the rat. 158:76-88.

Ni W, Mao S, Xi G, Keep RF, Hua Y (2016) Role of erythrocyte CD47 in intracerebral hematoma clearance. Stroke (United States) 47:505-511.

Nicotera P, Leist M, Manzo L (1999a) Neuronal cell death: A demise with different shapes. Trends Pharmacol Sci 20:46-51.

Nicotera P, Leist M, Ferrando-May E (1999b) Apoptosis and necrosis: Different execution of the same death. 66:69-73.

Numazawa S, Yamada H, Furusho A, Nakahara T, Oguro T, Yoshida T (1997) Cooperative induction of c-fos and heme oxygenase gene products under oxidative stress in human fibroblastic cells. Exp Cell Res (UNITED STATES) 237:434-444.

O'Dell DM, Gibson CJ, Wilson MS, DeFord SM, Hamm RJ (2000) Positive and negative modulation of the GABA(A) receptor and outcome after traumatic brain injury in rats. Brain Res (Netherlands) 861:325-332.

Oguro T, Hayashi M, Nakajo S, Numazawa S, Yoshida T (1998) The expression of heme oxygenase-1 gene responded to oxidative stress produced by phorone, a glutathione depletor, in the rat liver; the relevance to activation of c-jun n-terminal kinase. J Pharmacol Exp Ther (UNITED STATES) 287:773-778.

Oh LY, Larsen PH, Krekoski CA, Edwards DR, Donovan F, Werb Z, Yong VW (1999) Matrix metalloproteinase-9/gelatinase B is required for process outgrowth by oligodendrocytes. J Neurosci (United States) 19:8464-8475.

O'Keefe J, Conway DH (1978) Hippocampal place units in the freely moving rat: Why they fire where they fire. Exp Brain Res (Germany) 31:573-590.

Oldenborg PA, Zheleznyak A, Fang YF, Lagenaur CF, Gresham HD, Lindberg FP (2000) Role of CD47 as a marker of self on red blood cells. Science (United States) 288:2051-2054.

Olsen AS, Sozda CN, Cheng JP, Hoffman AN, Kline AE (2012) Traumatic brain injury-induced cognitive and histological deficits are attenuated by delayed and chronic treatment with the 5-HT1A-receptor agonist buspirone. J Neurotrauma (United States) 29:1898-1907.

O'Shaughnessy MC, Brunstrom GM, Fielding J (1966) Iron chelation in haematomas at fracture sites. J Clin Pathol (England) 19:364-367.

Palmer AM, Marion DW, Botscheller ML, Swedlow PE, Styren SD, DeKosky ST (1993) Traumatic brain injury-induced excitotoxicity assessed in a controlled cortical impact model. J Neurochem (England) 61:2015-2024.

Pappolla MA, Chyan YJ, Omar RA, Hsiao K, Perry G, Smith MA, Bozner P (1998) Evidence of oxidative stress and in vivo neurotoxicity of beta-amyloid in a transgenic mouse model of alzheimer's disease: A chronic oxidative paradigm for testing antioxidant therapies in vivo. Am J Pathol (UNITED STATES) 152:871-877.

Park JH, Park SW, Kang SH, Nam TK, Min BK, Hwang SN (2009a) Detection of traumatic cerebral microbleeds by susceptibility-weighted image of MRI. J Korean Neurosurg Soc (Korea (South)) 46:365-369.

Park K-, Rosell A, Foerch C, Xing C, Kim WJ, Lee S, Opdenakker G, Furie KL, Lo EH (2009b) Plasma and brain matrix metalloproteinase-9 after acute focal cerebral ischemia in rats. 40:2836-2842.

Pellman EJ, Viano DC, National Football League's Committee on Mild Traumatic Brain Injury (2006) Concussion in professional football: Summary of the research conducted by the national football league's committee on mild traumatic brain injury. Neurosurg Focus (United States) 21:E12.

Penkowa M, Giralt M, Carrasco J, Hadberg H, Hidalgo J (2000) Impaired inflammatory response and increased oxidative stress and neurodegeneration after brain injury in interleukin-6-deficient mice. 32:271-285.

Peres CM, Caldas JG, Puglia P,Jr, de Andrade AF, da Silva IA, Teixeira MJ, Figueiredo EG (2017) Endovascular management of acute epidural hematomas: Clinical experience with 80 cases. J Neurosurg (United States) 1-7.

Perris R (1997) The extracellular matrix in neural crest-cell migration. Trends Neurosci (England) 20:23-31.

Perris R, Perissinotto D (2000) Role of the extracellular matrix during neural crest cell migration. Mech Dev (Ireland) 95:3-21.

Petraglia AL, Dashnaw ML, Turner RC, Bailes JE (2014) Models of mild traumatic brain injury: Translation of physiological and anatomic injury. Neurosurgery (United States) 75 Suppl 4:S34-49.

Pettus EH, Christman CW, Giebel ML, Povlishock JT (1994) Traumatically induced altered membrane permeability: Its relationship to traumatically induced reactive axonal change. J Neurotrauma (United States) 11:507-522.

Phillips L, Lyeth B, Hamm R, Reeves T, Povlishock J (1998) Glutamate antagonism during secondary deafferentation enhances cognition and axo-dendritic integrity after traumatic brain injury. Hippocampus 8:390-401.

Phillips LL, Reeves TM (2001) Interactive pathology following traumatic brain injury modifies hippocampal plasticity. Restor Neurol Neurosci (Netherlands) 19:213-235.

Phillips LL, Chan JL, Doperalski AE, Reeves TM (2014) Time dependent integration of matrix metalloproteinases and their targeted substrates directs axonal sprouting and synaptogenesis following central nervous system injury. Neural Regen Res (India) 9:362-376.

Phillips S, Woessner D (2015) Sports-related traumatic brain injury. Prim Care (United States) 42:243-248.

Pimstone NR, Tenhunen R, Seitz PT, Marver HS, Schmid R (1971a) The enzymatic degradation of hemoglobin to bile pigments by macrophages. J Exp Med (UNITED STATES) 133:1264-1281.

Pimstone NR, Engel P, Tenhunen R, Seitz PT, Marver HS, Schmid R (1971b) Inducible heme oxygenase in the kidney: A model for the homeostatic control of hemoglobin catabolism. J Clin Invest (UNITED STATES) 50:2042-2050.

Pittman RN, Buettner HM (1989) Degradation of extracellular matrix by neuronal proteases. 11:361-375.

Planas AM, SolÃ© S, Justicia C (2001) Expression and activation of matrix metalloproteinase-2 and -9 in rat brain after transient focal cerebral ischemia. 8:834-846.

Platt JL, Nath KA (1998) Heme oxygenase: Protective gene or trojan horse. Nat Med (United States) 4:1364-1365.

Ponomarev ED, Maresz K, Tan Y, Dittel BN (2007) CNS-derived interleukin-4 is essential for the regulation of autoimmune inflammation and induces a state of alternative activation in microglial cells. J Neurosci (United States) 27:10714-10721.

Portera-Cailliau C, Price DL, Martin LJ (1997) Excitotoxic neuronal death in the immature brain is an apoptosis-necrosis morphological continuum. 378:10-87.

Poss KD, Tonegawa S (1997a) Reduced stress defense in heme oxygenase 1-deficient cells. Proc Natl Acad Sci U S A (United States) 94:10925-10930.

Poss KD, Tonegawa S (1997b) Heme oxygenase 1 is required for mammalian iron reutilization. Proc Natl Acad Sci U S A (UNITED STATES) 94:10919-10924.

Povlishock JT, Pettus E (1996) Traumatically induced axonal damage: Evidence for enduring changes in axolemmal permeability with associated cytoskeletal change. In: Mechanisms of secondary brain damage in cerebral ischemia and trauma Traumatically induced axonal damage: Evidence for enduring changes in axolemmal permeability with associated cytoskeletal change. pp81-86.Springer.

Povlishock JT (1992) Traumatically induced axonal injury: Pathogenesis and pathobiological implications. Brain Pathol (Switzerland) 2:1-12.

Povlishock JT, Kontos HA (1985) Continuing axonal and vascular change following experimental brain trauma. Cent Nerv Syst Trauma (United States) 2:285-298.

Povlishock JT, Becker DP (1985) Fate of reactive axonal swellings induced by head injury. Lab Invest (United States) 52:540-552.

Povlishock JT, Erb DE, Astruc J (1992) Axonal response to traumatic brain injury: Reactive axonal change, deafferentation, and neuroplasticity. J Neurotrauma (United States) 9 Suppl 1:S189-200.

Povlishock JT, Becker DP, Cheng CLY, Vaughan GW (1983) Axonal change in minor head injury. 42:225-242.

Povlishock JT, Katz DI (2005) Update of neuropathology and neurological recovery after traumatic brain injury. 20:76-94.

Povlishock JT, Christman CW (1995) The pathobiology of traumatically induced axonal injury in animals and humans: A review of current thoughts. 12:555-564.

Pravalie R (2014) Nuclear weapons tests and environmental consequences: A global perspective. Ambio (Sweden) 43:729-744.

Raghavendra Rao VL, Dhodda VK, Song G, Bowen KK, Dempsey RJ (2003) Traumatic brain injury-induced acute gene expression changes in rat cerebral cortex identified by GeneChip analysis. J Neurosci Res (United States) 71:208-219.

Raghupathi R, Conti AC, Graham DI, Krajewski S, Reed JC, Grady MS, Trojanowski JQ, McIntosh TK (2002) Mild traumatic brain injury induces apoptotic cell death in the cortex that is preceded by decreases in cellular bcl-2 immunoreactivity. 110:605-616.

Raisman G (1969) Neuronal plasticity in the septal nuclei of the adult rat. 14:25-48.

Ramlackhansingh AF, Brooks DJ, Greenwood RJ, Bose SK, Turkheimer FE, Kinnunen KM, Gentleman S, Heckemann RA, Gunanayagam K, Gelosa G, Sharp DJ (2011) Inflammation after trauma: Microglial activation and traumatic brain injury. 70:374-383.

Ransohoff RM, Brown MA (2012) Innate immunity in the central nervous system. J Clin Invest (United States) 122:1164-1171.

Rathore KI, Berard JL, Redensek A, Chierzi S, Lopez-Vales R, Santos M, Akira S, David S (2011) Lipocalin 2 plays an immunomodulatory role and has detrimental effects after spinal cord injury. J Neurosci (United States) 31:13412-13419.

Ratledge C (2007) Iron metabolism and infection. Food Nutr Bull (United States) 28:S515-23.

Reeves TM, Lyeth BG, Povlishock JT (1995) Long-term potentiation deficits and excitability changes following traumatic brain injury. Exp Brain Res (Germany) 106:248-256.

Regan RF, Panter SS (1996) Hemoglobin potentiates excitotoxic injury in cortical cell culture. J Neurotrauma (UNITED STATES) 13:223-231.

Reiss K, Maretzky T, Ludwig A, Tousseyn T, de Strooper B, Hartmann D, Saftig P (2005) ADAM10 cleavage of N-cadherin and regulation of cell-cell adhesion and beta-catenin nuclear signalling. EMBO J (England) 24:742-752.

Relton JK, Rothwell NJ (1992) Interleukin-1 receptor antagonist inhibits ischaemic and excitotoxic neuronal damage in the rat. 29:243-246.

Richmon JD, Fukuda K, Maida N, Sato M, Bergeron M, Sharp FR, Panter SS, Noble LJ (1998) Induction of heme oxygenase-1 after hyperosmotic opening of the blood-brain barrier. Brain Res (NETHERLANDS) 780:108-118.

Rizzardini M, Carelli M, Cabello Porras MR, Cantoni L (1994) Mechanisms of endotoxin-induced haem oxygenase mRNA accumulation in mouse liver: Synergism by glutathione depletion and protection by N-acetylcysteine. Biochem J (ENGLAND) 304 (Pt 2):477-483.

Rizzardini M, Terao M, Falciani F, Cantoni L (1993) Cytokine induction of haem oxygenase mRNA in mouse liver. interleukin 1 transcriptionally activates the haem oxygenase gene. Biochem J (ENGLAND) 290 (Pt 2):343-347.

Romanic AM, Madri JA (1994) Extracellular matrix-degrading proteinases in the nervous system. 4:145-156.

Rose P, Huang Q, Ong CN, Whiteman M (2005) Broccoli and watercress suppress matrix metalloproteinase-9 activity and invasiveness of human MDA-MB-231 breast cancer cells. Toxicol Appl Pharmacol (United States) 209:105-113.

Rosell A, Lo E (2008) Multiphasic roles for matrix metalloproteinases after stroke. 8:82-89.

Rosenberg GA (1995) Matrix metalloproteinases in brain injury. 12:833-842.

Rosenberg GA (2009) Matrix metalloproteinases and their multiple roles in neurodegenerative diseases. Lancet Neurol (England) 8:205-216.

Rosenberg GA, Navratil M (1997) Metalloproteinase inhibition blocks edema in intracerebral hemorrhage in the rat. Neurology (United States) 48:921-926.

Rosenberg GA, Estrada EY, Dencoff JE, Hsu CY (1998) Matrix metalloproteinases and TIMPs are associated with blood-brain barrier opening after reperfusion in rat brain Â editorial comment. 29:2189-2195.

Rosenberg GA, Cunningham LA, Wallace J, Alexander S, Estrada EY, Grossetete M, Razhagi A, Miller K, Gearing A (2001) Immunohistochemistry of matrix metalloproteinases in reperfusion injury to rat brain: Activation of MMP-9 linked to stromelysin-1 and microglia in cell cultures. 893:104-112.

Ross D, Graham D, Adams JH (1993) Selective loss of neurons from the thalamic reticular nucleus following severe human head injury. J Neurotrauma 10:151-165.

Rothman SM, Olney JW (1987) Excitotoxity and the NMDA receptor. 10:299-302.

Rothwell N (2000) Interleukin 1 in the brain: Biology, pathology and therapeutic target. 23:618-625.

Rothwell NJ, Luheshi GN (2000) Interleukin 1 in the brain: Biology, pathology and therapeutic target. Trends Neurosci (England) 23:618-625.

Rothwell NJ (1999) Cytokines - killers in the brain? 514:3-17.

Ruoslahti E (1996) Brain extracellular matrix. 6:489-492.

Rutland-Brown W, Langlois JA, Thomas KE, Xi YL (2006) Incidence of traumatic brain injury in the united states, 2003. 21:544-548.

Ryter S, Kvam E, Richman L, Hartmann F, Tyrrell RM (1998) A chromatographic assay for heme oxygenase activity in cultured human cells: Application to artificial heme oxygenase overexpression. Free Radic Biol Med (UNITED STATES) 24:959-971.

Ryter SW, Tyrrell RM (2000) The heme synthesis and degradation pathways: Role in oxidant sensitivity. heme oxygenase has both pro- and antioxidant properties. Free Radic Biol Med (United States) 28:289-309.

Ryter SW, Alam J, Choi AM (2006) Heme oxygenase-1/carbon monoxide: From basic science to therapeutic applications. Physiol Rev (United States) 86:583-650.

Ryter SW, Kvam E, Tyrrell RM (2000) Heme oxygenase activity. current methods and applications. Methods Mol Biol (UNITED STATES) 99:369-391.

Safciuc F, Constantin A, Manea A, Nicolae M, Popov D, Raicu M, Alexandru D, Constantinescu E (2007) Advanced glycation end products, oxidative stress and metalloproteinases are altered in the cerebral microvasculature during aging. Curr Neurovasc Res (Netherlands) 4:228-234.

Sardana MK, Sassa S, Kappas A (1982) Metal ion-mediated regulation of heme oxygenase induction in cultured avian liver cells. J Biol Chem (UNITED STATES) 257:4806-4811.

Sato M, Noble LJ (1998) Involvement of the endothelin receptor subtype A in neuronal pathogenesis after traumatic brain injury. Brain Res (NETHERLANDS) 809:39-49.

Saulle M, Greenwald BD (2012) Chronic traumatic encephalopathy: A review. 2012:1-9.

Saunders N, Habgood M, Dziegielewska K (1999) BARRIER MECHANISMS IN THE BRAIN, I. ADULT BRAIN. 26:11-19.

Saygili E, Schauerte P, Pekassa M, Saygili E, Rackauskas G, Schwinger RHG, Weis J, Weber C, Marx N, Rana OR (2010) Sympathetic neurons express and secrete MMP-2 and MT1-MMP to control nerve sprouting via pro-NGF conversion. 31:17-25.

Sbai O, Ferhat L, Bernard A, Gueye Y, Ould-Yahoui A, Thiolloy S, Charrat E, Charton G, Tremblay E, Risso J, Chauvin J, Arsanto J, Rivera S, Khrestchatisky M (2008) Vesicular trafficking and secretion of matrix metalloproteinases-2, -9 and tissue inhibitor of metalloproteinases-1 in neuronal cells. 39:549-568.

Scapagnini G, Foresti R, Calabrese V, Giuffrida Stella AM, Green CJ, Motterlini R (2002) Caffeic acid phenethyl ester and curcumin: A novel class of heme oxygenase-1 inducers. Mol Pharmacol (United States) 61:554-561.

Schallner N, Pandit R, LeBlanc R,3rd, Thomas AJ, Ogilvy CS, Zuckerbraun BS, Gallo D, Otterbein LE, Hanafy KA (2015) Microglia regulate blood clearance in subarachnoid hemorrhage by heme oxygenase-1. J Clin Invest (United States) 125:2609-2625.

Scheff S, Benardo I, Cotman C (1977) Progressive brain damage accelerates axon sprouting in the adult rat. 197:795-797.

Scheff SW, Price DA, Hicks RR, Baldwin SA, Robinson S, Brackney C (2005) Synaptogenesis in the hippocampal CA1 field following traumatic brain injury. 22:719-732.

Scherbel U, Raghupathi R, Nakamura M, Saatman KE, Trojanowski JQ, Neugebauer E, Marino MW, McIntosh TK (1999) Differential acute and chronic responses of tumor necrosis factor-deficient mice to experimental brain injury. 96:8721-8726.

Schipper HM, Cisse S, Stopa EG (1995) Expression of heme oxygenase-1 in the senescent and alzheimer-diseased brain. Ann Neurol (UNITED STATES) 37:758-768.

Schipper HM, Chertkow H, Mehindate K, Frankel D, Melmed C, Bergman H (2000) Evaluation of heme oxygenase-1 as a systemic biological marker of sporadic AD. Neurology (UNITED STATES) 54:1297-1304.

Schmidt RH, Grady MS (1993) Regional patterns of Bloodâ€“Brain barrier breakdown following central and lateral fluid percussion injury in rodents. 10:415-430.

Schousboe A, Waagepetersen HS (2005) Role of astrocytes in glutamate homeostasis: Implications for excitotoxicity. Neurotox Res (United States) 8:221-225.

Schousboe A, Scafidi S, Bak LK, Waagepetersen HS, McKenna MC (2014) Glutamate metabolism in the brain focusing on astrocytes. Adv Neurobiol (United States) 11:13-30.

Schuller DJ, Wilks A, Ortiz de Montellano PR, Poulos TL (1999) Crystal structure of human heme oxygenase-1. Nat Struct Biol (UNITED STATES) 6:860-867.

Schwarzmaier SM, Kim SW, Trabold R, Plesnila N (2010) Temporal profile of thrombogenesis in the cerebral microcirculation after traumatic brain injury in mice. J Neurotrauma (United States) 27:121-130.

Shi WZ, Ju JY, Xiao HJ, Xue F, Wu J, Pan MM, Ni WF (2017) Dynamics of MMP9, MMP2 and TIMP1 in a rat model of brain injury combined with traumatic heterotopic ossification. Mol Med Rep (Greece) 15:2129-2135.

Shibahara S (2003) The heme oxygenase dilemma in cellular homeostasis: New insights for the feedback regulation of heme catabolism. Tohoku J Exp Med (Japan) 200:167-186.

Shibahara S, Muller RM, Taguchi H (1987) Transcriptional control of rat heme oxygenase by heat shock. J Biol Chem (UNITED STATES) 262:12889-12892.

Shibahara S, Sato M, Muller RM, Yoshida T (1989) Structural organization of the human heme oxygenase gene and the function of its promoter. Eur J Biochem (GERMANY, WEST) 179:557-563.

Shibahara S, Muller R, Taguchi H, Yoshida T (1985) Cloning and expression of cDNA for rat heme oxygenase. Proc Natl Acad Sci U S A (UNITED STATES) 82:7865-7869.

Shibahara S, Yoshizawa M, Suzuki H, Takeda K, Meguro K, Endo K (1993) Functional analysis of cDNAs for two types of human heme oxygenase and evidence for their separate regulation. J Biochem (JAPAN) 113:214-218.

Shin EJ, Kim E, Lee JA, Rhim H, Hwang O (2012) Matrix metalloproteinase-3 is activated by HtrA2/omi in dopaminergic cells: Relevance to parkinsonâ€™s disease. 60:249-256.

Shohami E (1999) Dual role of tumor necrosis factor alpha in brain injury. 10:119-130.

Shohami E, Gallily R, Mechoulam R, Bass R, Ben-Hur T (1997) Cytokine production in the brain following closed head injury: Dexanabinol (HU-211) is a novel TNF-Î± inhibitor and an effective neuroprotectant. 72:169-177.

Shohami E, Novikov M, Bass R, Yamin A, Gallily R (1994) Closed head injury triggers early production of TNFÎ± and IL-6 by brain tissue. 14:615-619.

Shubayev VI, Myers RR (2004) Matrix metalloproteinase-9 promotes nerve growth factor-induced neurite elongation but not new sprout formation in vitro. 77:229-239.

Silver JM (2012) Effort, exaggeration and malingering after concussion. J Neurol Neurosurg Psychiatry (England) 83:836-841.

Silver J, Miller JH (2004) Regeneration beyond the glial scar. 5:146-156.

Silver JM, McAllister TW, Yudofsky SC (2011) Textbook of traumatic brain injury. Washington, DC: American Psychiatric Pub.

Singhal A, Baker AJ, Hare GMT, Reinders FX, Schlichter LC, Moulton RJ (2002) Association between cerebrospinal fluid interleukin-6 concentrations and outcome after severe human traumatic brain injury. 19:929-937.

Siow RC, Mann GE (2010) Dietary isoflavones and vascular protection: Activation of cellular antioxidant defenses by SERMs or hormesis? Mol Aspects Med (England) 31:468-477.

Sivanandam TM, Thakur MK (2012) Traumatic brain injury: A risk factor for alzheimer's disease. 36:1376-1381.

Skrzypiec AE, Shah RS, Schiavon E, Baker E, Skene N, Pawlak R, Mucha M (2013) Stress-induced lipocalin-2 controls dendritic spine formation and neuronal activity in the amygdala. PLoS One (United States) 8:e61046.

Smith DH, Meaney DF (2000) Axonal damage in traumatic brain injury. 6:483-495.

Smith DH, Hicks R, Povlishock JT (2013) Therapy development for diffuse axonal injury. 30:307-323.

Smith DH, Chen X, Xu B, McIntosh TK, Gennarelli TA, Meaney DF (1997) Characterization of diffuse axonal pathology and selective hippocampal damage following inertial brain trauma in the pig. 56:822-834.

Soane L, Li Dai W, Fiskum G, Bambrick LL (2010) Sulforaphane protects immature hippocampal neurons against death caused by exposure to hemin or to oxygen and glucose deprivation. J Neurosci Res (United States) 88:1355-1363.

Spangelo BL, Judd AM, MacLeod RM, Goodman DW, Isakson PC (1990) Endotoxin-induced release of interleukin-6 from rat medial basal hypothalami*. 127:1779-1785.

Speller CF, Spalding KL, Buchholz BA, Hildebrand D, Moore J, Mathewes R, Skinner MF, Yang DY (2012) Personal identification of cold case remains through combined contribution from anthropological, mtDNA, and bomb-pulse dating analyses. J Forensic Sci (United States) 57:1354-1360.

Stahel PF, Kossmann T, Joller H, Trentz O, Morganti-Kossmann MC (1998) Increased interleukin-12 levels in human cerebrospinal fluid following severe head trauma. Neurosci Lett (Ireland) 249:123-126.

Stamenkovic I (2003) Extracellular matrix remodelling: The role of matrix metalloproteinases. 200:448-464.

Sternlicht MD, Werb Z (2001) How matrix metalloproteinases regulate cell behavior. Annu Rev Cell Dev Biol (United States) 17:463-516.

Steward O (1992) Signals that induce sprouting in the central nervous system: Sprouting is delayed in a strain of mouse exhibiting delayed axonal degeneration. Exp Neurol (United States) 118:340-351.

Steward O (1976) Reinnervation of dentate gyrus by homologous afferents following entorhinal cortical lesions in adult rats. Science (United States) 194:426-428.

Steward O, Banker GA, Davis L, Phillips LL (1988) The process of reinnervation of CNS neurons: Evidence for local synthesis of synaptic constituents at postsynaptic sites. 469-480.

Steward O (1989) Reorganization of neuronal connections following CNS trauma: Principles and experimental paradigms. 6:99-152.

Steward O, Vinsant SL (1983) The process of reinnervation in the dentate gyrus of the adult rat: A quantitative electron microscopic analysis of terminal proliferation and reactive synaptogenesis. 214:370-386.

Stone JR, Okonkwo DO, Dialo AO, Rubin DG, Mutlu LK, Povlishock JT, Helm GA (2004) Impaired axonal transport and altered axolemmal permeability occur in distinct populations of damaged axons following traumatic brain injury. 190:59-69.

Strassmann G (1949) Formation of hemosiderin and hematoidin after traumatic and spontaneous cerebral hemorrhages. Arch Pathol (Chic) (United States) 47:205-210.

Strich S (1961) SHEARING OF NERVE FIBRES AS A CAUSE OF BRAIN DAMAGE DUE TO HEAD INJURY A pathological study of twenty cases. 278:443-448.

Stroemer RP, Kent TA, Hulsebosch CE (1995) Neocortical neural sprouting, synaptogenesis, and behavioral recovery after neocortical infarction in rats. Stroke (United States) 26:2135-2144.

Sullivan HG, Martinez J, Becker DP, Miller JD, Griffith R, Wist AO (1976) Fluid-percussion model of mechanical brain injury in the cat. J Neurosurg (United States) 45:521-534.

Sullivan PG, Bruce-Keller AJ, Rabchevsky AG, Christakos S, Clair DK, Mattson MP, Scheff SW (1999) Exacerbation of damage and altered NF-kappaB activation in mice lacking tumor necrosis factor receptors after traumatic brain injury. J Neurosci (United States) 19:6248-6256.

Sun D, McGinn MJ, Zhou Z, Harvey HB, Bullock MR, Colello RJ (2007) Anatomical integration of newly generated dentate granule neurons following traumatic brain injury in adult rats and its association to cognitive recovery. 204:264-272.

Sun D, Colello RJ, Daugherty WP, Kwon TH, McGinn MJ, Harvey HB, Bullock MR (2005) Cell proliferation and neuronal differentiation in the dentate gyrus in juvenile and adult rats following traumatic brain injury. 22:95-105.

Susan L. Hillier MHS (1997) Outcomes 5 years post traumatic brain injury (with further reference to neurophysical impairment and disability). 11:661-675.

Sutton RL, Lescaudron L, Stein DG (1993) Unilateral cortical contusion injury in the rat: Vascular disruption and temporal development of cortical necrosis. 10:135-149.

Szklarczyk A, Lapinska J, Rylski M, McKay RD, Kaczmarek L (2002a) Matrix metalloproteinase-9 undergoes expression and activation during dendritic remodeling in adult hippocampus. J Neurosci (United States) 22:920-930.

Szklarczyk A, Lapinska J, Rylski M, McKay RD, Kaczmarek L (2002b) Matrix metalloproteinase-9 undergoes expression and activation during dendritic remodeling in adult hippocampus. J Neurosci (United States) 22:920-930.

Takizawa S, Hirabayashi H, Matsushima K, Tokuoka K, Shinohara Y (1998) Induction of heme oxygenase protein protects neurons in cortex and striatum, but not in hippocampus, against transient forebrain ischemia. J Cereb Blood Flow Metab (UNITED STATES) 18:559-569.

Tanaka N, Ikeda Y, Ohta Y, Deguchi K, Tian F, Shang J, Matsuura T, Abe K (2011) Expression of Keap1-Nrf2 system and antioxidative proteins in mouse brain after transient middle cerebral artery occlusion. Brain Res (Netherlands) 1370:246-253.

Tanigawa S, Fujii M, Hou DX (2007) Action of Nrf2 and Keap1 in ARE-mediated NQO1 expression by quercetin. Free Radic Biol Med (United States) 42:1690-1703.

Teasell R, Bayona NA, Bitensky J (2005) Plasticity and reorganization of the brain post stroke. Top Stroke Rehabil (England) 12:11-26.

Tehranian R, Andell-Jonsson S, Beni SM, Yatsiv I, Shohami E, Bartfai T, Lundkvist J, Iverfeldt K (2002) Improved recovery and delayed cytokine induction after closed head injury in mice with central overexpression of the secreted isoform of the interleukin-1 receptor antagonist. 19:939-951.

Tenhunen R, Marver HS, Schmid R (1970) The enzymatic catabolism of hemoglobin: Stimulation of microsomal heme oxygenase by hemin. J Lab Clin Med (UNITED STATES) 75:410-421.

Tenhunen R, Marver HS, Schmid R (1969) Microsomal heme oxygenase. characterization of the enzyme. J Biol Chem (UNITED STATES) 244:6388-6394.

Terry CM, Clikeman JA, Hoidal JR, Callahan KS (1999) TNF-alpha and IL-1alpha induce heme oxygenase-1 via protein kinase C, Ca2+, and phospholipase A2 in endothelial cells. Am J Physiol (UNITED STATES) 276:H1493-501.

Thau-Zuchman O, Shohami E, Alexandrovich AG, Leker RR (2010) Vascular endothelial growth factor increases neurogenesis after traumatic brain injury. 30:1008-1016.

Tian L, Stefanidakis M, Ning L, Van Lint P, Nyman-Huttunen H, Libert C, Itohara S, Mishina M, Rauvala H, Gahmberg CG (2007) Activation of NMDA receptors promotes dendritic spine development through MMP-mediated ICAM-5 cleavage. 178:687-700.

Trakshel GM, Ewing JF, Maines MD (1991) Heterogeneity of haem oxygenase 1 and 2 isoenzymes. rat and primate transcripts for isoenzyme 2 differ in number and size. Biochem J (ENGLAND) 275 (Pt 1):159-164.

Trakshel GM, Kutty RK, Maines MD (1986) Purification and characterization of the major constitutive form of testicular heme oxygenase. the noninducible isoform. J Biol Chem (UNITED STATES) 261:11131-11137.

Truettner JS, Alonso OF, Dietrich WD (2005) Influence of therapeutic hypothermia on matrix metalloproteinase activity after traumatic brain injury in rats. J Cereb Blood Flow Metab (United States) 25:1505-1516.

Tulis DA, Durante W, Peyton KJ, Evans AJ, Schafer AI (2001) Heme oxygenase-1 attenuates vascular remodeling following balloon injury in rat carotid arteries. Atherosclerosis (Ireland) 155:113-122.

Turner CP, Bergeron M, Matz P, Zegna A, Noble LJ, Panter SS, Sharp FR (1998) Heme oxygenase-1 is induced in glia throughout brain by subarachnoid hemoglobin. J Cereb Blood Flow Metab (UNITED STATES) 18:257-273.

Ullian EM (2001) Control of synapse number by glia. 291:657-661.

Vaillant C (2003) MMP-9 deficiency affects axonal outgrowth, migration, and apoptosis in the developing cerebellum. 24:395-408.

Van den Steen PE, Dubois B, Nelissen I, Rudd PM, Dwek RA, Opdenakker G (2002) Biochemistry and molecular biology of gelatinase B or matrix metalloproteinase-9 (MMP-9). 37:375-536.

Van Hove I, Lemmens K, Van de Velde S, Verslegers M, Moons L (2012) Matrix metalloproteinase-3 in the central nervous system: A look on the bright side. 123:203-216.

Van Wart HE, Birkedal-Hansen H (1990) The cysteine switch: A principle of regulation of metalloproteinase activity with potential applicability to the entire matrix metalloproteinase gene family. 87:5578-5582.

Vanderbeken I, Kerckhofs E (2017) A systematic review of the effect of physical exercise on cognition in stroke and traumatic brain injury patients. NeuroRehabilitation (Netherlands) 40:33-48.

Vascak M, Jin X, Jacobs KM, Povlishock JT (2017) Mild traumatic brain injury induces structural and functional disconnection of local neocortical inhibitory networks via parvalbumin interneuron diffuse axonal injury. Cereb Cortex (United States) 1-20.

Venstrom KA, Reichardt LF (1993) Extracellular matrix. 2: Role of extracellular matrix molecules and their receptors in the nervous system. FASEB J (United States) 7:996-1003.

Verma A, Hirsch DJ, Glatt CE, Ronnett GV, Snyder SH (1993) Carbon monoxide: A putative neural messenger. Science (United States) 259:381-384.

Verslegers M, Lemmens K, Van Hove I, Moons L (2013) Matrix metalloproteinase-2 and -9 as promising benefactors in development, plasticity and repair of the nervous system. 105:60-78.

Vincent SR, Das S, Maines MD (1994) Brain heme oxygenase isoenzymes and nitric oxide synthase are co-localized in select neurons. Neuroscience (United States) 63:223-231.

Virgintino D, Girolamo F, Errede M, Capobianco C, Robertson D, Stallcup WB, Perris R, Roncali L (2007) An intimate interplay between precocious, migrating pericytes and endothelial cells governs human fetal brain angiogenesis. 10:35-45.

Wagner AK, Kline AE, Ren D, Willard LA, Wenger MK, Zafonte RD, Dixon CE (2007) Gender associations with chronic methylphenidate treatment and behavioral performance following experimental traumatic brain injury. Behav Brain Res (Netherlands) 181:200-209.

Wagner AK, Sokoloski JE, Ren D, Chen X, Khan AS, Zafonte RD, Michael AC, Dixon CE (2005) Controlled cortical impact injury affects dopaminergic transmission in the rat striatum. J Neurochem (England) 95:457-465.

Wakabayashi N, Dinkova-Kostova AT, Holtzclaw WD, Kang MI, Kobayashi A, Yamamoto M, Kensler TW, Talalay P (2004) Protection against electrophile and oxidant stress by induction of the phase 2 response: Fate of cysteines of the Keap1 sensor modified by inducers. Proc Natl Acad Sci U S A (United States) 101:2040-2045.

Wang G, Fang H, Zhen Y, Xu G, Tian J, Zhang Y, Zhang D, Zhang G, Xu J, Zhang Z, Qiu M, Ma Y, Zhang H, Zhang X (2016) Sulforaphane prevents neuronal apoptosis and memory impairment in diabetic rats. Cell Physiol Biochem (Switzerland) 39:901-907.

Wang KKW (2000) Calpain and caspase: Can you tell the difference? 23:20-26.

Wang W, Wu Y, Zhang G, Fang H, Wang H, Zang H, Xie T, Wang W (2014) Activation of Nrf2-ARE signal pathway protects the brain from damage induced by epileptic seizure. Brain Res (Netherlands) 1544:54-61.

Warden DL, Gordon B, McAllister TW, Silver JM, Barth JT, Bruns J, Drake A, Gentry T, Jagoda A, Katz DI (2006) Guidelines for the pharmacologic treatment of neurobehavioral sequelae of traumatic brain injury. J Neurotrauma 23:1468-1501.

Warren KM, Reeves TM, Phillips LL (2012) MT5-MMP, ADAM-10, and N-cadherin act in concert to facilitate synapse reorganization after traumatic brain injury. 29:1922-1940.

Weber J, Maas A (2007) **Neurotrauma: New insights into pathology and treatment, volume 161**. (NY, USA) .

Wee Yong V (2010) Inflammation in neurological disorders: A help or a hindrance? 16:408-420.

Wee Yong V, Forsyth PA, Bell R, Krekoski CA, Edwards DR (1998) Matrix metalloproteinases and diseases of the CNS. 21:75-80.

Wei EP, Hamm RJ, Baranova AI, Povlishock JT (2009) The long-term microvascular and behavioral consequences of experimental traumatic brain injury after hypothermic intervention. J Neurotrauma (United States) 26:527-537.

Weightman MM, Bolgla R, McCulloch KL, Peterson MD (2010) Physical therapy recommendations for service members with mild traumatic brain injury. 25:206-218.

Wells GMA, Catlin G, Cossins JA, Mangan M, Ward GA, Miller KM, Clements JM (1996) Quantitation of matrix metalloproteinases in cultured rat astrocytes using the polymerase chain reaction with a multi-competitor cDNA standard. 18:332-340.

Werner C, Engelhard K (2007) Pathophysiology of traumatic brain injury. 99:4-9.

Whishaw IQ, Pellis SM, Gorny BP, Pellis VC (1991) The impairments in reaching and the movements of compensation in rats with motor cortex lesions: An endpoint, videorecording, and movement notation analysis. Behav Brain Res (Netherlands) 42:77-91.

Whitman MC, Greer CA (2009) Adult neurogenesis and the olfactory system. Prog Neurobiol (England) 89:162-175.

Wilhelmsson U, Li L, Pekna M, Berthold CH, Blom S, Eliasson C, Renner O, Bushong E, Ellisman M, Morgan TE, Pekny M (2004) Absence of glial fibrillary acidic protein and vimentin prevents hypertrophy of astrocytic processes and improves post-traumatic regeneration. J Neurosci (United States) 24:5016-5021.

Wintermark M et al (2013) Acute stroke imaging research roadmap II. Stroke (United States) 44:2628-2639.

Wlodarczyk J, Mukhina I, Kaczmarek L, Dityatev A (2011) Extracellular matrix molecules, their receptors, and secreted proteases in synaptic plasticity. 71:1040-1053.

Wolf JA, Stys PK, Lusardi T, Meaney D, Smith DH (2001) Traumatic axonal injury induces calcium influx modulated by tetrodotoxin-sensitive sodium channels. J Neurosci (United States) 21:1923-1930.

Wu J, Hua Y, Keep RF, Nakamura T, Hoff JT, Xi G (2003) Iron and iron-handling proteins in the brain after intracerebral hemorrhage. Stroke (United States) 34:2964-2969.

Wu L, Du Y, Lok J, Lo EH, Xing C (2015) Lipocalin-2 enhances angiogenesis in rat brain endothelial cells via reactive oxygen species and iron-dependent mechanisms. J Neurochem (England) 132:622-628.

Xi G, Keep RF, Hoff JT (1998) Erythrocytes and delayed brain edema formation following intracerebral hemorrhage in rats. J Neurosurg (UNITED STATES) 89:991-996.

Xing C, Wang X, Cheng C, Montaner J, Mandeville E, Leung W, van Leyen K, Lok J, Wang X, Lo EH (2014) Neuronal production of lipocalin-2 as a help-me signal for glial activation. Stroke (United States) 45:2085-2092.

Yachie A, Niida Y, Wada T, Igarashi N, Kaneda H, Toma T, Ohta K, Kasahara Y, Koizumi S (1999) Oxidative stress causes enhanced endothelial cell injury in human heme oxygenase-1 deficiency. J Clin Invest (United States) 103:129-135.

Yamanaka M, Yamabe K, Saitoh Y, Katoh-Semba R, Semba R (1996) Immunocytochemical localization of heme oxygenase-2 in the rat cerebellum. Neurosci Res (Ireland) 24:403-407.

Yamauchi T, Lin Y, Sharp FR, Noble-Haeusslein LJ (2004) Hemin induces heme oxygenase-1 in spinal cord vasculature and attenuates barrier disruption and neutrophil infiltration in the injured murine spinal cord. J Neurotrauma (United States) 21:1017-1030.

Yan L, Borregaard N, Kjeldsen L, Moses MA (2001) The high molecular weight urinary matrix metalloproteinase (MMP) activity is a complex of gelatinase B/MMP-9 and neutrophil gelatinase-associated lipocalin (NGAL): MODULATION OF MMP-9 ACTIVITY BY NGAL. 276:37258-37265.

Yang J, McNeish B, Butterfield C, Moses MA (2013) Lipocalin 2 is a novel regulator of angiogenesis in human breast cancer. FASEB J (United States) 27:45-50.

Yang Y, Hill JW, Rosenberg GA (2011) Multiple roles of metalloproteinases in neurological disorders. Prog Mol Biol Transl Sci (Netherlands) 99:241-263.

Yokobori S, Mazzeo AT, Hosein K, Gajavelli S, Dietrich WD, Bullock MR (2013) Preconditioning for traumatic brain injury. Transl Stroke Res (United States) 4:25-39.

Yokoyama A, Sakamoto A, Kameda K, Imai Y, Tanaka J (2006) NG2 proteoglycan-expressing microglia as multipotent neural progenitors in normal and pathologic brains. 53:754-768.

Yong VW (2005) Metalloproteinases: Mediators of pathology and regeneration in the CNS. 6:931-944.

Yong VW, Power C, Forsyth P, Edwards DR (2001) Metalloproteinases in biology and pathology of the nervous system. 2:502-511.

Yoo MS, Chun HS, Son JJ, DeGiorgio LA, Kim DJ, Peng C, Son JH (2003) Oxidative stress regulated genes in nigral dopaminergic neuronal cells: Correlation with the known pathology in parkinson's disease. Brain Res Mol Brain Res (Netherlands) 110:76-84.

Yoshida T, Oguro T, Numazawa S, Kuroiwa Y (1987) Effects of phorone (diisopropylidene acetone), a glutathione (GSH) depletor, on hepatic enzymes involved in drug and heme metabolism in rats: Evidence that phorone is a potent inducer of heme oxygenase. Biochem Biophys Res Commun (UNITED STATES) 145:502-508.

Yoshida T, Biro P, Cohen T, Muller RM, Shibahara S (1988) Human heme oxygenase cDNA and induction of its mRNA by hemin. Eur J Biochem (GERMANY, WEST) 171:457-461.

Yoshinaga T, Sassa S, Kappas A (1982) Purification and properties of bovine spleen heme oxygenase. amino acid composition and sites of action of inhibitors of heme oxidation. J Biol Chem (UNITED STATES) 257:7778-7785.

Yoshino A, Hovda DA, Katayama Y, Kawamata T, Becker DP (1992) Hippocampal CA3 lesion prevents postconcussive metabolic dysfunction in CA1. J Cereb Blood Flow Metab (United States) 12:996-1006.

Youn JK, Kim DW, Kim ST, Park SY, Yeo EJ, Choi YJ, Lee HR, Kim DS, Cho SW, Han KH, Park J, Eum WS, Hwang HS, Choi SY (2014) PEP-1-HO-1 prevents MPTP-induced degeneration of dopaminergic neurons in a parkinson's disease mouse model. BMB Rep .

Yu H, Huang J, Wang S, Zhao G, Jiao X, Zhu L (2013) Overexpression of Smad7 suppressed ROS/MMP9-dependent collagen synthesis through regulation of heme oxygenase-1. Mol Biol Rep (Netherlands) 40:5307-5314.

Zhang H, Adwanikar H, Werb Z, Noble-Haeusslein LJ (2010) Matrix metalloproteinases and neurotrauma: Evolving roles in injury and reparative processes. Neuroscientist (United States) 16:156-170.

Zhang H, Chang M, Hansen CN, Basso DM, Noble-Haeusslein LJ (2011) Role of matrix metalloproteinases and therapeutic benefits of their inhibition in spinal cord injury. Neurotherapeutics (United States) 8:206-220.

Zhang L, Rzigalinski BA, Ellis EF, Satin LS (1996) Reduction of voltage-dependent Mg2+ blockade of NMDA current in mechanically injured neurons. 274:1921-1923.

Zhang R, Miao QW, Zhu CX, Zhao Y, Liu L, Yang J, An L (2015) Sulforaphane ameliorates neurobehavioral deficits and protects the brain from amyloid beta deposits and peroxidation in mice with alzheimer-like lesions. Am J Alzheimers Dis Other Demen (United States) 30:183-191.

Zhang R, Zhang J, Fang L, Li X, Zhao Y, Shi W, An L (2014) Neuroprotective effects of sulforaphane on cholinergic neurons in mice with alzheimer's disease-like lesions. Int J Mol Sci (Switzerland) 15:14396-14410.

Zhao J, Moore AN, Redell JB, Dash PK (2007) Enhancing expression of Nrf2-driven genes protects the blood brain barrier after brain injury. J Neurosci (United States) 27:10240-10248.

Zhao J, Xi G, Wu G, Keep RF, Hua Y (2016a) Deferoxamine attenuated the upregulation of lipocalin-2 induced by traumatic brain injury in rats. Acta Neurochir Suppl (Austria) 121:291-294.

Zhao J, Chen H, Zhang M, Zhang Y, Qian C, Liu Y, He S, Zou Y, Liu H (2016b) Early expression of serum neutrophil gelatinase-associated lipocalin (NGAL) is associated with neurological severity immediately after traumatic brain injury. J Neurol Sci (Netherlands) 368:392-398.

Zhao Z, Alam S, Oppenheim RW, Prevette DM, Evenson A, Parsadanian A (2004) Overexpression of glial cell line-derived neurotrophic factor in the CNS rescues motoneurons from programmed cell death and promotes their long-term survival following axotomy. Exp Neurol (United States) 190:356-372.

Zhu J, Hamm R, Reeves T, Povlishock J, Phillips L (2000) Postinjury administration of L-deprenyl improves cognitive function and enhances neuroplasticity after traumatic brain injury. Exp Neurol 166:136-152.

Ziebell JM, Adelson PD, Lifshitz J (2015) Microglia: Dismantling and rebuilding circuits after acute neurological injury. Metab Brain Dis (United States) 30:393-400.

Ziebell JM, Morganti-Kossmann MC (2010) Involvement of pro- and anti-inflammatory cytokines and chemokines in the pathophysiology of traumatic brain injury. 7:22-30.

6 Appendices

6.1 Description of Injury Model

In our hands the cFPI rat model produces a moderate injury with righting time ~7:00 minutes. In general animals that have righting times longer than ~9:00 minutes tend to either die or demonstrate remarkable hemorrhage which excludes them from further testing.

We frequently see that the hemorrhage induced by the cFPI has a tendency to lateralize. Although in many instances the hemorrhage is roughly equivalent in size on both sides of the brain for the purposes of presentation in circumstances where the hemorrhages are of unequal size we always represent the hemisphere with the larger hemorrhage.

We rarely observed animals with significant edema (identified by the brain swelling at the craniectomy site) and such animals were excluded from our studies.

6.2 Commentary on Randomization, Blinding, Animal Sex Selection

Where possible animals were randomized during surgery, behavioral testing, and western analysis and during behavioral testing were blinded to the extent possible. Unfortunately in the context of cFPI injury and drug treatment there were several relatively obvious changes that occurred in the animals after injury and during recovery. As an example Sham animals and drug treated TBI animals tended to recover faster and had noticeably better grooming ability.

Male rats were used without paired female counterparts due to concerns about the injury model with physically smaller animals and possible concerns about hormonal fluctuations in a drug treatment model. At the age of rat used female rats are roughly 2/3 the size of the male rats whielt he size of the craniectomy surgical tools would be unchanged and we had concerns that

changes to the cFPI impact overpressure to standardize for righting time may cause a reduction in hemorrhagic injury. We believe that future work should include the addition of female animals to establish if the injury and treatment effects observed are generalizable.

6.3 Drug Blood Brain Barrier Transport

There have been limited studies with either Hemin or Sulforaphane looking at how exactly they each cross the blood brain barrier. The majority of researchers have opted instead to inject the drugs peripherally and note changes that occur in the CNS as evidence of barrier transport. In the context of Sulforaphane it is interpreted that as a small relatively soluble molecule that barrier transport is relatively efficient and it has been observed in numerous models that sulforaphane given peripherally is capable of inducing a CNS response (Greco and Fiskum, 2010; Wang et al., 2014; Siow and Mann, 2010; Zhao et al., 2007; Tanaka et al., 2011; Morroni et al., 2013; Zhang et al., 2014; Alfieri et al., 2013). Hemin in contrast is considered to be a largely insoluble molecule which must be bound by some carrier to allow it to circulate systemically, typically either via binding to hemopexin or an albumin protein. Similar to sulforaphane most researchers have simply injected hemin peripherally and observed central effects and this has been observed reliably (He et al., 2011; Tulis et al., 2001; Yamauchi et al., 2004; Takizawa et al., 1998; Bhardwaj et al., 2016; Lu et al., 2014; Chen-Roetling et al., 2015)

6.4 Sham Drug Treated Animal Behavior

6.4.1 Morris Water Maze

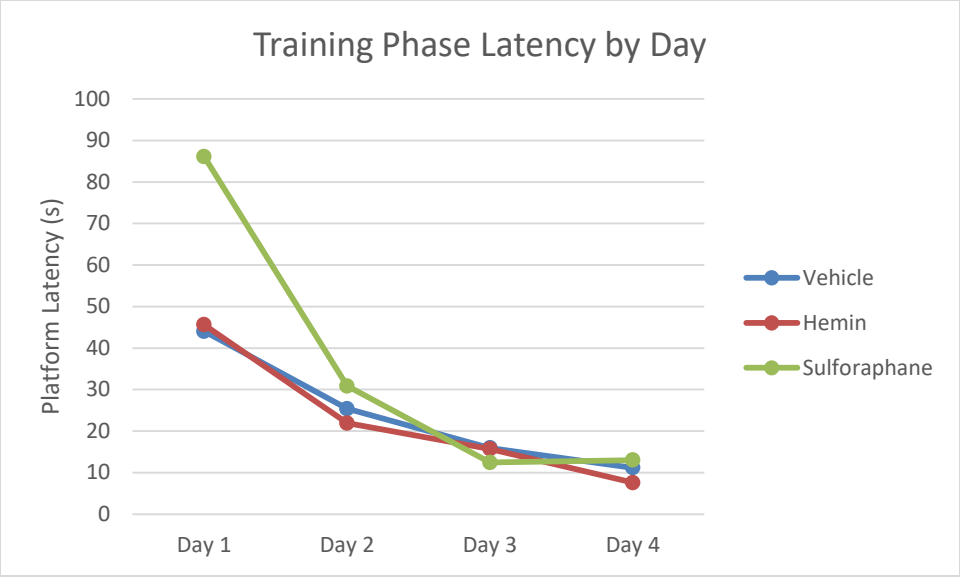

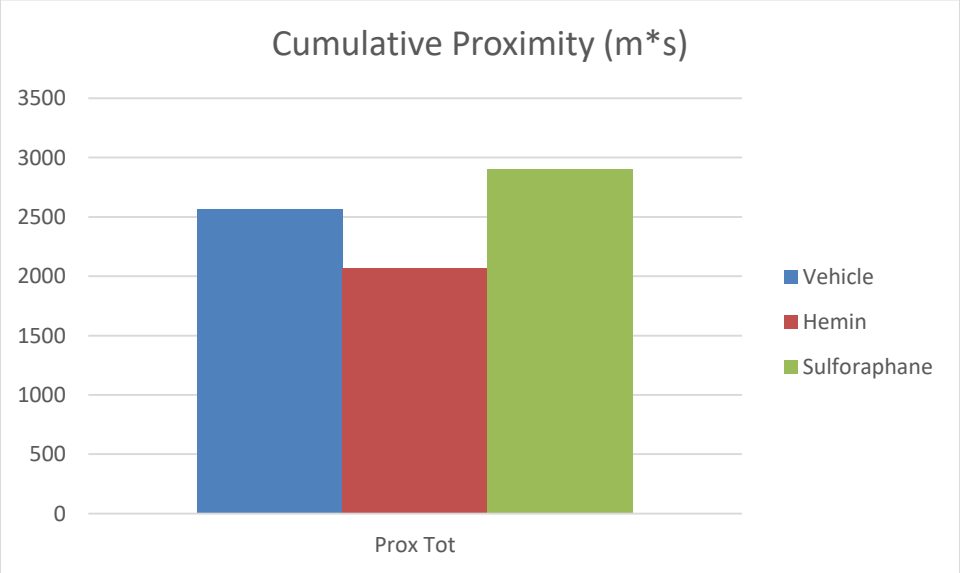

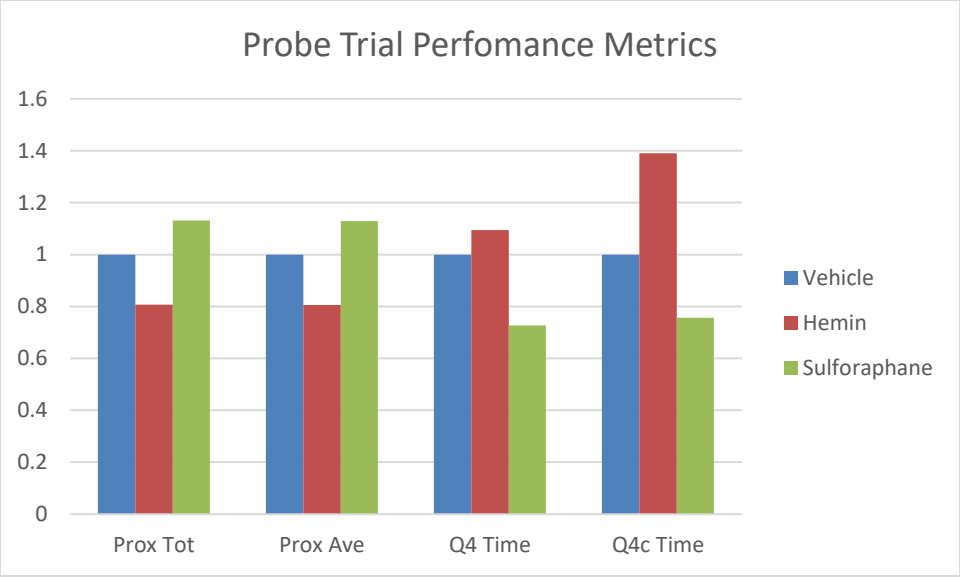
Probe Trial Perfomance Metrics
1.6
1.4
1.2
1
0.8
0.6
0.4
0.2
0
Prox Tot
Prox Ave
Q4 Time
Q4c Time
Vehicle
Hemin
Sulforaphane

6.5 Appendix Data for Chapter 3

6.5.1.1 HO-1 ANOVA Tables

Cortex							
Model:							
Value~Day*Condition							
	Df	Sum of Sq	RSS	AIC	F Value	Pr(>F)	Significance Code
<none>			297.5	139.6			
Day	3	283.79	581.29	193.89	23.5299	8.46E-11	***
Condition	3	180.59	478.09	176.3	14.9733	1.04E-07	***
Day:Condition	9	178.69	476.19	163.94	4.9385	3.41E-05	***

Hippocampus							
Model:							
Value~Day*Condition							
	Df	Sum of Sq	RSS	AIC	F Value	Pr(>F)	Significance Code
<none>			815.76	224.22			
Day	3	397.84	1213.6	251.99	11.2168	4.41E-06	***
Condition	3	386.19	1201.95	251.17	10.8885	6.09E-06	***
Day:Condition	9	562.04	1377.8	250.78	5.2822	1.82E-05	***

Combined Tissue							
Model:							
Value~Day*Condition							
	Df	Sum of Sq	RSS	AIC	F Value	Pr(>F)	Significance Code
<none>			1113.3	387.8			
Day	3	676.49	1789.8	464.88	28.9655	1.08E-14	***
Condition	3	548.54	1661.8	451.9	23.487	2.03E-12	***
Tissue	1	13.78	1127	387.95	1.77	0.1855	
Day:Condition	9	662.22	1775.5	451.48	9.4515	3.26E-11	***
Day:Tissue	3	6.73	1120	382.85	0.2881	0.8339	
Condition:Tissue	3	32.59	1145.8	386.85	1.3953	0.2467	
Day:Condition:Tissue	9	80.84	1194.1	382.06	1.1538	0.3293	

6.5.1.2 HO-1 TukeyHSD Table

Cortex				
$Condition				
	diff	lwr	upr	p
SFN-HMN	-0.22792	-1.89656	1.440714	0.98403
SHAM-HMN	-2.18211	-3.78609	-0.57813	0.003401
TBI-HMN	1.296586	-0.30739	2.900562	0.154848
SHAM-SFN	-1.95419	-3.51416	-0.39421	0.008126
TBI-SFN	1.524509	-0.03547	3.084484	0.057865
TBI-SHAM	3.478696	1.988089	4.969303	2E-07

Hippocampus				
$Condition				
	diff	lwr	upr	p
SFN-HMN	-0.608749	-3.549841	2.3323434	0.947608
SHAM-HMN	-2.491284	-5.289596	0.3070273	0.0981019
TBI-HMN	2.745812	-0.131258	5.6228835	0.0667616
SHAM-SFN	-1.882535	-4.598283	0.8332122	0.2705424
TBI-SFN	3.3545618	0.5577293	6.1513943	0.0123381
TBI-SHAM	5.2370972	2.5908176	7.8833768	0.000011

Combined				
$Condition				
	diff	lwr	upr	p
SFN-HMN	-0.4138939	-2.0585479	1.23076	0.9139269
SHAM-HMN	-2.3374022	-3.9102757	-0.7645288	0.0009637
TBI-HMN	1.9705039	0.3764247	3.564583	0.008715
SHAM-SFN	-1.9235083	-3.4516506	-0.395366	0.0072447
TBI-SFN	2.3843978	0.8344378	3.9343579	0.0005832
TBI-SHAM	4.3079061	2.8343321	5.7814802	0

6.5.1.3 FTL ANOVA Tables

Cortex							
Model:							
Value~Day*Condition							
	Df	Sum of Sq	RSS	AIC	F Value	Pr(>F)	Significance Code
<none>			45.37	-45.248			
Day	3	15.869	61.239	-21.554	9.6771	1.51E-05	***
Condition	3	20.845	66.214	-13.82	12.7112	6.48E-07	***
Day:Condition	9	19.09	64.459	-28.48	3.8803	0.0003856	***

Hippocampus							
Model:							
Value~Day*Condition							
	Df	Sum of Sq	RSS	AIC	F Value	Pr(>F)	Significance Code
<none>			99.626	30.617			
Day	3	27.793	127.419	49.468	7.9042	0.0001035	***
Condition	3	36.64	136.266	56.248	10.4203	6.57E-06	***
Day:Condition	9	17.979	117.605	29.373	1.7044	0.1004482	

Combined Tissue							
Model:							
Value~Day*Condition							
	Df	Sum of Sq	RSS	AIC	F Value	Pr(>F)	Significance Code
<none>			145	-0.323			
Day	3	36.649	181.65	38.748	14.1547	2.87E-08	***
Condition	3	54.747	199.74	57.743	21.1445	1.14E-11	***
Tissue	1	3.038	148.03	1.825	3.5204	0.0623535	.
Day:Condition	9	28.579	173.57	17.658	3.6792	0.0003153	***
Day:Tissue	3	6.885	151.88	2.956	2.6592	0.0499465	*
Condition:Tissue	3	2.375	147.37	-3.073	0.9174	0.4338092	
Day:Condition:Tissue	9	8.648	153.64	-6.736	1.1133	0.3559105	

6.5.1.4 FTL TukeyHSD Table

Cortex				
$Condition				
	diff	lwr	upr	p
SFN-HMN	-0.02568808	-0.64668855	0.59531238	0.9995398
SHAM-HMN	-0.66979575	-1.23814073	-0.10145076	0.0142169
TBI-HMN	0.45234532	-0.11599966	1.02069031	0.1659528
SHAM-SFN	-0.64410767	-1.20368588	-0.08452945	0.0174498
TBI-SFN	0.4780334	-0.08154481	1.03761162	0.1211002
TBI-SHAM	1.12214107	0.6216391	1.62264304	0.0000005

Hippocampus				
$Condition				
	diff	lwr	upr	p
SFN-HMN	-0.58554771	-1.4944497	0.32335424	0.3361946
SHAM-HMN	-1.34850479	-2.1701982	-0.52681134	0.0002607
TBI-HMN	0.05520891	-0.776626	0.88704381	0.9981158
SHAM-SFN	-0.76295709	-1.5716585	0.04574434	0.0716488
TBI-SFN	0.64075661	-0.1782472	1.45976039	0.1780772
TBI-SHAM	1.4037137	0.6827112	2.12471617	0.0000119

Combined				
$Condition				
	diff	lwr	upr	p
SFN-HMN	-0.3050221	-0.85112471	0.2410805	0.4705268
SHAM-HMN	-1.0049598	-1.501622	-0.5082976	0.0000027
TBI-HMN	0.254434	-0.24536383	0.7542318	0.550874
SHAM-SFN	-0.6999377	-1.18884104	-0.2110344	0.0015619
TBI-SFN	0.5594561	0.06736769	1.0515445	0.0188519
TBI-SHAM	1.2593938	0.82282047	1.6959671	0

6.5.1.5 LCN2 ANOVA Tables

Cortex							
Model:							
Value~Day*Condition							
	Df	Sum of Sq	RSS	AIC	F Value	Pr(>F)	Significance Code
<none>			3208.4	297.37			
Day	2	1544.29	4752.6	321.66	14.44	7.59E-06	***
Condition	3	1755.25	4963.6	322.79	10.9417	7.90E-06	***
Day:Condition	6	852.23	4060.6	302.33	2.6563	0.02369	*

Hippocampus							
Model:							
Value~Day*Condition							
	Df	Sum of Sq	RSS	AIC	F Value	Pr(>F)	Significance Code
<none>			18771	424.57			
Day	2	5524.8	24296	439.14	8.8298	0.0004352	***
Condition	3	11332.7	30104	452.57	12.0746	2.76E-06	***
Day:Condition	6	4071.9	22843	426.7	2.1692	0.0584626	.

Combined Tissue							
Model:							
Value~Day*Condition							
	Df	Sum of Sq	RSS	AIC	F Value	Pr(>F)	Significance Code
<none>			21980	772.04			
Day	2	5862.9	27842	802.09	16.0046	6.90E-07	***
Condition	3	10856.2	32836	823.84	19.757	1.78E-10	***
Tissue	1	4972.3	26952	799.41	27.1472	7.94E-07	***
Day:Condition	6	3913.8	25893	783.64	3.5613	0.002785	**
Day:Tissue	2	1206.2	23186	775.73	3.2928	0.040534	*
Condition:Tissue	3	2231.7	24211	779.97	4.0614	0.008674	**
Day:Condition:Tissue	6	1010.3	22990	766.51	0.9193	0.483632	

6.5.1.6 LCN2 TukeyHSD Table

Cortex				
$Condition				
	diff	lwr	upr	p
SFN-HMN	-1.2548569	-8.856656	6.346942	0.9719759
SHAM-HMN	-11.0792453	-17.911112	-4.247379	0.0003823
TBI-HMN	-0.3646	-7.299207	6.570007	0.9990321
SHAM-SFN	-9.8243883	-16.32279	-3.325987	0.0010063
TBI-SFN	0.8902569	-5.716073	7.496587	0.984374
TBI-SHAM	10.7146453	5.011081	16.418209	0.0000351

Hippocampus				
$Condition				
	diff	lwr	upr	p
SFN-HMN	0.437978	-17.949427	18.825384	0.9999095
SHAM-HMN	-29.177887	-45.702961	-12.652812	0.0001023
TBI-HMN	-6.692791	-23.466377	10.080795	0.7182618
SHAM-SFN	-29.615865	-45.334346	-13.897383	0.0000333
TBI-SFN	-7.130769	-23.110311	8.848772	0.6422002
TBI-SHAM	22.485095	8.689185	36.281006	0.0003554

Combined				
$Condition				
	diff	lwr	upr	p
SFN-HMN	-0.4084395	-10.2171	9.400217	0.9995406
SHAM-HMN	-20.128566	-28.94377	-11.313359	0.0000002
TBI-HMN	-3.5286957	-12.47647	5.419078	0.7336988
SHAM-SFN	-19.7201265	-28.10506	-11.335192	0.0000001
TBI-SFN	-3.1202562	-11.64445	5.403939	0.7758367
TBI-SHAM	16.5998703	9.24052	23.95922	0.0000002

6.5.1.7 Zymogram Data Tables Mean ± SEM

Hippocampus HMN Series

		Day 1	Day 3	Day 7
MMP2	Sham	100.00 ± 15.98	100.00 ± 15.20	100.00 ± 2.89
	TBI	152.78 ± 12.01	260.71 ± 24.05	165.06 ± 4.74
	HMN	158.43 ± 7.19	230.79 ± 13.24	168.53 ± 17.45

		Day 1	Day 3	Day 7
Pro-MMP9	Sham	100.00 ± 35.30	100.00 ± 30.36	100.00 ± 15.40
	TBI	769.01 ± 87.03	233.58 ± 107.17	85.65 ± 16.38
	HMN	763.17 ± 37.64	179.00 ± 19.25	123.55 ± 15.19

		Day 1	Day 3	Day 7
Active-MMP9	Sham	100.00 ± 10.39	100.00 ± 13.56	100.00 ± 2.13
	TBI	253.53 ± 33.99	180.04 ± 40.01	119.02 ± 23.40
	HMN	264.74 ± 39.79	134.98 ± 21.89	103.41 ± 12.87

Hippocampus SFN Series

		Day 1	Day 3	Day 7
MMP2	Sham	100.00 ± 10.64	100.00 ± 24.19	100.00 ± 4.36
	TBI	165.09 ± 5.24	239.06 ± 5.98	164.35 ± 7.64
	SFN	133.56 ± 11.46	196.50 ± 12.98	162.17 ± 12.14

		Day 1	Day 3	Day 7
Pro-MMP9	Sham	100.00 ± 57.95	100.00 ± 30.82	100.00 ± 5.89
	TBI	605.64 ± 57.34	197.05 ± 85.63	100.96 ± 6.50
	SFN	489.86 ± 120.39	124.45 ± 33.07	102.26 ± 32.98

		Day 1	Day 3	Day 7
Active-MMP9	Sham	100.00±31.16	100.00±15.15	100.00±8.76
	TBI	253.58±39.29	157.52±35.66	123.92±20.67
	SFN	222.50±23.66	119.46±20.65	95.56±9.53

Neocortex HMN Series

		Day 1	Day 3	Day 7
MMP2	Sham	100.00 ± 8.44	100.00 ± 9.56	100.00 ± 9.18
	TBI	141.60 ± 11.47	184.23 ± 8.99	177.03 ± 5.01
	HMN	157.37 ± 7.45	175.18 ± 23.22	141.68 ± 17.46

		Day 1	Day 3	Day 7
Pro-MMP9	Sham	100.00 ± 24.53	100.00 ± 26.38	100.00 ± 27.16
	TBI	2064.72 ± 203.07	411.21 ± 163.14	114.16 ± 36.44
	HMN	2268.62 ± 512.59	177.45 ± 96.87	106.54 ± 19.07

		Day 1	Day 3	Day 7
Active-MMP9	Sham	100.00 ± 12.47	100.00 ± 3.43	100.00 ± 3.61
	TBI	338.72 ± 16.06	191.78 ± 25.19	126.09 ± 9.90
	HMN	280.95 ± 43.90	104.19 ± 14.99	116.47 ± 11.35

Neocortex SFN Series

		Day 1	Day 3	Day 7
MMP2	Sham	100.00 ± 5.19	100.00 ± 11.25	100.00 ± 15.67
	TBI	145.96 ± 7.06	199.58 ± 3.89	181.22 ± 10.38
	SFN	147.24 ± 13.90	163.39 ± 14.27	156.61 ± 13.92

		Day 1	Day 3	Day 7
Pro-MMP9	Sham	100.00 ± 38.74	100.00 ± 13.92	100.00 ± 23.53
	TBI	2088.49 ± 136.02	315.00 ± 57.03	103.23 ± 17.05
	SFN	1789.10 ± 267.62	76.57 ± 15.23	201.33 ± 25.71

		Day 1	Day 3	Day 7
Active-MMP9	Sham	100.00 ± 7.27	100.00 ± 4.08	100.00 ± 12.41
	TBI	316.23 ± 16.37	194.89 ± 32.51	114.22 ± 10.90
	SFN	267.84 ± 44.79	147.43 ± 9.93	106.42 ± 12.16

6.5.1.8 Appendix Figure 2: Drug dosing Proof of Concepts

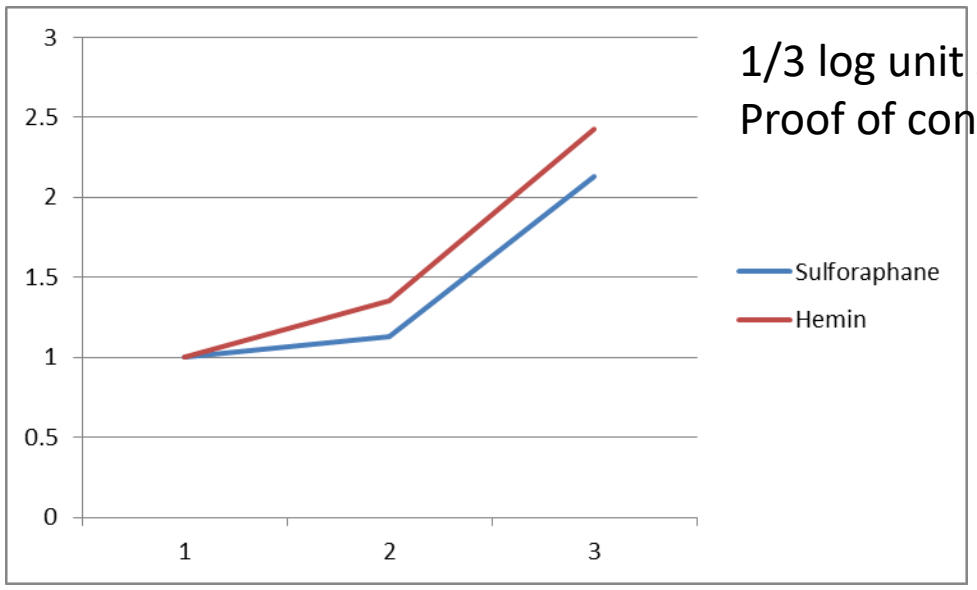

Hemin Doses: 10, 21.5, 46.4 mg/kg
Sulforaphane Doses: 2.2, 4.6, 10 mg/kg

6.5.1.9 Figure 3: Proof of concept of drug dosing influence on HO-1 in naïve untreated animals using 1/3 log ramp (4.6 mg/kg Hemin and 1 mg/kg Sulforaphane doses not shown since equal effect to next ramp step).

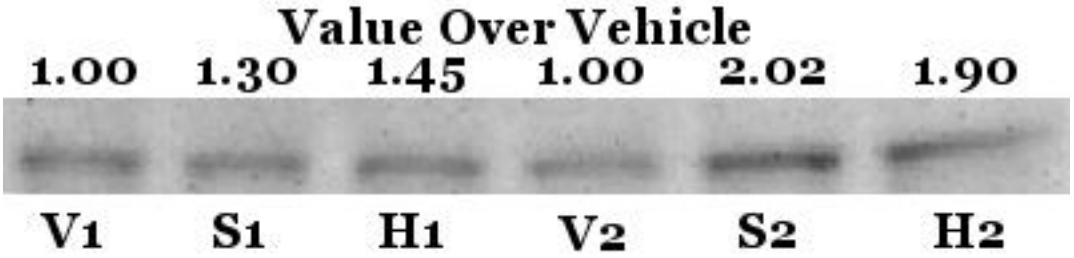

6.6 Affymetric Rat Genome Microarray Screening

Gene	Significant?	Nrf2 Target?	H 24h	Cx 24h	CC 24h	H 7d
HO-1	Yes	Yes	**2.5**	**3.8**	**4.3**	**2.7**
HO-2	No	No	-	-	-	-
LCN2	Yes	Yes	**36**	**34.2**	**10.9**	1.9
Trf	Yes	Yes	**1.7**	**2**	-3.51	1.3
FTL	No	Yes	-	-	-	-
Mgst1	Yes	Yes	1.8	1.8	1.26	**2.5**
Ugt1a1	Yes	Yes	1.4	1.6	1.31	**1.5**
Known HO-1 Transcription Factors						
Nrf2	No		1.1	1	-1.06	1.4
HIF1α	No		-	-	-	-
AP-1	No		-	-	-	-

(-) denotes no significance in Nrf2 target or no observed change

Bold denotes significant upregulation at time point indicated

7 Vita

Nicholas Hyatt Russell was born on 1987 August 25 in Houston, Texas, and is a citizen of the United States of America. He graduated from St. John's School in Houston, Texas, in 2006. He received his B.S. in Mechanical Engineering with an Additional Major in Biomedical Engineering in 2010 and his M.ChE in Chemical Engineering in 2011 both from Carnegie Mellon University. He then entered the M.D.-Ph.D. program at Virginia Commonwealth University in 2011, and anticipates a thesis defense in Neuroscience in May 2017 and a graduation date of May 2019.